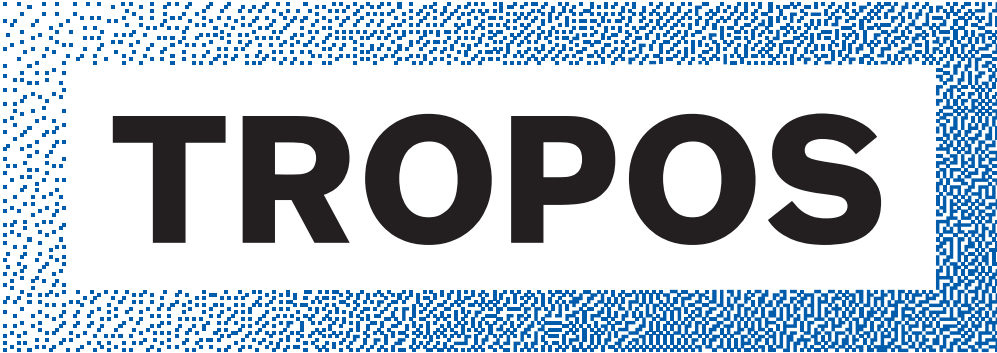


Biennial Report

Zweijahresbericht
2022/2023



Leibniz Institute for
Tropospheric Research



TROPOS

Leibniz Institute for
Tropospheric Research



Imprint

Published by

TROPOS

Leibniz Institute for Tropospheric Research
Leibniz-Institut für Troposphärenforschung e.V. Leipzig
Member of the Leibniz Association

Permoserstraße 15
04318 Leipzig
Germany

Phone: ++49 (341) 2717-7060
Fax: ++49 (341) 2717-7006
Email: info@tropos.de
Internet: <http://www.tropos.de>

Copy editors

Katja Schmieder, Ina Burkert, Konstanze Kunze,
Kerstin Müller, Beate Richter, Tilo Arnhold (Photographer)

Editorial board

Andres Macke, Hartmut Herrmann, Ina Tegen, Mira Pöhlker,
Ulla Wandinger, Frank Stratmann, Kathrin Niehuus

Photo and illustration credits © TROPOS / as described in
the captions

- p. 1: top - Rico Hengst / TROPOS
middle - tropos.de / TROPOS
bottom - Martin Riese / Forschungszentrum Jülich
- p. 39: top - Sebastian Duesing / TROPOS
middle - Martin Radenz / TROPOS
bottom - Edson Silva Delgado / GEOMAR
- p. 143: top - Michael Schmidt / www.schmidt.fm
middle - Tilo Arnhold / TROPOS
bottom - Falk Lange / SMWK

Table of contents

- 3 **Introduction / Einleitung**
- 13 **Overview of the individual contributions / Übersicht der Einzelbeiträge**
- 20 **Highlight Publications / Highlight-Publikationen**
- 22 **Transfer in science and society – overview / Transfer in Wissenschaft und Gesellschaft – Überblick**
- 37 **Facts and figures / Zahlen und Fakten**

Articles

- 41 D. van Pinxteren et al.: Ozone and its precursors in Saxony - Trends, impacts, and drivers
- 51 F. Stratmann et al.: Model assisted vertical in-situ investigation of aerosols, and aerosol-cloud-turbulence interactions in the Southern Hemisphere marine boundary layer: Indications for new particle formation from terrestrial precursors
- 60 K. Ohneiser et al.: UTLS wildfire smoke – a synopsis of Polly observations in Europe, the Arctic, and southern South America (2017-2021)
- 69 O. Hellmuth: A contribution to the discussion “What is a cloud?”
- 77 M. Radenzet al.: Ground-based remote sensing of aerosol, clouds, dynamics, and precipitation in Antarctica - First results from the one-year COALA campaign at Neumayer III Station in 2023
- 80 A. Babu Suja et al.: Measurements of Aerosol Particles in the Arctic during ATWAICE campaign
- 83 B. Wehner et al.: Vertical distributions of aerosol particles during fall 2021 and spring 2022 in Ny-Ålesund/Svalbard
- 86 F. Senf et al.: Global adjustments to stratospheric smoke injection from the extreme 2019–2020 Australian wildfires
- 90 T. Schaefer et al.: Peroxyl radicals in the atmospheric aqueous phase
- 93 M. B. E. Aiyuk et al.: Modelling of heterogeneous chemistry on dust aerosol particles
- 96 H. Wiedenhaus et al.: Sources of particulate matter identified by labelled species in a chemical transport model and a complementary measurement campaign
- 100 H. Deneke et al.: The Small-Scale Variability of Solar Radiation Campaign – Overview and First Results
- 103 D. Niedermeier et al.: Particle deliquescence in a turbulent humidity field
- 107 O. Valderrama et al.: BASS project: field campaigns
- 110 A. Leon-Marcos et al.: Modeling the emission of marine organic aerosol based on a detailed biogeochemical model output
- 113 S. Gómez Maqueo Anaya et al.: Mineralogy in COSMO5.05-MUSCAT: implications and comparison with in-situ measurements
- 116 B. Gast et al.: Fluorescence lidar at TROPOS – the new MARTHA
- 119 U. Käfer et al.: The Schmücke Cloud Observatory (SCO) and the Center for Cloud Water Chemistry (CCWaC)
- 122 A. Hünerbein et al.: Algorithm development work for EarthCARE
- 126 S. Mertes et al.: Aerosol properties of cloud particle residuals measured during CIRRUS-HL

Table of contents

- 130 A. A. Floutsi et al.: DeLiAn – a new aerosol climatology based on PollyXT lidars
- 134 U. Winkler et al.: Ultra-fine dust pollution from airports in Berlin (ULTRAFLEB) – the results of the stationary UFP measurements
- 137 E. J. dos S. Souza et al.: Assessing Mineral Dust Toxic Potency Using the Oxidative Potential Assays
- 140 M. Weger and B. Heinold: Urban modelling at the grey zone

Appendices

- 145 Publications
 - 145 Publication statistics
 - 145 Publications
- 165 University courses
- 168 Academic degrees
 - 168 Completed academic qualifications 2020/2021
 - 171 Summary of completed academic qualifications
- 171 Awards
- 172 Editorships
- 173 Memberships
- 175 Meetings
- 176 Reviews
- 176 Guest scientists
- 178 Visits of TROPOS scientists
- 179 International and national field campaigns
- 183 Cooperations
 - 183 International cooperations
 - 187 National cooperations
- 190 Boards
 - 190 Boards of trustees
 - 190 Scientific advisory board
 - 191 Members of the TROPOS association
- 192 Organigram

Introduction / Einleitung

Overview / Übersicht



Introduction

The Leibniz Institute for Tropospheric Research e. V. (TROPOS) has been located in the Leipzig Science Park/Permoserstrasse since 1992 in the neighbourhood of the Helmholtz Centre for Environmental Research, the Leibniz Institute for Surface Modification and other institutions. Its name identi-



Fig. / Abb. 1: TROPOS main building. / TROPOS-Hauptgebäude.
(Photo: Patric Seifert / TROPOS)

fies it as a member of the Gottfried Wilhelm Leibniz Society.

The institute is funded by the State of Saxony and the Federal Ministry of Education and Research with an annual basic budget of approx. 10.6 million euros, and approx. 13.1 million euros per year in third-party funding.

A total of 207 people are employed at TROPOS (including 53 student/scientific assistants, 3 apprentices), 159 of whom are scientists (as at 31 December 2023). TROPOS was founded to research physical and chemical processes in the polluted troposphere.

TROPOS has developed a clear and globally unique research profile, which today focuses on the



Fig. / Abb. 2: The new TROPOS chemistry laboratory. / Des neue TROPOS-Chemielaborgebäudes. (Photo: Tilo Arnhold / TROPOS)

Einleitung

Im Wissenschaftspark Leipzig/Permoserstraße befindet sich seit 1992 das Leibniz-Institut für Troposphärenforschung e. V. (TROPOS) in Nachbarschaft zum Helmholtz-Zentrum für Umweltforschung, zum Leibniz-Institut für Oberflächenmodifizierung sowie weiteren Einrichtungen. Sein Name weist es als Mitglied der Wissenschaftsgemeinschaft Gottfried Wilhelm Leibniz aus.

Das Institut wird vom Freistaat Sachsen und dem Bundesministerium für Bildung und Forschung mit einem jährlichen Grundetat von ca. 10,6 Millionen Euro gefördert, ca. 13,1 Millionen pro Jahr werden an Drittmitteln eingeworben.

Am TROPOS sind insgesamt 207 Mitarbeitende beschäftigt (inklusive 53 Studentische/Wissenschaftliche Hilfskräfte, 3 Lehrlinge), davon 159 Wissenschaftlerinnen und Wissenschaftler (Stichtag 31.12.2023). Gegründet wurde das TROPOS zur Erforschung physikalischer und chemischer Prozesse in der belasteten Troposphäre.



Fig. / Abb. 3: TROPOS cloud laboratory. / TROPOS-Wolkenlabor.
(Photo: Tilo Arnhold / TROPOS)

Das TROPOS hat ein klares und weltweit einzigartiges Forschungsprofil herausgebildet, in dessen Mittelpunkt heute die physikalischen und chemischen Wechselwirkungen zwischen atmosphärischen Schwebeteilchen (Aerosolpartikeln) und Wolkenpartikeln stehen. Trotz geringster absoluter Mengen sind diese Partikel wesentliche Bestandteile der Atmosphäre, weil sie den Energie-, Wasser- und Spurenstoffhaushalt des Erdsystems beeinflussen. Menschliche Aktivitäten können die Eigenschaften dieser hochdispersen Systeme verändern und damit sowohl direkt als auch indirekt auf den Menschen in den Bereichen Gesundheit und Klima zurückwirken.

Zur Klärung dieser wichtigen Beziehungen müssen die physiko-chemischen Prozesse von Aerosol- und Wolkenbildung und die Wirkungen auf

Introduction / Einleitung



Fig. / Abb. 4: The GoSouth team. From left to right / Das GoSouth-Team. Von links nach rechts: Silvia Henning (TROPOS), Sebastian Düsing (TROPOS), Juliane Kalla (Universität Hannover), Julian Hofer (TROPOS), Thomas Conrath (TROPOS), Frank Stratmann (TROPOS), Joel Rindelaub (University of Auckland) & Guy Coulson (NIWA). (Photo: Lana Young / NIWA)

physical and chemical interactions between atmospheric small airborne particles (aerosol particles) and cloud particles. Despite the smallest absolute quantities, these particles are essential components of the atmosphere because they influence the energy, water and trace substance balance of the earth system. Human activities can change the properties of these highly dispersed systems and thus have both a direct and indirect impact on human health and climate.

In order to clarify these strong connections, the physico-chemical processes of aerosol and cloud formation and the effects on health and climate still need to be investigated to a considerable extent. Particular challenges here are the analysis of the smallest quantities of substances involved and the complex behavior of atmospheric multiphase systems, whose individual processes in the atmosphere cannot be clearly observed separately. In the current state of knowledge on global climate change, this complexity is reflected in the much greater uncertainties in all published figures on aerosol and cloud effects compared to the state of knowledge on the effects of greenhouse gases.

In order to achieve a significant increase in the understanding of tropospheric multiphase processes and to improve their application to the prediction of the consequences of human intervention, TROPOS develops and carries out coordinated field, laboratory and modelling studies to investigate aerosol particles and clouds. The long-term measurements initiated by TROPOS are increasingly making it possible to record trends in regional and large-scale aerosol distribution and their impact on climate and health. The ACTRIS-D research infrastructure coordinated by TROPOS, which is part of the national roadmap and Germany's contribution to the European ACTRIS

Gesundheit und Klima noch zu einem erheblichen Teil erforscht werden. Besondere Herausforderungen hierbei sind die Analyse der beteiligten kleinsten Stoffmengen und das komplexe Verhalten atmosphärischer Mehrphasensysteme, deren Einzelprozesse in der Atmosphäre nicht klar getrennt beobachtet werden können. Beim gegenwärtigen Stand des Wissens zum globalen Klimawandel spiegelt sich diese Komplexität in den sehr viel größeren Unsicherheiten in allen zu Aerosol- und Wolkenwirkung veröffentlichten Zahlen im Vergleich zum Kenntnisstand der Auswirkungen von Treibhausgasen wider.

Um einen signifikanten Zuwachs im Prozessverständnis troposphärischer Mehrphasenprozesse zu erreichen und dessen Anwendung auf die Vorhersage der Folgen menschlicher Eingriffe zu verbessern, werden am TROPOS aufeinander abgestimmte Feld-, Labor- und Modellstudien zur Untersuchung von Aerosolpartikeln und Wolken entwickelt und durchgeführt. Die vom TROPOS maßgeblich initiierten Langzeitmessungen erlauben immer mehr auch die Erfassung von Trends in der regionalen und großräumigen Aerosolverteilung und deren Auswirkung auf Klima und Gesundheit. Hier spielt die vom TROPOS koordinierte Forschungsinfrastruktur ACTRIS-D, die Teil der Nationalen Roadmap und Beitrag Deutschlands zum europäischen Roadmap-Programm ACTRIS ist, eine zentrale Rolle und wird die Arbeiten am TROPOS sowie nationale und internationale Kooperationen langfristig und maßgeblich prägen.

Feldexperimente

Die Feldexperimente des Instituts dienen der Aufklärung des atmosphärischen Kreislaufs der



Fig. / Abb. 5: Leipzig meteorologist Dr Martin Radenz from TROPOS lived and worked in the Antarctic for a year and was one of the 10 people who overwintered at Neumayer Station III. / Der Leipziger Meteorologe Dr. Martin Radenz vom TROPOS lebte und arbeitete ein Jahr in der Antarktis und gehörte zu den 10 Personen, die an der Neumayer-Station III überwinterten. (Photo: Ronny Engelmann / TROPOS)

roadmap programme, plays a central role here and will significantly shape the work at TROPOS as well as national and international collaborations in the long term.

Field experiments

The Institute's field experiments serve to elucidate the atmospheric cycle of aerosol and cloud particles and the associated processes. The complexity of the aerosol-cloud system is determined, among other things, by the fact that particles and droplets occur in the atmosphere whose diameters vary by more than six orders of magnitude from the nanometre to the micrometre range. The size range of a few nanometres, which occurs directly after the formation of new particles, has been added to the measurement range of aerosol size distributions at TROPOS in the last two years. In addition, the liquid water droplet and ice crystal forming properties of aerosols interact with a regionally and globally changing Earth system. As a result of the diversity of microphysical, chemical and meteorological processes occurring, there is still a lack of quantitative understanding of the importance of aerosol-cloud interactions in the global climate system.

This uncertainty begins with the particle sources, which are also the subject of research at TROPOS. The combustion of fossil and renewable fuels for energy production and transport is a significant source of aerosols. Measurements taken by the institute at many urban measuring points and continental background stations show that the emissions of particles and their precursors are followed by a variety of physical and chemical transformations that need to



Fig. / Abb. 6: Inauguration of the new TROPOS remote sensing station on the roof of the Ocean Science Centre Mindelo (OSCM) with the Presidents of Germany and Cabo Verde. / Einweihung der neuen Fernerkundungstation des TROPOS auf dem Dach des Ocean Science Centre Mindelo (OSCM) mit den Präsidenten von Deutschland und Cabo Verde. (Photo: Edson Silva Delgado / GEOMAR)



Fig. / Abb. 7: Dr Khanneh Wadinga Fomba (TROPOS) explains the dust measurements at Cabo Verde Atmospheric Observatory (CVAO) to Frank-Walter Steinmeier (German Federal President) and José Maria Neves (President of the Republic of Cabo Verde) (from left to right). / Dr. Khanneh Wadinga Fomba (TROPOS) erklärt Frank-Walter Steinmeier (Bundespräsident) und José Maria Neves (Präsident der Republik Cabo Verde) die Staubmessungen am Cabo Verde Atmospheric Observatory (CVAO) (von links nach rechts). (Photo: Bundesregierung / Bergmann)

Aerosol- und Wolkenpartikel und der damit verbundenen Prozesse. Die Komplexität des Aerosol-Wolken-Systems wird dabei unter anderem dadurch bestimmt, dass in der Atmosphäre Partikel und Tropfen auftreten, deren Durchmesser sich vom Nano- bis zum Mikrometerbereich um mehr als sechs Größenordnungen unterscheiden. Dabei ist der Größenbereich weniger Nanometer, wie er direkt nach einer Neubildung von Partikeln auftritt, in den letzten zwei Jahren am TROPOS in den Messbereich von Aerosol-Größenverteilungen dazu gekommen. Außerdem stehen die Flüssigwassertröpfchen- und Eiskristall-bildenden Eigenschaften der Aerosole in Wechselwirkung mit einem sich regional und global ändernden Erdsystem. Als Folge der Vielfalt der auftretenden mikrophysikalischen, chemischen und meteorologischen Prozesse mangelt es nach wie vor an quantitativem Verständnis hinsichtlich der Bedeutung von Aerosol-Wolken-Wechselwirkungen im globalen Klimasystem.

Diese Unsicherheit beginnt schon bei den Partikelquellen, die ebenfalls Forschungsgegenstand am TROPOS sind. Die Verbrennung fossiler und nachwachsender Brennstoffe zur Energieerzeugung und im Verkehr ist eine maßgebliche Aerosolquelle. Messungen des Instituts an vielen urbanen Messstellen und kontinentalen Hintergrundstationen zeigen, dass den Emissionen von Partikeln und deren Vorläufern vielfältige physikalische und chemische Umwandlungen folgen, die mit hoher zeitlicher Auflösung analysiert werden müssen, um die beteiligten Prozesse aufzuklären.

Der Ballungsraum Leipzig mit der Hintergrundstation Melpitz ist immer wieder im Zentrum von

Introduction / Einleitung



Fig. / Abb. 8: View of Mindelo (Cabo Verde) from the observatory - with (01.02.2022) and without (07.02.2022) Saharan dust. / Blick vom Observatorium auf Mindelo (Cabo Verde) – mit (01.02.2022) und ohne (07.02.2022) Saharastaub. (Photo: Christian Nehls / Forschungszentrum Borstel)

be analysed with high temporal resolution in order to elucidate the processes involved.

The Leipzig conurbation with the Melpitz background station is repeatedly at the centre of studies on air pollution with a focus on particles, which are often integrated into national and international collaborations. Despite very far-reaching legal regulations, air pollution still exists in Germany and Europe with its consequences for the morbidity and mortality of the population. The Melpitz research station is increasingly being used for focused measurement campaigns, also to combine physico-chemical high-resolution in-situ characterisation on the ground with in-situ and remote sensing measurements of the entire column and the associated modelling.

The strongest polluted regions over North America, Europe, Asia with priority on China, Africa,

Untersuchungen zur Luftverschmutzung mit dem Schwerpunkt auf Partikeln, die oft in nationale und internationale Kooperationen eingebunden sind. Trotz sehr weitgehender gesetzlicher Regelungen existiert in Deutschland und Europa immer noch Luftverschmutzung mit ihren Folgen für Morbidität und Mortalität der Bevölkerung. Die Forschungsstation Melpitz wird zunehmend für fokussierte Messkampagnen genutzt, auch um die physikalisch-chemisch hoch aufgelöste In-situ-Charakterisierung am Boden mit In-situ- und Fernerkundungsmessungen der gesamten Säule und auch den zugehörigen Modellierungen zu kombinieren.

Die am stärksten belasteten Regionen über Nordamerika, Europa, Asien mit dem Schwerpunkt China, Afrika und über dem indischen Subkontinent und Südamerika sind bei weitem noch nicht hinreichend bezüglich ihrer Aerosolbelastungen und den daraus resultierenden Klimawirkungen untersucht. Auf diese Regionen konzentrieren sich daher in internationaler Zusammenarbeit die Feldexperimente des TROPOS, u. a. in Form von Messkampagnen und Langzeitmessungen in Asien, Südamerika und der Mittelmeerregion. Hier kommt auch die Untersuchung der zunehmenden großen Waldbrände eine wachsende Bedeutung zu. Aber auch die maritime Troposphäre über dem sauberen südlichen und dem belasteten nördlichen Atlantik wird langfristig vermessen, um Aerosol-Wolken-Wechselwirkungen besser zu verstehen.

Studien zum Mineralstaub und zu marinen Aerosolpartikeln und deren Wirkungen auf den Strahlungshaushalt, die Wolkenbildung und die atmosphärische Eisbildung bleiben ein Kernbestandteil der Arbeiten am TROPOS. Durch die Nutzung eines kommerziellen Verkehrsflugzeuges der Lufthansa werden im Rahmen der Europäischen Forschungsinfrastruktur

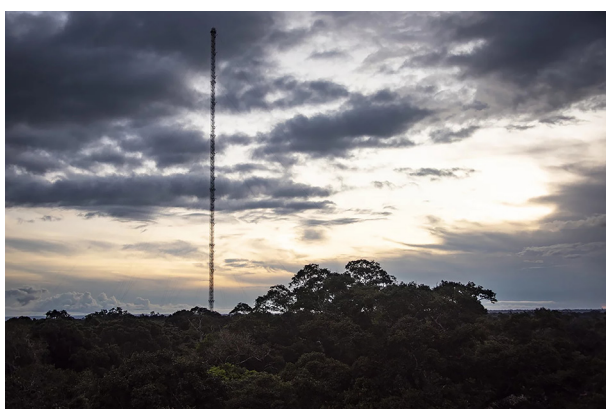


Fig. / Abb. 9: Clouds over the Amazon. Measurements at the Amazon Tall Tower Observatory (ATTO) in the central Amazon revealed that up to two thirds of the soot comes from Africa. / Messungen am Amazon Tall Tower Observatory (ATTO) im zentralen Amazonas enthielten, dass bis zu zwei Dritteln des Rußes aus Afrika stammt. (Photo: Dom Jack / Max Planck Institute for Chemistry)



Fig. / Abb. 10: BSOA measurements on the MyDiv area in Bad Lauchstädt in September 2022. / BSOA-Messungen auf der MyDiv-Fläche in Bad Lauchstädt im September 2022. (Photo: Loreen Alshaabi / TROPOS)

the Indian subcontinent, and South America are far from being sufficiently characterized in terms of aerosol burdens and ensuing climate effects. TROPOS field experiments, including measurement campaigns and long-term measurements in Asia, South America and the Mediterranean region, are therefore focused on these regions in international cooperation. The investigation of the increasing number of large forest fires is also becoming increasingly important here. The maritime troposphere over the clean southern and polluted northern Atlantic is also being observed over the long term in order to better understand aerosol-cloud interactions.

Studies on mineral dust and marine aerosol particles and their effects on the radiation budget, cloud formation and atmospheric ice formation remain a core component of the work at TROPOS. By using a Lufthansa commercial airliner, aerosol distributions in the upper troposphere are also measured and analysed on regularly flown intercontinental routes as part of the European research infrastructure IAGOS. TROPOS is a consortium partner in the operation of the German research aircraft HALO and is regularly involved in flight campaigns. The studies on mineral dust are integrated into increasing co-operation with countries on the African continent, such as Cape Verde, Morocco, Nigeria and Namibia.

Various ground-based remote sensing methods are developed and coupled at TROPOS in order to obtain a synergistic picture of the vertical distribution of aerosols and hydrometeors and their processing. The institute is now a leader in the development and application of international lidar networks for recording the four-dimensional aerosol distribution. The remote sensing methods developed at TROPOS are also used in international satellite programmes of various space agencies.

IAGOS auch Aerosolverteilungen in der oberen Troposphäre auf regelmäßig beflogenen interkontinentalen Routen gemessen und analysiert. TROPOS ist Konsortialpartner im Betrieb des deutschen Forschungsflugzeugs HALO und regelmäßig an Flugkampagnen beteiligt. Die Untersuchungen zum Mineralstaub sind eingebunden in zunehmende Kooperationen mit Ländern des afrikanischen Kontinents wie derzeit die Kapverden, Marokko, Nigeria und Namibia.

Am TROPOS werden verschiedene bodengebundene Fernerkundungsverfahren entwickelt und gekoppelt, um so zu einem synergetischen Bild der vertikalen Verteilung von Aerosolen und Hydrometeoren sowie deren Prozessierung zu gelangen. Mittlerweile ist das Institut federführend in der Entwicklung und Anwendung internationaler Lidarnetzwerke zur Erfassung der vierdimensionalen Aerosolverteilung. Die



Fig. / Abb. 11: The PyrNet devices from TROPOS measured global radiation, temperature and humidity during the S2VSR campaign in the fields of Oklahoma. / Die PyrNet-Geräte vom TROPOS haben bei der Kampagne S2VSR in den Feldern Oklahomas Globalstrahlung, Temperatur und Luftfeuchtigkeit gemessen. (Photo: Oscar Ritter / TROPOS)

Introduction / Einleitung



Fig. / Abb. 12: ACTRIS campaign at the Sonnblick Observatory - Austria's highest meteorological observation station. / ACTRIS-Kampagne am Observatorium Sonnblick - Österreichs höchstelegene meteorologische Beobachtungsstation. (Photo: Uwe Käfer / TROPOS)

On smaller scales, investigations into particle formation and interaction between aerosol particles and clouds and the influence of turbulent mixing processes on cloud development are carried out using airborne measuring platforms. In addition, mountain stations are used for process studies dedicated to understanding individual processes such as the formation of new particles, the physico-chemical changes in aerosol particles during cloud passage and the influence of aerosol particles on the development and freezing of clouds.

TROPOS is significantly involved in regional, national and European in-situ measurement networks for the local recording of atmospheric aerosol and cloud cover. As part of the WMO's Global Atmospheric Watch (GAW) programme, the institute operates the World Calibration Centre for Physical Aerosol Measurements (WCCAP) with the aim of quality assurance of in-situ measurements at national and international measuring stations.

TROPOS continues to play a leading role in the development and operation of the networked European and national research infrastructure for recording aerosols, clouds and trace gases (ACTRIS) in order to investigate and understand the processes of short-lived climate components on all relevant scales.

Field experiments are supported and extended by analyses based on meteorological satellite data. In particular, satellite products are used to analyse the spatiotemporal development of clouds and their radiative forcing, as well as the transport paths of aerosols.

am TROPOS entwickelten Fernerkundungsverfahren finden auch Anwendung in internationalen Satellitenprogrammen diverser Weltraumbehörden.

Auf kleineren Skalen werden Untersuchungen zur Partikelbildung und Wechselwirkung zwischen Aerosolpartikeln und Wolken und der Einfluss turbulenter Mischungsprozesse auf die Wolkenentwicklung mit Hilfe luftgestützter Messplattformen durchgeführt. Zusätzlich werden Bergstationen zu Prozessstudien genutzt, die sich dem Verständnis von Einzelprozessen, wie der Partikelneubildung, der physiko-chemischen Veränderung der Aerosolpartikel beim Wolkendurchgang und dem Einfluss von Aerosolpartikeln auf die Entwicklung und das Gefrieren von Wolken widmen.

TROPOS ist maßgeblich an regionalen, nationalen und Europäischen In-situ-Messnetzen zur lokalen Erfassung des atmosphärischen Aerosols und der Bewölkung beteiligt. Das Institut betreibt im Rahmen des Global Atmospheric Watch (GAW) Programms der WMO das Weltkalibrierzentrum für physikalische Aerosolmessungen (WCCAP) mit dem Ziel der Qualitätssicherung von In-situ-Messungen an nationalen und internationalen Messstationen.

TROPOS ist weiterhin federführend an der Entwicklung und dem Betrieb der vernetzten europäischen und nationalen Forschungsinfrastruktur zur Erfassung von Aerosolen, Wolken und Spurengasen (ACTRIS) beteiligt, um die Prozesse der kurzlebigen Klimakomponenten auf allen relevanten Skalen zu untersuchen und zu verstehen.

Feldexperimente werden durch Analysen, basierend auf meteorologischen Satellitendaten, unterstützt und erweitert. Insbesondere werden mit



Fig. / Abb. 13: Tethered balloon BELUGA in Ny-Ålesund on Svalbard during the international HALO-(AC)3 research campaign to study changes in air masses in the Arctic. / BELUGA-Fesselballon in Ny-Ålesund auf Svalbard während der Kampagne HALO-(AC)3 zur Untersuchung von Luftmassen-Wechsel in der Arktis. (Photo: Holger Siebert / TROPOS)

Laboratory experiments

Measurement technology

Numerous measurement methods are being developed in laboratory experiments that are used for particle characterisation in ground-based and airborne field measurement campaigns. This work includes, for example, the further development of aerosol size spectrometers and collection systems for the physical and chemical characterisation of cloud droplets and the interstitial aerosol, i.e. those aerosol particles that are suspended in the gas phase within clouds in addition to the cloud particles themselves.

Optical measurement methods are developed and applied to determine the extinction coefficient of particles. Multi-wavelength lidars, a fluorescence lidar and a novel coupled wind and aerosol lidar are being further developed in the laboratory and used in the field to measure aerosol properties, aerosol fluxes and meteorological parameters such as temperature, humidity and wind. The proportions of biogenic and mineral aerosol components in aerosol samples are determined by spectral absorption measurements.

Process analyses

The activation of cloud droplets and heterogeneous ice formation under realistic turbulent environmental conditions are being investigated at the LACIS-T wind tunnel. The objectives of these investigations are to gain a better understanding of the process at a fundamental level, to identify critical and controlling parameters and to develop suitable



Fig. / Abb. 14: Sampling of the surface film by inflatable boat from the Spanish research vessel B.I.O Hespérides (A33) 2023 during the PolarChange campaign in the Antarctic. / Probenahme vom Oberflächenfilm per Schlauchboot des Spanischen Forschungsschiffes B.I.O Hespérides (A33) 2023 während der Kampagne PolarChange in der Antarktis. (Photo: Christina Breitenstein / TROPOS)



Fig. / Abb. 15: Measurements of ultrafine particulate matter (UFP) in the area around BER Airport. Following on from Berlin, TROPOS is now also analysing UFP pollution in the around the Frankfurt Airport. / Messungen von Ultrafeinstaub (UFP) in der Nähe des Flughafens BER. Nach Berlin untersucht TROPOS jetzt auch die Belastung mit UFP im Umfeld des Flughafens Frankfurt/Main. (Photo: Ulf Winkler / TROPOS)

Satellitenprodukten die raumzeitliche Entwicklung von Wolken und deren Strahlungsantrieb untersucht, ebenso wie die Transportwege von Aerosolen.

Laborexperimente

Messtechnik

In Laborexperimenten werden zahlreiche Messmethoden entwickelt, die zur Partikelcharakterisierung in boden- und luftgestützten Feldmesskampagnen eingesetzt werden. Diese Arbeiten beinhalten z. B. die Weiterentwicklung von Aerosolgrößenspektrometern sowie Sammelsysteme zur physikalischen und chemischen Charakterisierung von Wolkentröpfchen und dem interstitiellen Aerosol, also denjenigen Aerosolpartikeln, die innerhalb von Wolken neben den Wolkenpartikeln selbst in der Gasphase suspendiert sind.

Optische Messmethoden werden zur Bestimmung des Extinktionskoeffizienten von Partikeln entwickelt und angewendet. Mehrwellenlängenlidare, ein Fluoreszenzlidar und ein neuartiges gekoppeltes Wind- und Aerosollidar werden zur Messung von Aerosoleigenschaften, Aerosolflüssen und meteorologischen Parametern wie Temperatur, Feuchte und Wind im Labor weiterentwickelt und im Feld eingesetzt. Die Anteile biogener und mineralischer Aerosolkomponenten in Aerosolproben werden durch spektrale Absorptionsmessungen bestimmt.

Prozessuntersuchungen

Am Feuchtluftwindkanal LACIS-T werden die Aktivierung von Wolkentröpfchen und die heterogene

Introduction / Einleitung

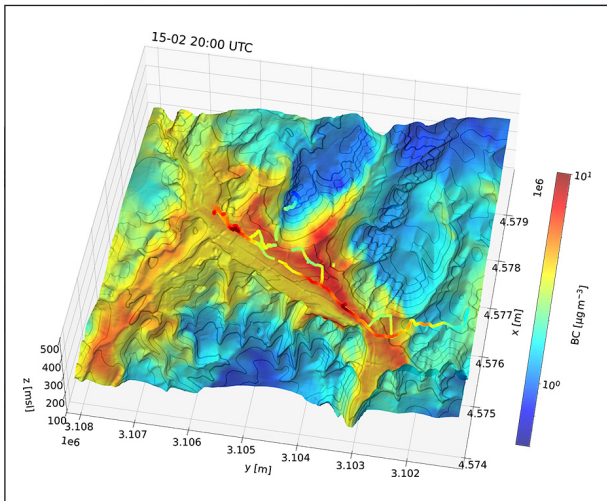


Fig. / Abb. 16: Spatial distribution of soot (black carbon, BC) in the Döhlen Basin, a side valley of the Dresden Elbe valley, in which the town of Freital is located. The concentration was computed with ICON-MUSCAT at 65-m grid spacing for 15 February 2024. In addition, lines show the concentrations of BC actually measured with two backpacks. / Räumliche Verteilung von Ruß (Black Carbon, BC) im Döhlen Becken, einem Seitental des Dresdner Elbtals, in dem die Stadt Freital liegt. Die Konzentration wurde mit ICON-MUSCAT bei 65- Gitterweite für den 15. Februar 2024 gerechnet. Darüber hinaus zeigen Linien die tatsächlich mit zwei Rucksäcken gemessenen Konzentrationen von BC.

parameterisations for describing droplet and ice formation in dynamic models.

Gas phase reactions of various radicals are investigated in flow reactors. The interactions of trace gases with particles and oxidative conditions are the working topic of the ACD-C aerosol chamber. These processes are of interest for ozone and particle formation caused by anthropogenic or biogenic volatile hydrocarbons. The particles produced are also investigated with regard to their moisture growth and activation behaviour.

At ACD-C, phase transfer parameters for trace gases and radicals are systematically analysed. The determination of phase transfer parameters and reactive uptake coefficients is being extended to chemical species and complex surfaces that have not yet been analysed.

In the field of liquid phase mechanisms, reactions of predominantly radical oxidants are investigated using time-resolved optical detection techniques. These reactions take place in the droplets of clouds, rain and fog as well as in aqueous aerosol particles. In order to understand the oxidation of organic trace gases in the tropospheric multiphase system, a large number of reactions of various radicals and reactions of halogen-containing oxidants are investigated. The latter species are of interest in the release of halogen compounds from marine sea salt particles, so-called halogen activation. One current research complex is

Eisbildung unter realitätsnahen turbulenten Umgebungsbedingungen erforscht. Ziele dieser Untersuchungen sind die Erlangung eines besseren Prozessverständnisses auf fundamentaler Ebene, die Identifikation kritischer und kontrollierender Parameter und die Entwicklung geeigneter Parametrisierungen zur Beschreibung von Tröpfchen- und Eisbildung in dynamischen Modellen.

Gasphasenreaktionen verschiedener Radikale werden in Strömungsreaktoren untersucht. Die Wechselwirkungen von Spurengasen mit Partikeln und oxidative Bedingungen sind das Arbeitsthema der Aerosolkammer ACD-C. Diese Prozesse sind von Interesse für die Ozon- und Partikelbildung, verursacht durch anthropogene oder biogene flüchtige Kohlenwasserstoffe. Die erzeugten Partikel werden auch hinsichtlich ihres Feuchtwachstums- und Aktivierungsverhaltens untersucht.

An ACD-C werden systematisch Untersuchungen bzgl. der Phasentransferparameter für Spurengase und Radikale durchgeführt. Die Bestimmung von Phasentransferparametern und reaktiven Aufnahmekoeffizienten wird dabei auf bisher nicht betrachtete chemische Spezies und komplexe Oberflächen ausgeweitet.

Im Bereich von Flüssigphasenmechanismen werden Reaktionen von vorwiegend radikalischen Oxidantien mit zeitaufgelösten optischen Nachweistechniken untersucht. Diese Reaktionen laufen in den Tröpfchen von Wolken, Regen und Nebel sowie in wässrigen Aerosolpartikeln ab. Hier werden zum Verständnis der Oxidation organischer Spurengase im troposphärischen Mehrphasensystem eine Vielzahl von Reaktionen verschiedener Radikale sowie Reaktionen von halogenhaltigen Oxidantien untersucht. Letztere Spezies sind von Interesse bei der Freisetzung von Halogenverbindungen aus maritimen Seesalzpartikeln, der so genannten Halogenaktivierung. Ein aktueller Forschungskomplex ist die Radikal- und Oxidantienbildung in der sog. Fenton-Reaktion zwischen Fe(II) und H₂O₂.

Das Flüssigphasen-Laserlabor zur Untersuchung der troposphärischen Flüssigphasenprozesse ist ein wichtiges Zentrum dieses Forschungsbereiches. Aus den Prozessuntersuchungen resultieren Verbesserungen chemischer Mechanismen, die in der Modellierung mit dem eigenen Mechanismus CAPRAM zunächst in Boxmodellen und dann zunehmend auch in höherskaligen Modellen angewendet werden. In der analytischen Messtechnik werden in Laborexperimenten Verfahren zur besseren chemischen Charakterisierung der organischen Bestandteile von Aerosolpartikeln entwickelt und getestet. Diese Techniken beruhen zumeist auf massenspektrometrischen Verfahren, die in verschiedenen Kopplungstechniken

the formation of radicals and oxidants in the so-called Fenton reaction between Fe(II) and H₂O₂.

The liquid-phase laser laboratory for investigating tropospheric liquid-phase processes is an important centre of this research area. The process investigations result in improvements to chemical mechanisms, which are used in modelling with our own CAPRAM mechanism, initially in box models and then increasingly in higher-scale models. In analytical measurement technology, methods for better chemical characterisation of the organic components of aerosol particles are developed and tested in laboratory experiments. These techniques are mostly based on mass spectrometric methods, which are used in various coupling techniques. In the area of sampling techniques, there is also close cooperation with the "Atmospheric Microphysics" department for the development of targeted separation of particles of specific sizes and their chemical analysis, as well as for the development of inlet systems and reactors.

Further calibration centres for quality assurance of chemical aerosol characterisation, the analysis of multiphase processes and cloud water (OGTAC-CC and CCWAC) are being established as part of ACTRIS.

Modelling

To describe the complex atmospheric processes, modelling systems of different dimensions, complexity and scales are developed, tested and applied, also in combination with data from field measurements and

eingesetzt werden. Im Bereich der Probenahmetechniken gibt es auch hier eine enge Kooperation mit der Abteilung „Atmosphärische Mikrophysik“ zur Entwicklung einer gezielten Abscheidung von Partikeln bestimmter Größe und deren chemischer Analyse aber auch zur Entwicklung von Einlasssystemen und Reaktoren.

Im Rahmen von ACTRIS entstehen weitere Kalibrierzentren zur Qualitätssicherung chemischer Aerosolcharakterisierung, der Analytik von Multiphasenprozessen und Wolkenwasser (OGTAC-CC und CCWAC)

Modellierung

Zur Beschreibung der komplexen atmosphärischen Vorgänge werden Modellsysteme verschiedener Dimension, Komplexität und Skalenbereiche entwickelt, überprüft und angewendet, auch in Kombination mit Daten aus Feldmessungen und Fernerkundung. Die Modelluntersuchungen sollen der Beschreibung von Kreisläufen, Wechselwirkungen und Phasenübergängen zwischen Aerosolpartikeln, Gasen und Wolken, sowie der direkten und indirekten Einflüsse von Aerosolpartikeln auf den Strahlungshaushalt dienen.

Regionale Chemie-Transportmodellierung wird durch das am TROPOS entwickelte 3D-Modellsystem COSMO-MUSCAT realisiert. Seine Eignung zur Simulation des Ausbreitungsverhaltens von Partikeln und Gasen auf regionaler Skala wurde in mehreren internationalen Modellvergleichen und bei der Bearbeitung

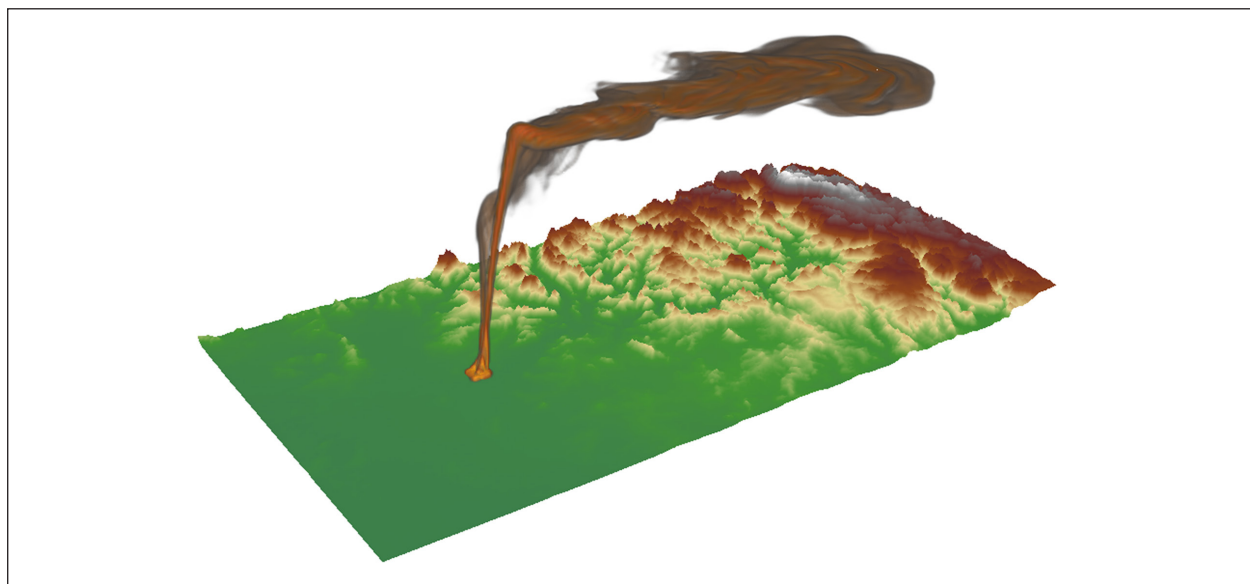


Fig. / Abb. 17: ICON simulation of the extreme Australian wildfire event around New Year's Eve 2019/2020. Shown here is a 3D rendering of tracer concentrations within the triggered Pyrocumulonimbus cloud./ ICON-Simulation des extremen australischen Waldbrandereignisses um den Jahreswechsel 2019/2020. Abgebildet ist eine 3D-Darstellung der Tracer-Konzentrationen in der durch die Feuer ausgelösten Pyrocumulonimbus-Wolke. (Graphic: Jason Müller / TROPOS)

Introduction / Einleitung

remote sensing. The modelling studies are intended to describe the cycles, interactions and phase transitions between aerosol particles, gases and clouds, as well as the direct and indirect influences of aerosol particles on the radiation budget.

Regional chemical transport modelling is implemented using the 3D model system COSMO-MUSCAT developed at TROPOS. Its suitability for simulating the dispersion behaviour of particles and gases on a regional scale has been demonstrated in several international model comparisons and in the processing of air quality issues. The dynamics of primary and secondary aerosol particles and their interaction with radiation and clouds are being simulated in several projects. An "urbanised" version of COSMO-MUSCAT, which uses a horizontal grid resolution of up to a few 100 m, has also been developed for further applications, in particular air quality studies. By transferring the results of the higher-resolution model studies into the aerosol scheme of the global aerosol climate model ECHAM-HAM or ICON-HAM, the model parameterisation of aerosol processes developed on high-resolution scales can be directly taken into account in climate studies. One research focus is the investigation of control factors and effects of natural aerosols such as mineral dust, marine aerosol, smoke particles from forest fires or organic aerosol from plant emissions.

In addition, one- and two-dimensional process models have been and are being further developed. SPECS (SPECtral bin cloud microphysicS) is used to describe cloud processes. It allows an explicit and very precise calculation of the processes condensation, collision or freezing, and can be used as a box model as well as for case studies coupled with the regional COSMO model. One focus for the investigation of aerosol-cloud processes is the investigation of the role of dust particles for heterogeneous ice formation processes in clouds. SPACCIM (SPectral Aerosol Cloud Chemistry Interaction Model) is a package model for the coupled size-resolved description of microphysics and multiphase chemistry. Process modelling is carried out in conjunction with field studies and laboratory experiments, often mediated by CAPRAM.

In addition to dynamic/microphysical/chemical modelling, radiative transfer models are developed and operated at TROPOS in order to design remote sensing algorithms and to better understand the solar and thermal radiative effect of aerosols and clouds.

von Fragen zur Luftqualität gezeigt. In mehreren Projekten wird die Dynamik primärer und sekundärer Aerosolpartikel simuliert und deren Wechselwirkung mit Strahlung und Wolken untersucht. Für weitere Anwendungsmöglichkeiten insbesondere Luftqualitätsstudien wurde zusätzlich eine „urbanisierte“ Version von COSMO-MUSCAT entwickelt, die eine horizontale Gitterauflösung bis zu wenigen 100 m nutzt. Durch Übertragung der Ergebnisse der höheraufgelösten Modellstudien in das Aerosolschema des globalen Aerosol-Klimamodells ECHAM-HAM bzw. ICON-HAM wird eine direkte Berücksichtigung der auf hochaufgelösten Skalen entwickelten Modellparametrisierung von Aerosolprozessen in Klimastudien möglich. Ein Forschungsschwerpunkt ist die Untersuchung von Kontrollfaktoren und Effekten natürlicher Aerosole wie Mineralstaub, marines Aerosol, Rauchpartikel aus Waldbränden oder organischem Aerosol aus Pflanzenemissionen.

Daneben wurden und werden ein- und zweidimensionale Prozessmodelle weiterentwickelt. SPECS (SPECtral bin cloud microphysicS) dient zur Beschreibung von Wolkenprozessen. Es erlaubt eine explizite und sehr genaue Berechnung der Prozesse Kondensation, Kollision oder Gefrieren, und kann als Boxmodell sowie auch für Fallstudien gekoppelt mit dem regionalen COSMO-Modell verwendet werden. Ein Schwerpunkt für die Untersuchung von Aerosol-Wolkenprozessen ist die Untersuchung der Rolle von Staubpartikeln für heterogene Eisbildungsprozesse in Wolken. SPACCIM (SPectral Aerosol Cloud Chemistry Interaction Model) ist ein Paketmodell zur gekoppelten großenaufgelösten Beschreibung von Mikrophysik und Mehrphasenchemie. Prozessmodellierungen werden im Zusammenspiel mit Feldstudien sowie mit Laborexperimenten, oft vermittelt über CAPRAM, durchgeführt.

Neben der dynamischen/mikrophysikalischen/chemischen Modellierung werden am TROPOS auch Strahlungstransportmodelle entwickelt und betrieben, um Fernerkundungsalgorithmen zu entwerfen und den solaren und thermischen Strahlungseffekt von Aerosolen und Wolken besser zu verstehen.

Overview of the individual contributions

This biennial report presents selected scientific TROPOS work from 2022 to 2023 in four long and 20 short articles. As in previous years, a broad spectrum of field, laboratory and modelling work is presented, which investigates both fundamental and novel physical and chemical mechanisms in aerosols and their interactions with clouds and the climate system, but also opens up new fields such as the question of the criteria for the existence of a cloud, the establishment of new research infrastructures or the development of new techniques for remote sensing of biogenic particles. The Institute's strategy of carrying out long-term or even permanent atmospheric observations as part of ACTRIS and including them in modeling is increasingly enabling research on trends and global patterns of the coupled aerosol-cloud system and their influence on health and climate, such as trends in regional ozone concentrations or the global effects of major forest fires.

Long articles

Tropospheric ozone contributes to both air pollution and global warming. A long-term study by **D. van Pinxteren et al.** of the last 20 years in the region of Saxony together with the Saxon State Environmental Agency (LfULG) shows that ozone concentrations are still too high and are even increasing slightly despite decreasing nitrogen oxide concentrations. A multivariate analysis of the influencing factors indicates that volatile organic hydrocarbons (VOCs) as important ozone precursor compounds can explain the stagnating trend and must therefore be integrated into future long-term observations. Implementation plans are being developed together with the LfULG.

Trace gases also play a fundamental role in aerosol formation and therefore also indirectly in cloud formation, weather and climate. This process chain is still insufficiently understood in the southern hemisphere, which is strongly characterised by maritime influences and is still subject to low levels of anthropogenic pollution. TROPOS has carried out and is planning a series of measurement campaigns on this problem area, some lasting several years. **Stratmann et al.** present goSouth, a first field campaign in southern New Zealand, which was carried out together with New Zealand partners, in particular on the coupling of ground-based in-situ and remote sensing measurements and process-resolved modelling. Here, the importance of precursor gases and their sources for understanding aerosol properties was also emphasised. For the first time, the

Übersicht der Einzelbeiträge

Der vorliegende Zweijahresbericht stellt in vier Lang- und 20 Kurzbeiträgen ausgewählte Arbeiten des TROPOS im Zeitraum 2022 bis 2023 vor. Wie auch in den Vorjahren liegt ein breites Spektrum von Feld-, Labor-, und Modellierungsarbeiten vor, die sowohl fundamentale und neuartige physikalische und chemische Mechanismen im Aerosol und deren Wechselwirkungen mit Wolken und Klimasystem untersuchen, aber auch neue Felder erschließen wie etwa die Fragestellung nach den Kriterien für das Vorhandensein einer Wolke, der Aufbau neuer Forschungsinfrastrukturen oder die Entwicklung neuer Techniken zur Fernerkundung biogener Partikel. Die Strategie des Instituts, im Rahmen von ACTRIS langfristig angelegte oder gar dauerhafte Atmosphärenbeobachtungen zu betreiben und im Modell aufzunehmen, ermöglicht zunehmend die Erforschung von Trends und globalen Mustern des gekoppelten Systems Aerosol-Wolke und deren Einfluss auf Gesundheit und Klima wie etwa Trends in der regionalen Ozonkonzentration oder globale Effekte großer Waldbrandereignisse

Langbeiträge

Troposphärisches Ozon trägt sowohl zur Luftbelastung als auch zur Klimaerwärmung bei. Eine Langzeitstudie von **D. van Pinxteren et al.** für die letzten 20 Jahre für die Region Sachsen gemeinsam mit dem sächsischen Landesumweltamt (LfULG) zeigt, dass die Ozonkonzentrationen weiterhin zu hoch sind und trotz abnehmender Stickoxidkonzentrationen sogar noch leicht zunehmen. Eine multivariate Analyse der Einflussfaktoren weist darauf hin, dass flüchtige organische Kohlenwasserstoffe (VOC) als wichtige Ozonvorläuferverbindungen den stagnierenden Verlauf erklären können und daher in zukünftige Langzeitbeobachtungen integriert werden müssen. Gemeinsam mit dem LfULG werden hierzu Umsetzungspläne entwickelt.

Spurengase spielen auch eine fundamentale Rolle in der Aerosolbildung und damit mittelbar auch für Wolkenbildung, Wetter und Klima. In der stark maritim geprägten und anthropogen noch gering belasteten Südhemisphäre ist diese Prozesskette noch unzureichend verstanden. TROPOS hat zu diesem Problemfeld eine Reihe von teilweise mehrjährigen Messkampagnen durchgeführt und in Planung. Insbesondere zur Kopplung bodengebundener in-situ und Fernerkundungsmessungen und prozessaufgelöster Modellierung stellen Insbesondere zur Kopplung bodengebundener in-situ und

Overview of the individual contributions / Übersicht der Einzelbeiträge

observations point to the forests of the Southern Alps as a source of aerosol precursor gases.

Both the northern and southern hemispheres have been exposed to massive forest fires in recent years. Using long-term measurements of the TROPOS polarisation Raman lidars at various stations, **Ohneiser et al.** were able to analyse the vertical dimensions and life cycles of the smoke aerosol clouds from the forest fires in Canada in 2017, Siberia in 2019, Australia in 2019/2020 and California in 2020. A self-lifting mechanism into the stratosphere due to solar heating, a depletion of stratospheric ozone presumably due to heterogeneous chemical processes on the smoke particles and increased cirrus formation in the troposphere due to sedimented smoke aerosol were identified. This means that forest fires are becoming an increasing threat to our climate system.

While aerosols can be found on all scales of the atmosphere, a distinction is made between cloudy and non-cloudy conditions in the case of hydrometeors, as general experience also suggests. However, it must be borne in mind that the physical decision on the presence of a cloud depends on the sensitivity of the sensors used and the threshold values selected in advance and is therefore not universal. Using a combination of different sensitivities of the usual sensors such as radiometers, lidar and radar, **Hellmuth et al.** at least succeeded in finding a consistent definition of the threshold values for deciding the presence of a cloud.

Short articles

Focal points

To gain a better understanding of the atmospheric state and its role in a changing Earth system, TROPOS is conducting longer measurement campaigns in neuralgic regions of our planet. In addition to the northern hemispheric dust belt from West Africa to Central Asia, the polar regions and the regional and global effects of massive forest fires (as described above) are playing an increasingly important role in the campaign and modelling activities. Increasing emphasis is being placed on long time series and global modelling studies in order to bring our understanding of processes to larger scales.

For the first time, the atmospheric column in the Antarctic was recorded for an entire year. **Radenz et al.** have successfully deployed the mobile OCEANET observatory at the AWI's Neumayer Station III and have already carried out the first aerosol cloud closure studies. In addition, permanent aerosol layers were discovered in the stratosphere, which make up half of the total aerosol volume.

Fernerkundungsmessungen und prozessaufgelöster Modellierung stellen **Stratmann et al.** mit goSouth eine erste Feldkampagne im Süden Neuseelands vor, die gemeinsam mit neuseeländischen Partnern durchgeführt wurde. Auch hier wurde die Bedeutung von Vorläufergasen und deren Quellen für das Verständnis der Aerosoleigenschaften unterstrichen. Die Beobachtungen weisen erstmalig auf die Wälder der südlichen Alpen als Quelle von Aerosolvorläufergasen hin.

Sowohl die Nord- als auch die Südhemisphäre waren in den letzten Jahren massiven Waldbränden ausgesetzt. Mittels Langzeitmessungen der Polarisations-Raman-Lidare des TROPOS an verschiedenen Stationen konnten **Ohneiser et al.** die vertikalen Ausmaße und Lebenszyklen der Rauchaerosolwolken der Waldbrände aus Kanada 2017, Sibirien 2019, Australien 2019/2020 sowie Kalifornien 2020 analysieren. Hierbei konnte ein Selbsthebungsmechanismus in die Stratosphäre durch solare Heizung, ein Abbau des stratosphärischen Ozons vermutlich durch heterogene chemische Prozesse an den Rauchpartikeln sowie eine erhöhte Cirrusbildung in der Troposphäre durch sedimentiertes Rauchaerosol identifiziert werden. Damit kommt Waldbränden eine zunehmend bedrohliche Bedeutung für unser Klimasystem zu.

Während Aerosole auf allen Skalen der Atmosphäre vorzufinden sind, unterscheidet man bei Hydrometeoren zwischen bewölkten und unbewölkten Zuständen, wie die allgemeine Erfahrung auch suggeriert. Dabei muss allerdings mitgedacht werden, dass die physikalische Entscheidung über das Vorhandensein einer Wolke von der Empfindlichkeit der verwendetet Sensorik und vorab gewählten Schwellwerten abhängt und somit nicht universell ist. Mittels einer Kombination unterschiedlicher Empfindlichkeiten der üblichen Sensoren wie Radiometer, Lidar und Radar gelang **Hellmuth et al.** zumindest eine in sich konsistente Definition der Schwellwerte zur Entscheidungsfindung des Vorhandenseins einer Wolke.

Kurzbeiträge

Brennpunkte

Zum besseren Verständnis des atmosphärischen Zustands und dessen Rolle in einem sich wandelnden Erdsystem führt TROPOS längere Messkampagnen an neuralgischen Regionen unseres Planeten durch. Neben dem nordhemisphärischen Staubgürtel von Westafrika bis zu nach Zentralasien spielen hierbei die Polarregionen und die regionalen und globalen Auswirkungen massiver Waldbrände (wie oben bereits beschrieben) eine zunehmende Rolle in den

Overview of the individual contributions / Übersicht der Einzelbeiträge

Following the MOSAiC expedition, which also lasted one year, TROPOS is also participating in trips to the Arctic by the research vessel Polarstern. **Suja et al.** present the results of the ATWAICE project, in which very detailed in-situ aerosol characterisations were combined with measurements of near-surface turbulent fluxes in order to quantify the sedimentation of soot in the polluted Arctic in particular.

In order to investigate aerosol-cloud interactions, such in-situ aerosol measurements should also be carried out in the cloud area. TROPOS uses its BELUGA tethered balloon system for this purpose. **Wehner et al.** report on two three-month measurement campaigns in autumn 2021 and spring 2022 at the research station in Ny Alesund on Spitsbergen. The vertical aerosol profiles reveal the extent to which locally produced aerosol or aerosol transported from afar influences cloud formation for different weather situations, which is also important information for modelling.

The most drastic examples of long-range aerosol transport with global impacts are large volcanic eruptions and extensive forest fires. For the aforementioned extreme forest fires of the 2019-2020 Australian forest fire season ("Black Summer"), **Senf et al.** were able to show using a global aerosol climate model that these cause significant warming of the southern hemispheric stratosphere and associated changes in global circulation patterns. This means that forest fires could play a significant role in future climate scenarios.

Processes

Chemical reactions in the aqueous phase driven by free radicals in aerosols and cloud droplets can contribute significantly to the formation of secondary organic aerosols (SOA). **Schaefer et al.** have successfully determined experimentally and using theoretical chemistry methods the reaction kinetics and mechanisms of organic peroxy radicals. Thereby an important process in SOA formation was identified.

In addition to chemical reactions in particles, heterogeneous processes on particle surfaces play an important role, particularly in the ageing of mineral dust aerosol. **Aiyuk et al.** have extended the CAPRAM multiphase chemistry model to include a module for the consideration of heterogeneous chemistry and applied this to an atmospheric box model. Sensitivity studies now make it possible to determine dominant heterogeneous chemical processes for given environmental conditions.

Four-dimensional atmospheric models cannot explicitly resolve such complex processes, but are able to determine the spatial transport of the aerosol. Using a new approach to consider different emission

Kampagnen- und Modellierungsaktivitäten. Dabei wird verstärkt Wert auf lange Zeitreihen und globale Modellstudien gelegt um unser Prozessverständnis auf größere Skalen zu bringen.

Erstmals wurde für ein gesamtes Jahr die Atmosphärensäule in der Antarktis erfasst. **Radenz et al.** haben hierzu das mobile OCEANET-Observatorium auf der Neumayer-Station III des AWI erfolgreich eingesetzt und bereits erste Aerosol-Wolken Schließungsstudien durchgeführt. Darüber hinaus wurden dauerhafte Aerosolschichten in der Stratosphäre entdeckt, die die Hälfte der gesamten Aerosolmenge ausmachen.

Auch nach der ebenfalls einjährigen MOSAiC-Expedition beteiligt sich TROPOS an Fahrten des Forschungsschiffes Polarstern in die Arktis. **Suja et al.** stellen Ergebnisse des ATWAICE-Projektes vor, bei dem sehr ausführliche in-situ Aerosolcharakterisierungen mit Messungen der bodennahen turbulenten Flüsse kombiniert wurden, um insbesondere die Sedimentation von Ruß in der belasteten Arktis zu quantifizieren.

Zur Untersuchung von Aerosol-Wolken-Wechselwirkungen sollten solche in-situ-Aerosolmessungen auch im Wolkenbereich durchgeführt werden. Hierzu setzt TROPOS sein Fesselballonsystem BELUGA ein. **Wehner et al.** berichten über zwei jeweils dreimonatige Messkampagnen im Herbst 2021 und Frühjahr 2022 an der Forschungsstation in Ny Alesund auf Spitzbergen. Die vertikalen Aerosolprofile verraten, inwieweit lokal produziertes oder aus der Ferne antransportiertes Aerosol die Wolkenbildung für unterschiedliche Wettersituationen beeinflussen, eine auch für Modellierung wichtige Information.

Die drastischsten Beispiele für Ferntransport von Aerosol mit globalen Auswirkungen sind große Vulkanausbrüche und ausgedehnte Waldbrände. Für die bereits erwähnten extremen Waldbrände der australischen Waldbrandsaison 2019-2020 ("Black Summer") konnten **Senf et al.** mittels eines globalen Aerosol-Klimamodells zeigen, dass diese deutliche Erwärmungen der südhemisphärischen Stratosphäre und damit verbundene Änderungen der globalen Zirkulationsmuster verursachen. Damit können Waldbrände in zukünftigen Klimaszenarien eine bedeutende Rolle spielen.

Prozesse

Chemische Reaktionen in der wässrigen Phase, die durch freie Radikale in Aerosolen und Wolkentröpfchen angetrieben werden, können signifikant zur Bildung sekundärer organischer Aerosole (SOA) beitragen. **Schaefer et al.** haben hierzu erfolgreich die Reaktionskinetik und -mechanismen organischer Peroxylradikale experimentell und mit Methoden der

Overview of the individual contributions / Übersicht der Einzelbeiträge

sources and comparing them with measurements, **Wiedenhaus et al.** were able to show that domestic heating has become increasingly important in the distribution of primary aerosol. However, SOA estimates indicate that the models still underestimate wood and coal combustion for the formation of precursor gases.

The spatial distribution of aerosols and clouds in particular significantly determine the radiation budget from the global to the process scale on a few decameters. Using a sensor network of 60 pyranometers, **Deneke et al.** measured the small-scale variability of solar irradiance in a three-month field campaign in the USA. Due to the simultaneous availability of high-resolution geostationary satellite data, case studies are planned that will also be possible over Europe in the future with the Meteosat Third Generation.

The prime example of small-scale and multi-scale processes is the omnipresent turbulence. In particular, microphysical processes for aerosol and cloud formation as well as aerosol-cloud interaction are subject to turbulent environmental conditions. **Niedermeier et al.** show empirically on the turbulent cloud channel LACIS-T and on the example of particle deliquescence (transition from hygroscopic particle to solution droplet) that this is determined not only by the mean ambient conditions, but also by their turbulent variability; an important indication for future parameterisations.

Compartments

It is obvious that the troposphere does not stand alone and is in dialogue with all components of the Earth system, but requires cooperation at many levels. A better understanding of this interdisciplinary significance is part of the long-term strategy of TROPOS. Permanent observations and modelling that captures atmospheric transport processes between land and ocean, targeted campaigns in marine or terrestrial source regions and method developments that identify and quantify biogenic components in the atmosphere, for example, all contribute to this.

TROPOS is a project partner in the DFG research group BASS (Biogeochemical Processes and Air-Sea exchange in the Sea Surface Microlayer) and contributes here with several years of expertise on the role of the sea surface film in ocean-atmosphere coupling. **Valderrama et al.** present how TROPOS in BASS will contribute to the study of the chemical and photochemical transformation of organic material in the surface film.

Sea surface films are sources of marine organic aerosol (MOA) in the troposphere, which contribute significantly to the activation of cloud droplets and ice formation. **Leon-Marcos et al.** combine a

theoretischen Chemie ermittelt und damit einen wichtigen Prozess in der SOA-Bildung ausfindig gemacht.

Neben chemischen Reaktionen in Partikeln spielen heterogene Prozesse an Partikeloberflächen eine wichtige Rolle insbesondere in der Alterung von Mineralstaubaerosol. **Aiyuk et al.** haben hierzu das Multiphasenchemiemodell CAPRAM um ein Modul zur Berücksichtigung heterogener Chemie erweitert und dieses auf ein atmosphärisches Box-Modell angewendet. Sensitivitätsstudien ermöglichen nun die Ermittlung dominanter heterogener chemischer Prozesse für vorgegebene Umgebungsbedingungen.

Vierdimensionale Atmosphärenmodelle können derart komplexe Prozesse nicht explizit auflösen, sind dafür aber in der Lage, räumliche Transporte des Aerosols zu bestimmen. Mit einem neuen Ansatz zur Berücksichtigung verschiedener Emissionsquellen und dem Vergleich zu Messungen konnten **Wiedenhaus et al.** zeigen, dass Hausbrand eine wachsende Bedeutung in der Verteilung des primären Aerosols gewonnen hat. Allerdings weisen Abschätzungen des SOAs darauf hin, dass die Modelle Verbrennung von Holz und Kohle für die Bildung von Vorläufergasen noch unterschätzen.

Die räumliche Verteilung von Aerosolen und insbesondere von Wolken bestimmen maßgeblich den Strahlungshaushalt von der globalen bis zur Prozess-Skala auf wenigen Dekametern. Mit einem Sensor-Metznetz von 60 Pyranometern haben **Deneke et al.** in einer dreimonatigen Feldkampagne in den USA die kleinskalige Variabilität der solaren Einstrahlung vermessen. Durch die gleichzeitige Verfügbarkeit hochauflöster geostationärer Satellitendaten sind hiermit Fallstudien vorgesehen, die in Zukunft auch über Europa mit dem Meteosat Third Generation möglich sein werden.

Das Paradebeispiel für klein- bzw. mehrskalige Prozesse ist die allgegenwärtige Turbulenz. Insbesondere mikrophysikalische Prozesse zu Aerosol- und Wolkenbildung sowie Aerosol-Wolkenwechselwirkung unterliegen den turbulenten Umgebungsbedingungen. **Niedermeier et al.** zeigen empirisch am turbulenten Wolkenkanal LACIS-T und am Beispiel der Partikel-deliqescenz (Übergang vom hygrokopischen Partikel zum Lösungströpfchen), dass diese nicht nur von den mittleren Umgebungsbedingungen, sondern auch von deren turbulenter Variabilität bestimmt wird; ein wichtiger Hinweis für zukünftige Parametrisierungen.

Kompartimente

Das die Troposphäre nicht für sich alleine steht, sondern im Austausch mit allen Komponenten des Erdsystems steht, ist offensichtlich, erfordert aber Kooperationen auf vielen Ebenen.

Overview of the individual contributions / Übersicht der Einzelbeiträge

biogeochemical model for the calculation of MOA precursors in seawater with a physically based model for the emission of MOA into the atmosphere and find good correlations with marine and atmospheric measurements in the Arctic.

The primary emission of aerosol from land surfaces also requires detailed information on the character, the scattering and absorption behaviour of the particles. The mineralogy of the land surface plays an important role, especially for mineral dust as the largest proportion of primary aerosol. **Gómez Maqueo Anaya et al.** show how mineralogically resolved dust distributions can be realised in the model and validated with active remote sensing. Conversely, the mineralogical fingerprint actively remotely sensed via lidar can also be used to identify source regions.

Active lidar remote sensing at TROPOS has developed into a tried and tested method for characterising atmospheric aerosol particles and their cloud and ice nucleation capacity. This characterisation has now significantly improved both the measurement accuracy and the detection of biogenic aerosol by using a spectral channel to measure fluorescence. **Gast et al.** demonstrate the potential of the fluorescence channel using the example of smoke aerosol and were thus able to detect, for example, previously unrecognised cirrus formation from forest fire aerosol; an important step towards understanding biosphere/atmosphere interactions.

Research infrastructures (FIS)

As the coordinating institute of the national roadmap project ACTRIS-D (Aerosol, Cloud and Trace gas Research InfraStructure - Germany), a strong partner in the European ACTRIS network and in space-based earth observation, RIS play a central role at TROPOS in understanding the processes of highly variable short-lived climate components on all scales. To this end, we develop our own RIS and utilise others in cooperation with partner institutions, such as the national research aircraft HALO or the German research vessel fleet (here Polarstern, Meteor, Sonne).

For the long-term and continuous observation and research of aerosol-cloud interactions, the Schmücke Cloud Observatory (SCO) in the Thuringian Forest is currently being set up as a national facility (NF) within the framework of ACTRIS. **Käfer et al.** present the concept of the observatory for the chemical and physical characterisation of air masses during cloud passage and the status of its implementation. The Schmücke Observatory is thematically linked to the ACTRIS Calibration Centre for Cloud Water Chemistry (CCWaC) to establish

Diese disziplinübergreifende Bedeutung besser zu verstehen, ist Teil der langfristigen Strategie des TROPOS. Hierzu tragen dauerhafte Beobachtungen und Modellierungen bei, die atmosphärische Transportprozesse zwischen Land und Ozean einfangen, gezielte Kampagnen in marin oder terrestrisch geprägten Quellregionen sowie Methodenentwicklungen, die z.B. biogene Anteile in der Atmosphäre erkennen und quantifizieren.

TROPOS ist Projektpartner in der DFG-Forschungsgruppe BASS (Biogeochemical Processes and Air-Sea exchange in the Sea Surface Microlayer) und trägt hier mit einer mehrjährigen Expertise zur Rolle des Meeresoberflächenfilms in der Ozean-Atmosphären-Kopplung bei. **Valderrama et al.** stellen vor, wie TROPOS in BASS zur Untersuchung der chemischen und photochemischen Umwandlung von organischem Material im Oberflächenfilm beitragen werden.

Meeresoberflächenfilme sind Quellen des marinen organischen Aerosols (MOA) in der Troposphäre, welche wesentlich zur Aktivierung von Wolkentröpfchen und zur Eisbildung beitragen. **Leon-Marcos et al.** verbinden hierzu ein biogeochemisches Modell zur Berechnung der MOA-Vorläufer im Meerwasser mit einem physikalisch basierten Modell zur Emission des MOA in die Atmosphäre und finden gute Übereinstimmungen mit marinen und atmosphärischen Messungen in der Arktis.

Auch die primäre Emission des Aerosols von Landoberflächen benötigt detaillierte Informationen zur Beschaffenheit und zum Streu- und Absorptionsverhalten der Partikel. Speziell für Mineralstaub als größter Anteil primären Aerosols spielt die Mineralogie der Landoberfläche eine wichtige Rolle. **Gómez Maqueo Anaya et al.** zeigen auf, wie man mineralogisch aufgelöste Staubverteilungen im Modell realisieren und mit aktiver Fernerkundung validieren kann. Umgekehrt kann der aktiv via Lidar fernerkundete mineralogische Fingerabdruck auch zur Identifikation von Quellregionen genutzt werden.

Aktive Lidarfernerkundung hat sich am TROPOS grundsätzlich zu einer bewährten Methode zur Charakterisierung der atmosphärischen Aerosolpartikel und ihrer Wolken- und Eiskeimfähigkeit entwickelt. Diese Charakterisierung hat nun durch den Einsatz eines spektralen Kanals zur Messung der Fluoreszenz sowohl die Messgenauigkeit als auch die Erfassung biogenen Aerosols erheblich verbessert. **Gast et al.** demonstrieren das Potential des Fluoreszenzkanals am Beispiel von Rauchaerosol und konnten so z.B. bislang unerkannte Cirrusbildung aus Waldbrandaerosol nachweisen; ein wichtiger Schritt zur Erkenntnis von Biosphäre/Atmosphäre-Wechselwirkungen.

Overview of the individual contributions / Übersicht der Einzelbeiträge

and harmonise the analysis of cloud water samples. Comparison campaigns have already been carried out here and initial guidelines have been drawn up.

The launch of the European-Japanese EarthCARE space mission in May 2024 is eagerly awaited, which represents a milestone in the global recording of aerosol-cloud radiation processes with a coupling of active and passive remote sensing. TROPOS has been involved in the development of the evaluation algorithms for many years. **Hünerbein et al.** summarise the contributions of TROPOS in obtaining aerosol and cloud properties from the EarthCARE lidar ATLID, the imager MSI and from a combination of both, while always ensuring physically consistent assumptions on the cloud microphysical properties across all sensors.

TROPOS is a consortium partner for the scientific operation of HALO and is involved in the determination of ice crystal residues with the HALO-CVI inlet system, among other things. **Mertes et al.** present the results of the HALO mission CIRRUS-HL, in which the microphysical properties of the ice particles and the background aerosol were almost completely recorded and provide important information on the formation of droplets and the nucleation of ice particles in clouds.

Ground-based remote sensing networks enable a statistically significant characterisation of global aerosol types. With DeLiAn, **Floutsi et al.** present such a data set based on the lidar network PollyNET. Here, permanent and temporary globally distributed measurement series of numerous lidar systems developed at TROPOS are summarised, thus creating an elementary basis for the fundamental development of aerosol typing.

Health

Research on (ultra)fine particulate matter in urban and rural areas, which are exposed to various transformations of climate change, (de)industrialisation, energy transition and land use changes, is an essential component of the socially relevant work at TROPOS. Measurement networks, focussed campaigns, laboratory and model studies continue to contribute equally to this.

As part of the project "Ultrafine particulate pollution from airports in Berlin (ULTRAFLEB), TROPOS is coordinating stationary and mobile field measurements of ultrafine particles (UFP) over a period of three years. **Winkler et al.** were able to show that air traffic emissions still dominate the UFP concentrations several kilometres downwind, especially for the smallest particles with a diameter of 10 - 20 nm, which are particularly harmful to health. However, these are mainly volatile particles with a short lifetime.

An important parameter for characterising the toxicity of aerosol particles is their oxidation potential

Forschungsinfrastrukturen (FIS)

Als koordinierendes Institut des nationalen Roadmap-Projektes ACTRIS-D (Aerosol, Cloud and Trace gas Research InfraStructure - Deutschland), starker Partner im Europäischen ACTRIS-Verbund und in der weltraumgestützten Erdbeobachtung spielen FIS eine zentrale Rolle am TROPOS zum Prozessverständnis der hochvariablen kurzlebigen Klimakomponenten auf allen Skalen. Hierzu werden sowohl eigene FIS entwickelt und andere im Verbund mit Partnerinstitutionen genutzt wie etwa das nationale Forschungsflugzeug HALO oder die deutsche Forschungsschiffslotte (hier Polarstern, Meteor, Sonne).

Für die langfristige und kontinuierliche Beobachtung und Erforschung von Aerosol-Wolken-Wechselwirkungen wird derzeit das Schmücke Cloud Observatory (SCO) im Thüringer Wald als nationale Einrichtung (NF) im Rahmen von ACTRIS aufgebaut. **Käfer et al.** stellen das Konzept des Observatoriums zur chemischen und physikalischen Charakterisierung von Luftmassen beim Wolkendurchgang und den Stand der Umsetzung vor. Thematisch gekoppelt ist das Schmücke-Observatorium mit dem ACTRIS-Kalibrierzentrum für Wolkenwasserchemie (CCWaC) zur Etablierung und Harmonisierung der Analytik von Wolkenwasserproben. Hier sind bereits Vergleichskampagnen durchgeführt und erste Richtlinien erarbeitet worden.

Mit Spannung wird der Start der europäisch-japanischen Weltraummission EarthCARE im Mai 2024 erwartet, die mit einer Kopplung von aktiver und passiver Fernerkundung einen Meilenstein in der globalen Erfassung von Aerosol-Wolken-Strahlungsprozessen darstellt. TROPOS ist seit vielen Jahren an der Entwicklung der Auswertungsalgorithmen beteiligt. **Hünerbein et al.** fassen die Beiträge des TROPOS zusammen, Aerosol- und Wolkeneigenschaften aus dem EarthCARE-Lidar ATLID, dem Imager MSI und aus einer Kombination beider zu erhalten, und dabei stets über alle Sensoren hinweg physikalisch konsistente Annahmen zu den wolkenmikrophysikalischen Eigenschaften sicherzustellen.

TROPOS ist Konsortialpartner für den wissenschaftlichen Betrieb von HALO und unter anderem mit dem Einlasssystem HALO-CVI an der Bestimmung von Eiskristallresiduen beteiligt. **Mertes et al.** stellen Ergebnisse der HALO-Mission CIRRUS-HL vor, bei der die mikrophysikalischen Eigenschaften der Eispartikel und des Hintergrund aerosols nahezu vollständig erfasst wurden und wichtige Hinweise auf die Bildung von Tröpfchen und die Nukleation von Eispartikeln in Wolken geben.

Netzwerke bodengebundener Fernerkundung ermöglichen eine statistisch signifikante

Overview of the individual contributions / Übersicht der Einzelbeiträge

(OP). **Souza et al.** report a remarkable application of this using the example of mineral dust over Cape Verde. As part of the DUSTRISK project of the Leibniz Competition, the OP could be recorded in size resolution for dust-intensive and low-dust events. This shows that toxicity is more than 50% greater for coarse particles and dust-intensive situations than in low-dust periods.

Knowledge of air pollution is particularly important in urban areas. However, stationary measurement networks are not necessarily representative of an entire city due to the complex orography and the highly variable traffic load over space and time. **Weger and Heinold** present the CAIRDIO air quality model developed at TROPOS, which makes it possible to simulate entire cities highly efficiently with sufficient accuracy. Using the examples of Leipzig and Dresden, they were able to show when building effects or orography effects dominate the spatiotemporal distribution of air pollution.

Charakterisierung der globalen Aerosoltypen. Mit DeLiAn stellen **Floutsi et al.** einen solchen Datensatz auf Basis des Lidarnetzwerkes PollyNET vor. Hierbei werden dauerhafte und temporäre global verteilte Messreihen zahlreicher am TROPOS entwickelter Lidarsysteme zusammenfasst und damit eine elementare Grundlage für die grundsätzliche Entwicklung von Aerosoltypisierungen geschaffen.

Gesundheit

Die Erforschung von (Ultra-)Feinstaub in urbanen und ländlichen Räumen, die verschiedenen Transformationen von Klimawandel, (De-)Industrialisierung, Energiewende und Landnutzungsänderungen ausgesetzt sind, ist eine wesentliche Komponente der gesellschaftsrelevanten Arbeiten am TROPOS. Messnetze, fokussierte Kampagnen, Labor- und Modellstudien tragen weiterhin gleichermaßen hierzu bei.

Im Rahmen des Projektes „Ultrafeinstaubbelastung durch Flughäfen in Berlin (ULTRAFLEB) koordiniert TROPOS über drei Jahre stationäre und mobile Feldmessungen von Ultrafeinpartikeln (UFP). **Winkler et al.** konnten zeigen, dass Luftverkehrsemissionen noch mehrere Kilometer im Abwind die UFP-Konzentrationen dominieren, insbesondere bei den gesundheitlich besonders schädlichen kleinsten Partikeln von 10 - 20 nm Durchmesser. Allerdings handelt es sich hierbei hauptsächlich um flüchtige Partikel mit geringer Lebensdauer.

Eine wesentliche Größe zur Charakterisierung der Toxizität von Aerosolpartikeln ist deren Oxidationspotential (OP). Eine bemerkenswerte Anwendung hierzu berichten **Souza et al.** am Beispiel des Mineralstaubs über den Kapverden. Im Rahmen des DUSTRISK-Projektes des Leibniz-Wettbewerbs konnte das OP größtenteils für staubintensive und staubarme Ereignisse erfasst werden. Hierbei zeigt es sich, dass die Toxizität bei groben Partikeln und staubintensiven Situationen um mehr als 50% größer ist als in staubarmen Zeiten.

Gerade in urbanen Räumen ist eine Kenntnis der Luftbelastung von großer Bedeutung. Allerdings sind stationäre Messnetze aufgrund der komplexen Orographie und der raumzeitlich hochvariablen Verkehrsbelastung nicht unbedingt repräsentativ für eine gesamte Stadt. **Weger und Heinold** stellen das am TROPOS entwickelte Luftqualitätsmodell CAIRDIO vor, das es ermöglicht, ganze Städte hocheffizient mit ausreichender Genauigkeit zu simulieren. Am Beispiel von Leipzig und Dresden konnte gezeigt werden, wann Gebäudeeffekte oder Orographie-Effekte die raumzeitliche Verteilung der Luftbelastung dominieren.

Highlight Publications / Highlight-Publikationen

Highlight Publications

Global organic and inorganic aerosol hygroscopicity and its effect on radiative forcing

Pöhlker, M.L., Pöhlker, C., Quaas, J. et al. Global organic and inorganic aerosol hygroscopicity and its effect on radiative forcing. *Nat Commun* **14**, 6139 (2023). <https://doi.org/10.1038/s41467-023-41695-8>

Through extensive investigations, an international research team led by the Max Planck Institute for Chemistry (MPIC) and the Leibniz Institute for Tropospheric Research (TROPOS) was able to reduce the relationship between the chemical composition and water absorption of aerosol particles to a simple linear formula. In a study published in the journal "Nature Communications", they showed that the hygroscopicity is essentially determined on a global average by the proportion of organic and inorganic substances in the aerosol composition.

Pöhlker, M.L., Pöhlker, C., Quaas, J. et al. Global organic and inorganic aerosol hygroscopicity and its effect on radiative forcing. *Nat Commun* **14**, 6139 (2023). <https://doi.org/10.1038/s41467-023-41695-8>

How the extreme 2019–2020 Australian wildfires affected global circulation and adjustments

Senf, F., Heinold, B., Kubin, A., Müller, J., Schrödner, R., and Tegen, I., *Atmos. Chem. Phys.*, **23**, 8939–8958, <https://doi.org/10.5194/acp-23-8939-2023>, 2023.

Smoke from wildfires is an important source of atmospheric particles that can absorb sunlight and thus may significantly influence the climate system. The change in circulation patterns due to smoke entering the stratosphere during the massive vegetation fires in Australia in December and January 2019–2020 was investigated in this model study. Adjustment processes in the stratosphere slowed down the meridional circulation, and a positive temperature perturbation developed in both hemispheres within the first 2 months after the event.

Daytime Atmospheric Halogen Cycling through Aqueous-Phase Oxygen Atom Chemistry

Evan Z. Dalton, Erik H. Hoffmann, Thomas Schaefer, Andreas Tilgner, Hartmut Herrmann, and Jonathan D. Raff, *Journal of the American Chemical*

Highlight-Publikationen

Globale organische und anorganische Aerosol-Hygroskopizität und ihr Einfluss auf den Strahlungsantrieb

Pöhlker, M.L., Pöhlker, C., Quaas, J. et al. Global organic and inorganic aerosol hygroscopicity and its effect on radiative forcing. *Nat Commun* **14**, 6139 (2023). <https://doi.org/10.1038/s41467-023-41695-8>

Durch umfangreiche Untersuchungen konnte ein internationales Forschungsteam unter Leitung des Max-Planck-Instituts für Chemie (MPIC) und des Leibniz-Instituts für Troposphärenforschung (TROPOS) den Zusammenhang zwischen chemischer Zusammensetzung und Wasseraufnahme von Aerosolpartikeln auf eine einfache lineare Formel reduzieren. In einer Studie, die im Fachjournal „Nature Communications“ erschien, zeigten sie, dass die Hygrokopizität global gemittelt im Wesentlichen durch den Anteil organischer und anorganischer Stoffe an der Aerosolzusammensetzung bestimmt wird.

Wie sich die extremen australischen Waldbrände 2019–2020 auf die globale Zirkulation und Anpassungen auswirkten

Senf, F., Heinold, B., Kubin, A., Müller, J., Schrödner, R., and Tegen, I., *Atmos. Chem. Phys.*, **23**, 8939–8958, <https://doi.org/10.5194/acp-23-8939-2023>, 2023.

Rauch von Waldbränden ist eine wichtige Quelle atmosphärischer Partikel, die Sonnenlicht absorbieren und somit das Klimasystem erheblich beeinflussen können. In dieser Modellstudie wurde die Veränderung von Zirkulationsmustern aufgrund des Raucheneintrags in die Stratosphäre während der massiven Vegetationsbrände in Australien im Dezember und Januar 2019–2020 untersucht. Anpassungsprozesse in der Stratosphäre verlangsamten die meridionale Zirkulation und eine positive Temperaturstörung entwickelte sich in beiden Hemisphären innerhalb der ersten zwei Monate nach dem Ereignis.

Atmosphärischer Halogenkreislauf am Tag durch die Chemie der Sauerstoffatome in wässriger Phase

Evan Z. Dalton, Erik H. Hoffmann, Thomas Schaefer, Andreas Tilgner, Hartmut Herrmann, and Jonathan D. Raff, *Journal of the American Chemical*

Highlight Publications / Highlight-Publikationen

Jonathan D. Raff, Journal of the American Chemical Society 2023 145 (29), 15652-15657. <https://doi.org/10.1021/jacs.3c03112>

Halogen atoms are important atmospheric oxidants that have unidentified daytime sources from photochemical halide oxidation in sea salt aerosols. Here, we show that the

photolysis of nitrate in aqueous chloride solutions generates nitryl chloride (ClNO_2) in addition to Cl_2 and HOCl. Experimental and modeling evidence suggests that $\text{O}({}^3\text{P})$ formed in the minor photolysis channel from nitrate oxidizes chloride to Cl_2 and HOCl, which reacts with nitrite to form ClNO_2 . This chemistry is different than currently accepted mechanisms involving chloride oxidation by OH and could shift our understanding of daytime halogen cycling in the lower atmosphere.

Self-lofting of wildfire smoke in the troposphere and stratosphere: simulations and space lidar observations

Ohneiser, K., Ansmann, A., Wittuhn, J., Deneke, H., Chudnovsky, A., Walter, G., and Senf, F., Atmos. Chem. Phys., 23, 2901–2925, <https://doi.org/10.5194/acp-23-2901-2023>, 2023

We analyzed long-term CALIOP (Cloud–Aerosol Lidar with Orthogonal Polarization) observations of smoke layers and plumes evolving in the UTLS (upper troposphere and lower stratosphere) height region over Siberia and the adjacent Arctic Ocean during the summer season of 2019. Our results indicate that self-lofting contributed to the vertical transport of smoke. We hypothesize that the formation of a near-tropopause aerosol layer, observed with CALIOP, was the result of self-lofting processes. This is in line with our self-lofting model based on ECRAD (European Centre for Medium-Range Weather Forecasts Radiation) scheme simulations.

Society 2023 145 (29), 15652-15657. <https://doi.org/10.1021/jacs.3c03112>

Halogenatome sind wichtige atmosphärische Oxidationsmittel, die tagsüber aus der photochemischen Halogenidoxidation in Meersalzaerosolen stammen. Hier zeigen wir, dass die

Photolyse von Nitrat in wässrigen Chloridlösungen neben Cl_2 und HOCl auch Nitrylchlorid (ClNO_2) erzeugt, zusätzlich zu Cl_2 und HOCl. Experimentelle und modelltechnische Beweise deuten darauf hin, dass $\text{O}({}^3\text{P})$, das im Nebenkanal der Photolyse von Nitrat gebildet wird, Chlorid zu Cl_2 und HOCl oxidiert, das mit Nitrit reagiert und ClNO_2 bildet. Diese Chemie unterscheidet sich von den derzeit akzeptierten Mechanismen der Chloridoxidation durch OH und könnte unser Verständnis des Halogenkreislaufs in der unteren Atmosphäre während des Tages verändern.

Selbstauwirbelung von Waldbrandrauch in der Troposphäre und Stratosphäre: Simulationen und Weltraum-Lidar-Beobachtungen

Ohneiser, K., Ansmann, A., Wittuhn, J., Deneke, H., Chudnovsky, A., Walter, G., and Senf, F., Atmos. Chem. Phys., 23, 2901–2925, <https://doi.org/10.5194/acp-23-2901-2023>, 2023

Wir haben langfristige CALIOP-Beobachtungen (Cloud-Aerosol Lidar with Orthogonal Polarization) von Rauchschichten und -fahnen analysiert, die sich in der UTLS-Höhenregion (obere Troposphäre und untere Stratosphäre) über Sibirien und dem angrenzenden Arktischen Ozean während der Sommersaison 2019 entwickelt haben. Unsere Ergebnisse deuten darauf hin, dass die Selbstauwirbelung zum vertikalen Transport von Rauch beiträgt. Wir stellen die Hypothese auf, dass die mit CALIOP beobachtete Bildung einer Aerosolschicht nahe der Tropopause das Ergebnis von Selbstauftreibsprozessen war. Dies steht im Einklang mit unserem Selbstauftreibsmodell, das auf Simulationen des ECRAD-Schemas (European Centre for Medium-Range Weather Forecasts Radiation) beruht.

Transfer in science and society – overview / Transfer in Wissenschaft und Gesellschaft – Überblick

Transfer in science and society – overview

Knowledge transfer and external impact

TROPOS research for specialist audiences.

Due to the Institute's focus on application-oriented basic research, the scientific results are mainly utilised in scientific publications and conference papers (see list, p. 145).

Of the **scientific conferences** in which TROPOS participated, the following stand out in the reporting period:

D-A-CH 2022: The German Meteorological Society (DMG), the Austrian Meteorological Society (ÖGM) and the Swiss Meteorological Society (SGM) organise the D-A-CH Meteorology Conference every three years. After 1998, Leipzig was the venue for the second time on 21-25 March 2022. TROPOS contributions reported on air pollutants, LACROS, BVOCs and ACTRIS-D, among other topics. TROPOS was also part of the excursion programme.

MOSAiC: At the “International MOSAiC Science Conference/Workshop”, researchers met at the Telegrafenberg in Potsdam from 25 to 29 April 2022 for the, due to the pandemic, first major conference to evaluate the extensive data from the 2019/20 MOSAiC expedition in the Arctic. The 2nd MOSAiC Science Conference was held on 13-17 February 2023 at the University of Colorado, Boulder, in the USA. TROPOS provided important atmospheric data for MOSAiC with its lidar and balloon measurements and is also working closely with the Biogeochemistry department to analyse the data.

ACTRIS-D kick-off event: From 20 to 22 June 2022 in Leipzig, around 120 stakeholders from science and politics discussed current research issues relating to ACTRIS-D - the German



Fig. / Abb. 1: The Rector of Leipzig University, Prof Dr Eva Inés Obergfell, visits TROPOS. / Die Rektorin der Universität Leipzig, Prof. Dr. Eva Inés Obergfell, zu Besuch am TROPOS. (Photo: Tilo Arnhold, TROPOS)

Transfer in Wissenschaft und Gesellschaft – Überblick

Wissenstransfer und Außenwirkung

TROPOS-Forschung für Fachpublikum.

Auf Grund der Ausrichtung des Institutes auf anwendungsorientierte Grundlagenforschung erfolgt die Verwertung der wissenschaftlichen Ergebnisse hauptsächlich in Fachpublikationen und Konferenzbeiträgen (siehe Liste, S. 145).

Aus den **wissenschaftlichen Tagungen**, an deren TROPOS beteiligt war, stechen im Berichtszeitraum folgende heraus:

D-A-CH 2022: Die Deutsche Meteorologische Gesellschaft (DMG), die Österreichische Gesellschaft für Meteorologie (ÖGM) und die Schweizerische Gesellschaft für Meteorologie (SGM) richten alle drei Jahre die D-A-CH-Meteorologie-Tagung aus. Nach 1998 war Leipzig am 21.-25.03.2022 zum zweiten Mal Austragungsort. TROPOS-Beiträge berichteten u.a. über Luftschadstoffe, LACROS, BVOCs und ACTRIS-D. TROPOS war auch Teil des Exkursionsprogramms.

MOSAiC: Bei der „International MOSAiC Science Conference/Workshop“ trafen sich Forschende vom 25. bis 29. April 2022 auf dem Telegrafenberg in Potsdam pandemiebedingt zur ersten größeren Tagung zur Auswertung der umfangreichen Daten der MOSAiC-Expedition 2019/20 in der Arktis. Die 2nd MOSAiC Science Conference wurde am 13.-17.02.23 an der University of Colorado, Boulder, in den USA durchgeführt. TROPOS hat bei MOSAiC mit den Lidar- und Ballonmessungen wichtige Daten im Bereich Atmosphäre geliefert und arbeitet bei der Auswertung auch eng mit der Biogeochemie zusammen.

Auftaktveranstaltung von ACTRIS-D: Rund 120 Akteure aus Wissenschaft und Politik diskutierten vom 20. bis 22. Juni 2022 in Leipzig aktuelle Forschungsfragen rund um ACTRIS-D – dem deutschen Beitrag zur EU-Forschungsinfrastruktur ACTRIS, der die Rolle kurzlebiger Bestandteile für das Klima in der Erdatmosphäre beobachtet. Nach zahlreichen Online-Meetings war die Jahrestagung pandemiebedingt die erste Gelegenheit zum persönlichen Austausch in größerem Rahmen. Die Festveranstaltung am 21. Juni bildete den offiziellen Auftakt: In ihren Grußworten unterstrichen unter anderem Mario Brandenburg (Parlamentarischer Staatssekretär im Bundesministerium für Bildung und Forschung) und Sebastian Gemkow (Staatsminister für Wissenschaft im Sächsischen Staatsministerium für Wissenschaft, Kultur und Tourismus) die Bedeutung für die Gesellschaft und sicherten ihre Unterstützung zu.

Transfer in science and society – overview / Transfer in Wissenschaft und Gesellschaft – Überblick

contribution to the EU research infrastructure ACTRIS, which monitors the role of short-lived components for the climate in the Earth's atmosphere. After numerous online meetings, the annual conference was the first opportunity for face-to-face dialogue on a larger scale due to the pandemic. The official kick-off event was held on 21 June: In their welcoming addresses, Mario Brandenburg (Parliamentary State Secretary at the Federal Ministry of Education and Research) and Sebastian Gemkow (Minister of State for Science at the Saxon State Ministry of Science, Culture and Tourism), among others, emphasised the importance for society and pledged their support.

ICAQ' Africa 2022: The first international conference on "Air Quality in Africa" took place on 11-14 October 2022. The conference took place online to enable as many people as possible to participate and was organised by Wadinga Fomba (TROPOS) together with colleagues from Alioune Diop University (Senegal) and the French CNRS.

IUGG 2023: The International Union of Geodesy and Geophysics (IUGG) met in Berlin on 11-20 July 23 for its 28th General Assembly. TROPOS used this major event to organise a session on "Upcoming Southern Ocean Initiatives" on 13.07.23 and to better network researchers on the Southern Ocean around Antarctica.

(AC)³ General Assembly: The annual meetings of the DFG Transregio TR172 on Arctic climate amplification are now also an essential part of TROPOS research. In 2022, the (AC)³ community met at the Klimahaus in Bremerhaven, 2023 at the Science Park Leipzig. Events for PhDs such as workshops on careers, communication and publishing are regularly organised.

Selected topics and activities for politics and society

The research results of TROPOS also serve as a contribution to **policy advice in the environmental sector**. For example, practical studies on the behaviour and future development of pollutants in the atmosphere are carried out for the State of Saxony and the Federal Environment Agency (UBA). In addition, measurement data on the concentrations of fine and ultrafine aerosol particles and on the chemical composition of particles in the atmosphere are collected, scientifically analysed and made available for further use as part of contract projects for the Federal Environmental Agency (UBA) and the Saxon State Office for Environment and Geology (LfULG).

Examples of this in 2022/23 are: The investigation of trends, causes and effects of ozone pollution in Saxony (LfULG), determination of characteristic



Fig. / Abb. 2: ACTRIS-D Annual Meeting 2022 at KUBUS Leipzig. / ACTRIS-D-Jahrestagung 2022 im KUBUS Leipzig. (Photo: Dr. Andreas Pohlmann)

ICAQ' Africa 2022: Am 11.-14.10.2022 fand die erste internationale Konferenz „Luftqualität in Afrika“ statt. Die Konferenz fand online statt, um möglichst vielen die Teilnahme zu ermöglichen, und wurde von Wadinga Fomba (TROPOS) zusammen mit Kolleg:innen der Alioune Diop University (Senegal) und dem französischen CNRS organisiert.

IUGG 2023: Die Internationale Union für Geodäsie und Geophysik (IUGG) traf sich am 11.-20.07.23 in Berlin zur 28. Generalversammlung. Diese Großveranstaltung nutzte TROPOS, um am 13.07.23 eine Session zu "Upcoming Southern Ocean Initiatives" zu organisieren und Forschende zum Südlichen Ozean rund um die Antarktis besser zu vernetzen.

(AC)³ General Assembly: Essentieller Bestandteil der TROPOS-Forschung sind inzwischen auch die Jahrestagungen des DFG-Transregios TR172 zur arktischen Klimaverstärkung. 2022 traf sich die (AC)³-Community im Klimahaus in Bremerhaven. 2023 im Wissenschaftspark Leipzig. Veranstaltungen für PhDs wie Workshops zu Karriere, Kommunikation oder Publizieren gehören regelmäßig dazu.

Ausgewählte Themen und Aktivitäten für Politik und Gesellschaft

Die Forschungsergebnisse des TROPOS dienen auch als ein Beitrag zur **Politikberatung im Umweltbereich**. So werden u.a. für das Land Sachsen oder das Umweltbundesamt (UBA) praxisrelevante Untersuchungen zum Verhalten und zur künftigen Entwicklung von Schadstoffen in der Atmosphäre durchgeführt. Außerdem werden im Rahmen von Auftragsprojekten für das UBA und das Sächsische Landesamt für Umwelt und Geologie (LfULG) über längere Zeiträume Messdaten zu den Konzentrationen feiner und ultrafeiner Aerosolpartikel sowie zur

Transfer in science and society – overview / Transfer in Wissenschaft und Gesellschaft – Überblick

exposure conditions for radon at indoor workplaces (Federal Office for Radiation Protection), conducting experimental studies on the atmospheric degradation of siloxanes (Wacker Chemie GmbH), integration of ammonia immission measurements into the Saxon air quality monitoring network (LfULG) or the investigation of ultrafine particles in indoor and ambient air (UBA).

The project “Ultrafine particulate pollution from airports in Berlin” (ULTRAFLEB) is investigating ultrafine particulate matter as a potential health hazard until the end of 2024 on behalf of the Federal Environment Agency. This involves stationary and mobile field measurements of ultrafine particles (UFP) in the vicinity of Berlin Brandenburg Airport BER using the TROPOS aerosol container as well as model calculations. In April 2023, the first of two central projects to assess the exposure of the Frankfurt/Main region to ultrafine particles (**UFP**) and their effects on health was launched with the “**UFP Exposure Study**”. The contracting authority of the consortium led by TROPOS is the Environmental and Neighbourhood House (UNH), which acts as the office of the Forum Airport and Region (FFR) and is 100% funded by the state of Hesse.

EDIAQI, a major EU project, was launched in 2022: a Europe-wide consortium of 19 universities, research institutions and companies will investigate indoor air pollution for four years. TROPOS is the only partner in Germany and will develop innovative tools for monitoring indoor air quality.

TROPOS is also involved in projects with partners from the medical field. Since 2021, the DUSTRISK project has been investigating the health effects of mineral dust, which can cause or exacerbate respiratory diseases such as asthma or

chemischen Partikelzusammensetzung in der Atmosphäre erhoben, wissenschaftlich ausgewertet und zur weiteren Nutzung zur Verfügung gestellt.

Beispiele in den Jahren 2022/23 hierfür sind: Die Untersuchung von Tendenzen, Verursachern und Auswirkungen der Ozonbelastung in Sachsen (LfULG), Ermittlung von charakteristischen Expositionsbedingungen bei Radon an Arbeitsplätzen in Innenräumen (Bundesamt für Strahlenschutz), Durchführung experimenteller Untersuchungen zum atmosphärischen Abbau von Siloxanen (Wacker Chemie GmbH), Integration von Ammoniak-Immissionsmessungen ins sächsische Luftgütemessnetz (LfULG) oder die Untersuchung ultrafeiner Partikel im Innenraum und in der Umgebungsluft (UBA).

Ultrafeinstaub als potenzielle Gesundheitsgefahr untersucht das Projekt „Ultrafeinstaubbelastung durch Flughäfen in Berlin“ (ULTRAFLEB) bis Ende 2024 im Auftrag des Umweltbundesamtes. Dazu finden stationäre und mobile Feldmessungen von ultrafeinen Partikeln (UFP) im Umfeld des Flughafens Berlin Brandenburg BER mit dem Aerosolcontainer des TROPOS sowie Modellrechnungen statt. Im April 2023 startete mit der „**UFP-Belastungsstudie**“ das erste von zwei zentralen Vorhaben zur Beurteilung der Belastung der Region Frankfurt/Main mit ultrafeinen Partikeln (**UFP**) und deren gesundheitlicher Auswirkungen. Auftraggeber des von TROPOS geleiteten Konsortium ist das Umwelt- und Nachbarschaftshaus (UNH), das als Geschäftsstelle des Forums Flughafen und Region (FFR) fungiert und zu 100% durch das Land Hessen finanziert wird.

Mit EDIAQI startete 2022 ein großes EU-Projekt: Ein europaweites Konsortium aus 19 Universitäten, Forschungseinrichtungen und Unternehmen wird vier Jahre lang die Schadstoffbelastung in Innenräumen untersuchen. TROPOS ist der einzige Partner in Deutschland und wird dabei innovative Werkzeuge zur Überwachung der Luftqualität in Innenräumen entwickeln.

TROPOS ist auch in Projekte mit Partnern aus dem medizinischen Bereich involviert. Das Projekt DUSTRISK untersucht seit 2021 die Gesundheitsauswirkungen von Mineralstaub, der Atemwegserkrankungen wie Asthma oder Lungenentzündung verursachen oder verschlimmern kann. Im interdisziplinären Projekt werden diese Aspekte in Kombination mit anhaftenden Mikroben untersucht. Feldstudien, Laboruntersuchungen sowie Modellierungsstudien werden in Zusammenarbeit mit Partnern der Leibniz-Institute DSMZ, FZB, IUF und TROPOS sowie der Kapverden durchgeführt, darunter Krankenhäuser, Universitäten und öffentliche Gesundheitsinstitute. DUSTRISK wird durch den Leibniz-Wettbewerb „Kooperative Exzellenz“ gefördert.



Fig. / Abb. 3: Festive event to mark 30 years of Leibniz in Saxony on 14 September 2022 in Dresden: Group photo of the directors with the Minister of Science, Minister President and Leibniz President. / Festveranstaltung zu 30 Jahre Leibniz in Sachsen am 14.09.2022 in Dresden: Gruppenfoto der Direktorinnen und Direktoren mit Wissenschaftsminister, Ministerpräsident und Leibniz-Präsidentin (Photo: Michael Schmidt)

Transfer in science and society – overview / Transfer in Wissenschaft und Gesellschaft – Überblick

pneumonia. The interdisciplinary project is investigating these aspects in combination with adhering microbes. Field studies, laboratory tests and modelling studies are being carried out in collaboration with partners from the Leibniz Institutes DSMZ, FZB, IUF and TROPOS as well as Cape Verde, including hospitals, universities and public health institutes. DUSTRISK is funded by the Leibniz competition "Cooperative Excellence".

In a project in collaboration with atmosfair and SaferRwanda, TROPOS backpack measurements documented the difference in emissions between new efficient and conventional cookstoves. The data collected was incorporated into a health study.

The EngageMINT project aims to make environmental research tangible for young people. As part of the project, the participants are developing a digital transfer tool that communicates the results and processes of current research at TROPOS on environmental and climate issues. This tool is aimed at environmentally aware young people and aims to promote interest and skills in STEM subjects, taking into account their interest profiles and using suitable feedback systems. The partners are Leibniz University Hannover (LUH) and the Leibniz Institute for Science and Mathematics Education (IPN).

TROPOS research for the general public.

TROPOS maintains a dialogue with the public - via print media, radio and television. 36 press releases were issued in 2022/23. This resulted in over 161 media publications in 2022 (as far as known). In 2023, there were 144 publications (as far as known).

Topics to which TROPOS researchers were able to contribute to the media were air quality (such as weekend effects from barbecues or positive effects from the corona lockdown), the warming of the Arctic and influences on the weather in Germany, smoke aerosol and the formation of an ozone hole over the Arctic. In 2023, the topic Antarctica was also added through Martin Radenz's one-year work at the Neumayer Station. Clouds in the north-south contrast were a topic in 2022 in the light of the GoSouth campaign in New Zealand. Clouds in general continued to fascinate media professionals in a wide variety of formats in 2023. The thematic focus shows that TROPOS research findings and activities can be successfully communicated to the public through press releases.

In the print sector, TROPOS is represented particularly frequently in the Sächsische Zeitung regional newspaper with 15 articles in the reporting period, alongside the Leipziger Volkszeitung and



Fig. / Abb. 4: Launch of the BMBF joint project EngageMINT (knowledge transfer for environmentally aware young people to raise awareness of STEM subjects). / Projektstart des BMBF-Verbundprojekts EngageMINT (Wissenstransfer für umweltbewusste Jugendliche zur Sensibilisierung für MINT). (Photo: Jan Uhing / IPN)

In einem Projekt in Zusammenarbeit mit atmosfair und SaferRwanda dokumentierten TROPOS-Rucksack-Messungen den Unterschied der Emissionen zwischen neuen effizienten und herkömmlichen Koch-Öfen. Die erhobenen Daten flossen in eine Gesundheitsstudie ein.

Das Projekt EngageMINT soll Umweltforschung für Jugendliche greifbar machen. Im Rahmen des Projekts entwickeln die Beteiligten ein digitales Transferinstrument, das Ergebnisse und Prozesse der aktuellen Forschung am TROPOS zu Umwelt- und Klimathemen vermittelt. Gerichtet ist dieses Instrument an umweltbewusste Jugendliche und hat zum Ziel, unter Berücksichtigung ihrer Interessensprofile und unter Einsatz geeigneter Feedback-Systeme, Interesse an und Kompetenzen in den MINT-Fächern zu fördern. Partner sind die Leibniz Universität Hannover (LUH) sowie das Leibniz-Institut für Pädagogik der Naturwissenschaften und Mathematik (IPN).

TROPOS-Forschung für die breite Öffentlichkeit. TROPOS steht im Dialog mit der Öffentlichkeit – u.a. auch über Printmedien sowie Hör- und Fernsehfunk. 2022/23 wurden 36 Pressemitteilungen herausgegeben. Daraus resultierten im Jahr 2022 über 161 Medienveröffentlichungen (soweit bekannt). Im Jahr 2023 waren es 144 Veröffentlichungen (soweit bekannt).

Themen zu denen TROPOS-Forschende medial beitragen konnte waren Luftqualität (wie z.B. Wochenendeffekte durch Grillen oder positive Effekte durch den Corona-Lockdown), die Erwärmung der Arktis und Einflüsse auf das Wetter in Deutschland, Rauch-aerosol und die Bildung eines Ozonlochs über der

Transfer in science and society – overview / Transfer in Wissenschaft und Gesellschaft – Überblick



Fig. / Abb. 5: Science cinema on 16.03.23 at the ZGF Leipzig: "Expedition Arctic" - panel discussion with Leipzig participants of the MOSAiC expedition and moderator Grit Krämer from MDR. / Wissenschaftskino am 16.03.23 im ZGF Leipzig: „Expedition Arktis“ - Diskussionsrunde mit Leipziger Teilnehmern der MOSAiC-Expedition und Moderatorin Grit Krämer vom MDR. (Photo: Tilo Arnhold / TROPOS)

BILD. Mira Pöhlker presented her research in a two-page interview in the German-language ZEIT magazine. The Southland Times reported on the GoSouth campaign in New Zealand; the Austrian Standard on ACTRIS. ACTRIS was officially founded as a European Research Infrastructure Consortium (ERIC) on 25 April 2023.

TROPOS researchers were also present on the radio: regionally on Sachsenradio or MDR aktuell, nationwide on Deutschlandfunk and DLF-Nova on smoke aerosol or dust topics and on Deutschlandsradio Kultur on climate change on the Cape Verde Islands or the climate impact of smoke.

Radio 1 from RBB and Bayern 2 from BR picked up on the press release on biogenic aerosols and interviewed Hartmut Herrmann.

In 2022, 11 TV programmes were produced on a wide range of topics, including regional programmes on MDR, WDR and SWR, as well as the ARD programme "Wetter vor Acht" and the arte documentary "The wind – motor of climate change," in which researchers from the Remote Sensing department took part. A TV highlight was the 5-minute appearance of TROPOS researcher Martin Radenz in the ORF documentary "Universum Spezial" with the title "Climate changes wilderness - Between adaptation and extinction of species" in 2023. He spent a year at the Neumayer Station researching the Antarctic atmosphere and climate change.

TROPOS doctoral student Gladiola Malollari from the Agricultural University of Tirana was a sought-after interviewee on Albanian television when the green lidar beam of the TROPOS PollyXT shone over Tirana

Arktis. 2023 kam auch das Thema Antarktis durch die einjährige Tätigkeit von Martin Radenz auf der Neumayer-Station dazu. Wolken im Nord-Süd-Kontast waren 2022 ein Thema vor dem Hintergrund der GoSouth-Kampagne in Neuseeland. Wolken im Allgemeinen faszinierten Medienschaffende auch 2023 in den verschiedensten Formaten. Die Themenausrichtung zeigt, dass es gelingt, die TROPOS-Forschungs ergebnisse und -tätigkeiten durch Pressemitteilungen in die Öffentlichkeit zu transportieren.

Im Print-Bereich ist TROPOS besonders häufig mit 15 Artikeln im Berichtszeitraum in der Sächsischen Zeitung regional vertreten, neben der Leipziger Volkszeitung und BILD. In der ZEIT als deutsch landweite Zeitschrift stellte Mira Pöhlker in einem zweiseitigen Interview ihre Forschung vor. Die Southland Times berichtete in Neuseeland zur GoSouth Kampagne; der österreichische Standard zu ACTRIS. ACTRIS wurde am 25. April 2023 offiziell als europäisches Forschungsinfrastruktur-Konsortium (ERIC) gegründet.

TROPOS-Forschende waren auch im Hörfunk präsent: regional im Sachsenradio oder MDR aktuell, deutschlandweit im Deutschlandfunk und DLF-Nova zu Rauch aerosol- oder Staubthemen und im Deutschlandradio Kultur zum Klimawandel auf den Kapverden oder der Klimawirkung von Rauch.

Radio 1 vom RBB und Bayern 2 vom BR griffen die Pressemitteilung zu Biogenen Aerosolen auf und interviewten Hartmut Herrmann.

2022 sind 11 Fernsehbeiträge zu den verschiedenen Themen entstanden, im regionalen Bereich in MDR, WDR und SWR, aber auch im Ersten (ARD) bei „Wetter vor Acht“ oder bei arte die Dokumentation „Der Wind - Motor des Klimawandels“; in der Forschende der Abteilung Fernerkundung mitwirkten. Ein TV-Highlight war der 5-minütige Auftritt von TROPOS-Forscher Martin Radenz in der ORF-Dokumentation „Universum Spezial. Klima wandelt Wildnis - Zwischen Anpassung und Artensterben“ in 2023. Er verbrachte ein Jahr an der Neumayer-Station und erforschte die Atmosphäre der Antarktis und die Veränderungen des Klimas.

TROPOS-Doktorandin Gladiola Malollari von der Landwirtschaftlichen Universität Tirana war eine gefragte Gesprächspartnerin im Albanischen Fernsehen als zum ersten Mal der grüne Lidarstrahl des TROPOS-PollyXT über Tirana leuchtete - so im Beitrag von KLAN-TV und im Studio von SCAN-TV.

An neuen Formaten sind 2023 verstärkt Podcasts mit TROPOS-Forschenden in Erscheinung getreten. So zum Beispiel Oscar Ritter für den Podcast der

Transfer in science and society – overview / Transfer in Wissenschaft und Gesellschaft – Überblick

for the first time - as featured on KLAN-TV and in the SCAN-TV studio.

In 2023, more podcasts featuring TROPOS researchers appeared in new formats. For example, Oscar Ritter for the Leibniz Association podcast with the topic "How was the summer?", Heike Wex for podcast.de on "Planetary boundaries. Aerosols and air pollution" or Mira Pöhlker for the podcast of weltderphysik.de on the topic of "Clouds".

For the first time, a TROPOS researcher was able to take part in a cinema film. In "Checker Tobi and the Journey to the Flying Rivers", Mira Pöhlker played herself as a researcher at the ATTO measuring tower in the Brazilian Amazon.

The website www.tropos.de is aimed not only at researchers but also at the general public. The "Discover" section therefore aims to explain research in an easily understandable way. For example, the website "Climate change continues - What we know about the climate today" provides information about climate change.

After measurement campaigns were cancelled due to the pandemic and therefore also the reports in the campaign blog, insights into the field research on the website could be made up for in 2023: Christina Breitenstein (ACD) reported on the PolarChange2023 ship campaign in the Antarctic & amino acids. Martin Radenz (RSD) also reported from the Antarctic on his year during the COALA campaign at Neumayer III. Jonas Withuhn and Oscar Ritter described the construction and dismantling of the TROPOS pyranometer network PyrNet at the ARM observatory Southern Great Plains as part of the S2VSR 2023 campaign in the USA.

With the X-channels "@TROPOS_de" & "@TROPOS_eu", the Institute is also active on social media in German and English. The German-language channel is primarily aimed at the general public in Germany; the English-language channel is also used for networking within the scientific community. Approximately 1120 and 1,072 people and institutions respectively have subscribed to the channel ("followers"). This means that the number has increased further compared to the previous period. The development of this microblogging service is being critically monitored by TROPOS and other Leibniz institutes. Despite all the criticism levelled at X, no alternative with a comparable reach has yet been able to establish itself.

Events

A total of 37 public events were realised in 2022/2023. The formats were diverse. Well-known

Leibniz-Gemeinschaft mit dem Thema „Wie war der Sommer?“; Heike Wex für podcast.de zu „Planetare Grenzen. Aerosole und Luftverschmutzung“ oder Mira Pöhlker für den Podcast von weltderphysik.de zum Thema „Wolken.“

Erstmals konnte eine TROPOS-Forscherin in einem Kinofilm mitwirken. In „Checker Tobi und die Reise zu den fliegenden Flüssen“ spielte Mira Pöhlker sich selbst als Forscherin am ATTO-Messturm im brasilianischen Amazonasgebiet.

Das Internetangebot www.tropos.de richtet sich neben Forschenden zugleich an die breite Öffentlichkeit. Die Rubrik „Entdecken“ hat daher zum Ziel, die Forschung leicht verständlich zu erläutern. So informiert z.B. die Webseite „Der Klimawandel geht weiter - Was wir heute übers Klima wissen“ über den Klimawandel.

Nachdem bedingt durch die Pandemie Messkampagnen und damit auch die Berichte im Kampagnen-Blog ausfielen, konnten 2023 Einblicke in die Feldforschung auf der Webseite nachgeholt werden: Über die Schiffskampagne PolarChange2023 in der Antarktis & Aminosäuren berichtete Christina Breitenstein (ACD). Über sein Jahr während der COALA-Kampagne an Neumayer III berichtete ebenfalls aus der Antarktis Martin Radenz (RSD). Den Auf- und Abbau des TROPOS-Pyranometer-Netzwerks PyrNet am ARM-Observatorium Southern Great Plains im Rahmen der Kampagne S2VSR 2023 in den USA beschrieben Jonas Withuhn und Oscar Ritter.

Mit den X-Kanälen „@TROPOS_de“ & „@TROPOS_eu“ ist das Institut auch in den sozialen Medien auf deutsch bzw. englisch aktiv. Der deutschsprachige Kanal richtet sich primär an die



Fig. / Abb. 6: Backpack measurements on behalf of the LfULG analysed summer barbecue fires in Dresden and Leipzig. / Rucksackmessungen im Auftrag des LfULG untersuchten sommerliche Grillfeuer in Dresden und Leipzig. (Photo: Susanne Bastian / LfULG)

Transfer in science and society – overview / Transfer in Wissenschaft und Gesellschaft – Überblick

formats such as group visits and lectures were of course not missing, but more unusual formats such as the online discussions at “Book a Scientist”, the chat format “I’m a Scientist” or film discussions were also represented. The Swiss documentary film “Expedition Arctic” (SRF) was shown at the “Science Cinema” in the Leipzig Forum of Contemporary History. Afterwards, the audience was able to ask questions to Andreas Macke and the MOSAiC expedition participants Julian Hofer, Christian Pilz, Dietrich Althausen and Hannes Griesche in the packed 200-seat auditorium.

At the “Silbersalz” media festival in Halle, schools were also offered a film screening and discussion in the Leopoldina on the film “Children of the climate crisis - 4 girls, 3 continents, one mission”. Afterwards, Ajit Ahlawat answered the students’ questions about the air quality section of the film.

TROPOS was represented with a programme at the annual Girls’ Day and the Long Night of Science 2023. Nine different groups visited TROPOS, five of which were students from schools or universities.

TROPOS scientists gave 8 lectures - for example at the City History Museum for the exhibition “Snow of Yesterday” or at the Annaberg Climate Days. These also focused on the Arctic and the MOSAiC expedition. The second event in the Leipzig Science Network’s new “LSN Science Club” series on 17 October 2022 took place at the IOM & TROPOS. Director Andreas Macke presented the EU research infrastructure ACTRIS-D.

“Thick air in the classroom” was the title of an event at the Karl Schubert School in Leipzig with a presentation and discussion on air hygiene measures and prevention in educational institutions and daycare

formats such as group visits and lectures were of course not missing, but more unusual formats such as the online discussions at “Book a Scientist”, the chat format “I’m a Scientist” or film discussions were also represented. The Swiss documentary film “Expedition Arctic” (SRF) was shown at the “Science Cinema” in the Leipzig Forum of Contemporary History. Afterwards, the audience was able to ask questions to Andreas Macke and the MOSAiC expedition participants Julian Hofer, Christian Pilz, Dietrich Althausen and Hannes Griesche in the packed 200-seat auditorium.

breite Öffentlichkeit in Deutschland; der englischsprachige dient auch der Vernetzung innerhalb der wissenschaftlichen Community. Ca. 1120 bzw. 1.072 Personen und Institutionen haben den Kanal abonniert („Follower“). Damit konnte die Anzahl im Vergleich zum vorigen Zeitraum weiter gesteigert werden. Die Entwicklung dieses Mikroblogging-Dienstes wird von TROPOS und anderen Leibniz-Instituten kritisch beobachtet. Trotz aller Kritik an X konnte sich aber bisher noch keine Alternative etablieren, die eine vergleichbare Reichweite hat.

Veranstaltungen

2022/2023 konnten insgesamt 37 öffentliche Veranstaltungen realisiert werden. Die Formate waren dabei vielfältig. Bekannte Formate wie Gruppenbesuche und Vorträge fehlten natürlich nicht, aber auch außergewöhnlicheres, wie die Online-Gespräche bei „Book a Scientist“, das Chat-Format „I’m a Scientist“ oder Filmgespräche waren vertreten. Beim „Wissenschaftskino“ im Zeitgeschichtlichen Forum Leipzig wurde der Schweizer Dokumentarfilm „Expedition Arktis“ (SRF) gezeigt. Danach konnte das Publikum im vollbesetzten Saal mit 200 Plätzen Fragen an Andreas Macke und die MOSAiC-Expeditionsteilnehmer Julian Hofer, Christian Pilz, Dietrich Althausen und Hannes Griesche stellen.

Auch beim „Silbersalz“ Medienfestival in Halle wurde Schulen eine Filmvorführung und Diskussion in der Leopoldina zum Film „Kinder der Klimakrise – 4 Mädchen, 3 Kontinente, eine Mission“ angeboten. Anschließend beantwortete Ajit Ahlawat die Fragen der Schüler:innen zum Themenpart Luftqualität im Film.

Beim jährlich stattfindenden Girls’ Day sowie bei der „Langen Nacht der Wissenschaften 2023“ war TROPOS mit Programm vertreten. Neun verschiedene Gruppen waren am TROPOS zu Besuch, darunter fünfmal Lernende aus Schulen oder Universitäten.

TROPOS-Wissenschaftler:innen hielten 8 Vorträge - zum Beispiel im Stadtgeschichtlichen Museum zur Ausstellung „Schnee von gestern“ oder den Annaberger Klimatagen. Hier ging es auch um das Thema Arktis und die MOSAiC-Expedition. Die zweite Veranstaltung der neuen Reihe „LSN Science Club“ des Leipzig Science Networks am 17. Oktober 2022 führte an das IOM & TROPOS. Director Andreas Macke stellte die EU-Forschungsinfrastruktur ACTRIS-D vor.

„Dicke Luft im Klassenzimmer“ nannte sich eine Veranstaltung in der Karl-Schubert-Schule in Leipzig mit Vortrag und Diskussion zu Lufthygienemaßnahmen und Prävention in Bildungseinrichtungen und



Fig. / Abb. 7: The TROPOS exhibition stand with exhibits as part of the launch event “SPIN2030 - Agenda for Science” in February 2023 in the Congress Hall at Leipzig Zoo. / Der TROPOS-Stand mit Exponaten im Rahmen der Auftaktveranstaltung „SPIN2030 - Agenda für die Wissenschaft“ im Februar 2023 in der Kongresshalle am Zoo Leipzig. (Photo: Tilo Arnhold / TROPOS)

Transfer in science and society – overview / Transfer in Wissenschaft und Gesellschaft – Überblick

centres. Hartmut Herrmann represented TROPOS here with his expertise.

TROPOS was active in direct policy advice as part of the “Leibniz in the Bundestag” format. Two talks on wood heating systems were held with members of the Bundestag in 2022 and one on indoor air quality and infection control in 2023.

The following events with a political focus should be emphasised for the reporting period:

The Leibniz Institutes in Saxony celebrated their 30th anniversary with a ceremony on 14 September 2022 at the International Congress Centre Dresden. In addition to the Minister President and the Minister of Science, other well-known representatives from the federal and state governments also took part. The Saxon science campaign SPIN2030 to showcase the achievements of Saxony as a science location was launched on 3 February with an opening event attended by the Minister President and Science Minister, at which TROPOS was represented with an information stand.

Pedro Ivo Ferraz da Silva, Head of the Department of Science, Technology & Innovation and Cooperation of the Brazilian Embassy in Berlin, visited the cloud laboratory on 6 April 2023 and spoke with Mira Pöhlker about the measurements at the ATTO rainforest station in Brazil.

TROPOS is also actively involved in the publicity campaigns of the German Climate Consortium (DKK) the Climate Navigator and the Leibniz Association. In 2023, the Leibniz Association's Press Working Group met in Leipzig, organised by the Leibniz Institutes in Leipzig.

Equal opportunities and promotion of young talent

Gender equality is implemented as a guiding principle at TROPOS. The institute therefore fulfils the equality standards of the Leibniz Association. A key instrument in this is the equality plan, the implementation of which is intended to promote and sustainably ensure equal opportunities for people of all genders at TROPOS. It focuses on measures to ensure absolutely non-discriminatory collaboration at the institute, from the recruitment process to further increasing the proportion of women in post-doctoral positions, permanent positions, scientific management positions and committees. The plan drawn up in August 2022 is valid for 4 years and is part of the newly implemented personnel development plan at TROPOS. TROPOS's targets for increasing the proportion of women are based on the Leibniz Association's cascade model, whereby a step-by-step



Fig. / Abb. 8: SILBERSALZ School Cinema on 21 June 2023 in the large hall of the LEOPOLDINA in Halle/Saale. / SILBERSALZ Schulkino am 21.06.2023 im großen Saal der LEOPOLDINA in Halle/Saale. (Photo: Agnes Fischer / Silbersalz)

Kita. Hartmut Herrmann vertrat hier mit seiner Expertise das TROPOS.

In der direkten Politikberatung war TROPOS im Rahmen des Formates „Leibniz im Bundestag“ aktiv. Zwei Gespräche zum Thema Holzheizungen wurden 2022 und ein Gespräch zu Luftqualität in Innenräumen und Infektionsschutz 2023 mit Bundestagsabgeordneten geführt.

Als weitere Veranstaltungen mit politischem Bezug sind für den Berichtszeitraum folgende hervorzuheben:

Die Leibniz-Institute in Sachsen feierten das
runde 30-jährige Jubiläum mit einem Festakt am 14.
September 2022 im Internationalen Kongresszentrum
Dresden. Daran nahmen neben dem Ministerpräsidenten
und dem Wissenschaftsminister auch weiteren
namhafte Vertretern von Bund und Land teil. Die säch-
sische Wissenschaftskampagne SPIN2030 zur Darstel-
lung der Leistungen des Wissenschaftsstandortes
Sachsen wurde am 3. Februar mit einer Eröffnungs-
veranstaltung unter Anwesenheit des Ministerpräsidenten
und Wissenschaftsministers gestartet, auf der
TROPOS mit einem Informationsstand vertreten war.

Pedro Ivo Ferraz da Silva, Leiter der Abteilung für Wissenschaft, Technologie & Innovation und Zusammenarbeit der brasilianischen Botschaft in Berlin, besuchte am 6. April 2023 das Wolkenlabor und sprach mit Mira Pöhlker über die Messungen an der Regenwald-Station ATTO in Brasilien.

Am 5. Oktober legte Bundespräsident Steinmeier, gemeinsam mit dem Präsidenten der Kapverden den Grundstein für ein neues Laborgebäude am Cabo-Verde-Atmosphären-Observatorium (CVAO) und besuchte anschließend das Ocean Science Centre Mindelo (OSCM) und hier auch die Fernerkundungs-Messstation des TROPOS.

Transfer in science and society – overview / Transfer in Wissenschaft und Gesellschaft – Überblick



Fig. / Abb. 9: Martin Radenz from TROPOS (2nd from right) was one of 10 nominees for the Leibniz Association's doctoral prize in 2022. / Martin Radenz vom TROPOS (2. v r.) war unter den 10 Nominierter für den Promotionspreis der Leibniz-Gemeinschaft im Jahr 2022. (Photo: Andreas Macke / TROPOS)

model adapted to the current position situation at the institute has been defined.

To promote the scientific careers of women, the workshop “Career Promotion” was offered at TROPOS in June 2023, and the regular FEM Café provides a platform for exchange, for example on applying for third-party funding and balancing work and career.

On 10.12.2020, the “berufundfamilie” audit certificate was confirmed following a successful dialogue process. This gives the certificate, which is regarded as a seal of quality for a strategically designed family and life-phase-conscious personnel policy, its permanent character. The 2023-2026 action programme was drawn up on Dialogue Day 2023.

Promoting young talent. TROPOS actively promotes young scientists in Bachelor's and Master's programmes, during doctoral projects and beyond. The institute is closely involved in the development and implementation of the new Bachelor's and Master's degree programmes at Leipzig University and is responsible for 12 modules.

Highly qualified employees participate in teaching at Leipzig University as joint appointments. In addition to students of meteorology, chemistry and physics students are also trained at TROPOS (see list, p. 168).

The institute offers young scientists individually tailored and supervised realisation of their doctorates within the framework of structured doctoral training. TROPOS staff hold courses at universities, international summer schools, training courses and networks (see list, p. 165).

The Leibniz Graduate School on “Clouds, Aerosols and Radiation”, founded in July 2012, has established a solid foundation for doctoral training at

Außerdem ist TROPOS an den Öffentlichkeitsaktionen des Deutschen Klimakonsortiums (DKK), des Klimanavigators und der Leibniz-Gemeinschaft aktiv beteiligt. 2023 traf sich der Arbeitskreis Presse der Leibniz-Gemeinschaft in Leipzig, organisiert von den Leipziger Leibniz-Instituten.

Chancengleichheit und Nachwuchsförderung

Gleichstellung ist am TROPOS als Leitprinzip implementiert. Das Institut erfüllt damit die Gleichstellungsstandards der Leibniz-Gemeinschaft. Ein wesentliches Instrument dabei ist der Gleichstellungsplan, dessen Umsetzung die Chancengleichheit für Menschen aller Geschlechter am TROPOS fördern und nachhaltig sichern soll. Er enthält schwerpunktmäßig Maßnahmen zur absolut diskriminierungsfreien Zusammenarbeit am Institut vom Einstellungsverfahren bis zur weiteren Erhöhung des Anteils von Frauen im Post-Doc-Bereich, in Festanstellungen, wissenschaftlichen Führungspositionen und Gremien. Der im August 2022 aufgestellte Plan gilt für 4 Jahre und ist Teil des am TROPOS neu implementierten Personalentwicklungsplanes. TROPOS orientiert sich in den Zielvorgaben für die Erhöhung des Frauenanteils am Kaskadenmodell der Leibniz-Gemeinschaft, wobei ein an die momentane institutsspezifische Stellsituation angepasstes Stufenmodell definiert wurde.

Zur Förderung der wissenschaftlichen Karrieren von Frauen wurde im Juni 2023 der Workshop „Karriereförderung“ am TROPOS angeboten, das regelmäßig stattfindende FEM-Café bietet eine Austauschplattform, zum Beispiel zur Beantragung von Drittmitteln und der Vereinbarkeit von Beruf und Karriere.

Zum 10.12.2020 wurde das Zertifikat zum Audit berufundfamilie nach erfolgreich durchlaufenem Dialogverfahren bestätigt. Damit erhält das Zertifikat, das als Qualitätssiegel für eine strategisch angelegte familien- und lebensphasenbewusste Personalpolitik gilt, seinen dauerhaften Charakter. Am Dialogtag 2023 wurde das Handlungsprogramm 2023-2026 ausgearbeitet.

Nachwuchsförderung. TROPOS fördert aktiv den wissenschaftlichen Nachwuchs in der Bachelor- und Masterausbildung, während der Promotionsvorhaben und darüber hinaus. Das Institut ist eng in die Entwicklung und in die Durchführung der neuen Bachelor- und Masterstudiengänge an der Universität Leipzig eingebunden und ist für 12 Module verantwortlich.

Hochqualifizierte Mitarbeiterinnen und Mitarbeiter beteiligen sich als gemeinsame Berufungen an der Lehre der Universität Leipzig. Neben Studierenden der

Transfer in science and society – overview / Transfer in Wissenschaft und Gesellschaft – Überblick

TROPOS together with the University of Leipzig and pools the joint expertise in the coupled areas of "aerosols-clouds-radiation". With currently 50 members, it is part of the Graduate Academy Leipzig (GA).

Promoting young talent contributes to the successful scientific function of the Institute and to securing its future. The Institute has also drawn up a personnel development plan for this purpose. This represents a framework in which specific measures and agreements are integrated and labelled accordingly (strategic instruments, personnel planning according to research strategy, measures and objectives for the selection and induction of personnel, health management, dual careers and teaming as well as support for transitions).

Creating the future. TROPOS supports the path to studying natural sciences by showing career prospects in the field of atmospheric research. Pupils learn about research work in a fun way and get to talk to researchers from the STEM field. As part of the STEM initiative, which aims to get young people interested in a career in maths, IT, science and technology, TROPOS also takes part in Girls' Day, the day of the future. On this day in 2022, interested schoolgirls were able to find out about research work and training opportunities in an interactive online programme and again directly at the institute in 2023. Two internships for school pupils and five internships to accompany their studies were realised in 2022/23.

TROPOS will continue to finance at least one apprenticeship training position from budget funds in the coming years.

Significant collaborations and networking in research

Numerous established networks within the Leibniz Association, with universities, with Max Planck Institutes, with institutes of the Helmholtz Association and at international level demonstrate the current status of TROPOS networking in interdisciplinary aerosol and cloud research. TROPOS is similarly networked at European and global level and is actively developing research programmes here (see list, p. 183).

Technological developments at TROPOS lead to international standards in the experimental direct and indirect detection of aerosols and hydrometeors from the ground to the high atmosphere as well as in the modelling of the complex multiphase system.

Cooperation opportunities within the Leibniz Association and beyond are being expanded as part of the Leibniz Association's competition fund. The

Meteorologie werden am TROPOS auch Chemie- und Physikstudierende ausgebildet (siehe Liste, S. 168).

Das Institut bietet jungen Wissenschaftlerinnen und Wissenschaftlern individuell abgestimmte und von einem Betreuungsteam begleitete Realisierung ihrer Promotionen im Rahmen der strukturierten Promovendenausbildung. Mitarbeitende des TROPOS halten Kurse an Universitäten, bei internationalen Sommerschulen, Ausbildungskursen und -netzwerken (siehe Liste, S. 165).

Die im Juli 2012 gegründete Leibniz-Graduiertenschule zu „Wolken, Aerosolen und Strahlung“ hat die Promovendenausbildung am TROPOS gemeinsam mit der Universität Leipzig auf eine solide Grundlage gestellt und bündelt die gemeinsame Expertise in den gekoppelten Bereichen „Aerosole-Wolken-Strahlung“. Sie ist mit aktuell 50 Mitgliedern in der „Graduate Academy Leipzig“ (GA) verortet.

Nachwuchsförderung trägt zu einer erfolgreichen wissenschaftlichen Funktion des Instituts und deren Sicherung für die Zukunft bei. Das Institut hat auch hierfür einen Personalentwicklungsplan erstellt. Dieser stellt einen Rahmen dar, in den konkrete Maßnahmen und Vereinbarungen eingebunden und entsprechend gekennzeichnet sind (strategische Instrumente, Personalplanung nach Forschungsstrategie, Maßnahmen und Ziele zur Auswahl und Einarbeitung von Personal, Gesundheitsmanagement, Dual Career und Teaming sowie Begleitung von Übergängen).

Zukunft schaffen. TROPOS unterstützt den Weg zum naturwissenschaftlichen Studium, indem berufliche Perspektiven im Bereich der Atmosphärenforschung aufgezeigt werden. Schülerinnen und Schüler lernen die Forschungsarbeit auf spielerische Art kennen und kommen mit Forschenden aus dem



Fig. / Abb. 10: Launch of a weather balloon at the "Langen Nacht der Wissenschaften 2023" in Leipzig. / Start eines Wetterballons bei der „Langen Nacht der Wissenschaften 2023“ in Leipzig. (Photo: Tilo Arnhold / TROPOS)

Transfer in science and society – overview / Transfer in Wissenschaft und Gesellschaft – Überblick

Institute is linked to numerous international organisations through cooperation agreements (see list, p. 183).

TROPOS continues to participate in the research network Integrated Earth System Research (iESF), which aims to gain action-relevant knowledge for society about people in the Earth system. In particular, the ecological carrying capacity of the Earth system is to be determined and sustainable development paths derived from this.

TROPOS continues to be involved in the Leibniz research network “Infections’21”, as well as in the research network “CrisEn” (Environmental Crisis - Crisis Environments), which emerged from the research network “Crises in a Globalised World”.

TROPOS plays a leading role in the European research infrastructure network ACTRIS (Aerosols, Clouds, and Trace Gases Research InfraStructure Network) and coordinates the German contribution ACTRIS-D as part of the National Roadmap of the Federal Ministry of Education and Research. More than 120 institutions in over 20 countries are already involved at European level. In June 2022, TROPOS organised the official ACTRIS-D kick-off event with partners from politics and science. ACTRIS was officially established as a European Research Infrastructure Consortium (ERIC) on 25 April 2023 and has thus become a mature and sustainable research infrastructure in 17 countries. The ACTRIS facilities form the world's largest multi-site infrastructure for atmospheric research, providing its users with free access



Fig. / Abb. 11: Film premiere on 01.10.2023 in Munich: Tobi Krell ('Checker Tobi'), cave expert Xuan-An Amy Truong, Marina M. Blanke ('Tobi's Best Friend'), cloud researcher Mira Pöhlker and director Johannes Honsell, who died in 2023 (from left to right). / Filmpremiere am 01.10.2023 in München: Tobi Krell ('Checker Tobi'), Höhlenexpertin Xuan-An Amy Truong, Marina M. Blanke ('Tobis beste Freundin'), Wolkenforscherin Mira Pöhlker und der 2023 verstorbene Regisseur Johannes Honsell (v.l.n.r.). (Photo: Christopher Poehlker / MPIC)

MINT-Bereich ins Gespräch. Im Rahmen der MINT-Initiative, die zum Ziel hat, Jugendliche für einen Beruf in den Fächern Mathematik, Informatik, Naturwissenschaften und Technik zu begeistern, beteiligt sich TROPOS auch am Girls' Day, dem Zukunftstag. 2022 konnten sich an diesem Tag interessierte Schülerinnen bei einem Online-Programm interaktiv über die Forschungsarbeit und Ausbildungsmöglichkeiten informieren und 2023 wieder am Institut direkt. Zwei Praktika für Schüler:innen und fünf studienbegleitende Praktika konnten 2022/23 realisiert werden.

TROPOS wird auch in den nächsten Jahren mindestens einen Lehrlingsausbildungssplatz aus Haushaltssmitteln finanzieren.

Bedeutende Kooperationen und Vernetzung in der Forschung

Zahlreiche bisher gewachsene Vernetzungen innerhalb der Leibniz-Gemeinschaft, mit Universitäten, mit Max-Planck-Instituten, mit Instituten der Helmholtz-Gemeinschaft sowie auf internationaler Ebene zeigen den derzeitigen Stand der Vernetzung des TROPOS in der interdisziplinären Aerosol- und Wolkenforschung. Ähnlich ist TROPOS auf der europäischen und weltweiten Ebene vernetzt und entwickelt hier aktiv Forschungsprogramme (siehe Liste, S. 183).

Technologische Entwicklungen am TROPOS führen zu internationalen Standards in der experimentellen direkten und indirekten Erfassung von Aerosolen und Hydrometeoren vom Boden bis zur hohen Atmosphäre sowie in der Modellierung des komplexen Multiphasensystems.

Im Rahmen des Wettbewerbsfonds der Leibniz-Gemeinschaft werden die Kooperationsmöglichkeiten innerhalb der Leibniz-Gemeinschaft und darüber hinaus ausgebaut. Durch Kooperationsvereinbarungen ist das Institut mit zahlreichen internationalen Einrichtungen verbunden (siehe Liste, S. 183).

TROPOS beteiligt sich weiterhin am Forschungsnetzwerk Integrierte Erdsystemforschung (iESF), das für die Gesellschaft handlungsrelevante Erkenntnisse über die Menschen im Erdsystem gewinnen will. Vor allem die ökologischen Tragfähigkeiten des Erdsystems sollen bestimmt und daraus nachhaltige Entwicklungspfade abgeleitet werden.

Am Leibniz-Forschungsverbund „Infections’21“ ist TROPOS weiterhin beteiligt; ebenso am Forschungsnetzwerk „CrisEn“ (Environmental Crisis - Crisis Environments), dass aus dem Forschungsverbund „Krisen einer globalisierten Welt“ entstanden ist.

TROPOS spielt eine führende Rolle im Netzwerk der europäischen Forschungsinfrastruktur

Transfer in science and society – overview / Transfer in Wissenschaft und Gesellschaft – Überblick

to instruments, expertise, training opportunities and data management services.

TROPOS is also still involved in the European and national roadmap project IAGOS (In-service Aircraft for a Global Observing System) and, together with its national partners, has successfully completed the set-up phase and commenced operations in December 2022.

In July 2022, the defence of the application for a new large-scale research centre for climate adaptation in Leipzig (CLAIRE) took place, to which TROPOS had contributed research ideas in the field of air quality and urban health. The decision was made in favour of the German Centre for Astrophysics (DZA) and the Centre for the Transformation of Chemistry (CTC).

To ensure that the close collaboration with the Physics and Technology Institute "S. U. Umarov" of the Academy of Sciences of the Republic of Tajikistan can continue in the long term, a Memorandum of Understanding between the two institutes on joint activities in the field of atmospheric dust research was signed in August 2022.

As part of the cooperation agreement with the German Weather Service (DWD), a joint meeting was held in December 2022 at which joint research in the five areas of boundary layer processes, remote measurement systems, satellite data validation, data provision and model development was specified. The next meeting is scheduled for summer 2024 and will also deal with the topic of air quality.

TROPOS is significantly involved in the development of the cluster project "Breathing Nature" (Breathing Nature: Interactions between Biodiversity, Climate and Human Behaviour), with which Leipzig University is entering the current round of the Excellence Strategy of the German federal and state governments.

The excellent cooperation with the Alfred Wegener Institute for Polar and Marine Research continued with workshops on Polarstern cruise planning, joint flight campaigns and participation in a wintering at the Neumayer III station with extensive measuring equipment from TROPOS.

TROPOS has also expanded its cooperation with the Max Planck Institute for Chemistry (MPIC) and is involved in the measurements and scientific publication of data from the Amazon Tall Tower Observatory (ATTO) in the tropical rainforest as part of the joint collaboration. Together with the University of Miami and the MPIC, TROPOS is responsible for measuring the physical parameters of aerosols at the Barbados Atmospheric Chemistry Observatory (BACO).

TROPOS plays a central role in the development and use of satellite-based earth observation and



Fig. / Abb. 12: Presentation of the 3 research projects with which Leipzig University is applying for the Excellence Strategy of the federal and state governments. Two of which, including "Breathing Nature", have reached the final round. / Vorstellung der 3 Forschungsvorhaben, mit denen sich die Universität Leipzig in der Exzellenzstrategie des Bundes und der Länder bewirbt. Zwei davon, darunter „Breathing Nature“, sind in die Endrunde gelangt. (Photo: Tilo Arnhold / TROPOS)

ACTRIS (Aerosols, Clouds, and Trace Gases Research InfraStructure Network) und koordiniert den deutschen Beitrag ACTRIS-D im Rahmen der Nationalen Roadmap des Bundesministeriums für Bildung und Forschung. Auf europäischer Ebene sind bereits mehr als 120 Institutionen in über 20 Ländern beteiligt. Im Juni 2022 führte TROPOS die offizielle Auftaktveranstaltung von ACTRIS-D mit Partnern aus Politik und Wissenschaft durch. ACTRIS wurde am 25. April 2023 offiziell als europäisches Forschungsinfrastruktur-Konsortium (ERIC) gegründet und ist damit zu einer ausgereiften und nachhaltigen Forschungsinfrastruktur in 17 Ländern geworden. Die ACTRIS-Einrichtungen bilden die weltweit größte, standortübergreifende Infrastruktur für die Atmosphärenforschung und bieten ihren Nutzern freien Zugang zu Instrumenten, Fachwissen, Schulungsmöglichkeiten und Datenverwaltungsdiensten.

Auch im europäischen und nationalen Roadmap-Projekt IAGOS (In-service Aircraft for a Global Observing System) ist TROPOS weiterhin beteiligt und hat gemeinsam mit den nationalen Partnern die Aufbau-Phase erfolgreich abgeschlossen und im Dezember 2022 den operationellen Betrieb aufgenommen.

Im Juli 2022 fand die Verteidigung des Antrags für ein neues Großforschungszentrum zur Klimaanpassung in Leipzig (CLAIRE) statt, zu dem TROPOS Forschungsideen im Bereich Luftqualität und urbane Gesundheit beigesteuert hatte. Die Entscheidung fiel auf das Deutsche Zentrum für Astrophysik (DZA) und das „Center for the Transformation of Chemistry“ (CTC).

Damit die enge Zusammenarbeit mit dem Physikalisch-Technischen Institut „S. U. Umarov“ der Akademie der Wissenschaften der Republik

Transfer in science and society – overview / Transfer in Wissenschaft und Gesellschaft – Überblick



Fig. / Abb. 13: Laying of the foundation stone for the new laboratory building at the international Cape Verde Atmospheric Observatory (CVAO) with Federal President Frank-Walter Steinmeier and the President of the Republic of Cabo Verde José Maria Neves. (from left to right) / Grundsteinlegung für das neue Laborgebäude am internationalen Cabo-Verde-Atmosphären-Observatorium (CVAO) mit Bundespräsident Frank-Walter Steinmeier und dem Präsident der Republik Cabo Verde José Maria Neves (v.l.n.r.). (Photo: Edson Silva Delgado, GEOMAR)

is involved in the international consortia of the first wind lidar AEOLUS of the European Space Agency ESA and the upcoming energy balance system EarthCARE. TROPOS contributed significantly to the great success of the AEOLUS mission by providing continuous global reference measurements for the validation of wind and aerosol/cloud products from the beginning to the end of the mission.

TROPOS continues to be involved in developing the ERATOSTHENES Remote Sensing Centre of Excellence (ECoE) in Cyprus into a leading digital innovation hub (DIH) for Earth observation and geodata. In June 2022, the representatives of all EXCELSIOR partner organisations met for the 2nd review meeting. In early February 2023, the TROPOS remote sensing team visited its Cypriot partners from the EXCELSIOR project to commission a new Doppler wind lidar as part of the CARO (Cyprus Atmospheric Remote Sensing Observatory) facility.

TROPOS participates in the National Initiative for Earth System Modelling (NatESM). This initiative aims to promote and efficiently utilise the use of future supercomputers for components of simulation-based climate research in Germany.

The Collaborative Research Centre/Transregio (CRC/TRR) 172 "Arctic Amplification: Climate-relevant Atmospheric and Surface Processes and Feedback Mechanisms (AC)³" will enter its third funding phase after a successful evaluation in June 2023 with the Universities of Leipzig (spokesperson), Bremen and Cologne as well as the AWI and TROPOS. The overarching goal is to achieve fundamental and ground-breaking progress in our understanding of Arctic

Tadschikistan langfristig weitergeführt werden kann, wurde im August 2022 ein Memorandum of Understanding zwischen den beiden Instituten zu gemeinsamen Aktivitäten auf dem Gebiet der atmosphärischen Staubforschung unterzeichnet.

Im Rahmen der Kooperationsvereinbarung mit dem Deutschen Wetterdienst (DWD) fand im Dezember 2022 ein gemeinsames Treffen statt, auf dem gemeinsame Forschung in den fünf Bereichen Grenzschichtprozesse, Fernmesssysteme, Satelliten-datenvalidierung, Datenbereitstellung, und Modellentwicklung konkretisiert wurde. Das nächste Treffen ist für Sommer 2024 angesetzt und soll zusätzlich das Thema Luftqualität behandeln.

TROPOS ist maßgeblich an der Entwicklung des Clustervorhabens „Breathing Nature“ (Atmende Natur: Wechselwirkungen zwischen Biodiversität, Klima und menschlichem Verhalten) beteiligt, mit dem die Universität Leipzig in die aktuelle Runde der Exzellenzstrategie des Bundes und der Länder geht.

Die exzellente Kooperation mit dem Alfred-Wegener-Institut für Polar- und Meeresforschung wurde im Rahmen von Workshops zur Polarstern-Fahrtplanung, gemeinsamen Flugkampagnen und der Beteiligung an einer Überwinterung an der Neumayer III-Station mit umfangreicher Messausstattung des TROPOS fortgeführt.

Zudem hat TROPOS seine Kooperationen zu dem Max-Planck-Institut für Chemie (MPIC) ausgebaut und beteiligt sich im Rahmen der gemeinsamen Zusammenarbeit an den Messungen und der wissenschaftlichen Veröffentlichung der Daten vom Amazon Tall Tower Observatory (ATTO) im tropischen Regenwald. Zusammen mit der Universität Miami und dem MPIC ist TROPOS für die Messung der physikalischen Parameter der Aerosole am Barbados Atmospheric Chemistry Observatory (BACO) verantwortlich.

TROPOS spielt eine zentrale Rolle in der Entwicklung und Nutzung der satellitengetragenen Erdbeobachtung und ist hier an den internationalen Konsortien des ersten Windlidars AEOLUS der Europäischen Weltraumorganisation ESA und des kommenden Energiebilanzsystems EarthCARE beteiligt. TROPOS trug maßgeblich zum großen Erfolg der AEOLUS-Mission bei, indem es von Beginn bis zum Ende der Mission weltweit kontinuierliche Referenzmessungen zur Validierung der Wind- und Aerosol-/Wolkenprodukte lieferte.

TROPOS ist weiterhin am Aufbau des Fernerkundungszentrums ERATOSTHENES Centre of Excellence (ECoE) in Zypern zu einem führenden digitalen Innovationszentrum (DIH) für Erdbeobachtung und Geodaten beteiligt. Im Juni 2022 trafen sich die Vertreter aller EXCELSIOR-Partnerorganisationen zum 2. Review-Meeting. Anfang Februar 2023

Transfer in science and society – overview / Transfer in Wissenschaft und Gesellschaft – Überblick

amplification and to improve the reliability of models for predicting dramatic warming in the Arctic.

Together with TROPOS and other partners, Leipzig University is applying for a DFG Collaborative Research Centre on Biodiversity and Climate (CRC “Biodiversity buffers Climate Extremes”). This application was positively reviewed on 6 December 2022 and invited to submit a full proposal. TROPOS is also participating in the new DFG Research Training Group Economics of Connected Natural Commons (ECO-N) at Leipzig University, which is researching the sustainable use of natural commons.

The President of the Republic of Cabo Verde José Maria Neves and German President Frank-Walter Steinmeier laid the foundation stone for a new laboratory building at the Cape Verde Atmospheric Observatory (CVAO) on 5 October 2013 and inaugurated the new TROPOS remote sensing station at the Ocean Science Center Mindelo (OSCM) of the GEOMAR Research Centre. CVAO is operated by a consortium of the Cape Verdean Institute of Meteorology and Geophysics (INMG), the Leibniz Institute for Tropospheric Research (TROPOS) in Leipzig, the Max Planck Institute for Biogeochemistry in Jena (MPI-BGC) and the University of York in the UK.

The Chacaltaya Observatory (CHC) in the Bolivian Andes has officially been one of the most important climate stations in the world since 11 October 2013. It is the second station in South America to become part of the “Global Atmospheric Watch” programme of the World Meteorological Organisation (WMO). The observatory has been continuously collecting data on the composition of the atmosphere for 12 years, in particular on aerosols, reactive gases and greenhouse gases. The station at an altitude of 5240 metres is the highest observatory of its kind in the world and is operated by an international consortium. TROPOS has contributed its expertise in measuring aerosols.

In the last two years, TROPOS has intensified its activities with the German research aircraft HALO (High Altitude and Long-Range Research Aircraft) and has been involved in two campaigns on particle formation in the upper troposphere. In addition, a campaign to investigate particle formation processes and their interaction with clouds in the Southern Ocean is planned for 2025 under the leadership of TROPOS.

Significant collaborations also exist with important research institutes in China, with which joint studies are often carried out, particularly on air quality and ocean-atmosphere interactions. The most important partners here are Fudan University in Shanghai and Shandong University with the School of Environmental Science and Engineering in Qingdao.

besuchte das TROPOS-Fernerkundungsteam seine zypriotischen Partner aus dem EXCELSIOR-Projekt, um ein neues Doppler-Wind-Lidar als Teil der CARO (Cyprus Atmospheric Remote Sensing Observatory) Anlage in Betrieb zu nehmen.

TROPOS beteiligt sich an der Nationalen Initiative für Erdsystemmodellierung (NatESM). Diese Initiative strebt an, den Einsatz zukünftiger Supercomputer für Komponenten der simulationsbasierten Klimaforschung in Deutschland voranzutreiben und effizient zu nutzen.

Der Sonderforschungsbereich/Transregio (SFB/TRR) 172 „Arktische Verstärkung: Klimarelevante Atmosphären- und Oberflächenprozesse und Rückkopplungsmechanismen (AC)³“ geht nach erfolgreicher Evaluierung im Juni 2023 mit den Universitäten Leipzig (Sprecher), Bremen und Köln sowie dem AWI und TROPOS in die dritte Förderphase. Übergeordnetes Ziel ist es, grundlegende und wegweisende Fortschritte in unserem Verständnis der arktischen Verstärkung zu erzielen und die Verlässlichkeit von Modellen zur Vorhersage der dramatischen Erwärmung in der Arktis zu verbessern.

Die Universität Leipzig bewirbt sich zusammen mit TROPOS und anderen Partnern um einen DFG-Sonderforschungsbereich zu Biodiversität und Klima (CRC „Biodiversity buffers Climate Extremes“). Dieser Antrag wurde am 06.12.2022 positiv begutachtet und zum Vollantrag aufgefordert. TROPOS beteiligt sich ebenfalls am neuen DFG-Graduiertenkolleg Economics of Connected Natural Commons (ECO-N) der Universität Leipzig, welches die nachhaltige Nutzung natürlicher Gemeinschaftsgüter erforscht.

Der Präsident der Republik Cabo Verde José Maria Neves und Bundespräsident Frank-Walter Steinmeier legten am 5.10.23 den Grundstein für ein neues Laborgebäude am Cape Verde Atmospheric



Fig. / Abb. 14: Brazilian delegation visits the TROPOS cloud lab on 6 April 2023. / Brasilianische Delegation zu Besuch im Wolkenturm des TROPOS am 06.04.2023. (Photo: Ina Burkert / TROPOS)

Transfer in science and society – overview / Transfer in Wissenschaft und Gesellschaft – Überblick



Fig. / Abb. 15: In November 2022, the green beam of a Polly lidar was seen over Tirana for the first time. The measurements are the first of their kind in Albania. / Im November 2022 war erstmals der grüne Strahl eines Polly-Lidars über Tirana zu sehen. Die Messungen sind die ersten ihrer Art in Albanien. (Photo: Dietrich Althausen, TROPOS)

Collaboration in research and teaching was agreed with the Federal University Oye, Ekiti in Nigeria with a MoU, which resulted from a very successful research stay at TROPOS by a member of this university.

Observatory (CVAO) und weihten die neue Fernerkundungsstation des TROPOS am Ocean Science Center Mindelo (OSCM) des GEOMAR Forschungszentrums ein. CVAO wird von einem Konsortium aus dem kapverdischen Institut für Meteorologie und Geophysik (INMG), dem Leibniz-Institut für Troposphärenforschung (TROPOS) in Leipzig, dem Max-Planck-Institut für Biogeochemie in Jena (MPI-BGC) und der Universität York in Großbritannien betrieben.

Das Chacaltaya Observatory (CHC) in den Bolivianischen Anden ist seit dem 11.10.23 offiziell eine der wichtigsten Klimastationen der Welt. Als zweite Station in Südamerika wurde sie Teil des Programmes „Global Atmospheric Watch“ der Weltmeteoroologieorganisation WMO. Das Observatorium sammelt seit 12 Jahren lang kontinuierlich Daten über die Zusammensetzung der Atmosphäre, insbesondere über Aerosole, reaktive Gase und Treibhausgase. Die Station auf 5240 m Höhe ist das höchste Observatorium seiner Art weltweit und wird von einem internationalen Konsortium betrieben. TROPOS hat dabei seine Expertise beim Messen von Aerosolen eingebracht.

In den letzten zwei Jahren hat TROPOS seine Aktivitäten mit dem deutschen Forschungsflugzeug HALO (High Altitude and Long Range Research Aircraft) verstärkt und war an zwei Kampagnen zur Partikelneubildung in der oberen Troposphäre beteiligt. Außerdem ist für 2025 eine Kampagne zur Untersuchung von Partikelneubildungsprozessen und deren Wechselwirkung mit Wolken im südlichen Ozean unter der Leitung von TROPOS geplant.

Bedeutende Kooperationen bestehen auch zu wichtigen Forschungsinstituten in China, mit denen oft gemeinsame Untersuchungen insbesondere zur Luftqualität und zur Ozean-Atmosphärenwechselwirkung durchgeführt werden. Die wichtigsten Partner hier sind die Fudan Universität in Shanghai und die Shandong-Universität mit der School of Environmental Science and Engineering in Qingdao.

Mit der Federal University Oye, Ekiti in Nigeria wurde eine Zusammenarbeit in Forschung und Lehre mit einem MoU vereinbart, die sich aus einen sehr erfolgreichen Forschungsaufenthalt eines Mitglieds dieser Universität am TROPOS ergab.



166 / 64 female
Employees

2022 / 2023

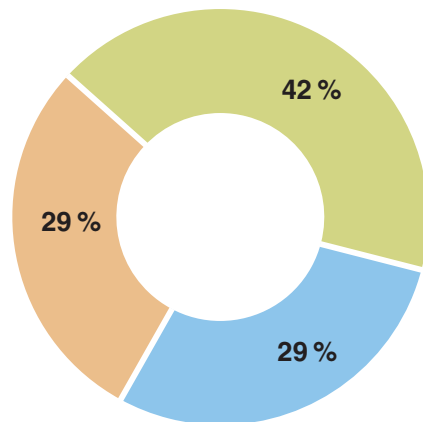
83 / 21 female
Scientists
36 / 18 female
Doctoral candidates

7 / 4
Doctoral theses

6 / 12
Master of Science
2 / 8
Bachelor of Sciences

21 Mio €

Budget in total



- Federal Ministry of Education and Research
- The Free State of Saxony
- External Funding



2022 / 2023

102 / 90

Publications
(peer-reviewed)

204 / 315

Reviews

6 / 9

Scientific events

2022 / 2023

8 / 6

National
campaigns

21 / 18

International
campaigns

4 / 4

Long-term
measurements

2022 / 2023

37

National
cooperations

49

International
cooperations

2022 / 2023

17 / 20

Public events

17 / 19

Press releases

140 / 161

Media publications

Articles



Ozone and its precursors in Saxony - Trends, impacts, and drivers

Dominik van Pinxteren, Yaru Wang, Vanessa Engelhardt, Max Hell, Bernd Heinold, Ralf Wolke, Hartmut Herrmann

Die mittleren Ozonkonzentrationen in Sachsen, Deutschland und Europa bewegen sich seit etwa 20 Jahren auf hohem Niveau und die chronische Belastung für Mensch und Vegetation ist immer noch zu hoch. In einem umfassenden Projekt für das sächsische Umweltlandesamt (LfULG) untersuchte TROPOS Konzentrationstrends, Auswirkungen auf die Vegetation und wichtige Einflussfaktoren bezüglich Ozon in Sachsen. Es ergaben sich eine Reihe von Befunden, die in den ersten Teilen dieses Beitrags beschrieben sind. Ein wichtiger Einflussfaktor, der mangels verfügbarer experimenteller Daten nicht untersucht werden konnte, sind die Konzentrationen flüchtiger organischer Kohlenwasserstoffe (VOC) als wichtige Ozonvorläuferverbindungen. Um diese Lücke zu schließen, prüft TROPOS in einem weiteren aktuellen Projekt die Eignung kommerzieller Online-GC-Instrumente für die Integration in Überwachungsnetze. Erste Ergebnisse und Bewertungen hierzu sind im letzten Teil des vorliegenden Beitrages wiedergegeben.

Introduction

Ozone is a trace gas acting both as an air pollutant and a short-lived climate forcer (SLCF). It has a strong impact on human health, vegetation including forests and agricultural crops, as well as on the Earth's climate.

Processes, sources, sinks and effects involving ozone have been studied for many decades [Clifton *et al.*, 2020; Cooper *et al.*, 2014; Monks *et al.*, 2015] and, for long, have been central in atmospheric chemistry research as a whole. Ozone is exclusively formed through secondary reactions in the atmosphere. Primarily emitted nitrogen oxides and volatile organic hydrocarbons (VOCs) as the most important ozone precursor compounds are linked in a complex chemical reaction system that contributes to the formation of tropospheric ozone depending on the prevailing chemical regime [Seinfeld und Pandis, 1998].

The understanding of these complex fundamental relationships led to a reduction in peak ozone levels, particularly in the 1990s, due to targeted reductions in emissions of precursor compounds which had often been guided by the respective atmospheric chemistry research. Since about the year 2000, however, average ozone concentrations in Germany and

Saxony have not shown any significant changes anymore and remain at chronically high levels.

Concerningly, target values for ozone for the protection of health and vegetation have not been met in recent years at several air quality monitoring stations [LfULG, 2019]. The Saxon State Office for the Environment, Agriculture and Geology (LfULG) therefore funded various projects where trends, effects and influencing factors of ozone in Saxony were comprehensively investigated and VOCs as important precursor substances were measured in a time-resolved manner using various devices. Selected results of these projects are presented in the following.

Trends of ozone in Saxony

First of all, and not surprisingly, Ozone in Saxony shows a clear concentration gradient across the different types of monitoring stations. As can be seen in Fig. 1, the 5-year average values in 2016 - 2020 are 40 - 45 $\mu\text{g m}^{-3}$ near traffic, 45 - 55 $\mu\text{g m}^{-3}$ in the urban background, around 50 - 60 $\mu\text{g m}^{-3}$ in the rural background and around 70 - 75 $\mu\text{g m}^{-3}$ on the Erzgebirge ridge. Forest stations, for which measured values are only available during the vegetation period from April to September, show ozone concentrations that are in

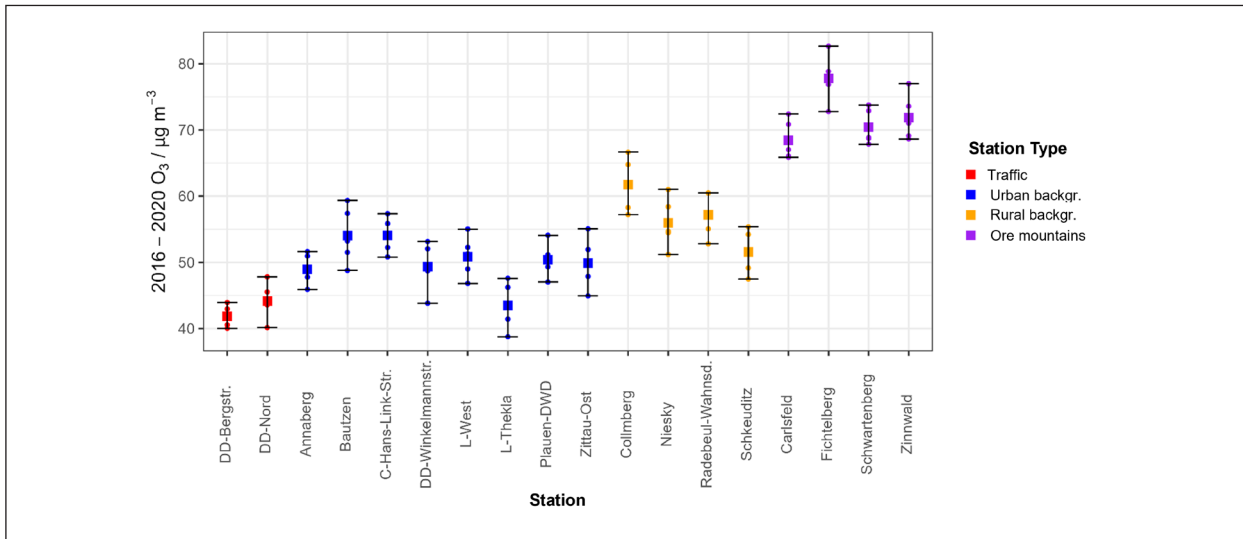


Fig. 1: Yearly mean values of ozone in Saxony (dots), their 5-year average (square) and min – max range (error bars) for 2016 to 2020.

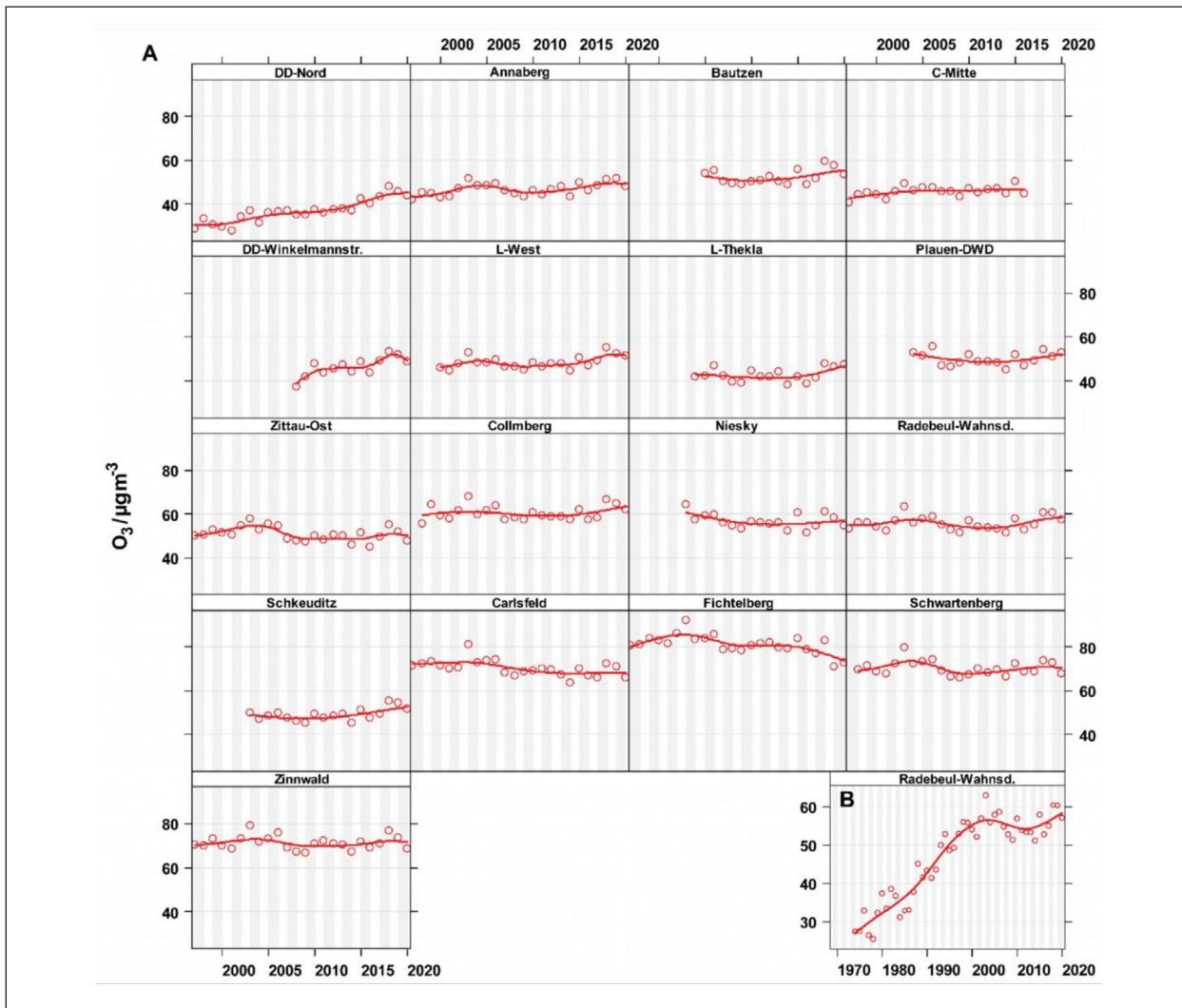


Fig. 2: Smoothed trends of yearly mean ozone concentrations for A) all stations from 1997 on, and B) the single station with a longer time series, starting in 1974 (Radebeul-Wahnsdorf)

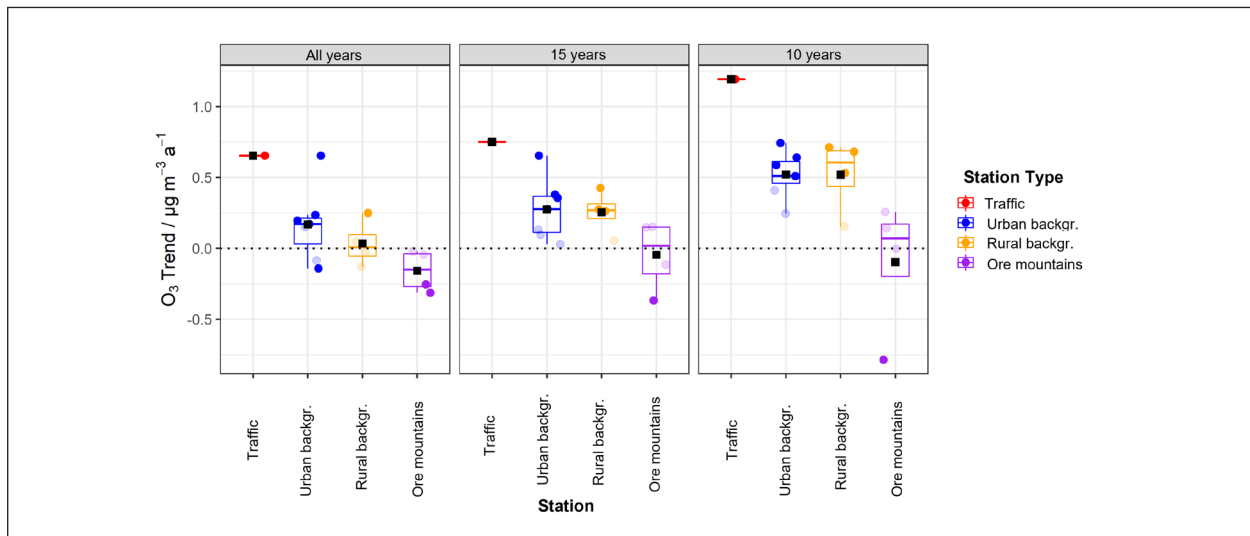


Fig. 3: Ozone trend values at 4 different station types and in 3 different periods (all years since 1997, 2006 – 2020, and 2011 – 2020). Solid dots indicate statistically significant values ($p < 0.05$), light dots represent non-significant values, the box-plot summarizes the individual station values and the black square gives the mean value across all stations of one type.

the range of urban and rural background concentrations for identical comparison periods.

The range of about a factor of 2 results from the locally different influencing factors such as ozone depletion due to freshly emitted NO from traffic, increased formation in the rural background from anthropogenic and biogenic precursors, as well as increased vertical mixing from higher atmospheric layers at higher stations.

Depending on the period under consideration, ozone concentrations in Saxony have changed to a greater or lesser extent over the past decades. The most significant changes occurred between 1974 and the early 2000s, when ozone at the Radebeul-Wahnsdorf station almost doubled from around 30 to almost 60 $\mu\text{g m}^{-3}$ as an annual average (Fig. 2). Since then, the concentrations at this and many other stations show some variation, but usually much less pronounced changes.

To determine trend values of ozone, the Theil-Sen method was used as a robust and non-parametric linear trend estimator. Because the exact value of a linear trend per year often depends on the exact period under consideration, trends were estimated for the entire period of available data as well as for the recent 15 and 10 years.

A significant increase of $0.65 \mu\text{g m}^{-3} \text{a}^{-1}$ is observed at the DD-Nord traffic station between 1997 and 2020, which is even more pronounced for shorter observation periods and amounts to $1.2 \mu\text{g m}^{-3} \text{a}^{-1}$ for the most recent decade from 2011 - 2020. This pattern of more pronounced concentration changes in more recent years is also observed at the other station types. In the urban and rural background,

ozone increases from 2011 - 2020 at an average of around $0.5 \mu\text{g m}^{-3} \text{a}^{-1}$ across all stations, whereby significantly lower, often stagnating and at one station even slightly decreasing trends are calculated for all available measurement data since 1997. At the mountain sites of the Erzgebirge, concentrations have essentially stagnated in the more recent decade; only at the Fichtelberg have they decreased significantly at $-0.8 \mu\text{g m}^{-3} \text{a}^{-1}$. For the overall period since 1997, the decrease was less strong.

Broken down by season, the highest ozone increasing trends in recent years are observed particularly in summer, whereas over longer periods of time, the most significant changes in concentration often occur in winter (not shown). This shift could be related to the increasing effects of climate change, which is increasingly leading to hot and dry summers in which ozone concentrations can rise sharply.

The trends in mean ozone result from trends in its concentration ranges, which vary significantly depending on the type of station. At the traffic station, mean concentrations increase most sharply around the 50th percentile, in the urban and rural background the highest increasing trend values are in the lower concentration range around the 10th - 25th percentile and on the Ore Mountain ridge the lowest concentrations increase most sharply around the 1st percentile (not shown). At the upper end, the highest concentrations decrease from around the 99th percentile in the urban and rural background and from around the 75th percentile in the Ore Mountains.

On the one hand, these different patterns illustrate the success of air pollution control measures in recent years and decades, which have led to a sig-

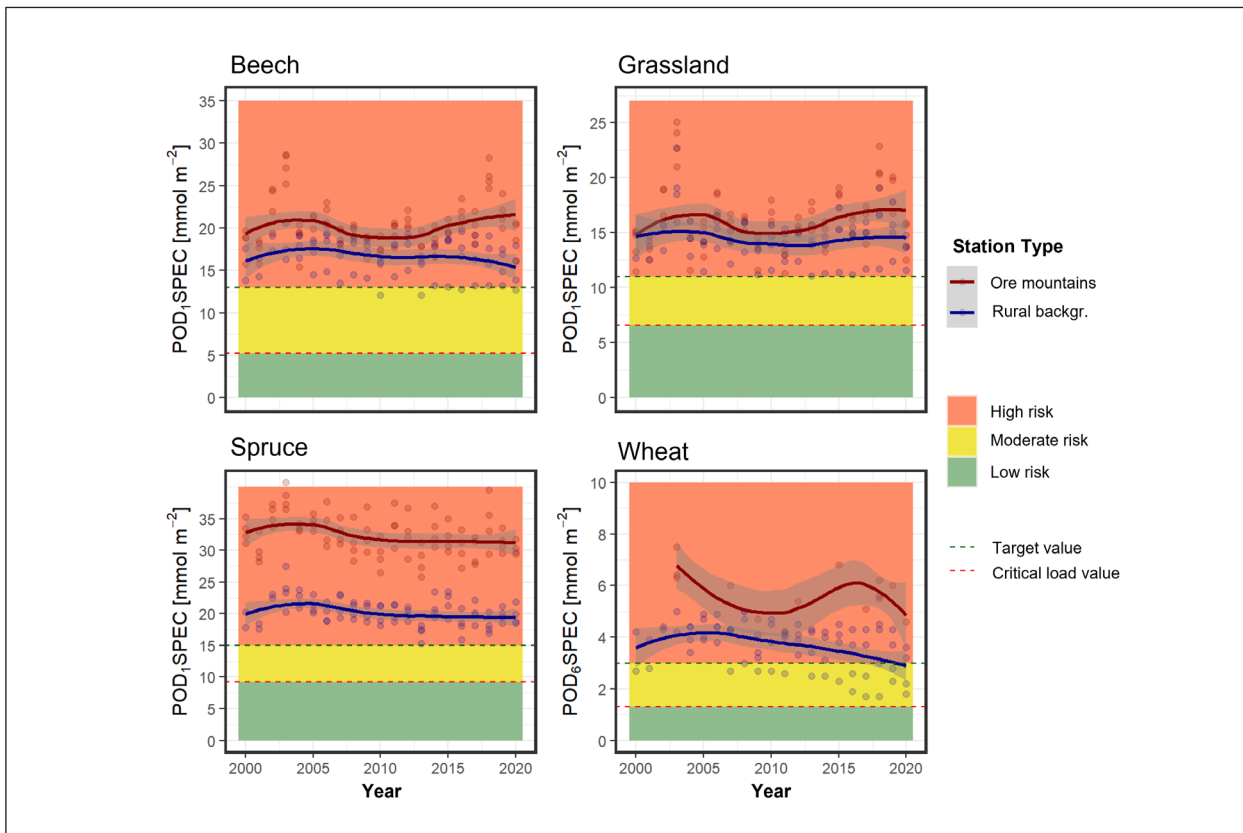


Fig. 4: Time series of POD values for 4 representative species at 2 station types. Dots indicate yearly mean values at individual stations, the red and blue lines represent the smoothed trend across all stations in the Ore Mountains and in the rural background. Critical load values and target values define ranges of no, moderate, and high risk of vegetation damage according to the literature [VDI, 2020].

nificant drop in peak ozone levels in some cases, but on the other hand they also show that the persistent total ozone pollution will probably remain high for some years to come due to increasing lower, medium and sometimes even high concentration levels.

An important reason for increasing ozone at many stations is the significant reduction in NO_x concentrations that have been observed at several stations, particularly through emission reductions in the transport sector. This reduces the significance of local ozone depletion by NO at the monitoring stations, although the total O_x as the sum of NO_2 and O_3 remains constant. This is also reflected in the studied O_x trends, which have essentially stagnated, particularly in the more recent decade, and have only decreased slightly over longer periods. The reductions in emissions of NO_x ozone precursors achieved to date have obviously not led to significantly lower O_x concentrations in the long term. A possible reason is the chemical interplay with VOCs as the second important precursor group. Continuous precursor VOC concentrations are, however, not available in Saxony and hardly available in Germany, which is the main motivation of the VOC project described below.

Impacts of ozone on vegetation

Various metrics including concentration-based ones such as AOT40 or flux-based ones such as the phytotoxic ozone dose (POD) exist for the assessment of prevailing ozone concentrations with respect to vegetation risk and damage. Flux-based metrics are considered advantageous as they better describe the actual physiologically relevant dose than purely exposure-based metrics [Denman et al., 2007; Grünhage et al., 2018].

In the project, the flux-based POD values were calculated for 4 species [VDI, 2020] and at all stations in the rural background and in the Ore Mountains. POD time series from 2000 to 2020 were generated and compared with critical load values and target values for the receptor species beech, spruce, grassland and winter wheat. These receptors are considered to be particularly sensitive to ozone and therefore serve as representative species for other types of vegetation.

As can be seen in Fig. 4, phytotoxic ozone doses were above the critical load values defined in the relevant guidelines for all receptors at all stations and in almost all years. The POD values at the stations in the

Ore Mountains are generally higher than in the rural background. There are only few exceptions, especially for winter wheat at 1 - 2 rural background stations, where POD values were below the critical load value in recent years, but the target value is still clearly exceeded.

Overall, the flux-based risk assessment showed that there is a high risk of vegetation damage in Saxony for all species investigated. This leads to losses in the biomass production of forests and grassland, in the grain yield of cereals and in the formation of flowers in grassland, which were quantitatively estimated in the project in relation to reference values. In comparison to the critical load value, losses of 2 to almost 20 % resulted, depending on the protection target and measurement station, which on the one hand mean significant economic damage and on the other hand also have an impact on CO₂ sequestration from the atmosphere and thus establish a stronger feedback to climate change.

Drivers of ozone revealed by statistical modelling

In order to investigate other factors influencing ozone, flexible tree-based machine learning models (gradient boosting machines) were fit to the data sets from various stations and the statistical dependencies of ozone on various predictor variables as resolved by the models were investigated.

In a base model, local meteorological measurements and temporal proxy variables were used as predictors, of which relative humidity, temperature, day of the year, wind direction and wind speed proved to be the most important for the model. Their influences were described in partial dependence plots (PDPs), which statistically describe the quantitative effects of a variable on mean ozone, adjusted for the influences of the other variables.

As can be seen in Fig. 5, the influences on mean ozone determined in the base model were retained in a similar form for some variables in an extended model that was supplemented by additional predictor variables, but also disappeared almost completely for other variables if one of the newly added variables was able to better describe the statistical influence on ozone.

In the extended model, the water vapour pressure deficit, the local concentrations of NO₂ and NO, the relative humidity, the day of the year, the radiation along the air mass trajectory and the temperature were the most important influencing variables for the Radebeul-Wahnsdorf station and are briefly summarized below. For the base model, it was shown that very similar statistical dependencies arise at other station types.

The water vapor pressure deficit regulates the opening width of plant stomata and thus has a decisive influence on the sink strength of stomatal deposition [Lin et al., 2019]. When the water vapor pressure deficit is high, i.e. the air is warm and dry, plants increasingly close their stomata in order to avoid excessive water loss. As a result, average ozone concentrations – when adjusted for the other influencing variables - rise by up to 30 µg m⁻³ as the water vapor pressure deficit increases.

Nitrogen oxides affect ozone in different ways. On the one hand, NO₂ is an important precursor compound in the chemical reaction system of ozone formation; on the other hand, however, together with NO it reduces locally measured ozone concentrations by shifting the photostationary equilibrium towards NO₂ during the day [Clapp und Jenkin, 2001] and reacting directly with O₃ at night [Seinfeld und Pandis, 1998]. Therefore, the local mean ozone concentrations in the statistical model decrease by up to 50 µg m⁻³ at higher NO_x concentrations after adjustment for other effects.

Relative humidity in the base model serves as a measure of the sink strength of stomatal and non-stomatal deposition. While stomatal deposition in the extended model is statistically better described by the water vapor pressure deficit, the still high significance of relative humidity for the extended model corroborates a strong influence of non-stomatal deposition on plant or other moist surfaces [Clifton et al., 2020]. The mean ozone concentrations decrease by up to 15 µg m⁻³ with increasing humidity.

In the statistical model, the day of the year describes the annual pattern of other influences that are not sufficiently represented by the other predictor variables. Compared to the measured values and also to the annual cycle in the base model, it is flatter in the extended model and only shows a spring maximum. Such a maximum is usually observed at remote background stations and presumably describes the strongest vertical ozone interference from the stratosphere in spring [Cooper et al., 2014]. The summer maximum observed in the measurement data in Saxony, as well as the typical November minimum, is determined by the interaction of other influencing variables included in the model, such as water vapor pressure deficit, temperature and nitrogen oxides, and is therefore no longer included in the annual cycle of the extended model adjusted for these other influences.

The global radiation along the 4-day backward trajectory of the sampled air mass is a measure of the photochemical activity in the history of the air mass. Since a large proportion of locally measured ozone is always transported to the site, the mean ozone concentrations in the statistical model increase by up

to $10 \mu\text{g m}^{-3}$ with increasing mean radiation intensity along the trajectory.

Temperature is one of the most important influencing variables in the base model, but in the extended model it no longer has a pronounced influence on mean ozone concentrations. In reality, temperature is well-known to impact ozone through increased organic reactivity at high temperatures due to faster chemical conversions [Pusede et al., 2015] and in particular through higher concentrations of biogenic precursor compounds at higher temperatures [Fuentes et al., 2000; Guenther et al., 2006]. These relationships are possibly described sufficiently well by the water vapor pressure deficit in the extended model, which is highly correlated with temperature with $r = 0.8$. At temperatures below 0°C , slightly increasing mean ozone concentrations are observed, which could be related to

increased precursor concentrations of anthropogenic VOCs from traffic (cold start) or wood combustion.

The other predictor variables of the extended model had significantly less impact on ozone, but most of them still showed interesting and plausible patterns. In addition, globally less important variables can still be important for the ozone concentration during certain times or shorter episodes.

Therefore, the influences of individual predictor variables adjusted for the effects of other variables were calculated for each model value using SHAP values [Lundberg und Lee, 2017] and discussed for selected variables over the course of their annual mean values. This clearly showed, for example, the influence of the hot and dry summers of 2003 and 2018 - 2020, which were characterized by a very high water vapour pressure deficit and very low soil moisture.

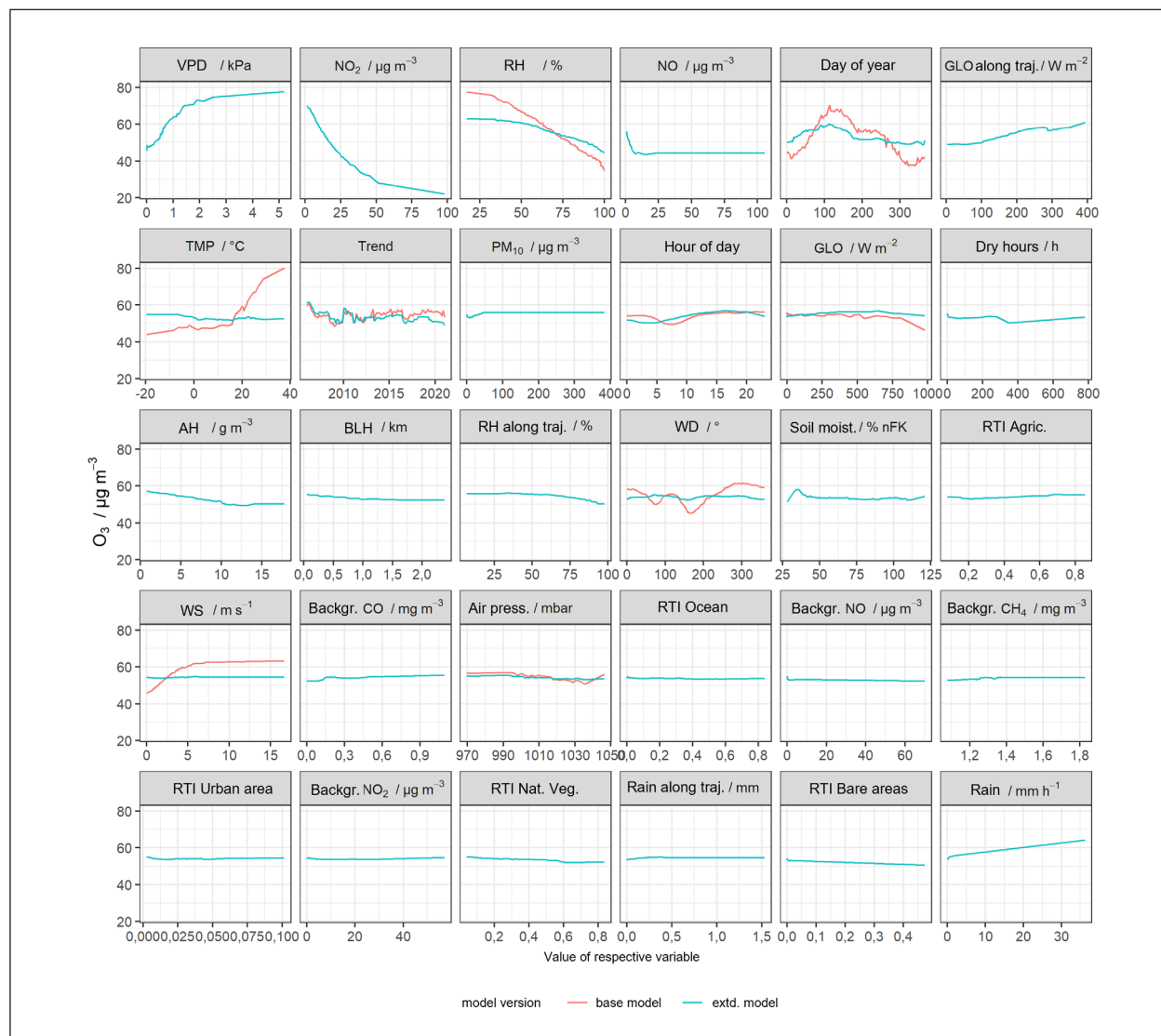


Fig. 5: Partial dependence plots describing the statistical dependencies of ozone on various predictor variables for the rural station Radebeul-Wahnsdorf. The base model contained local meteorological and temporal proxy variables, while many more predictors were added in the extended model.

These influences are depicted in the statistical model and are reflected in the above-average SHAP values of these variables in these years. These observations also indicate a slight increase in ozone in Saxony due to rising concentrations of methane in the continental background.

Overall, the statistical modelling and the methods used to explain the model values allowed for a number of interesting insights into the dependencies of ozone on various influencing variables. However, as these are of statistical nature, they are not necessarily causal and need to be interpreted with caution. Validation with process-oriented modelling would be beneficial for a deeper understanding.

Time-resolved measurements of VOC as important ozone precursors

In addition to nitrogen oxides, VOCs are important substances from which ground-level ozone can form in complex reaction chains. In contrast to ozone and nitrogen oxides, however, VOCs are only very rarely recorded in air quality monitoring networks in Germany and Europe, as there are few regulatory requirements for this. In particular, there are generally no requirements for recording VOC concentrations with good temporal resolution beyond a few point measurements per week.

In order to achieve a better understanding of ozone formation in the future, particularly with regard to anthropogenic and biogenic VOCs, the continuous determination of hourly VOC concentrations with devices from various manufacturers is therefore being tested in a current project. The aim is to assess the suitability of commercial systems for integration into monitoring networks and to assess the quality and usefulness of the obtained data.

To this purpose, two online GC systems listed in guideline VDI 2100/5 [2020] and developed for monitoring network operation by the manufacturers AMA Instruments (Ulm, Germany) and SynSpec (Groningen, Netherlands) were installed in the measurement container of the State Operating Company for Environment and Agriculture (BfUL) in Borna and operated in parallel for approx. 1.5 years. In addition, a similar system from Chromatotec (Orleans, France) was installed only in December 2023, but its data has still to be evaluated. The systems enable the continuous determination of approx. 60 C₂-C₁₂ VOCs in a wide range of boiling points by automated trapping on sorbents, transfer to 2 gas chromatographs (for low- and high-boiling VOCs) by thermal desorption, separation on suitable chromatographic columns, and detection by flame ionization or photoionization detectors (FID or PID).

Unfortunately, operation of both systems failed several times due to various software or hardware errors, but over a full year an availability of hourly or half-hourly measured values of around 70 - 80 % could still be achieved. Of the approximately 60 calibrated VOCs, around 20 were determined regularly with both systems, while the remaining VOCs only rarely or never showed concentrations above the detection limit. In addition to anthropogenic aliphatic and aromatic compounds, the most important biogenic isoprene precursor isoprene is also among the frequently determined VOCs.

The evaluation and peak assignment of the chromatograms is automated by the respective device software. However, significant shortcomings were found in both systems. Due to fluctuations in temperature or other external influences, the retention times of various VOCs sometimes shift and their peaks are then either assigned to the wrong substance by the evaluation algorithm or not assigned at all. As a result, the raw data from both devices often contain concentration values for some VOCs that do not correspond to the actual concentration, up to zero values, even though the VOC was present in a measurable concentration. The comparability of the VOC concentrations based on the raw data generated by the devices was therefore often unsatisfactory. In order to improve comparability, complex and time-consuming manual checks and corrections of the chromatograms were necessary to eliminate at least a large part of the misclassifications. After these corrections, a significantly better correlation with coefficients of determination of approx. 0.7 - 0.8 resulted for many VOCs, although individual substances still correlated significantly worse between the two devices even after the data correction. In addition to the temporal variability, the level of the concentration values between the devices is only partially consistent. For many VOCs, the AMA system often shows concentration ions that are on average 1.5 - 3 times higher than the Synspec system.

The partly large deviations in the concentrations determined between the two devices can have various causes. Although the design and measuring principle of both devices are very similar, they do differ in some details. For example, different sorbents and sampling volumes are used and it is unclear to what extent breakthroughs of the analytes are possible during sampling. It is also unclear to what extent losses of analytes could occur during drying of the sampled air masses. Further conclusions about possible reasons for the deviations are to be drawn from comparisons with the third device (Chromatotec), with separately conducted cartridge sampling and offline analysis, as well as from laboratory tests at the end

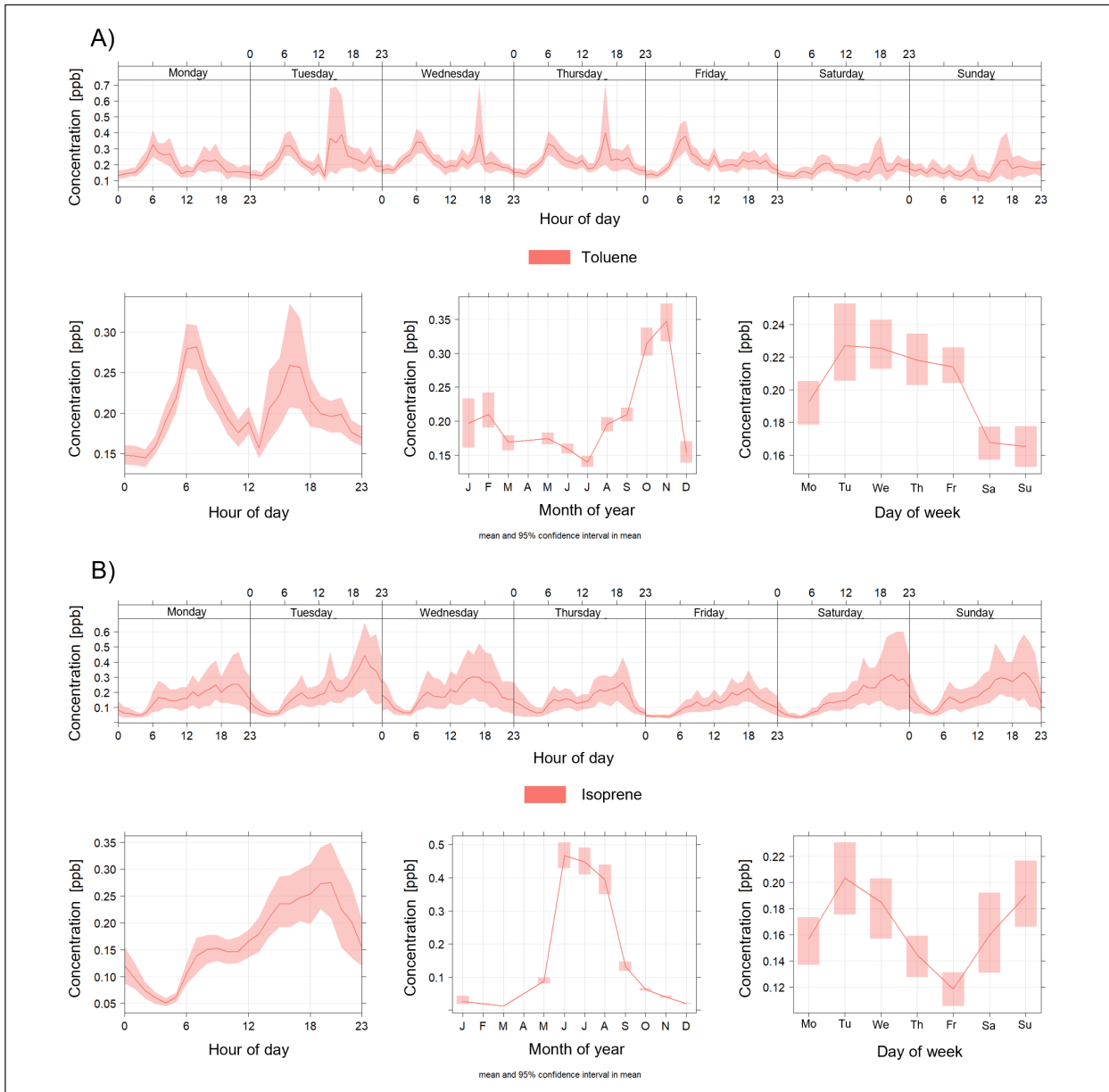


Fig. 6: Temporal profiles of A) toluene and B) isoprene obtained over 1 year with the AMA online GC system.

of the measurement campaign. These measurements are still ongoing.

Even though the comparability between the devices has not always been convincing, a large data set of time-resolved VOC concentrations has been obtained with both systems, which would not be achievable with manual methods. Figure 6 shows various temporal profiles for toluene and isoprene as examples.

For toluene as a marker for petrol emissions, a peak can be seen in the daily cycle with the morning rush hour and a drop in concentration by midday. In the weekly cycle, the concentrations are higher on working days than on weekends, which is due to the lower rush-hour traffic on Saturdays and Sundays.

As a typical marker of biogenic VOC emissions, a clear diurnal cycle can also be seen for isoprene. At sunrise, the isoprene concentration rises sharply in the morning, only to fall again at night after reaching a peak in the late afternoon. Due to the lack of light, plants do not emit isoprene at night, so that it can only react away or be deposited. The annual cycle shows a strong increase during the vegetation period in the summer months. From the fall months onwards, the isoprene concentration drops significantly again.

In general, these initial and preliminary results show that the data set promises interesting insights into the temporal progression of various VOCs at the Borna station, which can also be used in future studies for a better understanding of local ozone

sources, in particular through more precise modelling of ozone formation chemistry. However, further quality assurance studies measures are required to better ensure the reliability of the concentration values obtained with the various devices.

Summary

Average ozone concentrations in Saxony, Germany and Europe have remained at high levels for the past about 20 years and chronic exposure to humans and vegetation is still too high. In a comprehensive project on ozone in Saxony, stagnant or even increasing trends up to $1.2 \mu\text{g m}^{-3} \text{ a}^{-1}$ were derived for the station of the Saxonian air quality monitoring network. Phytotoxic ozone doses were calculated to lie in a “high risk” range at basically all rural and mountain sites, causing economic losses in the range of a few up to 20 %, depending on the species and protection target. Statistical modelling using machine learning techniques revealed a number of important factors driving annual and interannual ozone variations. The most important ones included the water vapour pressure deficit, the local concentrations of NO_2 and NO , the relative humidity, the day of the year, the radiation along the air mass trajectory and the temperature. The non-linear ways in which ozone depends on these drivers was visualized from the model output and found to be in general agreement with current theoretical understanding. Even factors which do not strongly influence average

concentrations throughout the years were shown to be important during specific episodes, e. g. soil moisture during drought. One important driver that could not be studied by the statistical model due to a lack of measured concentrations, are VOCs. Their trend is a likely cause of ozone staying high in the past 20 years, despite significant reductions in NO_x emissions. To fill this gap of experimental information, TROPOS is currently assessing the suitability of commercial online GC instruments for integration into monitoring networks. Despite a not yet satisfactory data quality, the continuous measurements over 1.5 years with hourly or half-hourly time resolution allows promising insights into short- and longer-term temporal patterns of about 20 important ozone precursor VOCs.

Due to its three important impacts in health, vegetation and climate, ozone will certainly remain an important topic in air pollution control in the coming years and decades and may become even more important in the course of the ongoing change in Earth's climate. Ozone research in atmospheric chemistry is undergoing a strong re-activation as increasing ozone concentrations are occurring in many areas of the world. As demonstrated in this combined project report, atmospheric chemistry research is both resuming and extending its effort to understand tropospheric ozone formation in the multiphase system in order to direct adequate reduction measures in the 21st century and to restrict adverse impacts on ozone regarding health, vegetation damage and climate, thus addressing a factor of very high societal impact.

References

- Clapp, L. J., and M. E. Jenkin (2001), Analysis of the relationship between ambient levels Of O₃, NO₂ and NO as a function of NO_x in the UK, *Atmospheric Environment*, 35(36), 6391-6405, doi: [https://doi.org/10.1016/S1352-2310\(01\)00378-8](https://doi.org/10.1016/S1352-2310(01)00378-8).
- Clifton, O. E., A. M. Fiore, W. J. Massman, C. B. Baublitz, M. Coyle, L. Emberson, S. Fares, D. K. Farmer, P. Gentine, G. Gerosa, A. B. Guenther, D. Helmig, D. L. Lombardozzi, J. W. Munger, E. G. Patton, S. E. Pusede, D. B. Schwede, S. J. Silva, M. Sörgel, A. L. Steiner, and A. P. K. Tai (2020), Dry Deposition of Ozone Over Land: Processes, Measurement, and Modeling, *Reviews of Geophysics*, 58(1), doi: <https://doi.org/10.1029/2019rg000670>.
- Cooper, O. R., D. D. Parrish, J. Ziemke, N. V. Balashov, M. Cupeiro, I. E. Galbally, S. Gilge, L. Horowitz, N. R. Jensen, J. F. Lamarque, V. Naik, S. J. Oltmans, J. Schwab, D. T. Shindell, A. M. Thompson, V. Thouret, Y. Wang, and R. M. Zbinden (2014), Global distribution and trends of tropospheric ozone: An observation-based review, *Elementa: Science of the Anthropocene*, 2, doi: <https://doi.org/10.12952/journal.elementa.000029>.
- Denman, K. L., G. Brasseur, A. Chidthaisong, P. Ciais, P. M. Cox, R. E. Dickinson, D. Hauglustaine, C. Heinze, E. Holland, D. Jacob, U. Lohmann, S. Ramachandran, P. L. da Silva Dias, S. C. Wofsy, and X. I. C. T. P. S. B. Zhang (2007), Couplings Between Changes in the Climate System and Biogeochemistry, in *Climate Change*
- 2007: The Physical Science Basis. Contribution of Working Group I to the Fourth Assessment Report of the Intergovernmental Panel on Climate Change., edited, Cambridge University Press, Cambridge, United Kingdom and New York, NY, USA.
- Fuentes, J. D., L. Gu, M. Lerdau, R. Atkinson, D. Baldocchi, J. W. Bottenheim, P. Ciccioli, B. Lamb, C. Geron, A. Guenther, T. D. Sharkey, and W. Stockwell (2000), Biogenic Hydrocarbons in the Atmospheric Boundary Layer: A Review, *Bulletin of the American Meteorological Society*, 81(7), 1537-1575, doi: [https://doi.org/10.1175/1520-0477\(2000\)081<1537:Bhitab>2.3.Co;2](https://doi.org/10.1175/1520-0477(2000)081<1537:Bhitab>2.3.Co;2).
- Grünhage, L., J. Bender, H. J. Weigel, and R. Matyssek (2018), Kritische Dosis-Kenngrößen für Ozon zum Schutz der Vegetation, *Gefahrst Reinhalt L*, 78(4), 173-180.
- Guenther, A., T. Karl, P. Harley, C. Wiedinmyer, P. I. Palmer, and C. Geron (2006), Estimates of global terrestrial isoprene emissions using MEGAN (Model of Emissions of Gases and Aerosols from Nature), *Atmospheric Chemistry and Physics*, 6(11), 3181-3210, doi: <https://doi.org/10.5194/acp-6-3181-2006>.
- LfULG (2019), Luftqualität in Sachsen - Jahresbericht 2019 Report, Sächsisches Landesamt für Umwelt, Landwirtschaft und Geologie, Dresden.
- Lin, M. Y., S. Malyshev, E. Shevliakova, F. Paulot, L. W. Horowitz, S. Fares, T. N. Mikkelsen, and L. M. Zhang (2019), Sensitivity of

- Ozone Dry Deposition to Ecosystem-Atmosphere Interactions: A Critical Appraisal of Observations and Simulations, *Global Biogeochemical Cycles*, 33(10), 1264-1288, doi: <https://doi.org/10.1029/2018gb006157>.
- Lundberg, S. M., and S.-I. Lee (2017), A Unified Approach to Interpreting Model Predictions, in *Advances in Neural Information Processing Systems 30*, edited by I. Guyon, U. V. Luxburg, S. Bengio, H. Wallach, R. Fergus, S. Vishwanathan and R. Garnett, pp. 4765-4774, Curran Associates, Inc.
- Monks, P. S., A. T. Archibald, A. Colette, O. Cooper, M. Coyle, R. Derwent, D. Fowler, C. Granier, K. S. Law, G. E. Mills, D. S. Stevenson, O. Tarasova, V. Thouret, E. von Schneidemesser, R. Sommariva, O. Wild, and M. L. Williams (2015), Tropospheric ozone and its precursors from the urban to the global scale from air quality to short-lived climate forcer, *Atmospheric Chemistry and Physics*, 15(15), 8889-8973, doi: <https://doi.org/10.5194/acp-15-8889-2015>.
- Pusede, S. E., A. L. Steiner, and R. C. Cohen (2015), Temperature and recent trends in the chemistry of continental surface ozone, *Chem Rev*, 115(10), 3898-3918, doi: <https://doi.org/10.1021/cr5006815>.
- Seinfeld, J. H., and S. N. Pandis (1998), Atmospheric and physics of air pollution, *Ed.: J. Wiley & Sons*.
- VDI 2100/5 (2020), Messen von leicht flüchtigen organischen Verbindungen, insbesondere Ozonvorläufersubstanzen - Gaschromatografisches VerfahrenReport, VDI/DIN-Kommission Reinhaltung der Luft (KRdL) - Normenausschuss.
- VDI (2020), Maximale Immissions-Werte zum Schutz der Vegetation - Kritische Dosis-Kenngrößen für OzonReport, VDI/DIN-Kommission Reinhaltung der Luft (KRdL) - Normenausschuss.

Funding

Saxon State Office for the Environment, Agriculture and Geology (LfULG), Dresden-Pillnitz, for both projects

Model assisted vertical in-situ investigation of aerosols, and aerosol-cloud-turbulence interactions in the Southern Hemisphere marine boundary layer: Indications for new particle formation from terrestrial precursors

Frank Stratmann¹, Guy Coulson², Silvia Henning¹, Baseerat Romshoo¹, Roland Schrödner¹, Thomas Conrath¹, Sebastian Düsing¹, Julian Hofer¹, Juliane Kalla³, Daniel Morrish², Sally Gray², Tony Bromley², Khanneh Wadinga Fomba¹, Holger Siebert¹, Birgit Wehner¹, Heike Wex¹, Sarah Grawe¹, Stephan Mertes¹, Mira Pöhlker¹, Hartmut Herrmann¹, Ina Tegen¹, Richard Querel², Gustavo Olivares², Gunther Seckmeyer³, and Andreas Macke¹

¹ Leibniz Institute for Tropospheric Research (TROPOS)

² National Institute of Water and Atmospheric Research (NIWA)

³ Institute of Meteorology and Climatology (IMUK)

Modellierte Wolken über dem Südlichen Ozean (SO) lassen zu viel Sonnenlicht bis an die Meeresoberfläche dringen. Dies führt, im Vergleich zu Beobachtungen, zu einer Überschätzung der Meeresoberflächentemperatur, und damit verbunden einer unterschätzten Meereisausdehnung, einer falschen Lage der Ozeanzirkulationsgürtel sowie einer Verlagerung der Sturmwege nach Süden. Ein wichtiger Teil dieses Problems ist unser immer noch unvollständiges Wissen über die mikrophysikalischen Eigenschaften von SO-Wolken, sowie hinsichtlich der kombinierten Einflüsse von Aerosolpartikeln, Thermodynamik, Grenzschichtdynamik und atmosphärischen und Wolkenturbulzenzen auf die Wolkeneigenschaften.

Zur Verbesserung unseres Verständnisses bzgl. der Eigenschaften und des Verhaltens südhemisphärischer Wolken, wurde im Rahmen des BMBF geförderten goSouth-Projekts, in enger Zusammenarbeit zwischen dem Institut für Troposphärenforschung (TROPOS), Leipzig, dem Institut für Meteorologie und Klimatologie (IMUK), Hannover, und dem National Institute of Water and Atmospheric Research (NIWA), Neuseeland, eine modellbegleitete mehrwöchige Messkampagne durchgeführt. Die Kampagne fand im Süden Neuseelands an einem Küstenstandort in der Nähe von Pahia statt und umfasste boden- und ballongestützte meteorologische und physikochemische Messungen von Aerosolpartikeln, sowie bodengestützte Fernerkundung und regionale Modellierung.

Auf Grundlage der gewonnenen experimentellen Daten stellen wir zum jetzigen Zeitpunkt die Hypothese auf, dass die beobachteten Partikelneubildung auf Vorläufergase aus terrestrischen Quellen in Neuseeland zurückgeführt werden können. Eine tiefgreifende Datenauswertung ist im Gange, um diese Hypothese zu überprüfen.

Die gewonnenen Ergebnisse und Erkenntnisse werden dazu beitragen, unser quantitatives Verständnis und die Modellierung von Aerosol-Wolken-Turbulenz-Wechselwirkungen in der südlichen Hemisphäre zu verbessern und damit die Einflüsse von Wolken auf Wetter und Klima in der Region des südlichen Ozeans zukünftig besser zu quantifizieren.



Fig. 1: Measurement location (left), site (middle), and NIWA, IMUK and TROPOS researches (right) at the measurement site near Pahia, NZ.

Introduction

Southern-Ocean (SO) clouds are routinely misrepresented in the present generation of climate models that informed the 5th Assessment Report of IPCC. The modeled SO clouds allow too much sunlight to penetrate to the ocean surface, causing a warm sea-surface temperature bias and associated consequences such as underestimated sea ice extent, incorrect locations of the ocean circulation belts, and a southward displacement of the storm track [Flato et al., 2013]. Also, for the latest generation of climate models, such misrepresentations of cloud properties reduce the ability of climate models to correctly reproduce such important climate properties such as climate sensitivity [Zelinka et al., 2020].

A major part of this problem is our still incomplete knowledge concerning the microphysical properties [e.g. droplet size distribution and phase state (liquid or frozen), Choi et al., 2010; Kanitz et al., 2011; Vergara-Temprado et al., 2018; Villanueva et al., 2020] of SO clouds, including the combined influences of aerosol particles, boundary layer dynamics, atmospheric and cloud turbulence, and thermodynamics on these properties. Respective investigations have been carried out in the Northern [e.g., Siebert and Shaw, 2017; Ditas et al., 2012], but to our knowledge not in the Southern Hemisphere.

Some - certainly not enough - data concerning aerosol particles, CCN, and INP at ground-/sea-levels in the SO region do exist [e.g., Schmale et al., 2019; Tatzelt et al., 2022; Quinn et al., 2017; McCluskey et al., 2018], however the sources of CCN and INP in the Southern Hemisphere are still unclear. Data from collocated vertically resolved measurements of particle properties and the vertical energy and mass transport (including the exchange between the marine boundary layer and the free troposphere, i.e., entrainment), to our knowledge, do not exist in the SO region.

To contribute to closing this significant gap of knowledge, the Leibniz Institute for Tropospheric

Research (TROPOS), Germany, the National Institute of Water and Atmospheric Research (NIWA), New Zealand, and the Institute for Meteorology and Climatology (IMUK), Germany, carried out a model-assisted vertical in-situ investigation of aerosols, clouds and aerosol-cloud-turbulence interactions in a Southern Hemisphere marine boundary layer. The respective project was named *goSouth*, and supported by the German Federal Ministry of Education and Research and the New Zealand Ministry of Business, Innovation & Employment.

Goals

goSouth had two main purposes, a) the characterization of climate-relevant aerosol processes in the turbulent boundary layer in the Southern Ocean region, and b) proof of concept for collaboration between Germany and NZ with a view to a larger ship and air-borne program to follow.

To meet these goals, a measurement campaign was carried out in November 2022 at a site overlooking Te Waewae Bay near Pahia (46.31°S, 167.71°W, 10 m a.s.l.), about 50 km west of Invercargill (Fig. 1). Five researchers from TROPOS and one researcher from IMUK joined the NZ contingent for three weeks of aerosol and turbulence measurements from ground level to 1 km.

The measurement activities were accompanied by modelling efforts using a convection-permitting regional configuration of the Met Office Unified Model (UM) and the aerosol chemistry transport model ICON-MUSCAT providing local weather predictions, regional aerosol and gas phase chemistry information, and derived CCN and INP concentrations.

Methods

The *goSouth* project comprised both joined experimental and modeling activities. Ground-based and balloon-borne measurements of aerosol physi-

cochemical properties, as well as meteorological parameters, including turbulence, were carried out. At ground level, measured properties were aerosol particle total number concentration (Condensation Particle Counter), aerosol particle number size distribution (Mobility Particle Size Spectrometer), cloud condensation nuclei number concentration (Cloud Condensation Nucleus Counter), particle chemical composition (offline analysis of filter samples) and the cloud cover (Hemispherical-Sky-Imager). Vertically measured were the ice nucleating particle concentration (offline analysis of low volume samples and air-borne filter samples taken with HALFBAC), the full suite of meteorological parameters, turbulence, and number concentration of aerosol particles with a diameter between 160 nm and 2.5 μm (Handix POPS).

The partner project *LOSTECCA* [Lidar Observations of SpatioTemporal Contrasts in Clouds and Aerosols, Hofer et al., 2023] contributed continuous observations of the vertical distribution of aerosol, clouds and atmospheric dynamics from multi-wavelength Raman polarization lidar and Doppler lidar, as well as integrated measurements of

atmospheric water vapor, liquid water, and aerosol optical thickness from microwave radiometer and sun-photometer.

The modeling activities comprised simulations with regional chemistry transport model ICON-MUSCAT and the meteorological model UM. The UM was applied in a tailored version for New Zealand (NZCSM). The model simulations were already utilized during the campaign for forecasts. Both, the UM and ICON-MUSCAT are performed in a nested approach. The outermost domain covers the Australian deserts and the Southern Ocean upwind of New Zealand with a horizontal resolution of ~ 12 km. The smallest domain is centered around the campaign measurement site and allows for a more explicit treatment of many of the atmospheric processes of interest to this project.

Results

Exemplary results from the goSouth project are presented in the following, together with initial scientific interpretations and conclusions.

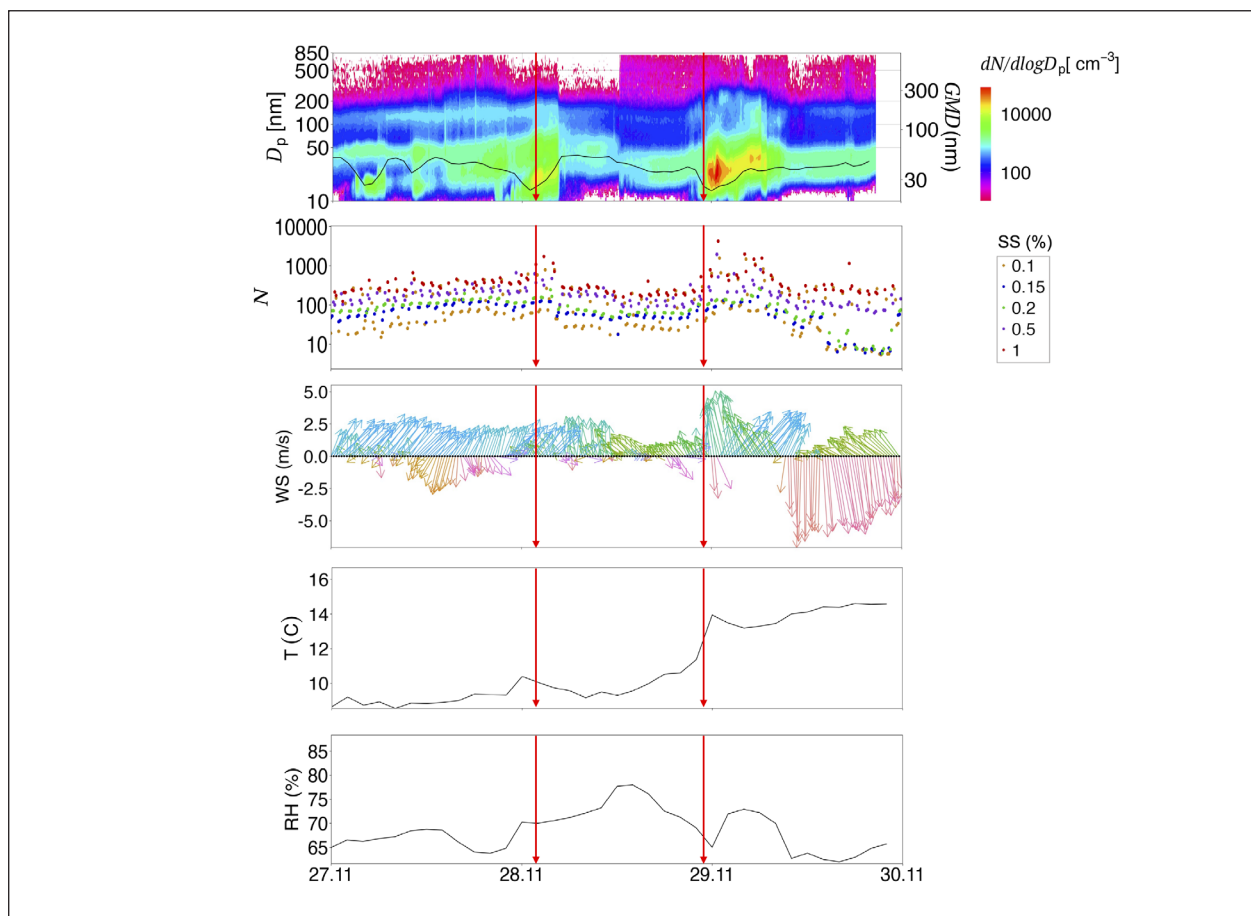


Fig. 2: From top to bottom, time series (time in UTC) of particle number size distribution and geometric mean diameter (GMD, right axis), CCN number concentration at different supersaturation SS, wind speed and direction, temperature and relative humidity. Red arrows indicate Helikite launches (cf. Fig. 5).

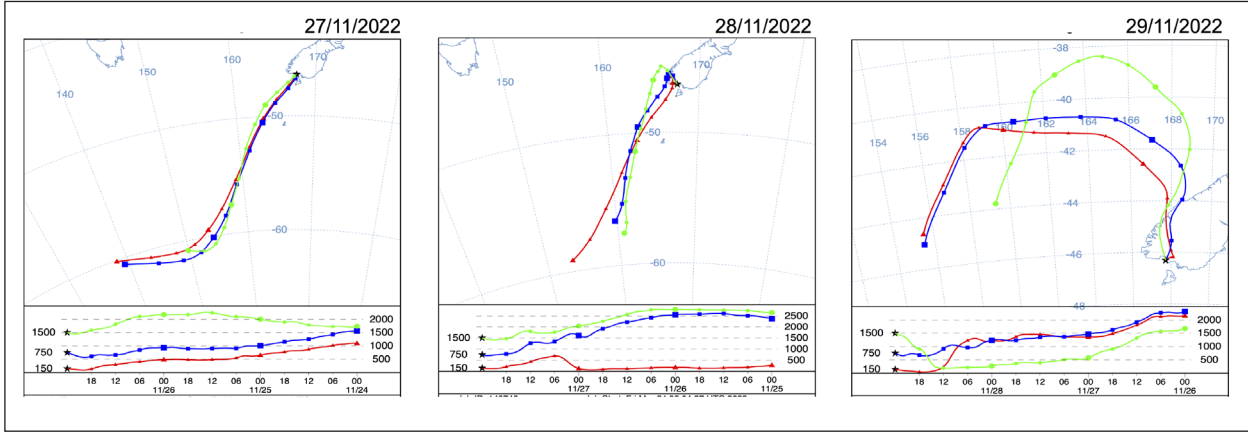


Fig. 3: 3-day back trajectories for the period from 27th to 29th of November 2022.

Ground-based measurements

Data collected during the ground-based measurements, which are representative of the scenarios for which new particle formation (NPF) was observed, are shown in Fig. 2. Depicted are, from top to bottom, time series (time in UTC) of particle number size distribution and geometric mean diameter (GMD, right axis), CCN number concentration at different supersaturation SS, wind speed and direction, temperature and relative humidity.

Figure 3 depicts 3-day back-trajectories as calculated with the hybrid single-particle Lagrangian integrated trajectory (HYSPLIT) model for the time period from the 18th to the 29th of November 2022. Red squares indicate time periods during which NPF was observed.

Based on our analysis (cf. Fig. 2 and 3) we have identified two distinct NPF events, characterized

by elevated number concentrations (yellowish and/or reddish colors appearing in the size range below 50 nm). The two events show clearly different behavior. The late 27th / early 28th (midday local time) of November, near ground features air masses from the Southern Ocean region, however with some influence from the Southern Alps at higher altitudes, together with slightly increased number concentrations of small particles. The late 28th / early 29th of November features air masses with significant influences from the Southern Alps at all altitudes, and compared to the late 27th / early 28th, significantly higher concentrations in the size range below 50 nm. It is noteworthy that no NPF was observed earlier on November 27th, when pristine air masses with low particle number concentrations from the Southern Ocean region were present, which did not pass over the Southern Alps. It should be mentioned that the wind directions measured at the site do not coincide



Fig. 4: Helikite carrying a radio sonde of NIWA and the two TROPOS sondes.

with back trajectories most of the time. This is presumably due to local orographic influences (nearby hill and bay) on wind direction and speed.

In summary, during the *goSouth* campaign we have found clear indications for NPF presumably from terrestrial (Southern Alps) precursors taking place. However, the in total four observed events (two presented herein) feature different characteristics concerning both the formation of new particles and their growth to CCN size.

Balloon-borne activities

The balloon-borne activities aimed at characterizing the stratification of meteorological and aerosol particle properties in- and above the atmospheric boundary layer at the measurement site. The measurements were carried out using a TROPOS-owned Helikite (Fig. 4, left) and were accompanied by regular radio sonde launches by NIWA. From the data we

expect indications concerning momentum, heat, water vapor and aerosol fluxes from and into the boundary layer. This information is important in context of identifying where (free troposphere, boundary layer) NPF and growth to CCN size took place. Worth mentioning is that partially strong and fast changing wind conditions at the site made the balloon-borne activities difficult and lead to a lower than anticipated number of successful flights.

A total of 7 Helikite flights were conducted. Figure 5 shows Helikite observations of wind velocity (hot-wire anemometer; left panel), potential temperature (thermocouple; middle panel), and relative humidity (slow response, right panel) as measured on November 28th, 2022 starting at 02:05 UTC (upper panel) and 23:03 UTC (lower panel) with the TROPOS turbulence probe.

On early November 28th, 2022 (launch at 02:05 UTC, upper panel of Fig. 5) the investigated air masses were approaching from the south, i.e., from

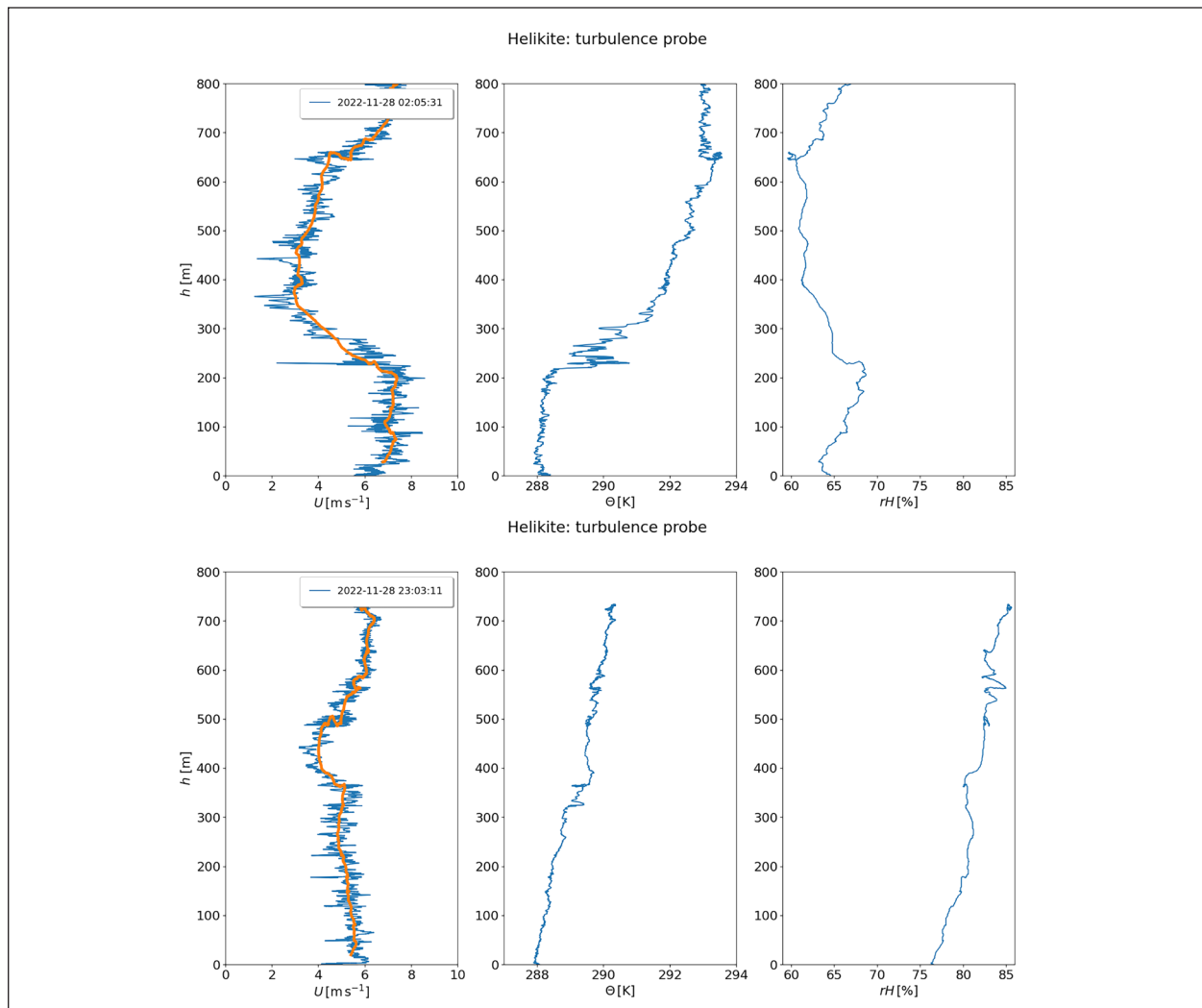


Fig. 5: Helikite observations of wind velocity (hot-wire anemometer; left panel), potential temperature (thermocouple; middle panel), and relative humidity (slow response, right panel) as measured on November 28th, 2022 starting at 02:05 UTC (upper panel) and 23:03 UTC (lower panel).

the Southern Ocean (see red back trajectory in Fig. 3, middle panel). A well-mixed surface layer with a depth of about 200 m had developed. Significant temperature fluctuations at the top of the surface layer are indicative for effective mixing probably caused by wind shear (gradually decreasing wind velocity from about 7 ms^{-1} at 200 m to 4 ms^{-1} at 350 m altitude). Within the well-mixed surface layer an increase of relative humidity with height is observed with about 65% at ground level.

About 20 hours later (lower panels in Fig. 5), the situation has changed. According to the back trajectories (Fig. 3, right panel), the flow has turned to a northerly direction, i.e., the investigated air masses have now passed over the mountains of the Southern Alps. Compared to the air masses approaching from the South, the vertical profiles now exhibit a general cooling of the column with an increased relative humidity, but also a stabilization of the atmosphere near the ground. The observed temperature and velocity fluctuations are dampened and vertical mixing can be considered as minor.

The aerosol chemical composition of particles collected during the Helikite flight on November 28th and on the ground, using a PM10 impactor sampling system, showed organic carbon concentrations of up to $16 \mu\text{g m}^{-3}$ with organic alkane compounds such as heneicosane (3.1 ng m^{-3}), docosane (3.8 ng m^{-3}) and pentacosane (4.4 ng m^{-3}) being observed. These are compounds that can originate from various organic materials, including plant waxes, algae, and other biological sources [Ramasamy and Gopalakrishnan, 2013]. During the flight on November 29th, nonacosane (5.4 ng m^{-3}) and tetracosane (4.4 ng m^{-3}) compounds were also observed. The presence of

these organic compounds as well as the elevated carbon preference index (> 3) observed, highlight the contribution of biological and terrestrial emissions [Deabji et al., 2021] to the PM composition on November 28th and 29th.

From these observations, we hypothesize, that the newly formed particles observed on the late 28th / early 29th of November result either from a local event, or stem from an upstream near Southern Alps event and are advected to the measurement site. A further indication for the latter hypothesis could be the elevated particle concentrations observed on late 27th / early 28th of November, which may as well result from NPF near the Southern Alps, together with advection at higher levels and downward mixing. However, further investigations are needed to verify or falsify this hypothesis.

Modeling activities

The coupled chemistry transport model ICON-MUSCAT was set up for a domain covering most of Australia and New Zealand and finer domains inside. Simulations were conducted for the time period 15 - 30 November. ICON-MUSCAT model simulations are driven by reanalysis data of the global ICON forecast of German Weather Service (DWD) and the CAMS aerosol and trace gas reanalysis. The emissions of natural aerosol and trace gases (sea salt, mineral dust, biogenic VOCs) are described in an online manner, whereas anthropogenic emissions are prescribed using the global emission inventory EDGAR. MUSCAT is a mass-based model, i.e., it directly simulates aerosol mass, but not number. For sea salt and mineral dust, however, a size-resolved

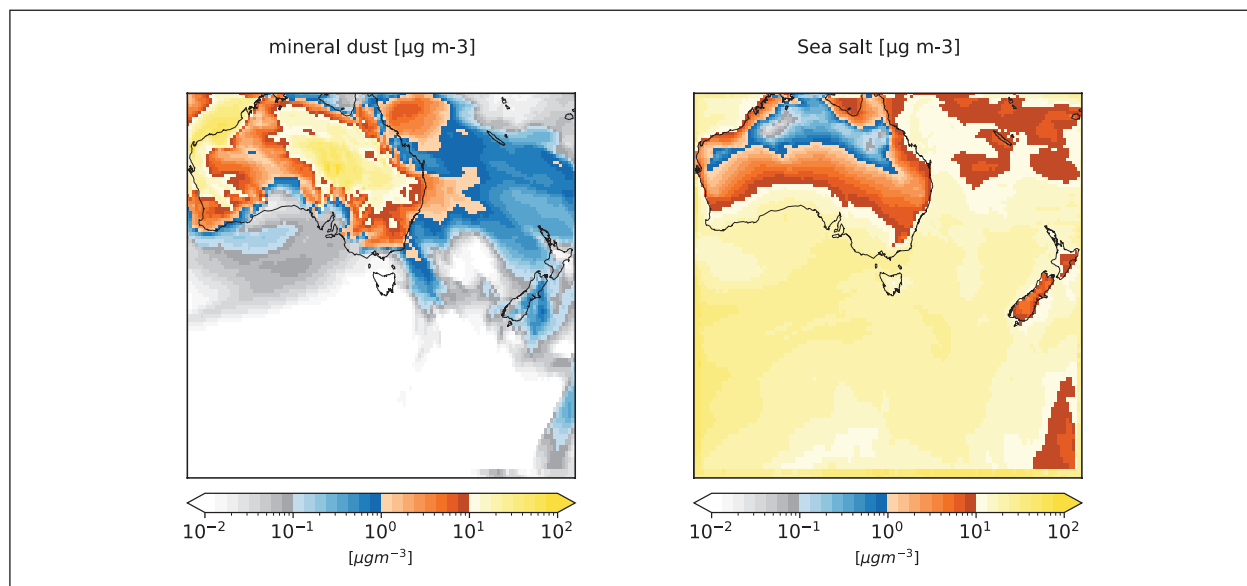


Fig. 6: Modeled temporal mean mass concentrations of mineral dust (left) and sea salt (right) during 27-30 November 2022.

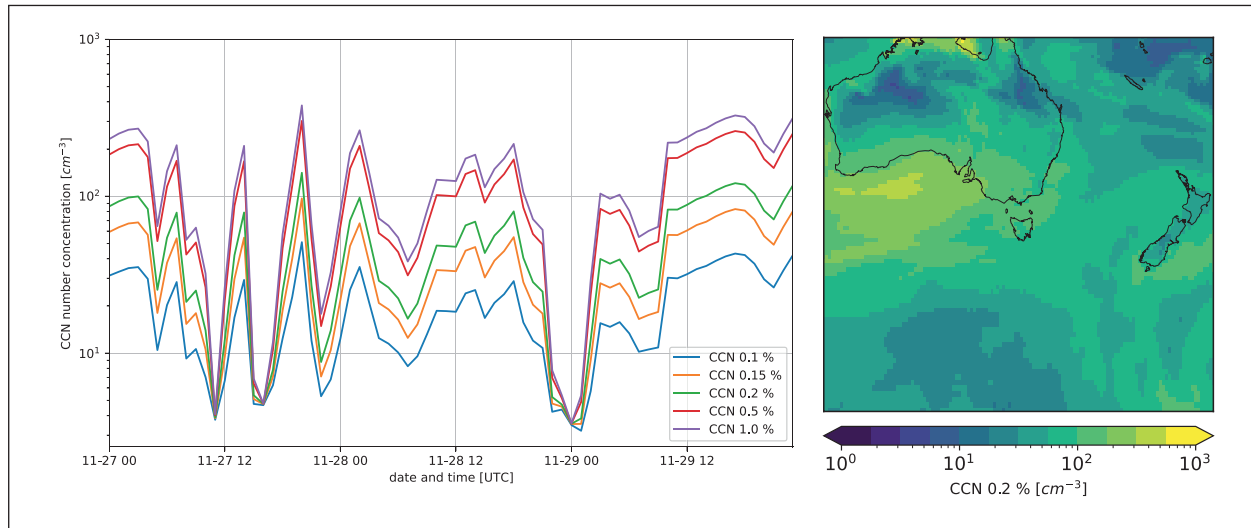


Fig. 7: Modeled time series of CCN concentration at the measurement site for supersaturations as presented in Figure 2 (left). Modeled temporal mean CCN concentration at 0.2 % supersaturation during 27-29 November 2022 (right).

treatment with fixed size bins is used. For all aerosol constituents other than mineral dust and sea salt, aerosol number concentrations are inferred by assuming typical size distributions for these. From these number concentrations and the already size resolved aerosol components, CCN concentrations can be estimated.

The online emission schemes of mineral dust and sea salt perform reasonably well (Fig. 6). Both mass and number concentration are in the expected concentration range. Sea salt thereby provides ubiquitous spatially and temporally rather constant background CCN, however on a low level of only a few up to 50 cm^{-3} . This is offset by anthropogenic contributions in the model from organic carbon and occasional mineral dust from Australia. In total at the measurement site for 1 % supersaturation, CCN concentration of a few 100 cm^{-3} can be reached in the model (Fig. 7, left). The modeled CCN concentration generally match the observations (see Fig. 2), however, the large CCN number concentrations measured during the two nucleation events are not seen in the model. This can be explained by missing NPF, which is not available in ICON-MUSCAT at present. This process caused a large increase of the observed CCN for high supersaturations (0.5 and 1.0 %) during these events. Due to the lack of very small aerosol particles in the model during the two NPF events, the CCN number concentration for low supersaturations (0.1 - 0.2 %) still roughly fits to the observed concentrations (despite its temporal uncertainty), but are underestimated dramatically for higher supersaturations. Wet deposition seems to be too efficient in the model as sudden decreases to very low CCN concentrations

(such as modeled during the November 29 around 0 UTC and November 27th in the afternoon) were not seen in the observations (compare to Fig. 2).

Remote sensing activities

In connection with the *goSouth*-campaign, remote sensing activities were carried out by the partner project *LOSTECCA*. Exemplary Doppler wind lidar measurements of the vertical wind velocity during the period of interest from 27-29th November 2022 are presented Fig. 8.

All these periods are characterized by alternating up- (yellow and red colors) and downdrafts (green and blue colors). Periods of persisting up- and downdrafts are largest on 27th, followed by 28th, and lowest on 29th November (00:00 UTC±3 h, respectively). Also, the magnitudes, apart from those related to clouds above about 1 km (strong downdrafts), are lower on 29th November.

The elevated particle concentrations, mentioned above, observed on late 27th / early 28th November might be related to these changing up- and downdraft patterns. However, at the Pahia measurement site, the likelihood of strong upward motion due to orographic mountain waves might be generally pronounced due to Pahia Hill (227 m a.s.l.), a landmark in direct vicinity of the measurement site. Besides the observations of the Doppler wind lidar, including vertically resolved information on the horizontal wind velocity, further investigations in this direction will comprise the full suite of available remote sensing observations in combination with above mentioned in-situ observations and modelling outputs.

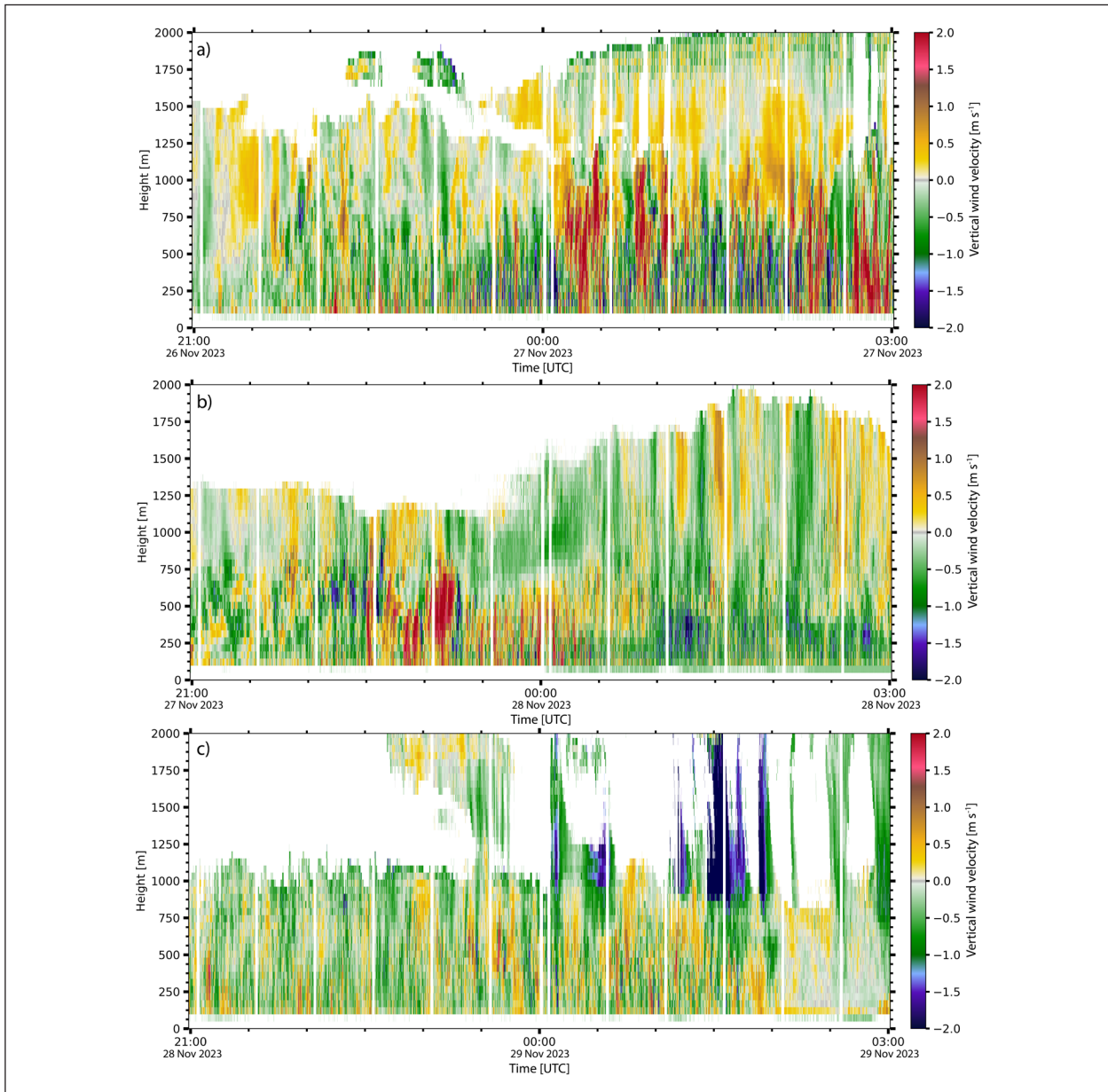


Fig. 8: Temporal development of vertical wind velocity measured by Doppler wind lidar for ± 3 h hours around 00:00 UTC on 27th November (a), 28th November (b), and 29th November 2023 (c).

Conclusions and Outlook

In the framework of the *goSouth* project, bringing together existing experimental and modeling systems from TROPOS, NIWA, and IMUK, a joint model-accompanied measurement campaign was conducted in southern New Zealand at a shore site near Pahia, NZ. The campaign comprised ground-based and airborne meteorological and aerosol particle physico-chemical measurements, as well as regional modeling.

From the gained experimental data, at this stage, we hypothesize new particle formation from gaseous precursors emitted from New Zealand terrestrial

sources. Thorough data evaluation is ongoing to verify or falsify this hypothesis.

Concerning modeling, ICON-MUSCAT in its present form is not able to resolve the effect of the short passage of the air mass over land that presumably led to or favored the observed new particle formation and growth events. Further refinements in terms of precursor gas emission and oxidation as well as nucleation mechanisms making use of precursor gas mixtures from different sources (marine and terrestrial VOC, DMS, amines) are planned. Moreover, INP measurements are still scarce, despite the many campaigns in the Southern Ocean region in the recent years. Such data is needed to increase the

knowledge on spatial and temporal variability of INP and to utilize such comprehensive data sets for model evaluation and development.

Despite the new and very interesting findings concerning new particle formation in Southern New Zealand, future related investigations should be carried out at a less locally influenced site to obtain information for marine conditions. Longer measurement periods are favored as challenging conditions

(e.g. harsh wind conditions close to the ocean) might limit feasibility of in-situ measurements.

All in all, the *goSouth* project has enabled us to establish a sustainable collaboration, specifically between TROPOS and NIWA. The results obtained contribute to improving the quantitative understanding of aerosol-cloud-turbulence interactions in the Southern Hemisphere.

References

- Choi, Y. S., R. S. Lindzen, C. H. Ho, and J. Kim (2010), Space observations of cold-cloud phase change, *Proc. Natl. Acad. Sci. USA*, 107(25), 11211-11216, doi: <https://doi.org/10.1073/pnas.1006241107>.
- Deabji, N., K. W. Fomba, S. El Hajjaji, A. Mellouki, L. Poulin, S. Zeppenfeld, and H. Herrmann (2021), First insights into northern Africa high-altitude background aerosol chemical composition and source influences, *Atmos. Chem. Phys.*, 21(24), 18147-18174, doi: <https://doi.org/10.5194/acp-21-18147-2021>.
- Ditas, F., R.A. Shaw, H. Siebert, M. Simmel, B. Wehner, and A. Wiedensohler (2012), Aerosols-cloud microphysics-thermodynamics-turbulence: evaluating supersaturation in a marine stratocumulus cloud, *Atmos. Chem. Phys.*, 12, 2459–2468, doi: <https://doi.org/10.5194/acp-12-2459-2012>.
- Flato, G., et al. (2013). Evaluation of Climate Models. *Climate Change 2013: The Physical Science Basis. Contribution of Working Group I to the Fifth Assessment Report of the Intergovernmental Panel on Climate Change, Chapter 9: Evaluation of Climate Models*. Cambridge, United Kingdom and New York, NY, USA, Cambridge University Press.
- Hamilton, D. S., L. A. Lee, K. J. Pringle, C. L. Reddington, D. V. Spracklen, and K. S. Carslaw (2014), Occurrence of pristine aerosol environments on a polluted planet, *Proc. Natl. Acad. Sci. USA*, 111(52), 18466-18471, doi: <https://doi.org/10.1073/pnas.1415440111>.
- Hofer, J., P. Seifert, J. B. Liley, M. Radenz, O. Uchino, I. Morino, T. Sakai, T. Nagai, and A. Ansmann (2023), Aerosol-related effects on the occurrence of heterogeneous ice formation over Lauder, New Zealand/Aotearoa, EGUsphere [preprint, accepted for publication in *Atmos. Chem. Phys.*], doi: <https://doi.org/10.5194/egusphere-2023-2173>.
- Kanitz, T., P. Seifert, A. Ansmann, R. Engelmann, D. Althausen, C. Casiccia, and E. G. Rohwer (2011), Contrasting the impact of aerosols at northern and southern midlatitudes on heterogeneous ice formation, *Geophys. Res. Lett.*, 38(L17802), doi: <https://doi.org/10.1029/2011gl048532>.
- McCluskey, C. S., T. C. J. Hill, R. S. Humphries, A. M. Rauker, S. Moreau, P. G. Strutton, S. D. Chambers, A. G. Williams, I. McRobert, J. Ward, M. D. Keywood, J. Harnwell, W. Ponsonby, Z. M. Loh, P. B. Krummel, A. Protat, S. M. Kreidenweis, and P. J. DeMott (2018), Observations of Ice Nucleating Particles Over Southern Ocean (e.g. harsh wind conditions close to the ocean) might limit feasibility of in-situ measurements.
- Waters, *Geophys. Res. Lett.*, 45(21), 11989-11997, doi: <https://doi.org/10.1029/2018gl079981>.
- Quinn, P. K., D. J. Coffman, J. E. Johnson, L. M. Upchurch, and T. S. Bates (2017), Small fraction of marine cloud condensation nuclei made up of sea spray aerosol, *Nat. Geosci.*, 10(9), 674-679, doi: <https://doi.org/10.1038/ngeo3003>.
- Ramasamy, V. and V. K. Gopalakrishnan (2013), Chemical Composition of Spirulina by Gas Chromatography Coupled with Mass Spectrophotometer (GC-MS), *Int. J. Pharm. Phytopharmacological Res.*, 3(3), 239-244, <https://ejippr.com/s3gVln>.
- Schmale, J., A. Baccarini, I. Thurnherr, S. Henning, A. Efraim, L. Regayre, C. Bolas, M. Hartmann, A. Welti, K. Lehtipalo, F. Aemisegger, C. Tatzelt, S. Landwehr, R. L. Modini, F. Tummon, J. S. Johnson, N. Harris, M. Schnaiter, A. Toffoli, M. Derkani, N. Bukowiecki, F. Stratmann, J. Dommen, U. Baltensperger, H. Wernli, D. Rosenfeld, M. Gysel-Beer, and K. S. Carslaw (2019), Overview of the Antarctic Circumnavigation Expedition: Study of Preindustrial-like Aerosols and their Climate Effects (ACE-SPACE), *Bull. Am. Meteorol. Soc.*, doi: <https://doi.org/10.1175/BAMS-D-18-0187.1>.
- Siebert, H., and R. A. Shaw (2017), Supersaturation fluctuations during the early stage of cumulus formation, *J. Atmos. Sci.*, 74(4), 975-988, doi: <https://doi.org/10.1175/jas-d-16-0115.1>.
- Tatzelt, C., S. Henning, A. Welti, A. Baccarini, M. Hartmann, M. Gysel-Beer, M. van Pinxteren, R. L. Modini, J. Schmale, and F. Stratmann (2022), Circum-Antarctic abundance and properties of CCN and INPs, *Atmos. Chem. Phys.*, 22(14), 9721-9745, doi: <https://doi.org/10.5194/acp-22-9721-2022>.
- Vergara-Temprado, J., A. K. Miltenberger, K. Furtado, D. P. Grosvenor, B. J. Shipway, A. A. Hill, J. M. Wilkinson, P. R. Field, B. J. Murray, and K. S. Carslaw (2018), Strong control of Southern Ocean cloud reflectivity by ice-nucleating particles, *Proc. Natl. Acad. Sci. USA*, 115(11), 2687-2692, doi: <https://doi.org/10.1073/pnas.1721627115>.
- Villanueva, D., B. Heinold, P. Seifert, H. Deneke, M. Radenz, and I. Tegen (2020), The day-to-day co-variability between mineral dust and cloud glaciation: a proxy for heterogeneous freezing, *Atmos. Chem. Phys.*, 20(4), 2177-2199, doi: <https://doi.org/10.5194/acp-20-2177-2020>.
- Zelinka, M. D., T.A. Myers, D.T. McCoy, S. Po-Chedley, P.M. Caldwell, P. Ceppi, P., S.A. Klein, K.E. Taylor, (2020), Causes of higher climate sensitivity in CMIP6 models, *Geophys. Res. Lett.*, 47, e2019GL085782, doi: <https://doi.org/10.1029/2019GL085782>.

Funding

The *goSouth* and *LOSTECCA* projects were funded by the BMBF (German Federal Ministry of Education and Research, projects 01LK2003A and 01DR20002) and the Deep South Challenge and NIWA through SSIF (Strategic Science Investment Fund, New Zealand Ministry of Business, Innovation & Employment).

UTLS wildfire smoke – a synopsis of Polly observations in Europe, the Arctic, and southern South America (2017-2021)

Kevin Ohneiser, Albert Ansmann, Ronny Engelmann, Holger Baars, Patric Seifert, Moritz Haarig, Cristofer Jimenez, Martin Radenz, Julian Hofer, Dietrich Althausen, Johannes Bühl, Hartwig Deneke, Athina Floutsi, Henriette Gebauer, Hannes Griesche, Karsten Hanbuch, Birgit Heese, Andi Klamt, Fabian Senf, Annett Skupin, Philipp Sobek, Audrey Teisseire, Gregor Walter, Ulla Wandinger, Jonas Witthuhn, and Andreas Macke

Enorme Mengen an Waldbrandrauch von außerordentlich starken Waldbränden in Kanada (2017), Sibirien (2019), Australien (2019-2020) und Kalifornien (2020) gelangten in den letzten Jahren in die obere Troposphäre und untere Stratosphäre (UTLS: Upper Troposphere and Lower Stratosphere). Die Auswirkungen des Rauchs auf das Klimasystem der Erde wurden am TROPOS in den vergangenen Jahren intensiv untersucht. Mithilfe von Polarisations-Raman-Lidarmessungen (Polly: POrtabLe Lidar sYtem) wurden die optischen Eigenschaften des Rauchs vermessen und einige Aspekte der Auswirkungen auf das Klimasystem untersucht, insb. der Einfluss des Rauchs auf die stratosphärische Ozonschicht sowie auf die heterogene Eisbildung in Zirruswolken.

Introduction

Record-breaking wildfires were raging in the past years in many parts of the world. Extreme examples were happening in Canada 2017, Siberia 2019, Australia 2019-2020, and California 2020. Enormous amounts of wildfire smoke were injected into the upper troposphere and lower stratosphere (UTLS) which resulted in a stratospheric aerosol perturbation never observed before in the case of forest fire events.

The strong wildfires in British Columbia during the summer of 2017 were coupled with rather favorable weather conditions on 12 August 2017 that triggered the evolution of five major thunderstorms over western Canada in the afternoon of this day. Exceptionally strong and well-organized pyrocumulonimbus (pyroCb) clusters developed over the fire areas and lofted enormous amounts of fire smoke into the UTLS [Haarig et al., 2018; Ansmann et al., 2018; Baars et al., 2019].

In the summer of 2019, extreme and long-lasting wildfires in central and eastern Siberia developed and were responsible for the UTLS smoke layer that was observed during the MOSAiC (Multidisciplinary drifting Observatory for the Study of Arctic Climate) campaign in the central Arctic between Autumn 2019 and Spring 2020 [Engelmann et al. 2021; Ohneiser et al., 2021]. The main burning phase lasted from 19 July

to 14 August 2019. The most intense fires occurred between 55 and 70°N in close proximity to the Arctic region. In the absence of strong pyroCb activity, self-lofting processes were responsible for the vertical transport of smoke up to the tropopause [Ohneiser et al., 2021, 2023].

The strongest fires, ever observed in the Southern Hemisphere, developed in southeastern Australia in the second half of 2020 [Ohneiser et al., 2020, 2022; Ansmann et al., 2021]. In combination with extraordinarily strong pyrocumulonimbus (pyroCb) activity during the last days of December 2019 and the first days of January 2020, a rather strong perturbation of the stratospheric aerosol conditions was observed from ground and space.

In 2020, the strongest and longest wildfire season, ever monitored in California, occurred. A large amount of smoke was injected into the free troposphere. The biomass-burning-aerosol (BBA) layers were partly transported from the US west coast toward central Europe within 3 – 4 days [Baars et al., 2020].

Wildfire smoke particles, mainly consisting of brown carbon with a few percent of black carbon, considerably absorb solar radiation and can perturb shortwave and longwave radiative fluxes and thus dynamical processes. Several Australian smoke plumes were found to significantly alter the dynamic

circulation in the lower stratosphere. The potential of smoke to ascend over several months by heating the air due to strong light absorption is an important aspect that significantly prolongs the residence time of wildfire smoke in the stratosphere. Record-breaking stratospheric ozone holes formed partly (Arctic, 2020) and fully (Antarctica, 2020 and 2021) in smoke-polluted air [Ohneiser et al., 2021, 2022]. Clear indications for an impact of smoke on ozone hole formation (most pronounced over Antarctica) was found for the first time [Ansmann et al., 2022]. Evidence was also found that wildfire smoke particles can initiate cirrus formation in the tropopause region at -47 to -53°C [Ansmann et al., 2023; Mamouri et al., 2023].

Long-term observations of Canadian smoke over Europe, Siberian smoke over the Arctic, Australian smoke over South America, and Californian smoke over Cyprus using a powerful multiwavelength polarization Raman lidar [Engelmann et al., 2016] provided valuable information on the decay behavior of the stratospheric perturbation in terms of optical and microphysical smoke properties. These unique measurements with TROPOS lidars are presented in more detail in this report.

Results

Canadian fire smoke observed with PollyNET over Europe in 2017–2018

The smoke of the Canadian forest fires was transported towards Europe within a week and was observable with PollyNET (the network of Polly lidar instruments built by TROPOS; Polly stands for POrtable Lidar sYstem) in the stratosphere for almost half a year. For the first time, the large advantage of a continent-wide network of continuously measuring lidars [Baars et al., 2016] to monitor the spread of UTLS aerosol particles and the decay of the stratospheric perturbation could be demonstrated in detail.

The Polly observations in Fig. 1a were performed at Évora (Portugal), the central European stations of Hohenpeissenberg (Germany), Košetice (Czech Republic), and Warsaw (Poland) and in the eastern Mediterranean (Finokalia on the Greek island of Crete, Limassol in Cyprus, and Haifa, Israel) show that the layer top frequently exceeded 20 km (up to around 23 km) from mid-September 2017 until the end of the year (Fig. 1a). The main smoke layer extended from 15 to 20 km. The smoke was frequently detected over southwestern and central Europe in the beginning of the smoke period (August–September 2017) and then mostly over the eastern Mediterranean (October 2017 to January 2018). The data analysis was stopped at the end of January 2018 because

no significant smoke layer was found anymore over Finokalia, Limassol, and Haifa during the following months. As shown in Fig. 1b, the stratospheric aerosol optical thickness (AOT) at 532 nm decreased rapidly from values > 0.2 in August 2017 to values between 0.005 and 0.03 in the beginning of September 2017, and afterwards the AOT ranged from 0.002 (almost stratospheric background conditions) to 0.008 with most values between 0.003 and 0.004 (over Finokalia, Limassol, and Haifa; mid-September to December 2017).

The AOT fluctuations are partly caused by the relatively strong impact of signal noise on the retrieval results. However, atmospheric variability also contributed to the observed AOT fluctuations and varying vertically averaged 532 nm extinction coefficients shown in Fig. 1c. We observed vertical mean particle extinction coefficients for the smoke layers from 10 to 200 Mm^{-1} in August 2017, from 2 to 50 Mm^{-1} until 5 September 2017, from 1 to 10 Mm^{-1} until the end of September, and from 0.5 to 5 Mm^{-1} (accumulating around 1 Mm^{-1}) until the end of January 2018. Based on 731 clear-sky EARLINET nighttime lidar observations at Leipzig from January 2000 to June 2008, we conclude that the minimum (or background) stratospheric AOT is on the order of 0.001 to 0.002 for the layer from 1 km above the tropopause to the top of the identified aerosol structures ($< 30 \text{ km}$ in height). When using a typical extinction-to-backscatter ratio of 50 sr (for non-soot particles), the particle extinction coefficients for stratospheric background conditions are in the range of $0.1\text{--}0.2 \text{ Mm}^{-1}$ at 532 nm. More details are given by Ansmann et al. [2018], Haarig et al. [2018] and Baars et al. [2019].

The rotating, ascending Australian smoke disk: A unique atmospheric observation

A new atmospheric phenomenon, never observed before, was detected in January–March 2020 with the Polly at Punta Arenas, Chile, and the fleet of spaceborne instrumentation. It coupled smoke occurrence, aerosol–radiation interaction, and dynamical processes. A striking discovery was the observation of several rotating stratospheric smoke disks with diameters of up to 1000 km and vertical extents of up to 5 km. These disk-like aerosol layers self-organized themselves as so-called quasi-ellipsoidal anticyclonic vortices, persisted over weeks to months, and traveled around the globe. The smoke disks partly ascended from 15–20 km to up to 35 km height as a result of self-lofting processes (absorption of solar radiation by the smoke particles, heating of the smoke-containing air layers, and subsequent lofting of these heated layers in the colder environment).

Wildfire smoke, at such great heights, was never observed before. The upward moving smoke disks started to rotate. The heating of the air resulted in an anticyclonic (i.e., counterclockwise) circulation, with winds rotating around the plume at about 15 m s^{-1} .

This is the first evidence of smoke causing changes to winds in the stratosphere. This unique observation opened up a whole new vein of scientific research. This highly stable vortex persisted in the stratosphere for over 13 weeks, crossed the Pacific (from New Zealand to Chile) within 2 weeks, and hovered above the tip of South America for more than a week. It then followed a 10-week westbound round-the-world journey that could be tracked over 66 000 km until the beginning of April 2020. Rotation was essential in maintaining (stabilizing) the structure of the vortex for such a long time. All available satellite observations were analyzed and summarized in the bachelor thesis of *Gregor Walter [2021]*.

The rotating smoke field drifted with the prevailing westerly air flow towards South America and stayed close to the southernmost tip of South America (see Fig. 2) for 10–12 days, until the beginning of February 2020, and ascended by about 500 m per day. The

center of the vortex was closest to Punta Arenas on 29–30 January 2020. Figure 2a shows the disk-like structure southwest of two lidar stations at Punta Arenas (TROPOS Polly) and Río Grande (lidar of DLR, Oberpfaffenhofen). The Sentinel-5 UV aerosol index from 340 and 388 nm is shown for 26 January 2020. Bright blue colors indicate the presence of absorbing aerosol. The smoke plume was well detected by the spaceborne CALIOP (Cloud Aerosol Lidar with Orthogonal Polarization) instrument on 25 January 2020, as shown in Fig. 2b (dashed curve in Fig. 2a shows the CALIOP track). The smoke vortex was detected between 19 and 26 km height at latitudes from 52 to 65°S. According to the Punta Arenas lidar observations in Fig. 2c, parts of the rotating smoke field covered southern Chile from 24–31 January 2020. The flat base of the dome-like plume structure (see Fig. 2b) ascended from 19 km on 24 January to 22 km on 30 January and thus with a speed of about 500 m per day over the Polly lidar site. During the steady and monotonic ascent, the smoke reached heights above 22–25 km, at which easterly winds dominated, and started to move towards southern Africa in the following weeks.

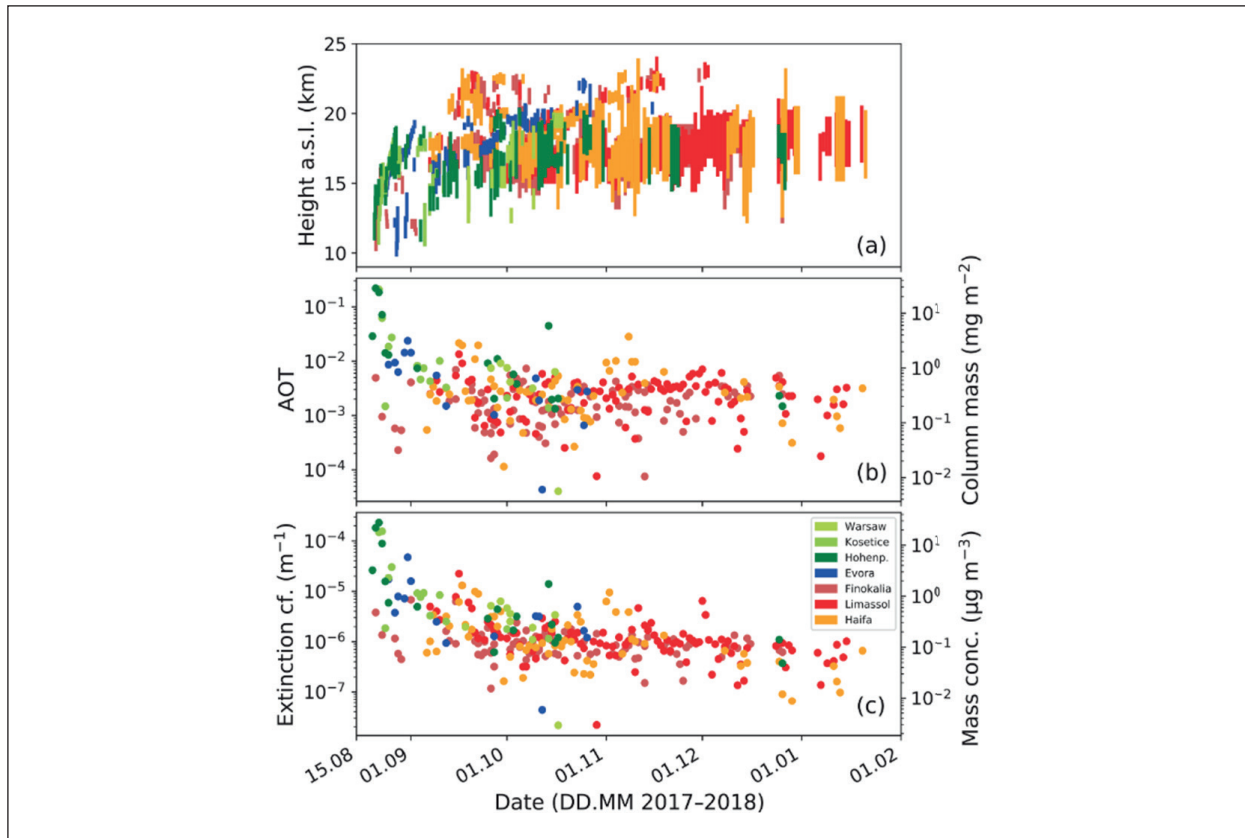


Fig. 1: (a) Overview of lidar observations with seven PollyNET instruments at sites in central Europe, in Portugal, and in the eastern Mediterranean (see legend in c) of the stratospheric smoke layer [from base to top as colored vertical lines, Baars et al., 2019]. For each station, one nighttime observation per day is considered. (b) Corresponding smoke layer AOT at 532 nm and estimated column-integrated smoke particle mass concentration and (c) vertically averaged smoke particle extinction coefficient and corresponding mean particle mass concentration.

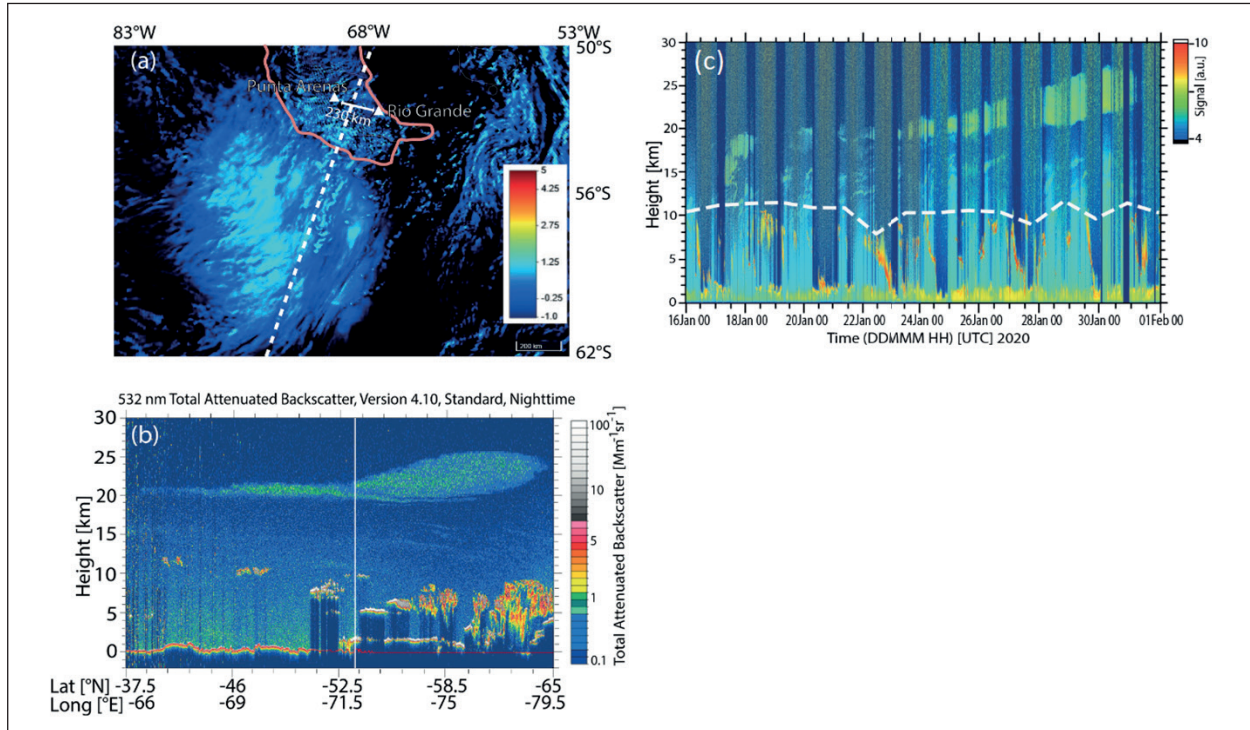


Fig. 2: (a) Sentinel-5 aerosol index (340–380 nm), showing the location of the rotating and ascending smoke vortex southwest of the southernmost tip of South America on 26 January 2020 from 00:00 to 20:00 UTC. Indicated are two ground-based lidar stations at Punta Arenas and Rio Grande (white triangles). The white dashed line indicates the CALIOP overpass. (b) CALIOP observation along the overpass track on 25 January 2020 between 05:50 and 06:02 UTC, showing smoke plumes above 20 km and the smoke-filled vortex at latitudes south of 52.5°S in terms of the 532 nm attenuated backscatter coefficient. The thin vertical line at 52.3°S indicates the shortest distance to the two ground-based lidars (triangles in panel a). (c) The rotating and ascending smoke vortex, as observed with ground-based lidar at Punta Arenas from 24–31 January 2020. Shown is the range-corrected signal at 1064 nm wavelength in arbitrary units in a logarithmic color scale. The tropopause is indicated by the white dashed line. Tropospheric clouds and day and night signal background changes caused the many interruptions in the high-quality observations of the stratospheric smoke. The figures are shown and discussed in detail in Ohneiser et al. [2022].

Comparison of the Canadian (2017), Siberian (2019–2020) and Australian (2020–2021) smoke events: Geometrical properties, AOT, and decay behavior

In Fig. 3, the three major stratospheric smoke events (PNE, Pacific Northwest Event, Canada; ANYSO, Australian New Year Super Outbreak; SILBE, Siberian Lake Baikal Event) are compared regarding their geometrical and optical properties. As can be seen, the vertical extent of the Canadian smoke layers was of the order of 1–4 km, and these smoke layers were clearly observable over Europe with lidar up to 150 days after injection only. The Siberian smoke formed a 7–10 km thick layer and was monitored from day 80 up to about 300 days after injection over the central Arctic during the MOSAiC expedition 2019–2020. From December 2019 to May 2020, the smoke was trapped around the North Pole under the influence of a rather strong polar vortex. The stratospheric perturbation could be observed until the strong polar vortex collapsed in May 2020 so that the smoke became dispersed over a larger

region towards the midlatitudes in the late spring and summer of 2020. The Australian fires were by far the strongest and produced a 10–15 km thick layer over Punta Arenas (and the entire southern part of the Southern Hemisphere according to the literature). These smoke layers were clearly detectable even 2 years after injection [Ohneiser et al., 2022]. The layer base height of the ANYSO and SILBE smoke layers was always close to or slightly below the tropopause (mostly at 8–10 km height). In contrast, the base height of the PNE smoke layer was typically several kilometers above the tropopause. The top height was mostly around 20 (PNE), 18 (SILBE), and 23–24 km (ANYSO). The different top heights had a sensitive impact on the decay of the stratospheric perturbation described in terms of e-folding decay times.

In Fig. 3b, the AOT data sets of the three wildfire events are compared, and the decay behavior of the different stratospheric perturbations is shown. As expected, the PNE AOTs were, on average, 3 to 4 times lower than the ANYSO AOTs. In order to see a clear reduction in the AOT with time, the PNE and ANYSO AOTs were computed from the smoke

extinction coefficients between 13 and 30 km height and thus for a height range several kilometers above the tropopause. The decay behavior is indicated by straight lines in Fig. 3b. In addition, the e-folding decay times are given as numbers. They were computed by using the AOT time series from day 40 to 160 (PNE) and from day 60 to 560 (ANYSO). The first 40–60 days (after smoke injection) were excluded because they showed a rather strong AOT variability and no clear trend. The MOSAiC expedition started in October 2019 (2–3 months after the strong Siberian fires) so that all measured AOT values could be considered in the decay time computation in the case of the Siberian smoke (SILBE data, in blue in Fig. 3). In terms of AOT, the ANYSO and SILBE smoke events were similar. However, strong differences in the decay behavior of the stratospheric perturbation in the Northern and Southern Hemispheres were found. A very large value of the e-folding decay time of 19 months was obtained from the ANYSO AOT data set and a quite short decay time of 8 months in the case of PNE (2017). Several processes influence the decay time.

Besides the sedimentation of particles and self-lofting of the absorbing smoke particle, horizontal (meridional) dispersion, and even the growth of the smoke particles by water uptake and condensation of gases on the particles have to be considered. Larger particles produce larger optical effects and

thus lead to an increase in AOT. The top height of the smoke layer plays an important role as well. The main ANYSO smoke layer reached to around 24 km height. And this comparably large top height in combination with particle sedimentation was responsible for the e-folding decay time of 19 months. The PNE smoke was mostly confined between 14 and 20 km height and thus could be removed relatively quickly (from the stratosphere above 13 km). Furthermore, complex horizontal dispersion features in the Northern Hemisphere have been reported in the case of the Canadian smoke event. The smoke became efficiently distributed towards the tropics and towards the North Pole within a few weeks. The short decay time for the High Arctic smoke (SILBE, 2019–2020) of 5 months is related to the specific polar meteorological conditions (impact of the strong polar vortex) and specific vertical air mass exchange mechanisms (related to the Brewer–Dobson circulation) and also to the fact that the top of the aerosol layer was clearly below 20 km height.

Impact of wildfire smoke on stratospheric ozone depletion

Figure 4 shows the deviation in the ozone partial pressure (from the 2000–2019 mean value) over the Neumayer research station of the Alfred Wegener Institute (70.6°S , 8.3°W). The daily smoke

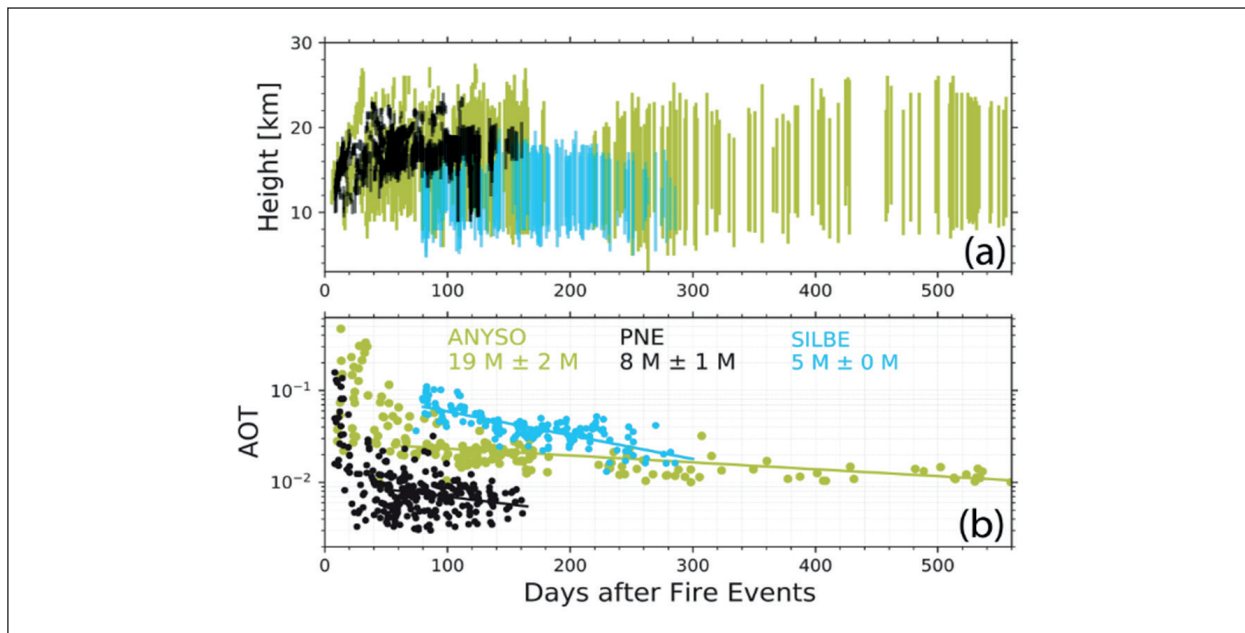


Fig. 3: Comparison of geometrical and optical properties of three stratospheric fire smoke events measured with different Polly instruments [Ohneiser et al., 2022]. Day 0 is the 12 August 2017 (PNE), 23 July 2019 (SILBE), and 31 December 2019 (ANYSO). Canadian (PNE), Siberian (SILBE), and Australian (ANYSO) fire smoke data are taken from Baars et al. [2019], Ohneiser et al. [2021], and Ohneiser et al. [2022], respectively. (a) Overview of Polly observations of UTLS smoke layers (colored bars from layer base to top) in the days after smoke injection into the UTLS height regime. (b) The 532 nm AOT time series for the different wildfire events; straight lines indicate the decay of the perturbations according to the given e-folding decay times in months (M).

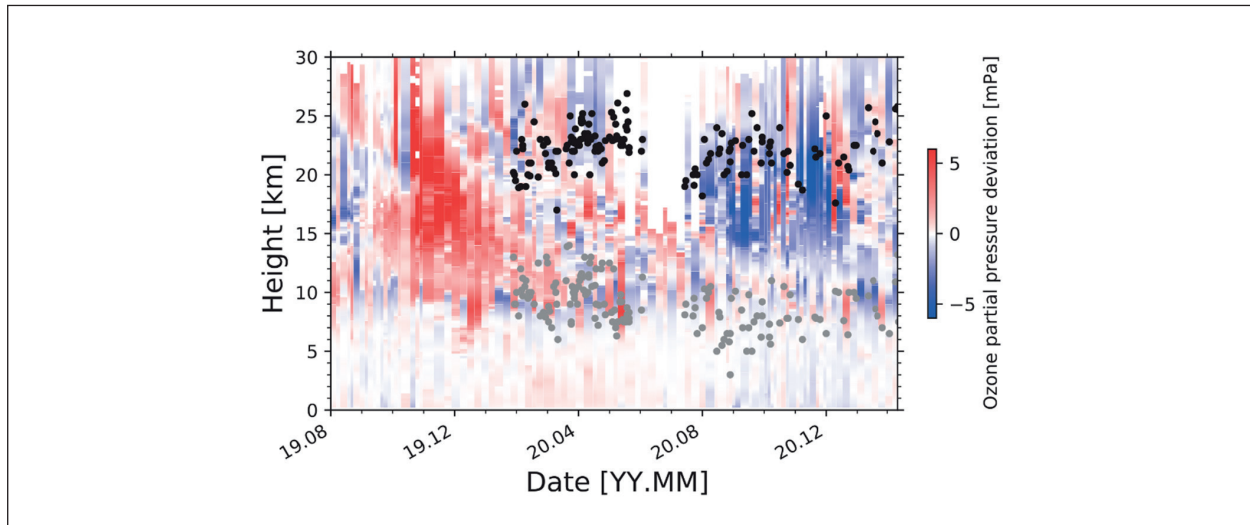


Fig. 4: Deviation of each individual ozone profile measured at the Neumayer Station from the respective long-term (2000–2019) monthly mean ozone profile [Ohneiser et al., 2022]. The base (gray dots) and top heights (black dots) of the Australian smoke layer measured with Polly at Punta Arenas indicate the smoke-polluted height range.

layer base and top heights, as measured over Punta Arenas (53.2°S , 70.9°W), are indicated by gray and black circles, respectively. We assume that the general structures of the smoke layers as measured over Punta Arenas were similar to the ones over the Neumayer station (about 1900 km further south). Large positive ozone deviations from the long-term mean were observed in November and December 2019 before the long-lasting decrease in the ozone partial pressure over about 10 months started. From October 2020 to January 2021, the largest negative ozone deviations were found between 12 and 25 km, well within the Australian smoke layer [Ohneiser et al., 2022; Ansmann et al., 2022]. As in the case of the strong ozone depletion over the High Arctic [Ohneiser et al., 2021], the polar vortex was unusually strong over Antarctica in July and August 2020. The large-scale warming of the southern hemispheric stratosphere as a result of strong absorption of solar radiation by smoke in January to April 2020 may have contributed to the development of a strong vortex over Antarctica in the July–September 2020 by suppressing large-scale wave activity.

We observed a clear coincidence between the layer with strongest ozone reduction over the ozone-sonde stations (14–25 km height range) and the layer showing an enhanced particle surface area concentration over Punta Arenas (10–24 km height range) and the height range in which CALIOP detected PSCs (mostly over Antarctica at heights from 13–26 km, Ohneiser et al., 2022; Ansmann et al., 2022).

We assume that, in the PSC height range from 13–26 km, all background particles and most of the $\text{H}_2\text{SO}_4/\text{H}_2\text{O}$ -coated smoke particles grew due to

HNO_3 condensation during PSC events. Compared to PSC-free conditions, the particle surface area concentration and thus the potential for halogen activation strongly increased within the PSCs. The total particle number concentration is typically a factor of 1.3–2 higher than the number concentration of particles larger than 50 nm. High numbers of smoke particle concentrations were found in the PSC height region during the southern hemispheric winter and spring months in 2020 and were probably involved in PSC formation, strong halogen activation, and the resulting record-breaking ozone depletion. The findings in Ohneiser et al. 2021 were highlighted in the Science magazine by Voosen [2021]. More details are also given in Ansmann et al. [2022]. Recently, Dinneen [2023] highlighted our findings regarding Arctic and Antarctic ozone loss caused by wildfire smoke in the New Scientist magazine.

Impact of wildfire smoke on ice nucleation in the upper troposphere

Strong ice nucleation and virga evolution were observed over Limassol, Cyprus, over many hours in the evening of 30 October 2020 [Mamouri et al., 2023]. The top height of the virga zone always coincided with the lower part of the smoke layer as shown in Fig. 5. The measurements were performed with a TROPOS Polly instrument as part of CARO (Cyprus Atmospheric Remote Sensing Observatory) of the Eratosthenes Centre of Excellence, Limassol. The smoke originated from strong Californian wildfires. The pronounced virga structures point to a relatively small number of comparably large ice crystals that

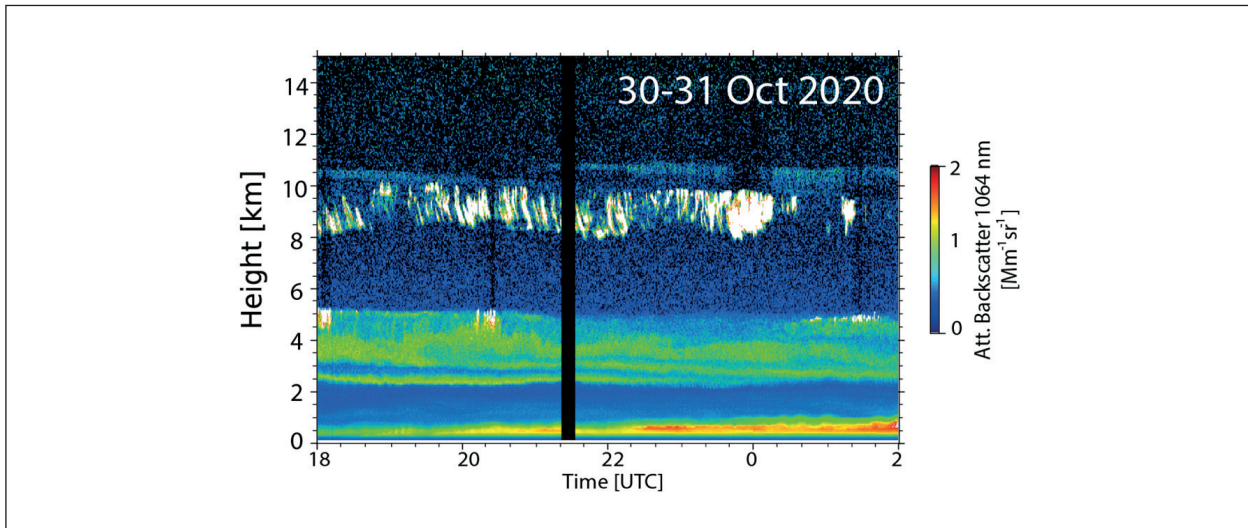


Fig.5: The height-time displays of the range-corrected 1064 nm backscatter signal (equivalent to the 1064 nm attenuated backscatter coefficient), measured with the TROPOS Polly, shows Californian wildfire smoke layers at 10–11 km height [Mamouri et al., 2023]. Ice nucleation started at the top of the ice virga zone (white features, at about -50°C). The virga tops coincided with the lower part of the smoke layers.

grew fast and formed these well-organized virga signatures. A broad crystal size spectrum (causing a respectively broad spectrum of sedimentation velocities) would probably not be able to produce such coherent virga structures over many hours.

Patchy and incoherent cirrus structures would be more likely. The smoke layer sufficiently overlapped with the humid region in the uppermost troposphere and thus was able to influence the development of cirrus clouds and virga significantly. All this is discussed in detail in Mamouri et al. [2023]. Based on lidar observations at Limassol, Cyprus, in the eastern Mediterranean we found clear evidence for the impact of wildfire smoke on cirrus formation in the tropopause region. The study of Mamouri et al. [2023] was selected by the Nature journal as research highlight [Liverpool, 2023].

Self-lofting of smoke in the free troposphere

Optically thick wildfire smoke layers absorb a sufficient amount of solar radiation, so that they heat up and start to ascend as a result of so-called self-lofting processes. Such a behavior was frequently observed in the stratosphere but only rarely in the troposphere.

Figure 6 shows ECRAD (European Centre for Medium-Range Weather Forecasts Radiation scheme) model simulations [for details see Ohneiser et al., 2023] of the ascent of a 2.5 km thick smoke layer from the lower troposphere to the stratosphere as a function of AOT. The initial layer center was at 3 km height (at day 0). The profiles were scaled to an AOT of 1, 2, and 3, as shown in the legend.

Three different BC fractions are considered. Again, daily average heating rates are used, and respective daily average lofting rates are calculated. In reality, the smoke layers diverge with time so that the AOT decreases. In the scenarios in Fig. 6, the AOT decreases by 15 % from day to day. On each next day, the new smoke layer center in terms of extinction is calculated from the layer center height of the last day plus the 24 hour mean lofting rate. The layer thickness is always 2.5 km, and the AOT is 15 % less compared to the day before. All curves in Fig. 6 indicate ascending layers that accelerate in the higher troposphere, although AOT decreases by 15 % per day. At the tropopause all aerosol layers ascend slowly. The higher the BC fraction, the higher the finally reached altitude. After 14 days of lofting, a smoke layer with a 2.5 % BC content would typically be found 1–3 km below the height of an aerosol layer with a 3.5 % BC content. A higher BC fraction is directly related to a larger ascent rate; however, there are too many free parameters that influence the ascent rate, which makes it hard to determine the BC fraction from model simulations when comparing to an observed lofting rate.

Our simulations show that it is in principle possible to loft an aerosol layer to the tropopause in the absence of any pyroCb convection. As the lofting process is quite efficient in the upper troposphere, even in the case of moderate pyroCb development with cloud tops reaching 8–10 km height only, smoke layers can easily be lofted higher up into the stratosphere.

The self-lofting rate was found to sensitively depend on the AOT, layer thickness, layer height,

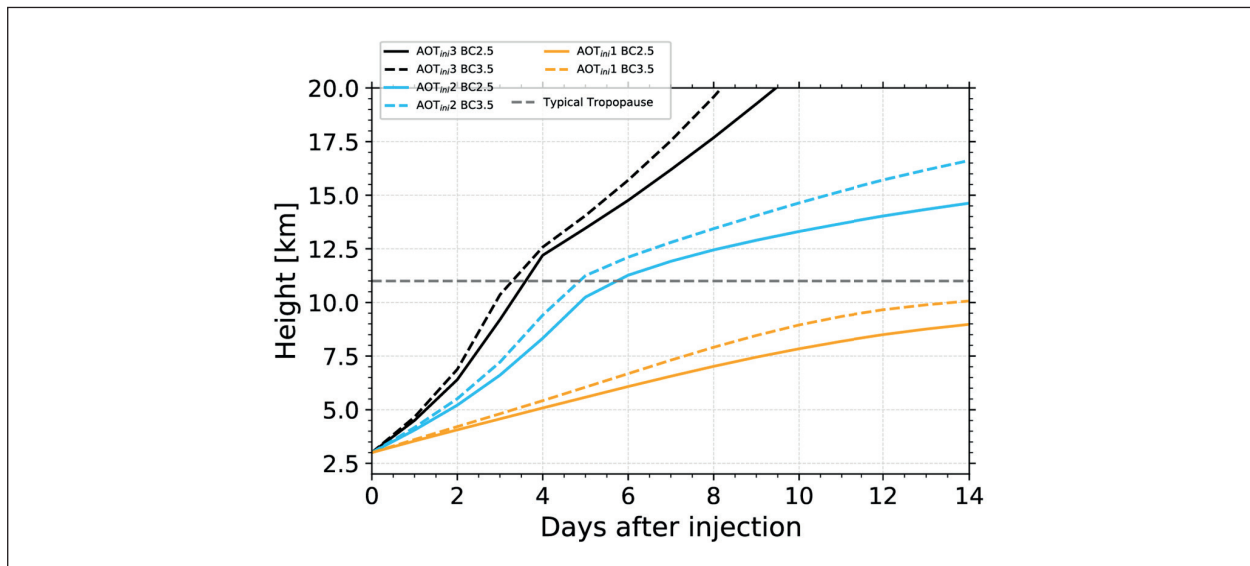


Fig. 6: Change in the center height of a 2.5 km thick aerosol layer, initially at 3 km height (day 0), during 14 d of continuous lofting (black, blue, orange, Ohneiser et al., 2023). In the ECRAD simulation, the AOT continuously decreases by 15 % from day to day. Different scenarios with different initial AOT of 1, 2, and 3 (indicated by index *ini*) and BC fraction of 2.5 %, 3.5 %, and 15 % are simulated. The dashed gray line represents a typical tropopause height in the mid-latitudes.

black-carbon-to-organic-carbon ratio, cloudiness, relative humidity, potential temperature gradient, and longevity of the smoke layers. The modelling results showed that smoke can ascend from the lower free troposphere to the tropopause within 3–7 days by these self-lofting processes in stable and stagnant weather conditions.

Summary

Lidar observations of the geometrical, optical, and microphysical properties of stratospheric smoke layers originating from four major wildfire events, occurring in the years 2017–2021, were presented and the decay of the smoke-related major stratospheric

aerosol perturbations was discussed. There were four outstanding events: the Canadian wildfires 2017, Siberian wildfires 2019, Australian wildfires 2019/2020, and Californian wildfires 2020. The observations of the resulting UTLS smoke plumes with powerful multi-wavelength polarization Raman lidars up to 30 km height are unique long-term data sets. The smoke in the stratosphere had a radiative impact, influenced dynamics and circulation pattern, caused ozone depletion in the stratosphere, and the particles that reentered the troposphere also influenced cirrus evolution. The TROPOS lidar observation significantly contributed to the investigation of the role of wildfire smoke in the climate system during recent years.

References

- Ansmann, A., H. Baars, A. Chudnovsky, I. Mattis, I. Veselovskii, M. Haarig, P. Seifert, R. Engelmann, and U. Wandinger (2018): Extreme levels of Canadian wildfire smoke in the stratosphere over central Europe on 21–22 August 2017, *Atmos. Chem. Phys.*, 18, 11831–11845, <https://doi.org/10.5194/acp-18-11831-2018>
- Ansmann, A., K. Ohneiser, R.-E. Mamouri, D.A. Knopf, I. Veselovskii, H. Baars, R. Engelmann, A. Foth, C. Jimenez, P. Seifert, and B. Barja (2021): Tropospheric and stratospheric wildfire smoke profiling with lidar: mass, surface area, CCN, and INP retrieval, *Atmos. Chem. Phys.*, 21, 9779–9807, <https://doi.org/10.5194/acp-21-9779-2021>
- Ansmann, A., K. Ohneiser, A. Chudnovsky, D.A. Knopf, E.W. Eloranta, D. Villanueva, P. Seifert, M. Radenz, B. Barja, F. Zamorano, C. Jimenez, R. Engelmann, H. Baars, H. Griesche, J. Hofer, D. Althausen, and U. Wandinger (2022): Ozone depletion in the Arctic and Antarctic stratosphere induced by wildfire smoke, *Atmos. Chem. Phys.*, 22, 11701–11726, <https://doi.org/10.5194/acp-22-11701-2022>
- Ansmann, A., K. Ohneiser, R. Engelmann, M. Radenz, H. Griesche, J. Hofer, D. Althausen, J.M. Creamean, M.C. Boyer, D.A. Knopf, S. Dahlke, M. Maturilli, H. Gebauer, J. Bühl, C. Jimenez, P. Seifert, and U. Wandinger (2023): Annual cycle of aerosol properties over the central Arctic during MOSAiC 2019–2020 – light-extinction, CCN, and INP levels from the boundary layer to the tropopause, *Atmos. Chem. Phys.*, 23, 12821–12849, <https://doi.org/10.5194/acp-23-12821-2023>
- Baars, H., A. Ansmann, K. Ohneiser, M. Haarig, R. Engelmann, D. Althausen, I. Hanssen, M. Gausa, A. Pietruckzuk, A. Szkop, I.S. Stachlewska, D. Wang, J. Reichardt, A. Skupin, I. Mattis, T. Trickl, H. Vogelmann, F. Navas-Guzmán, A. Haefele, K. Acheson,

- A.A. Ruth, B. Tatarov, D. Müller, Q. Hu, T. Podvin, P. Goloub, I. Veselovskii, C. Pietras, M. Haeffelin, P. Fréville, M. Sicard, A. Comerón, A.J. Fernández García, F. Molero Menéndez, C. Córdoba-Jabonero, J.L. Guerrero-Rascado, L. Alados-Arboledas, D. Bortoli, M.J. Costa, D. Dionisi, G.L. Libert, X. Wang, A. Sannino, N. Papagiannopoulos, A. Boselli, L. Mona, G. D'Amico, S. Romano, M.R. Perrone, L. Belegante, D. Nicolae, I. Grigorov, A. Gialitaki, V. Amiridis, O. Soupiona, A. Papayannis, R.-E. Mamouri, A. Nisantzi, B. Heese, J. Hofer, Y.Y. Schechner, U. Wandinger, and G. Pappalardo (2019): The unprecedented 2017–2018 stratospheric smoke event: decay phase and aerosol properties observed with the EARLINET, *Atmos. Chem. Phys.*, 19, 15183–15198, <https://doi.org/10.5194/acp-19-15183-2019>
- Baars, H., T. Kanitz, R. Engelmann, D. Althausen, B. Heese, M. Komppula, J. Preißler, M. Tesche, A. Ansmann, U. Wandinger, J.-H. Lim, J.Y. Ahn, I.S. Stachlewska, V. Amiridis, E. Marinou, P. Seifert, J. Hofer, A. Skupin, F. Schneider, S. Bohlmann, A. Foth, S. Bley, A. Pfüller, E. Giannakaki, H. Lihavainen, Y. Viisanen, R.K. Hooda, S.N. Pereira, D. Bortoli, F. Wagner, I. Mattis, L. Janicka, K.M. Markowicz, P. Achtert, P. Artaxo, T. Pauliquevis, R.A.F. Souza, V.P. Sharma, P.G. van Zyl, J.P. Beukes, J. Sun, E.G. Rohwer, R. Deng, R.-E. Mamouri, and F. Zamorano (2016): An overview of the first decade of Polly^{NET}: an emerging network of automated Raman-polarization lidars for continuous aerosol profiling, *Atmos. Chem. Phys.*, 16, 5111–5137, <https://doi.org/10.5194/acp-16-5111-2016>
- Baars, H., M. Radenz, A.A. Floutsi, R. Engelmann, D. Althausen, B. Heese, A. Ansmann, T. Flament, A. Dabas, D. Trapon, O. Reitebuch, S. Bley, U. Wandinger (2021): Californian wildfire smoke over Europe: A first example of the aerosol observing capabilities of Aeolus compared to ground-based lidar, *Geophysical Research Letters*, 48, e2020GL092194, <https://doi.org/10.1029/2020GL092194>
- Dinneen, J. (2023): How smoke from Australia's megafires ate away at the ozone, *NewScientist*, <https://www.newscientist.com/article/2363372-how-smoke-from-australias-megafires-ate-away-at-the-ozone/>
- Engelmann, R., T. Kanitz, H. Baars, B. Heese, D. Althausen, A. Skupin, U. Wandinger, M. Komppula, I. Stachlewska, V. Amiridis, E. Marinou, I. Mattis, H. Linné, and A. Ansmann (2016): The automated multiwavelength Raman polarization and water-vapor lidar PollyXT: the neXT generation, *Atmospheric Measurement Techniques*, 9, 1767–1784, <https://doi.org/10.5194/amt-9-1767-2016>
- Engelmann, R., A. Ansmann, K. Ohneiser, H. Griesche, M. Radenz, J. Hofer, D. Althausen, S. Dahlke, M. Maturilli, I. Veselovskii, C. Jimenez, R. Wiesen, H. Baars, J. Bühl, H. Gebauer, M. Haarig, P. Seifert, U. Wandinger, and A. Macke (2021): Wildfire smoke, Arctic haze, and aerosol effects on mixed-phase and cirrus clouds over the North Pole region during MOSAiC: an introduction, *Atmos. Chem. Phys.*, 21, 13397–13423, <https://doi.org/10.5194/acp-21-13397-2021>
- Haarig, M., A. Ansmann, H. Baars, C. Jimenez, I. Veselovskii, R. Engelmann, and D. Althausen (2018): Depolarization and lidar ratios at 355, 532, and 1064 nm and microphysical properties of aged tropospheric and stratospheric Canadian wildfire smoke, *Atmos. Chem. Phys.*, 18, 11847–11861, <https://doi.org/10.5194/acp-18-11847-2018>
- Liverpool, L. (2023): Huge California wildfires seeded cirrus clouds half a world away, *Nature*, <https://www.nature.com/articles/d41586-023-03560-y>
- Mamouri, R.-E., A. Ansmann, K. Ohneiser, D.A. Knopf, A. Nisantzi, J. Bühl, R. Engelmann, A. Skupin, P. Seifert, H. Baars, D. Ene, U. Wandinger, and D. Hadjimitsis (2023): Wildfire smoke triggers cirrus formation: lidar observations over the eastern Mediterranean, *Atmos. Chem. Phys.*, 23, 14097–14114, <https://doi.org/10.5194/acp-23-14097-2023>
- Ohneiser, K., A. Ansmann, H. Baars, P. Seifert, B. Barja, C. Jimenez, M. Radenz, A. Teisseire, A. Floutsi, M. Haarig, A. Foth, A. Chudnovsky, R. Engelmann, F. Zamorano, J. Bühl, and U. Wandinger (2020): Smoke of extreme Australian bushfires observed in the stratosphere over Punta Arenas, Chile, in January 2020: optical thickness, lidar ratios, and depolarization ratios at 355 and 532 nm, *Atmospheric Chemistry and Physics*, 20, 8003–8015, <https://doi.org/10.5194/acp-20-8003-2020>
- Ohneiser, K., A. Ansmann, A. Chudnovsky, R. Engelmann, C. Ritter, I. Veselovskii, H. Baars, H. Gebauer, H. Griesche, M. Radenz, J. Hofer, D. Althausen, S. Dahlke, and M. Maturilli (2021): The unexpected smoke layer in the High Arctic winter stratosphere during MOSAiC 2019–2020, *Atmos. Chem. Phys.*, 21, 15783–15808, <https://doi.org/10.5194/acp-21-15783-2021>
- Ohneiser, K., A. Ansmann, B. Kaifler, A. Chudnovsky, B. Barja, D.A. Knopf, N. Kaifler, H. Baars, P. Seifert, D. Villanueva, C. Jimenez, M. Radenz, R. Engelmann, I. Veselovskii, and F. Zamorano (2022): Australian wildfire smoke in the stratosphere: the decay phase in 2020/2021 and impact on ozone depletion, *Atmos. Chem. Phys.*, 22, 7417–7442, <https://doi.org/10.5194/acp-22-7417-2022>
- Ohneiser, K., A. Ansmann, J. Witthuhn, H. Deneke, A. Chudnovsky, G. Walter, and F. Senf (2023): Self-lofting of wildfire smoke in the troposphere and stratosphere: simulations and space lidar observations, *Atmos. Chem. Phys.*, 23, 2901–2925, <https://doi.org/10.5194/acp-23-2901-2023>
- Voosen, P. (2021): High-flying wildfire smoke may threaten ozone layer: Record Arctic ozone loss linked to Siberian wildfires, *Science*, 374, 921–922, <https://doi.org/10.1126/science.acx9655>
- Walter, G. (2021): Stratospheric smoke layers in the Northern and Southern Hemisphere: Impact of pyrocumulonimbus convection and self-lifting effects, *Bachelor thesis*

A contribution to the discussion “What is a cloud?”

Olaf Hellmuth¹, Dietrich Spänkuch², Ulrich Görsdorf³, Rainer Feistel⁴

¹ Leibniz Institute for Tropospheric Research e. V. (TROPOS), Berlin, Germany

² Leibniz-Sozietät der Wissenschaften zu Berlin e. V., Berlin, Germany

³ Deutscher Wetterdienst, Meteorologisches Observatorium Lindenberg–Richard-Aßmann-Observatorium–OT Lindenberg, Tauche, Germany

⁴ Leibniz Institute for Baltic Sea Research (IOW), Warnemünde, Germany

Ungeachtet der evidenten Bedeutung von Wolken für die Energiebilanz der Erde und ihren hydrologischen Zyklus sowie der Tatsache, dass praktisch jedermann in der Lage ist eine Wolke intuitiv bzw. phänomenologisch zu beschreiben, ist das Problem der metrologischen Wolkendefinition nach wie vor ungeklärt. Eine Ursache hierfür sind die Unterschiede in den Wolkendefinitionen, wie sie durch die AMS und die WMO festgelegt sind. Während die AMS-Definition auf der Wolkeneigenschaft der Sichtbarkeit ("visibility") basiert, ist in der WMO-Definition die Wahrnehmbarkeit ("perceivability") der Wolke das bestimmende Kriterium. Auf der Grundlage einer Analyse des Paradoxons der subvisiblen Wolken haben Spänkuch et al. (2022) zur Wolkendefinition tageszeitabhängige Schwellenwerte der wolkenoptischen Dicke unter Verwendung der Koschmiederschen Theorie der meteorologischen Sichtbarkeit abgeleitet. Um die mit einem einparametrischen Definitionskriterium einhergehende Umbestimmtheit der Wolke zu umgehen, ist in einer weiterführenden Analyse unter Verwendung theoretischer Beziehungen und semiempirischer Korrelationen ein Kalkulus zur Bestimmung des volumetrischen Extinktionskoefizienten, der Radarreflektivität, des effektiven Wolkentropfenradius, der Wolkentropfenkonzentration und des Formparameters der zugrundgelegten Wolkentropfenverteilung als Funktion des Wolkenflüssigwassergehaltes entwickelt worden. Die Bestimmung des wolkendefinierenden Flüssigwassergehaltes als Schließungsbedingung erfolgt auf der Grundlage des thermodynamischen und hydrostatischen Konzeptes der "Archimedischen Wolke" unter Berücksichtigung empirischer Befunde zur Turbulenz an den Wolkenrändern ("twilight zone"). Anhand eines Vergleiches mit mikrophysikalischen Observablen stratiformer Wolken werden die Möglichkeiten und Grenzen des entwickelten Ansatzes diskutiert sowie Ansatzpunkte für weitere Verbesserungen identifiziert.

Introduction

With a global annual mean cover of $\approx 66\%$ clouds are omnipresent in the Earth atmosphere. They strongly affect the radiation budget of the Earth both in the solar and thermal spectral ranges, thus having a significant impact on weather, hydrology, climate, air chemistry, and several practical implications with respect to atmospheric aviation hazards and solar energy use. The definition of a cloud in terms of metrology is much more complicated than suggested by its phenomenological perception through an observer at the ground. In studies on regulation and harmonization of terminology in cloud physics Mazin and Minervin [1993] and Mazin et al. [2000] emphasized that the concept of "cloud" has

no clear quantitative definition. In order to eliminate the existing ambiguity of terminology the authors demanded precise definitions of principal terms. Despite extensive studies for decades, Hirsch et al. [2014] concluded that there is no clear definition of a cloud. A driving motive for a unique cloud definition is the dependence of cloud detectability on the employed instrumentation and the corresponding measurands by which clouds are characterized.

Cloud definition by the American Meteorological Society (AMS) and the World Meteorological Organization (WMO). According to the AMS [2020b] a "cloud" is defined as (i) a visible aggregate of minute water droplets and/or ice particles in the atmosphere above the Earth's surface. (ii) A cloud differs from fog

only in that the latter is, by definition, close (a few meters) to the Earth's surface. Clouds form in the free atmosphere as a result of condensation of water vapor in rising currents of air, or by the evaporation of the lowest stratum of fog. For condensation to occur at a low degree of supersaturation, there must be an abundance of cloud condensation nuclei for water clouds, or ice nuclei for ice-crystal clouds, at temperatures substantially above -40°C . The size of cloud drops varies from one cloud type to another, and within any given cloud there always exists a finite range of sizes. Generally, cloud drops (droplets) range from 1 to $100\ \mu\text{m}$ in diameter, and hence are very much smaller than raindrops. (iii) Any collection of particulate matter in the atmosphere dense enough to be perceptible to the eye, as a dust cloud or smoke cloud. According to the AMS standing orders “fog” is defined as water droplets suspended in the atmosphere in the vicinity the Earth's surface that affect visibility. According to international definition, fog reduces visibility below 1 km. Fog differs from cloud only in that the base of fog is at the Earth's surface while clouds are above the surface [AMS, 2020c]. According to the WMO [2018, p. 487] a cloud is defined as an aggregate of very small water droplets, ice crystals, or a mixture of both, with its base above the Earth's surface, which is perceivable from the observation location.

While the AMS defines a cloud in terms of visibility, i.e., by the eye of an human observer, the WMO defines it in terms of perceptibility, i.e., the perception can be realized both by a human observer or by an appropriate instrument. Both definitions are based on observations or measurements and rely on more or less arbitrarily defined thresholds of the optical thickness.

Definition obstacles. The main difficulty of a precise and unambiguous cloud definition is the variety of cloud metrics across the atmospheric science community. For example, emphasizing the dependence of cloud detection on the employed instrumentation, Mazin *et al.* [2000] argued that e.g. the statistics of the occurrence frequency of cirrus clouds derived from lidar instrumentation will differ dramatically from measurements conducted during aircraft field experiments or based on radar observations. The traditional classification of clouds into genera, classes, subclasses, special forms, etc., is strongly based on cloud phenomenology and its perception by a skilled observer. This includes the visual estimation of cloud height and shape, morphological and textural features, etc., which are conditioned by the atmospheric layer stability, thermally and mechanically induced turbulence, the aggregation

state of water, the evolution stage of the cloud, the multiscale driving forces such as circulation pattern, orography, land use. Such phenomenological cloud classification relies on the primary, empirically scaled visual observation of atmospheric water condensates. In contrast to a phenomenological approach to cloud classification, the treatment of clouds in atmospheric modeling requires “sharp” metrics that (i) do not rely on phenomenological features, (ii) are free from subjective impressions and observational biases, and (iii) do not require deduction from the notions of cloud morphology. Instead, cloud description is usually based on the numerical (and empirically constrained) evaluation of the conservation laws for energy (first law), momentum (Navier–Stokes equation), and mass (mass-continuity equations of humid air and water in all thermodynamic phases). The integration of these equations delivers spatiotemporally evolving cloud variables such as cloud temperature and pressure together with the mass mixing ratio and number concentration of water in different thermodynamic states of aggregation and hydrometeoric agglomeration. Cloud formation and dissipation are controlled by highly nonlinear and interlinked microphysical processes, which also set constraints on cloud definition. From the point of view of modeling, Spänkuch *et al.* [2022] tentatively defined a cloud as a hydrothermodynamic nonequilibrium system of the coexisting macrophases of water in a turbulent humid-air atmosphere including (i) the metastable states of water (supersaturated water vapor, under-cooled water), (ii) the different hydrometeoric forms of water condensates, and (iii) primarily emitted and secondarily formed atmospheric soles (aerosol, hydrosol) and plasmosols, which are involved in the phase transitions of atmospheric water by triggering the removal of metastable states of water into stable ones by heterogeneous nucleation. This perception of a cloud is close to those of Schmauß [1919] [cited in Jaenicke, 2020], who considered a cloudy state of the atmosphere as a metastable mix moving towards a stable condition, resembling e.g. a colloidal solution, which could be constantly changing for years, but which is not predictable about the time the change occurs. Comparing colloid chemistry and meteorology, Schmauß considered e.g. dust as a colloidal solution of water in air. Considering the notion hydrosol for a solution of colloids in water and alkosols for a solution of colloids in alcohol, dust should be classified as aerosol [Schmauß 1920, 1922, Jaenicke 2020]. Furthermore, aerosol and clouds should be considered as an entity, the atmospheric aerosol. With respect to aerosols there the same discrepancy in the definitions as for clouds [for details see AMS 2020a and discussion in Spänkuch *et al.* 2022].

The requirement for a general cloud definition arises from the need for harmonizing notions between atmospheric modeling and observation as well as for standardizing cloud observations within the framework of the international meteorological observation network. For a comprehensive review and discussion of the multifaceted aspects of cloud definition the reader is referred to Spänkuch et al. [2022]. Depending on the object of investigation and the observation system, the criteria for the definition of a cloud might differ [see Spänkuch et al. 2022, Table 1]. For example, cloud physicists define clouds by their particle concentration or their water and ice content. Modelers define clouds by their relative humidity and/or water and ice water content. Radiation experts define clouds by their optical thickness, and remote sensing specialists by their reflectance, backscatter, and/or cloud brightness temperature. Thus, observable cloud characteristics are quite different from the variables that are used in models to characterize clouds [Pincus et al. 2012]. The multitude of available metrics for cloud characterization, however, cannot be strictly classified according to special application; i.e., the one and the same metric can be meaningful for different applications.

Cloud definition based on the optical concept of meteorological visibility

Owing to its paramount importance for the meteorological practice Spänkuch et al. [2022] proposed a new cloud definition on the base of meteorological visibility as an integral metric that considers both radiative as well as microphysical observables. Starting point is the paradox of subvisible clouds (SVCs) [Spänkuch 2018]. Against the background of the AMS visibility criterion for cloud definition the author raised the question: Are SVCs clouds or not? Evaluating the visibility theory of Koschmieder [1924], Spänkuch et al. [2022, Appendix E] thought about a new visibility-based criterion for such objects. Brightness is a basic notion in the visibility theory to scale the subjective perception of the luminance of a visual target. Let us consider a black target (subscript t) at a distance x from an observer (setting $x = 0$ at the target) in front of a background (subscript b) that is homogeneously illuminated with monochromatic light in the visible range of the electromagnetic spectrum. The atmospheric reflectance $r(x)$ between an observer and the target is defined by the ratio of the luminance of the target E_t to the background luminance $E_b(\Psi)$ [Koschmieder 1924, Eq. (30)]:

$$r(x) = \frac{E_t}{E_b(\Psi)} = \frac{1}{1+\varepsilon}, \quad \varepsilon = \frac{E_b(\Psi)-E_t}{E_t}. \quad (1)$$

Here, ε denotes the contrast between the target and the background at the location x . Assuming a horizontal tangential plane touching the Earth surface at the location of a groundbased observer, the angle Ψ denotes the azimuth between two horizontal lines defined in this plane. The first line connects the point of the observer with the nadir of the sun in the tangential plane, and the second line connects the point of the observer with the nadir of the target in this plane. At $\Psi = 0$ the nadirs of the target and the sun are identical, and at $\Psi = \pi$ the target is placed opposite to the sun (target illuminated by the sun). If the atmosphere between the target and the observer completely reflects the background light, i.e., $r(x) = 1$, then the brightness of the target is indistinguishable from that of the background, $E_t = E_b(\Psi)$, and the target remains “invisible” to the observer. Vice versa, if the atmospheric reflectance between the observer and the target is zero, $r(x) = 0$, the target must be completely dark, $E_t(\Psi) = 0$ corresponding to $\varepsilon \rightarrow 0$. To ensure energy conservation, the reflectance $r(x)$ and the transmittance $t(x)$ of the atmosphere must fulfil the following constraint:

$$r(x) + t(x) = 1. \quad (2)$$

The atmospheric transmittance depends on the optical thickness τ , which in turn is a function of light extinction (absorption plus scattering) along the airmass pathway between the observer and the target:

$$t(x) = \exp[-\tau(x)], \quad \tau(x) = \beta_{v,e}x. \quad (3)$$

The quantity $\beta_{v,e}$ is the volumetric extinction (or attenuation) coefficient of the atmosphere (in units of m^{-1}). By virtue of Eq. (1) the luminance contrast C_L is defined by the following relation:

$$\begin{aligned} C_L(x) &= \frac{|\Delta E|}{E_b(\Psi)} = t(x) = \exp[-\beta_{v,e}x] \\ &= \frac{\varepsilon(x)}{1+\varepsilon(x)} \approx \varepsilon(x) \text{ for } \varepsilon(x) \ll 1, \Delta E = E_b(\Psi) - E_t. \end{aligned} \quad (4)$$

Defining the contrast in Eq. (4) by taking the absolute amount of ΔE , we ensure a positive definite contrast $C_L(x) \approx \varepsilon > 0$ also for the case that the target is brighter than the background, $E_t > E_b(\Psi)$. Setting a certain minimum contrast threshold $\varepsilon = \varepsilon_0$, one can immediately determine the visibility of the target $x = x_{vis}$ from Eq. (4) [Koschmieder 1924]:

$$\begin{aligned} x_{vis} &= \frac{1}{\beta_{v,e}} \ln \left(\frac{1+\varepsilon_0}{\varepsilon_0} \right) \approx \frac{1}{\beta_{v,e}} \ln \left(\frac{1}{\varepsilon_0} \right) \\ \rightarrow \quad \tau_{vis} &= \beta_{v,e} x_{vis} = \ln \left(\frac{1}{\varepsilon_0} \right). \end{aligned} \quad (5)$$

The contrast ratio between two different distances x_2 and x_1 reads:

$$\begin{aligned} t(x_1, x_2) &= \frac{C_L(x_2)}{C_L(x_1)} = \exp[-\tau(x_1, x_2)] \\ &= \frac{\varepsilon(x_2)}{\varepsilon(x_1)} \left[\frac{1+\varepsilon(x_1)}{1+\varepsilon(x_2)} \right] \approx \frac{\varepsilon(x_2)}{\varepsilon(x_1)}, \quad \tau(x_1, x_2) = \beta_{v,e}(x_2 - x_1). \end{aligned} \quad (6)$$

The quantities $\tau(x_1, x_2)$ and $t(x_1, x_2)$ denote the optical depth and the transmittance of the airmass between x_1 and x_2 . The transmittance is a product of three contributions [Spänkuch 2018]:

$$t(x_1, x_2) \approx t_R(x_1, x_2) t_G(x_1, x_2) t_A(x_1, x_2). \quad (7)$$

Here, t_R denotes the transmittance of a dry Rayleigh atmosphere, t_G the transmittance of a greenhouse gas atmosphere (with absorber gases H₂O, O₃, etc.), and t_A the transmittance of an aerosol atmosphere. For the wavelength $\lambda = 550$ nm, at which the daytime sensitivity of the human eye exceeds its maximum, Spänkuch [2018, see references therein] conducted a monochromatic first-guess approximation of t_R , t_G , and t_A for an atmosphere with infinite geometrical thickness. With reference to Baur [1970, p. 525, Table 73], Spänkuch [2018] assumed $t_R(550 \text{ nm}) = 0.9066$. For the greenhouse gas and aerosol transmittances the author arrived at first guesses of $t_G \approx 1$ and $t_A \approx 0.65$ (for the U.S. Standard Atmosphere with rural aerosol at a visibility of 25 km), which yields $t \approx 0.59$. This value refers to the whole atmosphere at vanishing zenith distance and represents the upper limit of the atmospheric transmittance.

The recognition of a cloud either by a human observer or an automatic device at the ground (at distance x_2) requires a certain (minimum) contrast. Investigating a dark target against a bright background, $\Delta E > 0$, Koschmieder [1924, 47–48] adopted $\varepsilon_0(x_2) = 0.02$. In the present case, however, we consider a bright cloud against a darker (blue) clear-sky background, $\Delta E < 0$. By virtue of the definition given by Eq. (4), we adopt $\varepsilon_0(x_2) \approx C_L(x_2) \approx 0.02$ with the constraint $\Delta E < 0$, which delivers an estimate of the contrast between the cloud and the clear-sky background in the vicinity of the cloud (i.e., at a distance $x_1 < x_2$):

$$C_L(x_1) = \frac{C_L(x_2)}{t(x_1, x_2)} \approx \varepsilon_0(x_1) \approx 0.034. \quad (8)$$

As a consequence, the detection of a cloud against the clear sky requires the cloud luminance (target) at distance x_1 to be

$$\frac{|E_b - E_t(x_1)|}{E_b} = \frac{\varepsilon_0(x_1)}{1 + \varepsilon_0(x_1)} \approx \varepsilon_0(x_1) = 3.4 \% \quad (9)$$

higher than that of the clear-sky background. These values can be interpreted as a required

increment in cloud reflectance (subscript c) of $\Delta r_c = r_c(x_1) - r_{c,0}(x_1) = 0.034$ above a certain reference state (indicated by subscript 0). By virtue of $t_c(x_1) = 1 - r_c(x_1)$ the corresponding increment in cloud transmittance is $\Delta t_c(x_1) = t_c(x_1) - t_{c,0}(x_1) = -\Delta r_c(x_1) = -0.034$. Taking into account $t_c = \exp(-\tau_c)$ with τ_c denoting the cloud optical thickness, the corresponding increment in cloud optical thickness is given by $\Delta \tau_c(x_1) = \tau_c(x_1) - \tau_{c,0}(x_1) = -\Delta t_c(x_1) / t_{c,0}(x_1)$. As a reference state we define a completely transparent (i.e., in fact not existent) cloud, defined by $r_{c,0}(x_1) = 0$, $t_{c,0}(x_1) = 1$, and $\tau_{c,0}(x_1) = 0$. Therewith, one has $r_c(x_1) = 0.034$ and $t_c(x_1) = 1 - 0.034 = 0.966$, allowing the determination of the minimum (threshold) value of the cloud optical thickness $\tau_c(x_1)$ at which a cloud becomes visible against its clear-sky background for a contrast threshold value at the location of the observer of $\varepsilon_0(x_2) = 0$:

$$\tau_c(x_1) = -\ln t_c(x_1) = 0.035. \quad (10)$$

Interestingly, such a threshold cloud with a transmittance of $t_c(x_1) = 0.966$, which just ensures visibility at $\lambda = 550$ nm, has a higher transmittance than the Rayleigh atmosphere with $t_R(550 \text{ nm}) = 0.9066$. The relative enhancement in transmittance is $(t_c - t_R)/t_R \approx 9.9 \%$. The AMS identifies an aggregate of minute water droplets and/or ice particles in the atmosphere above the Earth's surface as a cloud as soon as it becomes visible [AMS 2020b]. Therewith the reverse conclusion suggests that aggregates of minute water droplets and/or ice particles, which are invisible, i.e. with $0 < r_c(x_1) < 0.034$, $0.966 < t_c(x_1) < 1$, and $0 < \tau_c(x_1) < 0.35$ are not clouds. However, if they are not a cloud in terms of visibility, what they are? They are “subvisible clouds”, a paradox in terms of the AMS definition [Spänkuch 2018].

On the base of these considerations, Spänkuch et al. [2022] proposed the following cloud definition: A meteorological cloud is an aggregate of minute particulate matter (solid, liquid, or mixed) in the atmosphere above ground that becomes visible from ground at a line-of-sight optical depth of at least about $\tau = 0.03$ at day and $\tau = 0.05$ at night.

Figure 1 displays the integral liquid water path (LWP) together with the corresponding liquid water content for a cloud thickness of $\Delta z = 100$ m as a function of the effective cloud drop radius R_e for the two cloud-defining threshold values of the optical thickness, i.e., $\tau = 0.03$ for daytime and $\tau = 0.05$ for nighttime. The graphs are calculated according to Hu and Stamnes [1993]. Analogously, in Fig. 2 the integral ice water path (IWP) together with the corresponding

ice water content for a cloud thickness of $\Delta z = 100$ m as function of the effective width of the ice crystals D_e is shown. These curves are based on *Fu and Liou* [1993]. Fixing the cloud optical thickness allows the definition of either a warm cloud along the discrimination line $LWP = LWP(R_e)$ or of a cold cloud along the discrimination line $IWP = IWP(D_e)$; i.e., the cloud is defined except for one degree of freedom.

Additional microphysical and optical constraints defining a warm cloud

Owing to the dependence of τ on both the volumetric extinction coefficient $\beta_{v,e}$ and the cloud geometrical thickness Δz , a τ -based cloud definition criterion implies a certain microphysical and geometrical indeterminacy of the cloud. To remove this indeterminacy, *Hellmuth et al.* [2024a] made an attempt to extend the τ -based cloud definition of *Spänkuch et al.* [2022] by consideration of further cloud-defining criteria. The idea of this extension goes back to *Mazin and Minervin* [1993], who introduced the notion “demarcation microstructure diagram” (DMD), and to *Mazin et al.* [2000] who defined clouds by means of the dependence of the cloud drop concentration N on the effective cloud drop radius R_e with either radar reflectivity Z , volume extinction coefficient $\beta_{v,e}$, or liquid water content (LWC) ρ_c serving as a free parameter. In a double-logarithmic plot the graphs N vs. R_e appear as straight lines named demarcation lines, the slope and offset of which depend on

instrument-specific threshold values of Z , $\beta_{v,e}$ or LWC, respectively. Each line separates the parameter pair (N, R_e) into two regions. In one region, clouds remain undetected, in the other region (to the right of the line) clouds are detectable. Thus, the DMD allows an instrument-specific definition of a cloud at the edges of detectability upon prescription of threshold values for instrument-specific measurands together with R_e of the underlying cloud drop population. Based on a generalization of the DMD concept, *Hellmuth et al.* [2024a] proposed a calculus, which is based on five microphysical and optical constraints to describe (i) clouds detected by airborne microphysical instruments (AMCs), defined by ρ_c , (ii) LIDAR visible clouds (LVCs), defined by $\beta_{v,e}$, and (iii) RADAR visible clouds (RVCs), defined by Z .

These five constraints are described below:

- 1) The AMC-defining LWC is described by the relation $\rho_c = \rho_c(T, P, p, N, R_e)$ derived from the underlying theoretical cloud drop size distribution. The quantity p denotes the shape parameter of the assumed drop size distribution, and T and P are the temperature and pressure.
- 2) The LVC-defining volumetric extinction coefficient, $\beta_{v,e}$, is described by two alternative semi-empirical expressions. The first relation is given by a functional dependence $\beta_{v,e} = \beta_{v,e}(\rho_c)$, which is derived by *Kunkel* [1984] from measurements of fog droplet spectra data in several advection fogs. The second relation is given by a functional dependence $\beta_{v,e} = \beta_{v,e}(\rho_c, N)$, which is obtained

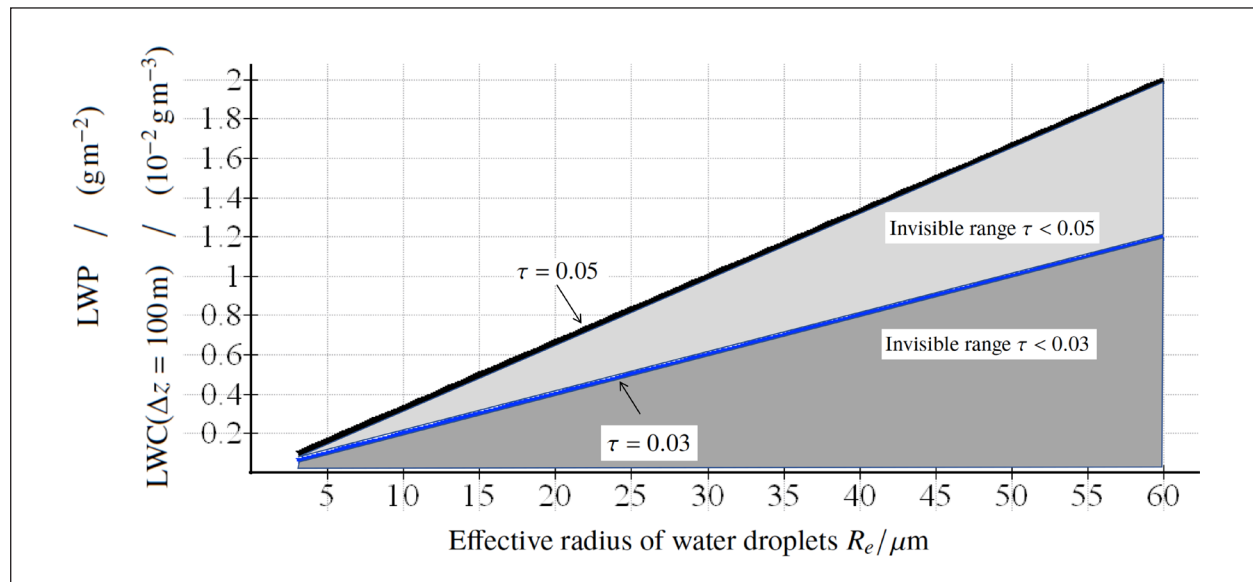


*Fig. 1: Integral liquid water path (LWP) and corresponding liquid water content (LWC) for a water-cloud thickness $\Delta z = 100$ m near zenith as function of the effective cloud drop radius R_e for two different cloud-defining threshold values of the optical thickness: $\tau = 0.03$ for daytime and $\tau = 0.05$ for nighttime. The areas below the two isolines ($\tau = \text{const.}$) represent cloud invisibility. The ordinate values are valid for both the LWP in units of $g\ m^{-2}$ and the LWC in units of $10^{-2}\ g\ m^{-3}$. Thus, this cloud will be visible when $R_e = 12\ \mu\text{m}$ at night and $20\ \mu\text{m}$ during day (taken from *Spänkuch et al.* 2022, Fig. 1).*

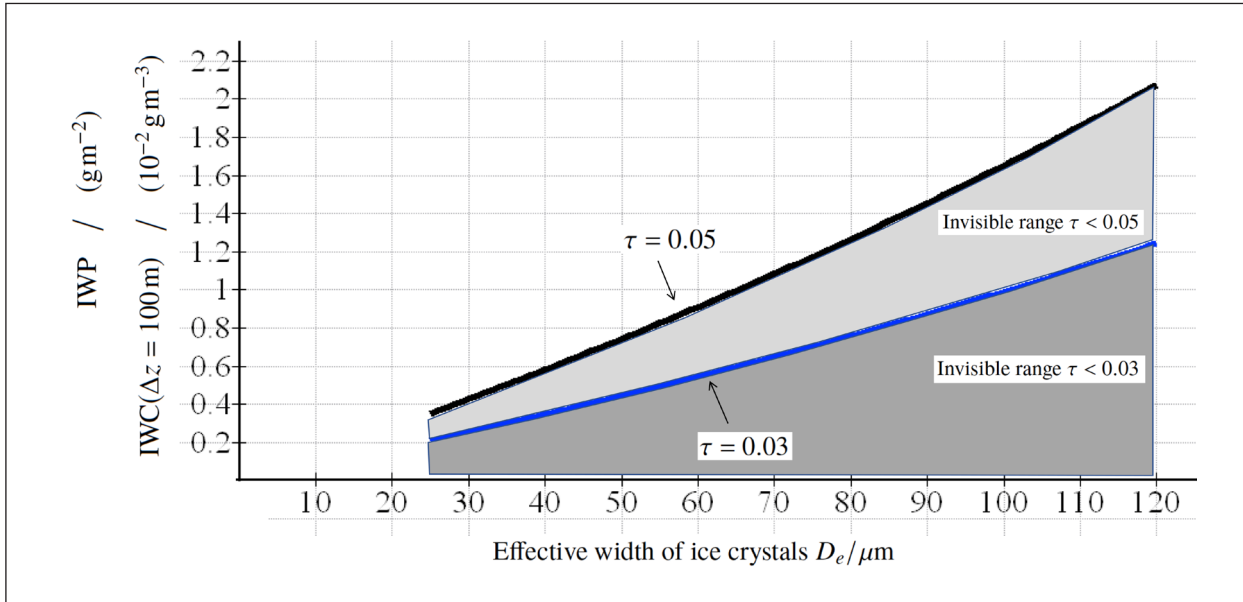


Fig. 2: Integral ice water path (IWP) and corresponding ice water content (IWC) for an ice-cloud thickness $\Delta z = 100 \text{ m}$ at zenith as function of the effective width of the ice crystal D_e for two different cloud-defining threshold values of the optical thickness: $\tau = 0.03$ for daytime and $\tau = 0.05$ for nighttime. The areas below the two isolines ($\tau = \text{const.}$) represent cloud invisibility. The ordinate values are valid for both the IWP in units of g m^{-2} and the IWC in units of 10^{-2} g m^{-3} . An ice cloud at zenith consisting of crystals with $D_e = 60 \mu\text{m}$ will be visible when IWP is greater than 0.6 g m^{-2} at day and greater than 0.9 g m^{-2} during night [taken from Späckuch et al. 2022, Fig. 2].

from a combination of Koschmieder's formula for the meteorological visibility $x_{\text{vis}} = x_{\text{vis}}(\beta_{v,e})$ [Stoelinga and Warner 1999], with a semi-empirical relation $x_{\text{vis}} = x_{\text{vis}}(\rho_c, N)$ proposed by Gultepe et al. [2006].

- 3) The third relation is a regression function for the effective radius $R_e = R_e(\rho_c, \beta_{v,e})$, which is derived from a parameterization proposed by Hu and Stamnes [1993] on the base of Mie-theory calculations.
- 4) The fourth relation is the RVC-defining radar reflectivity $Z = Z(p, N, R_e)$ derived from the underlying theoretical cloud drop size distribution.
- 5) Finally, the fifth relation is given by a semi-empirical power-law dependence of the RVC-defining radar reflectivity $Z = Z(\rho_c)$ proposed by Plank [1991] and Pujol et al. [2007].

These relations constitute a simple diagnostic cloud-defining model (CDM) for the determination of the parameter set $\{N, R_e, p, \beta_{v,e}, Z\}$ as a function of ρ_c under steady-state condition, i.e. the LWC serves as a free parameter.

Closure condition: thermodynamic and aerodynamic constraints defining a warm cloud

The determination of the cloud-defining LWC requires a closure condition. The conditio sine qua non for cloud being – regardless of being visible or

perceivable – is thermodynamic buoyancy, i.e. "floatability of wet air in a sea of humid air". This requirement sets a constraint on the LWC, which depends on the thermo-humid conditions of the ambient air in the near-cloud environment (the twilight zone). Based on this requirement Hellmuth et al. [2024b] formulated constraints for a diagnostic determination of the cloud-defining value of ρ_c for a quasi-steady state warm cloud. Such cloud can be approximated by a wet-air parcel, defined as a composite of humid air and liquid water. Humid air is described as a non-ideal mixture of dry air and water vapor. The wet-air parcel is subject of two restrictive conditions: (i) The humid air in wet air and the liquid water in wet air are in thermodynamic equilibrium, and (ii) the wet-air parcel is in hydrostatic equilibrium with its ambient humid air. Such cloud is called "Archimedean cloud". Evaluating the criterion of cloud floatability by means of the advanced international seawater standard TEOS-10 [McDougall et al. 2010, Feistel et al. 2010a,b, 2016, 2018, Wright et al. 2010, IOC, SCOR, and IAPSO 2010, Lovell-Smith et al. 2016], Hellmuth et al. [2024b] arrived at a governing equation for the LWC threshold value, $\rho_{c,\text{th}} = \rho_c (\langle \text{RH} \rangle_{\text{th}}, \langle T \rangle, \langle P \rangle)$, which ensures the floatability of the cloud in ambient air (denoted by angle brackets) with relative humidity $\langle \text{RH} \rangle_{\text{th}}$, temperature $\langle T \rangle$, and pressure $\langle P \rangle$. The definition of a cloud at the edges of its detection requires the consideration of small-scale fluctuations in the determination of the threshold relative humidity $\langle \text{RH} \rangle_{\text{th}}$ in the cloud environment.

This requires an additional closure condition in form of a metric of cloud fluctuability. With consideration of disposable phenomenological findings on cloud-water statistics, a rather heuristic approach to the determination of a cloud-defining LWC, $\rho_{c,th}$, has been used. The constraint $\rho_{c,th} = \rho_c (\langle RH \rangle_{th} = 0, \langle T \rangle, \langle P \rangle) = 0$ implies the requirement of subsaturation of the environmental air, i.e. $\langle RH \rangle_{th} < 1$, for cloud-water condensation, $\rho_c > 0$, and cloud floatability. The threshold value $\langle RH \rangle_{th}$ is tentatively determined employing the aerodynamic concept of cloud fluctuability in terms of the turbulence-induced standard deviation of the relative humidity σ_{RH} at the cloud boundaries. The ad hoc assumption $\langle RH \rangle_{th} = 1 - \sigma_{RH}$ with $\sigma_{RH} > 0$ ensures subsaturation of the ambient humid air [Kulmala et al. 1997] and $\rho_{c,th} = \rho_c (\langle RH \rangle_{th}, \langle T \rangle, \langle P \rangle) > 0$, i.e. cloud floatability. Based on a comprehensive survey of empirical data from the literature, for the present purpose $\sigma_{RH} = 0.001$ ($= 0.1\%rh$) is used as observed by Ditas et al. [2012] in the calm region at the cloud base of marine stratocumulus.

First results

The combination of (i) Koschmieder's theory of meteorological visibility to describe VVCs, with (ii) the generalized Mazin-Minervin approach to describe AMCs, LVCs, and RVCs, and (iii) the thermodynamic concept of cloud floatability in conjunction with the aerodynamic concept of cloud fluctuability allows a self-consistent diagnostic definition of a cloud at the edges of its detection in terms of the parameter set $\{\tau_c, N, R_e, p, \beta_{ve}, Z, \rho_c\}$. The solution of the system of equations strongly depends on the special choice of the empirical correlation functions entering the CDM equations and revealed the existence multiple mathematical solutions. A comparison of the calculated values of $\{N, R_e, p_c\}$ as functions of ρ_c

with the corresponding parameters derived by Miles et al. [2000] from empirical droplet size distributions for marine stratus and continental stratocumulus clouds shows that the approach delivers physically meaningful solutions, demonstrating the straightforwardness of the approach. Disclosed deviations between the model and the observations can be traced back to mispredicted values of the shape parameter, the determination of which responds very sensitive against the settings of the regression parameters in the employed empirical correlation functions. The reason for this misprediction could not be doubtlessly disclosed; different sources of uncertainties in both the employed empirical correlation equations and the observations are discussed. Next to unimodality of the droplet size distribution, mutual inconsistencies in the parameter settings underlying the employed correlation functions must be challenged. An extension of both the observational database and the set of correlation functions is pending to define the expectation range of the CDM predictions. Further studies must aim at bringing the effective shape parameter closer to those directly derived from observed drop size distributions. Cloud floatability in combination with cloud fluctuability is a meaningful concept to determine the cloud-defining LWC as a function of the ambient relative humidity, temperature and pressure. For the formulation of empirical constraints, the study includes a comprehensive survey of cloud-radiative, microphysical and turbulence measurements data.

In view of the recognized differences between the calculated “effective” and the “quasi-observed” shape parameter the present approach is a contribution to the discussion “What is a cloud?” but not a final answer. The details of the calculus and results are prepared for publication [Hellmuth et al. 2024a,b]. Starting points for further physical refinements of the CDM are identified.

References

- AMS (2020a), Aerosol. Glossary of Meteorology, URL <http://glossary.ametsoc.org/wiki/aerosol>, accessed 6 February 2024.
- AMS (2020b), Cloud. Glossary of Meteorology, URL <http://glossary.ametsoc.org/wiki/cloud>, accessed 6 February 2024.
- AMS (2020c), Fog. Glossary of Meteorology, URL <http://glossary.ametsoc.org/wiki/fog>, accessed 6 February 2024.
- Baur, F. (1970), Meteorologisches Taschenbuch. Begründet von Franz Linke, Neue Ausgabe, II. Band, Akademische Verlagsgesellschaft Geest & Portig K.-G., 712 pp.
- Ditas, F., R. A. Shaw, H. Siebert, M. Simmel, B. Wehner, and A. Wiedensohler (2012), Aerosols-cloud microphysics-thermodynamics-turbulence: evaluating supersaturation in a marine stratocumulus cloud, *Atmos. Chem. Phys.*, 12, 2459–2468, URL <https://doi.org/10.5194/acp-12-2459-2012>.
- Feistel, R. (2018), Thermodynamic properties of seawater, ice and humid air: TEOS-10, before and beyond, *Ocean Sci.*, 14, 471–502, URL <https://doi.org/10.5194/os-14-471-2018>.
- Feistel, R., R. Wielgosz, S. A. Bell, M. F. Camoes, J. R. Cooper, P. Dexter, A. G. Dickson, P. Fisicaro, A. H. Harvey, M. Heinonen, O. Hellmuth, H.-J. Kretzschmar, J. W. Lovell-Smith, T. J. McDougall, R. Pawlowicz, P. Ridout, S. Seitz, P. Spitzer, D. Stoica, and H. Wolf (2016), Metrological challenges for measurements of key climatological observables: oceanic salinity and pH, and atmospheric humidity. Part 1: overview, *Metrologia*, 53 (1), R1, URL <http://stacks.iop.org/0026-1394/53/i=1/a=R1>.
- Feistel, R., D. G. Wright, H.-J. Kretzschmar, E. Hagen, S. Herrmann, and R. Span (2010a), Thermodynamic properties of sea air, *Ocean Sci.*, 6, 91–141, URL <http://www.ocean-sci.net/6/91/2010/>.

- Feistel, R., D. G. Wright, D. R. Jackett, K. Miyagawa, J. H. Reissmann, W. Wagner, U. Overhoff, C. Guder, A. Feistel, and G. M. Marion (2010b), Numerical implementation and oceanographic application of the thermodynamic potentials of liquid water, water vapor, ice, seawater and humid air—Part 1: Background and equations, *Ocean Sci.*, 6, 633–677, doi:10.5194/os-6-633-2010, URL <http://www.ocean-sci.net/6/633/2010/>.
- Fu, Q. and K. N. Liou (1993), Parameterization of radiative properties of cirrus clouds, *J. Atmos. Sci.*, 50, 2008–2025, URL [https://doi.org/10.1175/1520-0469\(1993\)050<2008:POTRPO>2.0.CO;2](https://doi.org/10.1175/1520-0469(1993)050<2008:POTRPO>2.0.CO;2).
- Gultepe, I., M. D. Müller, and Z. Boybeyi (2006), A new visibility parameterization for warm-fog applications in Numerical Weather Prediction models, *J. Appl. Met. Clim.*, 45, 1469–1480, doi: <https://doi.org/10.1175/JAM2423.1>.
- Hellmuth, O., D. Spänkuch, R. Feistel, U. Görsdorf, and S. E. Schwartz (2024a), A contribution to the discussion “What is a cloud?” Part 1: Microphysical and optical constraints defining a warm cloud, prepared for submission to *J. Appl. Met.*
- Hellmuth, O., R. Feistel, D. Spänkuch, U. Görsdorf, and S. E. Schwartz (2024b), A contribution to the discussion “What is a cloud?” Part 2: Thermodynamic constraints defining a warm cloud, prepared for submission to *J. Appl. Met.*
- Hirsch, E., I. Koren, Z. Levin, O. Altaratz, and E. Agassi (2014), On transition-zone water clouds, *Atmos. Chem. Phys.*, 14, 9001–9012, URL <https://doi.org/10.5194/acp-14-9001-2014>.
- Hu, Y. X., and K. Stamines (1993), An accurate parameterization of the radiative properties of water clouds suitable for use in climate models, *J. Climate*, 6, 728–742, URL [https://doi.org/10.1175/1520-0442\(1993\)006<0728:AAPOTR>2.0.CO;2](https://doi.org/10.1175/1520-0442(1993)006<0728:AAPOTR>2.0.CO;2).
- IOC, SCOR, and IAPSO, 2010: The International Thermodynamic Equation of Seawater – 2010: Calculation and Use of Thermodynamic Properties. Written by: McDougall, T. J., Feistel, R., Wright, D. G., Pawlowicz, R., Millero, F. J., Jackett, D. R., King, B. A., Marion, G. M., Seitz, S., Spitzer, P., Chen, C. T. A. Tech. rep., Intergovernmental Oceanographic Commission, Manuals and Guides No. 56, UNESCO (English), 196 pp., Paris 2010. URL <http://www.teos-10.org>.
- Jaenicke, R. (2020), August Schmauß, 26 November 1877 – 10 October 1954. The Atmosphere as a Colloid – Pioneering Work of August Schmauß, G. J. Sem, Ed., International Aerosol Research Assembly, 2 pp.
- Koschmieder, H. (1924), Theorie der horizontalen Sichtweite. *Beitr. Phys. Atmos.*, 12, 33–55.
- Kulmala, M., Ü. Rannik, E. L. Zapadinsky, and C. F. Clement (1997), The effect of saturation fluctuations on droplet growth, *J. Aerosol Sci.*, 28, 1395–1409.
- Kunkel, B. A. (1984), Parameterization of droplet terminal velocity and extinction coefficient in fog models, *J. Climate Appl. Meteorol.*, 23, 34–41.
- Lovell-Smith, J., R. Feistel, A. H. Harvey, O. Hellmuth, S. A. Bell, M. Heinonen, and J. R. Cooper (2016), Metrological challenges for measurements of key climatological observables. Part 4: atmospheric relative humidity, *Metrologia*, 53 (1), R40, URL <http://stacks.iop.org/0026-1394/53/i=1/a=R40>.
- Mazin, I. P., G. A. Isaac, and J. Hallett (2000), Harmonization of terminology in cloud physics, 13th International Conference on Clouds and Precipitation, Nevada, 14–18 August 2000, Elsevier, Atmospheric Research, 59–60, 9–12.
- Mazin, I. P., and V. E. Minervin (1993), Regulation of terminology in cloud physics. *Russian Meteorology and Hydrology*, 4, 1–8.
- McDougall, T. J., R. Feistel, F. J. Millero, D. R. Jackett, D. G. Wright, B. A. King, G. M. Marion, C.-T. A. Chen, P. Spitzer, and S. Seitz (2010), The International Thermodynamic Equation Of Seawater 2010 (TEOS-10): Calculation and Use of Thermodynamic Properties, UNESCO 2009, IOC Manuals and Guides, 150 pp., URL www.teos-10.org.
- Pincus, R., S. Platnick, S. A. Ackerman, R. S. Hemler, and R. J. Patrick Hofmann (2012), Reconciling simulated and observed views of clouds: MODIS, ISCCP, and the limits of instrument simulators, *J. Climate*, 25, 4699–4720, URL <https://doi.org/10.1175/JCLI-D-11-00267.1>.
- Plank, V. G. (1991), Implications of the Khrgian-Mazin distribution function for water clouds and distribution consistencies with aerosols and rain. *Environmental Research Papers*, no. 1096, pltr-91-2293, 189 pp., Tech. rep., Phillips Laboratory, Hanscom Air Force Base, MA 01731-5000.
- Pujol, O., J.-F. Georgis, and H. Sauvageot (2007), Influence of drizzle on Z-M-relationships in warm clouds, *Atmos. Research*, 86 (3), 297–314, URL <https://doi.org/10.1016/j.atmosres>.
- Schmauß, A. (1919), Randbemerkungen II. *Meteor. Z.*, 36, 11–16.
- Schmauß, A. (1920), Kolloidchemie und Meteorologie. *Meteor. Z.*, 37 (1/2), 1–8.
- Schmauß, A. (1922), Kolloidchemie und Meteorologie. *Kolloid-Zeitschrift*, 31, 266–269, URL <https://doi.org/10.1007/BF01423586>.
- Schmauß, A., and A. Wigand (1929), Die Atmosphäre als Kolloid. Friedr. Vieweg & Sohn, 74 pp.
- Spänkuch, D. (2018), Was ist eine Wolke? Gedanken zu einer präziseren Definition, *Leibniz Online*, 35, 25 pp., URL <https://leibnizsozietaet.de/wp-content/uploads/2018/12/Spaenkuch.pdf>.
- Spänkuch, D., O. Hellmuth, and U. Görsdorf (2022), What is a cloud? Toward a more precise definition, *Bull. Amer. Meteor. Soc.*, 103, E1894–E1929, URL <https://doi.org/10.1175/BAMS-D-21-0032.1>.
- Stoelinga, M. T., and T. T. Warner (1999), Nonhydrostatic, mesobeta-scale model simulations of cloud ceiling and visibility for an East Coast winter precipitation event, *J. Appl. Met.*, 38 (4), 385–404, URL [https://doi.org/10.1175/1520-0450\(1999\)038<0385:NMSMSO>2.0.CO;2](https://doi.org/10.1175/1520-0450(1999)038<0385:NMSMSO>2.0.CO;2).
- WMO (2018), Measurement of meteorological variables. Vol. 1, Guide to Meteorological Instruments and Methods of Observation, WMO-8, World Meteorological Organization, 548 pp., URL https://library.wmo.int/doc_num.php?expnum_id=10616.
- Wright, D. G., R. Feistel, J. H. Reissmann, K. Miyagawa, D. R. Jackett, W. Wagner, U. Overhoff, C. Guder, A. Feistel, and G. M. Marion (2010), Numerical implementation and oceanographic application of the thermodynamic potentials of liquid water, water vapour, ice, seawater and humid air – Part 2: The library routines, *Ocean Sci.*, 6, 695–718, doi:10.5194/os-6-695-2010, URL <http://www.ocean-sci.net/6/695/2010/>.

Funding

The contribution of O. Hellmuth was provided within the framework of the research theme 2 “Aerosols & Clouds of Leibniz Institute for Tropospheric Research (TROPOS), Leipzig and is part of the TROPOS activities within the framework of the EU project “Aerosol, Clouds and Trace gases Research InfraStructure” (ACTRIS). This work contributes to the task of the IAPWS/SCOR/IAPSO Joint Committee on the Properties of Seawater (JCS).

Ground-based remote sensing of aerosol, clouds, dynamics, and precipitation in Antarctica - First results from the one-year COALA campaign at Neumayer III Station in 2023

Martin Radenz, Ronny Engelmann, Cristofer Jimenez, Silvia Henning, Holger Schmithüsens, Holger Baars, Markus M. Frey, Rolf Weller, Johannes Bühl, Johanna Roschke, Lukas Ole Muser, Nellie Wullenweber, Sebastian Zeppenfeld, Hannes Griesche, Ulla Wandinger, Patric Seifert

Die mobile OCEANET-Atmosphäre Fernerkundungsstation wurde während des gesamten Jahres 2023 an der deutschen Antarktisstation Neumayer III (70.67°S , 8.27°W) betrieben. Der entstandene ACTRIS-Datensatz mit höhenauflösten Aerosol- und Wolkeneigenschaften ist der erste seiner Art in diesem Bereich der Antarktis. Bereits jetzt konnten drei wissenschaftliche Höhepunkte aus dem Herbst und Winter identifiziert werden: 1. Häufig auftretende, langlebige Mischphasenwolken in Schichten marinen Aerosols; neuartige kombinierte Auswertealgorithmen erlauben für diese Wolken eine Schließung zwischen Aerosol- und Wolkeneigenschaften; 2. Außergewöhnliche Warmlufteinbrüche, die starken Schneefall beziehungsweise extrem warme Temperaturen und unterkühlten Nieselregen verursachten; 3. Allgegenwärtige Aerosolschichten in der Stratosphäre, die bis zu 50% zur gesamten aerosoloptischen Dicke von rund 0.06 bei 500 nm Wellenlänge beigetragen haben. Tiefgreifendere Auswertungen werden folgen, wie zum Beispiel die Analyse der am Spurenstoffobservatorium gesammelten Filterproben auf Eisaktivität im Kontext der Fernerkundungsbeobachtungen.

Introduction

The OCEANET-Atmosphere observatory of TROPOS was deployed at the Neumayer III station [70.67°S , 8.27°W , 42 m a.s.l.; Wesche *et al.* 2016] from January to December 2023 (Fig. 1) in the framework of the DFG-funded project Continuous Observations of Aerosol-cLoud interaction over Antarctica (COALA). The station is located at the northern edge of the Ekström Ice Shelf in the Dronning Maud Land (DML) of the Atlantic Sector of Antarctica. The coastal area of the DML is often subject to advection of air masses from lower latitudes triggered by cyclones over the Weddell Sea. These warm and moist air masses usually also bring marine and, to a lesser extent, terrestrial aerosol into the otherwise pristine environment. Such advection events, which occur mainly in winter, are usually accompanied by heavy snowfall. Neumayer III is the only station on a floating ice shelf that is manned throughout the year,

providing excellent conditions for studying atmospheric effects on the ice shelf.

For this deployment, the standard OCEANET-Atmosphäre instrumentation (PollyXT Raman polarization Lidar, HATPRO microwave radiometer, Cimel sun and lunar photometer, and radiation sensors) was complemented by a Mira-35 cloud radar, a LITRA-S scanning Doppler lidar, and a Parsivel² optical disdrometer. Together, these instruments brought the full ACTRIS aerosol and cloud profiling capabilities to a region where sophisticated ground-based observations were not available. The synergy of the different instruments allows for detailed retrievals of aerosol and cloud properties. The retrieval of ice crystal number concentrations and sizes is one of the major challenges. Recently, the variational retrieval CAPTIVATE [Mason *et al.* 2017, 2018, 2023] has been adapted for the ground-based sensors of the TROPOS lidar-radar remote-sensing stations.



Fig. 1: OCEANET-Atmosphere container as set up during COALA 400 m south of Neumayer III station.

Closure study in a shallow mixed-phase cloud

The radiative properties of a shallow mixed-phase cloud are mainly controlled by the amount of liquid water that can be maintained despite ice formation. A detailed understanding of the mechanisms that form and maintain such clouds requires constraints on the number concentrations of cloud-relevant aerosol

particles (cloud condensation nuclei, CCN, and ice-nucleating particles, INP) as well as the number and size of supercooled droplets and ice crystals. A typical shallow supercooled cloud was observed on 18 June 2023. A liquid layer with cloud-top temperatures between -23 and -26°C was observed for several hours, as shown in Fig. 2. Ice was continuously precipitating from this liquid layer. Lidar observations of the clear atmosphere surrounding the cloud revealed the presence of aerosol up to 3.2 km height. Using the retrievals of Mamouri and Ansmann [2016], Ansmann et al. [2019], Bühl et al. [2019], and Jimenez et al. [2020], the aerosol optical properties were converted into microphysical properties. The concentrations of CCN and INP were in the order of 10 to 50 cm^{-3} and 10 to 100 m^{-3} , respectively. Cloud droplet number concentrations derived from the lidar dual-field-of-view channels were in the range of 20 to 50 cm^{-3} with effective radii of 7 – $10 \mu\text{m}$. The amount of ice sedimenting from the liquid layer was about $1.0 \times 10^{-6} \text{ kg m}^{-3}$ with a median number concentration of 150 m^{-3} and a mean diameter of $260 \mu\text{m}$. Hence, the concentrations of cloud-relevant aerosol particles matched the concentrations of cloud droplets and ice crystals, respectively, demonstrating that the cloud

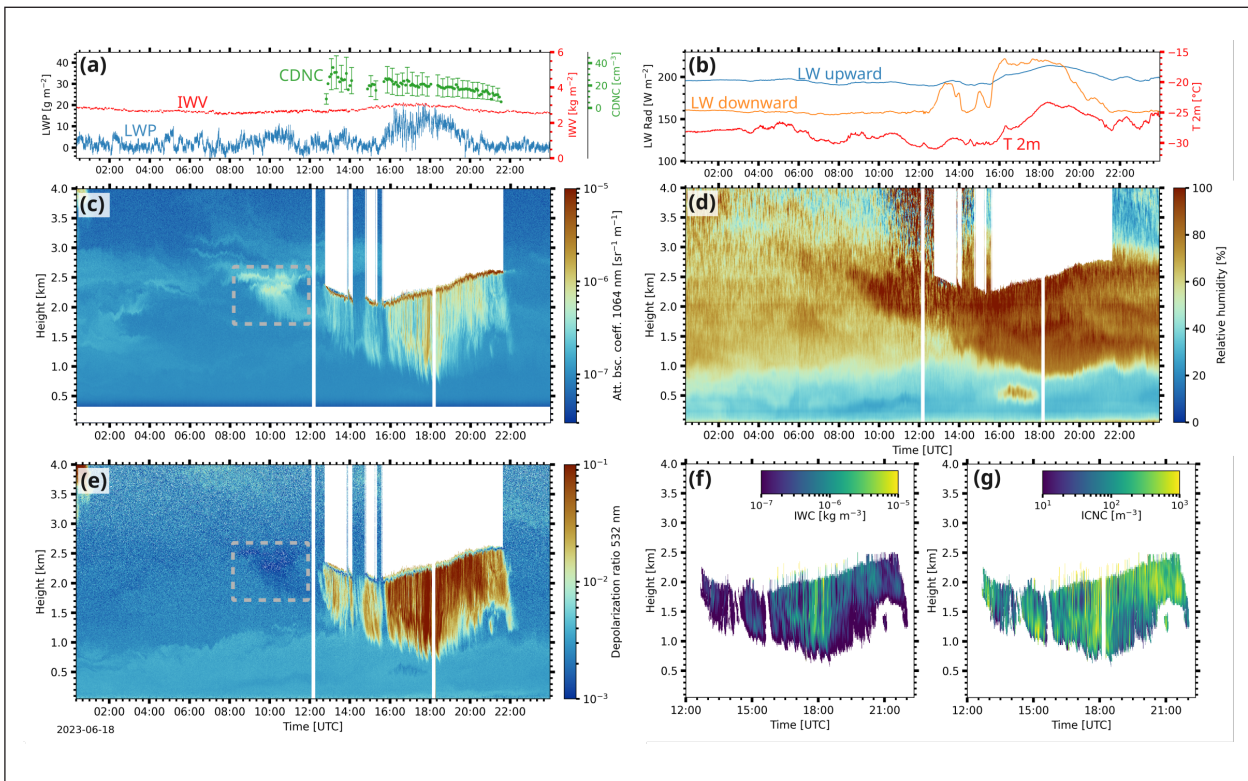


Fig. 2: Mixed-phase cloud developing in a layer of marine aerosol on 18 June 2023. (a) Time series of integrated water vapor (IWP), liquid water path (LWP), and cloud droplet number concentration (CDNC) 75 m above cloud base. (b) Time series of longwave radiation (LW) and temperature at the surface. (c) Time-height cross-section of lidar attenuated backscatter coefficient at 1064 nm with temperature from ECMWF's IFS analysis. (d) Relative humidity derived from the Raman water vapor channel and the temperature fields from ECMWF's IFS analysis. (e) Lidar volume linear depolarization ratio at 532 nm. (f) Time-height cross-section of retrieved ice water content (IWC). (g) Time-height cross-section of retrieved ice crystal number concentration (ICNC). The dashed boxes in (c) and (e) indicate the plume of strong hygroscopic growth.

formed in an aerosol-limited regime. In response to the longwave radiative forcing of the cloud, the temperature at the surface increased by almost 7 K within three hours.

Future Work

An overview on the COALA campaign setup and initial highlights are currently under review for the Bulletin of the American Meteorological Society (BAMS). Additionally to the closure between aerosol and cloud microphysics presented above, two more scientific highlights during austral fall and winter have been identified: (1) Two extraordinary warm air intrusions, one with intense snowfall produced the equivalent of 10% of the yearly snow accumulation and a second one accompanied by record high temperatures and heavy icing due to supercooled drizzle; (2)

Omnipresent aerosol layers in the stratosphere, which contributed almost 50% to the aerosol optical depth of around 0.06 at 500 nm wavelength. The lidar-derived optical signatures revealed sulfate aerosols in the stratosphere - most likely linked to the Hunga Tonga eruption in January 2022. Analysis of the full dataset will continue in 2024 and will focus on two main issues: (1) The role of long-range-transported and locally produced aerosol on clouds and radiation and the associated impact of atmospheric turbulence will be investigated. Comparative information on ice activity and CCN concentration of the local aerosol will be obtained from available co-located in-situ observations. (2) The relationship between cloud microphysics, thermodynamical structure, precipitation formation and radiation will be characterized, with special focus on atmospheric river events.

References

- Ansmann, A., R.-E. Mamouri, J. Hofer, H. Baars, D. Althausen, and S. F. Abdullaev, (2019), Dust mass, cloud condensation nuclei, and ice-nucleating particle profiling with polarization lidar: updated POLIPHON conversion factors from global AERONET analysis. *Atmos. Meas. Tech.*, 12, 4849–4865, doi: <https://doi.org/10.5194/amt-12-4849-2019>.
- Bühl, J., P. Seifert, M. Radenz, H. Baars, and A. Ansmann, (2019), Ice crystal number concentration from lidar, cloud radar and radar wind profiler measurements. *Atmos. Meas. Tech.*, 12, 6601–6617, doi: <https://doi.org/10.5194/amt-12-6601-2019>.
- Jimenez, C., A. Ansmann, R. Engelmann, D. Donovan, A. Malinka, P. Seifert, R. Wiesen, M. Radenz, Z. Yin, J. Bühl, J. Schmidt, B. Barja, and U. Wandinger, (2020), The dual-field-of-view polarization lidar technique: a new concept in monitoring aerosol effects in liquid-water clouds – case studies. *Atmos. Chem. Phys.*, 20, 15265–15284, doi: <https://doi.org/10.5194/acp-20-15265-2020>.
- Mason, S. L., J. C. Chiu, R. J. Hogan, and L. Tian, (2017), Improved rain rate and drop size retrievals from airborne Doppler radar. *Atmos. Chem. Phys.*, 17, 11567–11589, doi: <https://doi.org/10.5194/acp-17-11567-2017>.
- Mason, S. L., C. J. Chiu, R. J. Hogan, D. Moisseev, and S. Kneifel, (2018), Retrievals of Riming and Snow Density From Vertically Pointing Doppler Radars. *J. Geophys. Res. Atmos.*, 123, doi: <https://doi.org/10.1029/2018JD028603>.
- Mason, S. L., R. J. Hogan, A. Bozzo, and N. L. Pounder, (2023), A unified synergistic retrieval of clouds, aerosols, and precipitation from EarthCARE: the ACM-CAP product. *Atmos. Meas. Tech.*, 16, 3459–3486, doi: <https://doi.org/10.5194/amt-16-3459-2023>.
- Wesche, C., R. Weller, G. König-Langlo, T. Fromm, A. Eckstaller, U. Nixdorf, and E. Kohlberg, (2016), Neumayer III and Kohnen Station in Antarctica operated by the Alfred Wegener Institute. *JLSRF*, 2, A85.

Funding

DFG Priority Programme 1158 (funding number 463307613)

Cooperation

Alfred-Wegener-Institut, Bremerhaven, Germany
British Antarctic Survey, Cambridge, UK

Measurements of Aerosol Particles in the Arctic during ATWAICE campaign

Arun Babu Suja¹, Thomas Müller¹, Mira Pöhlker¹, Heike Wex¹, Andreas Held², Philipp Oehlke¹, Sabine Lüchtrath², Manuela van Pinxteren¹, Holger Siebert¹, Yifan Yang¹, Theresa Mathes², Kay Weinhold¹, Maik Merkel¹, Birgit Wehner¹

¹Leibniz Institute for Tropospheric Research, Leipzig, Germany

²Technische Universität Berlin, Germany

Der Klimawandel in der Arktis vollzieht sich immer schneller und die Erwärmung hat sich seit Mitte der 1960er-Jahre mehr als doppelt so schnell beschleunigt wie im globalen Durchschnitt. Aerosolpartikel in der Atmosphäre spielen eine wesentliche Rolle für den arktischen Klimawandel. Allerdings gibt es nur wenige Messungen von Aerosolpartikeln in dieser Region. Ziel des ATWAICE-Projekts ist es, die Rußkonzentration im luftgetragenen Zustand und die Deposition von Ruß zu verstehen, ebenso wie den Beitrag der lokalen Partikelemission aus dem Ozean zum gesamten Haushalt der Aerosolkonzentrationen in der arktischen Meeresgrenzschicht. Weiterhin werden die steuernden Faktoren für turbulente Partikelströme und die Variabilität über verschiedenen Oberflächen untersucht, sowie Hauptquellen für Partikel in der arktischen Meeresgrenzschicht, die zur Eisnukleation beitragen.

Introduction

Atmospheric aerosol particles are considered as important contributors to climate change in the Arctic climate system. Therefore, it is important to identify and quantify the aerosol particle sources and sinks, including vertical transport, and to characterize their optical properties as well as their impact on cloud formation. But there are very limited in-situ observations of aerosol particles over the Arctic Ocean. With this in mind, we have conducted aerosol measurements using aerosol particle measuring instruments installed aboard the German ice breaker research vessel Polarstern (PS-131) during the ATWAICE (Atlantic Water pathways to the ice in the Nansen Basin and Fram Strait) cruise. The major objectives of this study are to understand: (i) What are the contributions of local particle emission from the ocean and of new particle formation (NPF) to the entire budget of Arctic marine boundary layer (MBL) aerosol concentrations, and what are the controlling factors of these processes? (ii) How are refractory black carbon (rBC) concentrations in the airborne state linked to those of ocean surface water? (iii) What are the magnitude and sign of turbulent particle fluxes, and how do they vary for different surfaces and MBL conditions? (iv) What are the major sources for ice nucleating particles (INPs) in the Arctic MBL, and particularly to what

extent does the ocean contribute INPs to the Arctic atmosphere?

Method

The atmospheric aerosol particle measurements were carried out from 29th June to 12th August 2022. This includes continuous aerosol particle sampling using various measurement techniques, and particle flux and INP measurements during selected periods where calm conditions allowed us to set up instruments at the frontal outrigger and the crane (Fig. 1). For continuous measurements of physical, chemical and optical aerosol parameters, a laboratory container equipped with aerosol instrumentation was placed on the top deck of the ship. Continuous aerosol container measurements included particle number size distributions from 10 nm to 10 µm using a combination of SMPS (Scanning Mobility Particle Sizer) and APS (Aerodynamic Particle Sizer), and optical properties, such as absorption and scattering coefficients, which were continuously measured by MAAP (Multiangle Absorption Photometer), aethalometer (AE33), and nephelometer. Near real-time measurements of the mixing state and size distribution of airborne BC-containing particles were carried out using the Single Particle Soot Photometer (SP2). In addition, a high-volume filter sampler was installed on the roof of the

container to collect aerosol particles (PM_{10}) with a sampling time of 24 h during the cruise to provide information on the total particle mass concentration and the chemical composition of the aerosol particles. Sea water samples were taken regularly throughout the cruise from the onboard sea water pipeline in addition to sea ice samples from the ice floe stations. Frequent occurrence of fog events was observed during the campaign period. During these events, fog and cloud water samples were collected with a sampler placed on top of the aerosol container.

Further, we installed two systems at the bow crane of the ship for measuring vertical particle fluxes above different surfaces using the Eddy covariance and gradient method. For estimating particle fluxes using Eddy covariance, one temperature-stabilized box (box 1) equipped with an ultrasonic anemometer and a fast mixing-type condensation particle counter (MCPC) was installed at the frontal end of the bow crane's outrigger. The data acquisition rate was 20 Hertz. These measurements were carried out under favourable meteorological conditions and ship movements. Measurements were avoided when the ship was breaking the ice due to the heavy shaking of the bow's crane. A second box equipped with an ultrasonic distance sensor and an MCPC was used to measure the vertical profiles using a winch installed at a custom-built aluminium rack mounted at the end of the crane to move them up and down. These measurements were conducted at specific field stations under favourable meteorological conditions. Each profile measurement took 30 minutes with six measurements of five minutes intervals at different heights starting from 50 cm to 12 m above the ice/ocean surface. In addition, filter samples for INPs were collected using the system installed at the frontal outrigger. The filter sampler was operated simultaneously with the particle flux measurement systems. Sea water samples were also collected from the

onboard sea water pipeline for INP analysis during the beginning and end of each filter sample collection at the frontal outrigger. These samples were later analysed for INPs using LINA (Leipzig Ice Nucleation Array) and INDA (Ice Nucleation Droplet Array) [Wex et al., 2019; Sze et al., 2023] at TROPOS.

Results and Outlook

The aerosol particle size distribution measured during the cruise is shown in Figure-2. A dominance of aerosol particles below 100 nm can be seen, especially in the central Arctic region. Few new particle formation (NPF) events and subsequent growth were observed during the cruise. We observed the highest values of BC concentrations and light scattering coefficients during the initial phase of the cruise up to 70°N. These higher values were driven by the relatively higher contributions from the nearby continental region with higher anthropogenic emission sources. In addition to this, the observed higher light scattering coefficient during this period was found to be modulated by emissions from the open ocean sectors. Further, the measurement period from 16th-19th July was influenced by a warm airmass intrusion [Kanzow et al., 2023] when the ship was in the northern part of marginal ice zone. During this period, we observed significant enhancement in the light scattering and absorption properties. Specifically, the values of the rBC mass concentration enhanced nearly 8-fold compared to the previous period. The observed mass median diameters (MMD) of rBC cores were found to be lowest during 29th June -06th July (~155 nm) whereas the highest MMD were observed during the warm airmass intrusion period (>250 nm). The highest values of MMD during the warm airmass intrusion period indicates the atmospheric processing of BC during long-range airmass transport associated with biomass burning sources. The average MMD

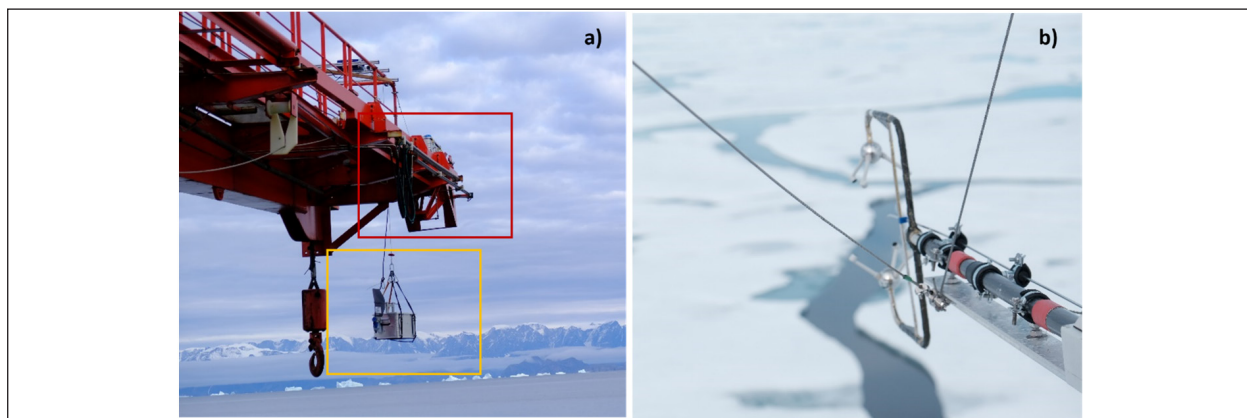


Fig. 1: Illustration of the two installed systems: a) One at the end of the bow crane's outrigger (red), the second underneath the crane at different heights (yellow). b) ultrasonic wind anemometer with the integrated inlet of box 1 above the ice.

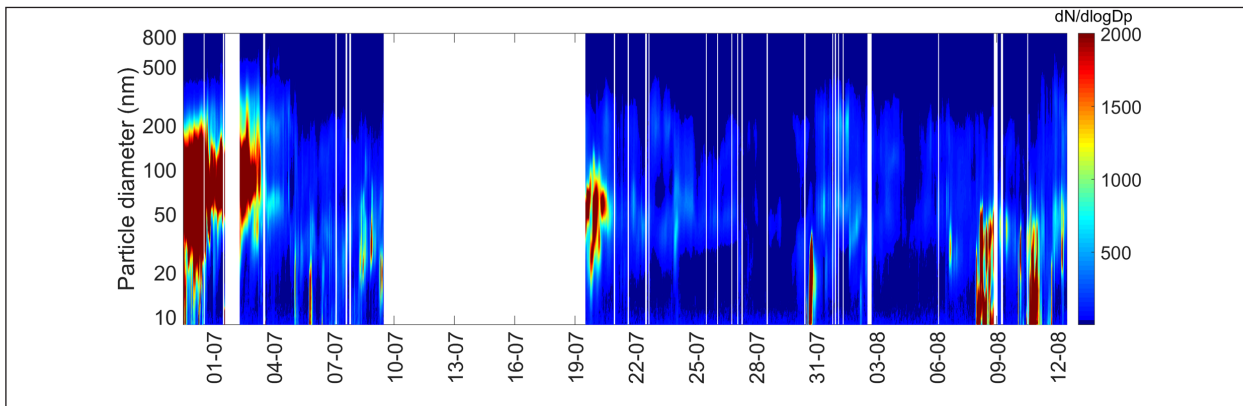


Fig. 2: Size distribution of aerosol particles (10-800nm) measured during ATWAICE cruise

in the central Arctic during the campaign period is ~220nm. This is comparable to earlier observations in the Arctic region [Zanatta et al., 2018; Taketani et al., 2016]. In addition, lower values of MMD were found to be comparable to smaller BC cores reported from urban areas [Laborde et al., 2013]. Differences in BC properties connected to various emission source could be the reason for this spatial systematic size difference. Long-range transport could additionally alter the BC mass mode, either by coagulation or by preferential wet removal of larger BC cores. Comparably high INP concentrations of highly ice active INPs were often found during the cruise. These highly ice active INPs were destroyed by heating to 90°C

for 1 hour. INP data during the ATWAICE campaign often were close to the highest ones found in summer in other parts of the Arctic, as e.g., on Northern Spitzbergen [Sze et al. 2023]. Analysis of sea water, aerosol and fog water samples will show how INP in these compartments are connected, and, together with other analyses in this study, will help to reveal if the ocean can be a major contributor to atmospheric INPs. The parallel sampling of particulate matter, fog, and ocean water, combined with particle flux measurements will provide a unique opportunity to better understand ocean - sea ice - atmosphere interactions in the Arctic.

References

- Kanzow, T. (2023). The Expedition PS131 of the Research Vessel POLARSTERN to the Fram Strait in 2022. Reports on Polar and Marine Research, ISSN 1866-3192. https://doi.org/10.57738/BzPM_0770_2023.
- Laborde, M., Crippa, M., Tritscher, T., Jurányi, Z., Decarlo, P. F., Temime-Roussel, B., Marchand, N., Eckhardt, S., Stohl, A., Baltensperger, U., Prévôt, A. S. H., Weingartner, E., & Gysel, M. (2013). Black carbon physical properties and mixing state in the European megacity Paris. *Atmospheric Chemistry and Physics*, 13(11), 5831–5856. <https://doi.org/10.5194/acp-13-5831-2013>
- Sze, K. C. H., Wex, H., Hartmann, M., Skov, H., Massling, A., Villanueva, D., & Stratmann, F. (2023). Ice-nucleating particles in northern Greenland: Annual cycles, biological contribution and parameterizations. *Atmospheric Chemistry and Physics*, 23(8), 4741–4761. <https://doi.org/10.5194/acp-23-4741-2023>
- Taketani, F., Miyakawa, T., Takashima, H., Komazaki, Y., Pan, X., Kanaya, Y., & Inoue, J. (2016). Shipborne observations of atmospheric black carbon aerosol particles over the Arctic Ocean, Bering Sea, and North Pacific Ocean during september 2014. *Journal of Geophysical Research*, 121(4), 1914–1921. <https://doi.org/10.1002/2015JD023648>
- Wex, H., Huang, L., Zhang, W., Hung, H., Traversi, R., Becagli, S., Sheesley, R. J., Moffett, C. E., Barrett, T. E., Bossi, R., Skov, H., Hünerbein, A., Lubitz, J., Löffler, M., Linke, O., Hartmann, M., Herenz, P., & Stratmann, F. (2019). Annual variability of ice-nucleating particle concentrations at different Arctic locations. *Atmospheric Chemistry and Physics*, 19(7), 5293–5311. <https://doi.org/10.5194/acp-19-5293-2019>
- Zanatta, M., Laj, P., Gysel, M., Baltensperger, U., Vratolis, S., Eleftheriadis, K., Kondo, Y., Dubuisson, P., Winiarek, V., Kazadzis, S., Tunved, P., & Jacobi, H. W. (2018). Effects of mixing state on optical and radiative properties of black carbon in the European Arctic. *Atmospheric Chemistry and Physics*, 18(19), 14037–14057. <https://doi.org/10.5194/acp-18-14037-2018>

Funding

We gratefully acknowledge the funding by the Deutsche Forschungsgemeinschaft (DFG, German Research Foundation) –WE 2757/6-1 and HE 5214/10-1. We also acknowledge the funding of RV Polarstern cruise PS131 (Expedition Grant No. AWI_PS131_04) by AWI.

Vertical distributions of aerosol particles during fall 2021 and spring 2022 in Ny-Ålesund/Svalbard

Birgit Wehner¹, Elisa Akansu¹, Thomas Conrath¹, Andre Ehrlich², Mona Kellermann¹, Michel Michalkow¹, Joshua Müller², Michael Lonardi², Christian Pilz¹, Michael Schäfer², Jens Voigtländer¹, Manfred Wendisch² and Holger Siebert¹

¹ Atmospheric Microphysics Department, Leibniz Institute for Tropospheric Research, Leipzig, Germany

² Leipzig Institute for Meteorology (LIM), Leipzig University, Leipzig, Germany

Mit dem Fesselballonsystem BELUGA wurden Profile vertikaler Aerosolanzahlkonzentration, Aerosolgrößenverteilung, Absorption sowie meteorologischer Parameter im arktischen Frühling und Herbst gemessen. Vertikalprofile sind von entscheidender Bedeutung für das Verständnis von Aerosol- und Aerosol-Wolken-Interaktionsprozessen und können als Grundlage für Modellierungsprozesse wie Strahlungstransferrechnungen dienen. Dank der umfassenden Forschungsinfrastruktur am Messort können bodengebundene Messungen als Ergänzung und zu Vergleichszwecken hinzugezogen werden. Anhand einer Fallstudie im März 2022 werden diese Ergebnisse beispielhaft präsentiert. Dieser Tag ist durch starke Verschmutzung durch Partikeltransport aus Sibirien geprägt und zeichnet sich durch hohe Anzahlkonzentrationen, sowie einen starken Absorptionskoeffizienten aus.

Introduction

Particle dynamics and stratification contribute to the direct radiative effect through the scattering and absorption of radiation. Additionally, particles indirectly influence radiative cooling or warming through cloud formation processes, serving as cloud condensation nuclei or ice nucleating particles. This is particularly relevant under Arctic conditions, as the system is sensitive to changes in radiative properties through feedback mechanisms, resulting in faster warming compared to the rest of the globe. Vertically resolved profiles of aerosol particles play a crucial role in understanding aerosol processes in the Arctic troposphere.

Balloon-borne measurements can bridge the gap between remote sensing data available from higher altitudes and ground measurements, providing a comprehensive profile of the lower troposphere in terms of aerosol and meteorological parameters.

Methods

In fall 2021 (Sep - Nov) and spring 2022 (Mar – May) a total of 60 flights up to an altitude of 1500 m were conducted south of the village Ny-Ålesund on

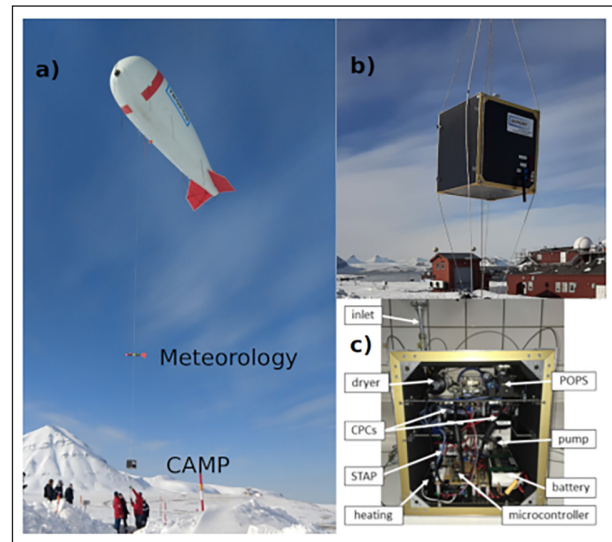


Fig. 1: Tethered balloon system BELUGA instrument deployment (a) and the Cubic Aerosol Measurement Platform with instrument labelling (b, c).

the western coast of Svalbard using the tethered balloon BELUGA (Balloon-born moduLar Utility for profilinG the lower Atmosphere) (Fig. 1) [Egerer et al., 2019]. The system was equipped with the Cubic Aerosol Measurement Platform (CAMP) [Pilz et al.,

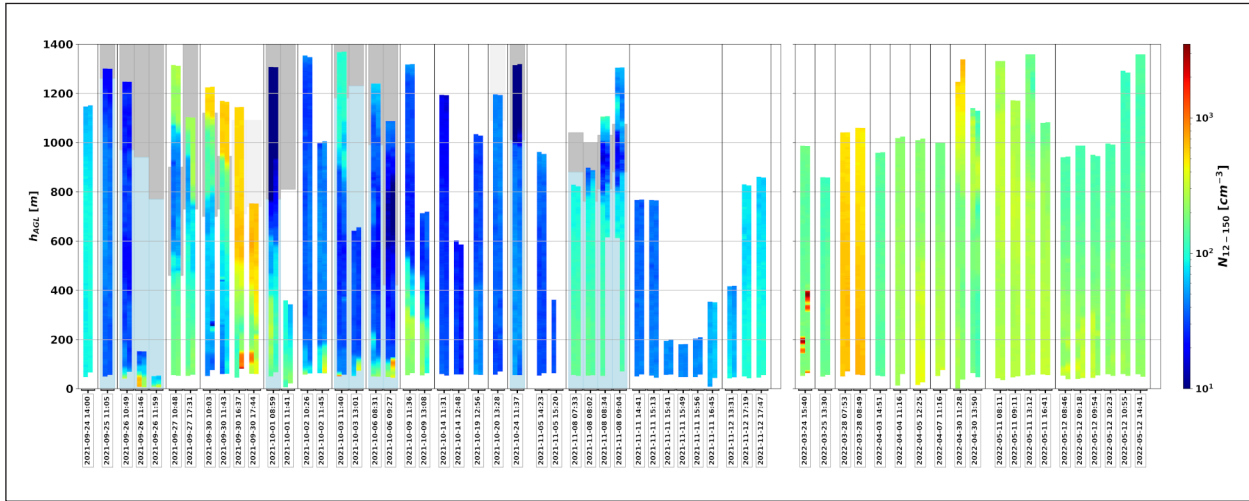


Fig. 2: Overview of the measured aerosol profiles. Different days are separated by black vertical lines. Starting times are denoted. Every flight consists of ascent and descent depicted touching. Aerosol number concentrations between 12–150 nm in cm⁻³ are colored on a logarithmic colorscale. The presence of clouds is marked by the gray background and the that of precipitation by a blue background.

2022] housing two CPCs, measuring particle number concentration above 8 nm (N_8) and 12 nm (N_{12}), a Portable Optical Particle Spectrometer providing particle number concentration from 150 to 2500 nm (N_{12-150}) and a Single Tricolor Absorption Photometer (absorption coefficient) as depicted in Fig. 1 b, c. The quantity N_{12-150} is derived by subtracting $N_{150-2500}$ from N_{12} .

Equivalent black carbon was derived from the absorption coefficient using a MAC (mass absorption cross section) of 13.1 m² g⁻¹ [Pilz et al., 2022]. A Standard Meteo sonde provided temperature, pressure, humidity and wind measurements. The close-by Zeppelin Observatory, situated at 472 m altitude and Gruvebadet Laboratory at the ground provide with long term measurements of aerosol properties.

Results

Flights Overview. An overview of all flights is shown in Fig. 2. Concentrations of particles between 12 and 150 nm (N_{12-150}) are depicted according to a logarithmic colormap. The presence of clouds was derived from ceilometer cloud base height and radar data. Presence of precipitation was concluded by agreement of radar data and flight reports. In the fall of 2021, the frequent occurrence of low-level clouds was accompanied partly by precipitation and resulted from multiple low-pressure systems, stemming from the Icelandic region. Precipitation- and in-cloud-scavenging lead often to pristine conditions with the exception of the 3rd October, where concentrations increased steadily towards and inside the cloudy layer. Elevated concentrations above clouds were observed for three cases, where Beluga surpassed

cloud top, namely: 27th Oct., 30th Oct. and 8th Nov.. On several occasions, highly polluted layers have been observed close to the ground, which may originate from local sources or be trapped under a stable atmosphere. The influence of atmospheric stratification is e.g. visible on the 9th Oct., where an inversion at ~1300 m suppressed mixing of the aerosol-rich layers near ground. In this case new-particle formation is a contributor, if not the main source, of the elevated concentrations. During spring 2022 on the other hand, mainly high pressure and clear sky conditions dominated the measurement period, leading to more homogeneous profiles. Exceptions are the 24th March, with sharp layers of extreme concentrations trapped under an inversion just below 1000 m, and the 30th April, with denser aerosol towards a higher ice cloud between 3 and 6 km.

Case study Arctic Haze. As shown in Fig. 3, the profiles from 28th March 2022 reveal enhanced aerosol number concentration of 500 to 650 cm⁻³ for N_{12-150} and 350 to 475 cm⁻³ for $N_{150-2500}$. This case fits typically into the Arctic Haze season, that is characterised by events of high particle number concentration in the late winter and spring Arctic. Backward trajectory analysis with Hysplit indicates that these particles were transported from northern Siberia to the measurement site and are most likely a product of anthropogenic pollution from high industrial activities in this area [Kirdyanov et al., 2020]. A layer with constant aerosol concentration indicates a well-mixed boundary layer, thus the particles from long range transport in higher altitudes got mixed to the ground. Equivalent black carbon shows values of 0.23 µg m⁻³ to 0.3 µg m⁻³, which highly exceeds the background

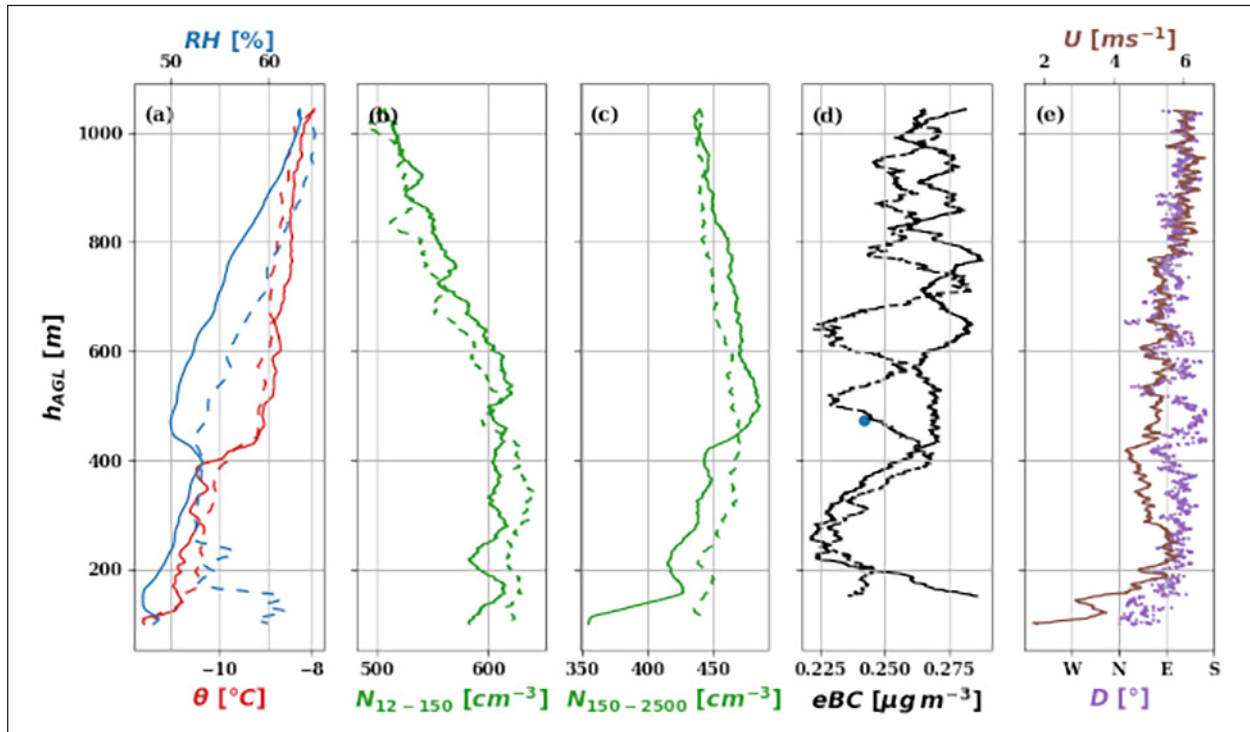


Fig.3: Vertical profiles of a) potential temperature and relative humidity, b) aerosol number concentration 12-150 nm , c) aerosol number concentration 150-2500 nm , d) equivalent black carbon and e) wind direction and speed measured on March 28, 2022..

value from 2009 to 2015 of $0.025 \mu\text{g m}^{-3}$ [Matsui et al., 2022].

Values of aerosol extinction coefficient of 45.2 Mm^{-1} for 532 nm from mie modelling with PyMiScatt [Sumlin, Heinson, and Chakrabarty, 2018]

agree well with measured values from ground station at Gruvebadet Lab. The vertically resolved optical aerosol properties provide a dataset for radiative transfer equations, incorporating the effects of aerosol stratification on radiative transfer.

References

- Egerer, U., M. Gottschalk, H. Siebert, A. Ehrlich and M. Wendisch (2019). „The new BELUGA setup for collocated turbulence and radiation measurements using a tethered balloon: first applications in the cloudy Arctic boundary layer.“ *Atmos. Meas. Tech.* 12(7): 4019-4038, doi: <https://doi.org/10.5194/amt-12-4019-2019>.
- Kirdyanov, A. V., P. J. Krusic, V. V. Shishov, E. A. Vaganov, A. I. Fertikov, V. S. Myglan, V. V. Barinov, J. Browse, J. Esper, V. A. Ilyin, A. A. Knorre, M. A. Korets, V. V. Kukarskikh, D. A. Mashukov, A. A. Onuchin, A. Piermattei, A. V. Pimenov, A. S. Prokushkin, V. A. Ryzhkova, A. S. Shishikin, K. T. Smith, A. V. Taynik, M. Wild, E. Zorita and U. Büntgen (2020). „Ecological and conceptual consequences of Arctic pollution.“ *Ecology Letters* 23(12): 1827-1837, doi: <https://doi.org/10.1111/ele.13611>.
- Matsui, H., T. Mori, S. Ohata, N. Moteki, N. Oshima, K. Goto-Azuma, M. Koike and Y. Kondo (2022). „Contrasting source contributions of Arctic black carbon to atmospheric concentrations, deposition flux, and atmospheric and snow radiative effects.“ *Atmos. Chem. Phys.* 22(13): 8989-9009, doi: <https://doi.org/10.5194/acp-22-8989-2022>.
- Pilz, C., S. Düsing, B. Wehner, T. Müller, H. Siebert, J. Voigtlander and M. Lonardi (2022). „CAMP: an instrumented platform for balloon-borne aerosol particle studies in the lower atmosphere.“ *Atmos. Meas. Tech.* 15(23): 6889-6905, doi: <https://doi.org/10.5194/amt-15-6889-2022>.
- Sumlin, B. J., W. R. Heinson and R. K. Chakrabarty (2018). „Retrieving the aerosol complex refractive index using PyMieScatt: A Mie computational package with visualization capabilities.“ *Journal of Quantitative Spectroscopy and Radiative Transfer* 205: 127-134, doi: <https://doi.org/10.1016/j.jqsrt.2017.10.012>.

Cooperation

Alfred Wegener Institute for Polar and Marine Research
Leipzig Institute for Meteorology

Global adjustments to stratospheric smoke injection from the extreme 2019–2020 Australian wildfires

Fabian Senf, Bernd Heinold, Anne Kubin, Jason Müller, Roland Schrödner, and Ina Tegen

Waldbrände sind eine bedeutende Quelle für absorbierende Aerosole in der Atmosphäre. Insbesondere extreme Brände, wie sie in der australischen Waldbrandsaison 2019–2020 (Black-Summer-Brände) auftraten, können erhebliche großräumige Auswirkungen haben unter anderem aufgrund des Rauchaerosols, das bis zu einer Höhe von 17 km freigesetzt wurde. Mit Hilfe von Simulationen mit einem globalen Aerosol-Klimamodell können wir zeigen, dass die Absorption der Sonnenstrahlung durch den im emittierten Rauch enthaltenen schwarzen Kohlenstoff zu einem kurzweligen Strahlungsantrieb von mehr als +5 W m⁻² in den südlichen mittleren Breiten der unteren Stratosphäre führt. Nachfolgende Anpassungsprozesse in der Stratosphäre verlangsamten die diabatisch angetriebene meridionale Zirkulation, wodurch die Störung auf globaler Ebene umverteilt wurde. Infolge dieser stratosphärischen Anpassungen entwickelte sich in beiden Hemisphären eine positive Temperaturstörung, die eine zusätzliche langwellige Ausstrahlung verursachte. Die langwelligen Anpassungen führten zu einer Kompensation der anfänglich positiven Strahlungsantriebs. Die simulierten Veränderungen in der unteren Stratosphäre wirkten sich durch dynamische Kopplung auch auf die Wolkeneigenschaften der oberen Troposphäre aus. Dies unterstreicht, dass künftige Veränderungen von extremen Waldbränden in die Klimaprojektionen des Aerosol-Strahlungsantriebs einbezogen werden müssen.

Introduction

Atmospheric aerosol particles from both anthropogenic and natural sources are important climate factors. The magnitudes of the different aerosol effects remain, however, highly uncertain [see *Forster et al.*, 2021]. While the overall average effect of aerosol particles on the radiation balance and surface temperatures is negative leading to reduction of surface temperatures [*Forster et al.*, 2021; *Thornhill et al.*, 2021], certain aerosol types, such as black carbon or soot particles, which originate from incomplete combustion processes and strongly absorb light in the spectral range of incident solar radiation, cause a positive radiative effect that counteracts the cooling caused by the non-absorbing aerosol types. This absorption of radiation results in heating rate changes within the aerosol-containing atmospheric layers. In turn, this heating causes rapid atmospheric adjustments to the instantaneous aerosol forcing [*Sherwood et al.*, 2015], and has the potential to alter atmospheric dynamics and circulation. Such atmospheric adjustments are complex and include the effects of changes in heating rates on

boundary layer stability or cloud cover as summarized by *Koch and Del Genio* [2010].

Exceptionally strong vegetation fires occurred in southeastern Australia in December and January 2019–2020 during Australia's so-called Black Summer. Several intense pyroconvective events injected massive smoke amounts into the lower stratosphere [*Kablick et al.*, 2020; *Khaykin et al.*, 2020]. The resulting smoke was transported across the southern hemisphere and was detected in the stratosphere for as long as 2 years after the event [*Ohneiser et al.*, 2022a]. It had significant effects on the radiation budget and its instantaneous positive radiative forcing in the Southern Hemisphere was estimated to be as high as +0.5 W m⁻² by *Heinold et al.* [2022]. The actual radiative effect by the smoke aerosol is however lower due to longwave adjustments in the stratosphere [*Yu et al.*, 2021; *Liu et al.*, 2022]. For various reasons, a large spread of values for radiative forcing (RF) by Australian smoke can be found in the current literature, ranging from around 0.8 W m⁻² [cloud case in *Sellitto et al.*, 2022] to –1.0 W m⁻² [*Hirsch and*

Koren, 2021]. To shed more light on the Australian smoke effects and to extend the work of Heinold et al. [2022], our recent study [Senf et al., 2023] comprehensively quantifies the impact of fire aerosol on global circulation and adjustments using the global simulations with an aerosol–climate model.

Methods

Global simulations with ECHAM6.3–HAM2.3 were initialized on 1 October 2019 and integrated forward until 31 March 2020, i.e., 6 months ahead. Two type model simulations are performed: nudged runs and freely running ensemble simulations. For nudging, additional tendencies are introduced into the momentum equations such that the horizontal winds simulated by ECHAM are relaxed towards ERA5 winds. This strategy is applied to keep the model as close as possible to the observed meteorology. For the freely running simulations, an ensemble with 36 members was set up with slightly perturbed mixing in the upper model layers. As in Heinold et al. [2022], the chosen global model setup applies prescribed wildfire emissions from the Global Fire Assimilation System. To realistically represent pyroconvection, the smoke aerosol is directly introduced in the model layer above the tropopause with emitted aerosol masses of 0.6 and 0.2Tg for the two event periods.

Results and Summary

Shortwave heating by the extreme Australian smoke event triggers local and non-local temperature increases in the stratosphere. As part of the stratospheric

adjustments, a positive temperature perturbation emerges (see Fig. 1). Initially the temperature perturbation develops in the southern mid-latitudes in both the nudged and the ensemble simulations and subsequently spreads towards north and south in the following weeks. While the expansion of the positive temperature perturbation towards the south, i.e., in the poleward direction, can mainly be attributed to the transport of smoke aerosol and is therefore much more pronounced in the nudged runs, the expansion towards the tropics is related to the changes in the stratospheric circulation (Fig. 2). In the southern tropics at around 10°S, upward motion lofts air towards the tropopause region. Between 100 and 200 hPa, the mean flow divides into a northward- and southward-directed branch of the global atmospheric circulation. The northward-directed branch reaches high into the stratosphere and is known as the Brewer–Dobson circulation [Butchart, 2014]. Nudged and ensemble simulations agree with confidence that due to the effects of absorbing wildfire smoke, a positive anomaly of the residual streamfunction develops in southern mid-latitudes and in the tropics. This leads to a reduction in the strength of the poleward circulation in the Southern Hemisphere and to an increase in the circulation strength in the upper northern hemispheric branch. In addition, Senf et al. [2023] discusses impact of the Australian smoke onto the troposphere. The amount of cirrus clouds appeared to be reduced which was caused by a reduction in relative humidity in the upper troposphere. The resulting tropospheric adjustments impacted the hydrological cycle, with subsequently reduced amounts of ice water path, surface precipitation, and evaporation. Due to energetic constraints, tropospheric circulation was also affected, with a link between precipitation changes and

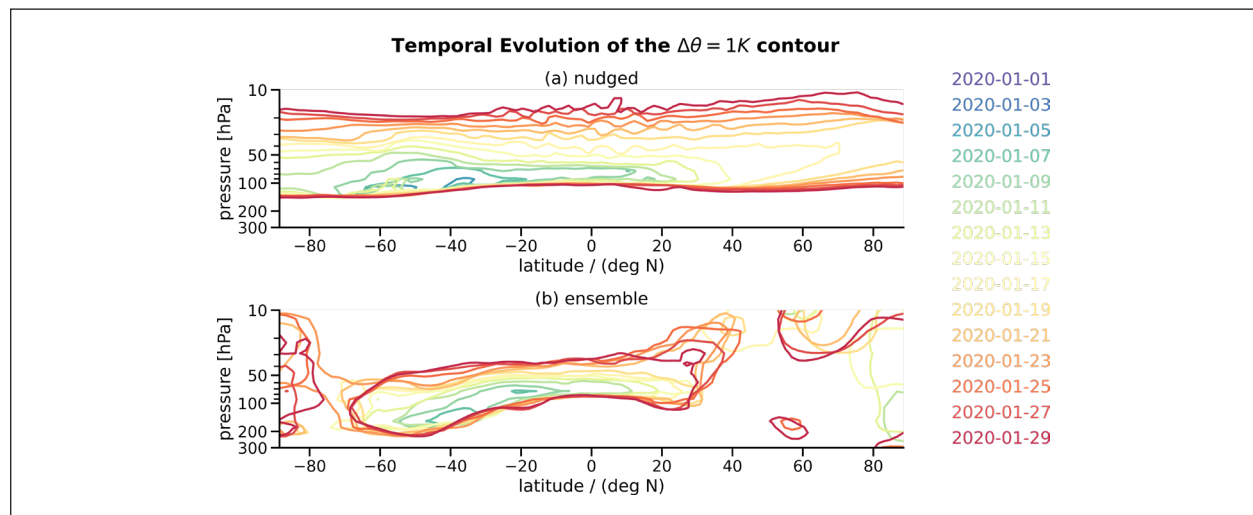


Fig. 1: Temporal evolution of the potential temperature perturbation for the Australian fire case with respect to a no-fire case. Shown is the 1 K contour of the average potential temperature perturbation for the (a) nudged simulations and (b) ensemble simulation that is color coded by time (see legend). Each second day is presented as beginning with 1 January 2020. Note that the pressure at the vertical axes ranges between 300 and 10 hPa [from Senf et al., 2023].

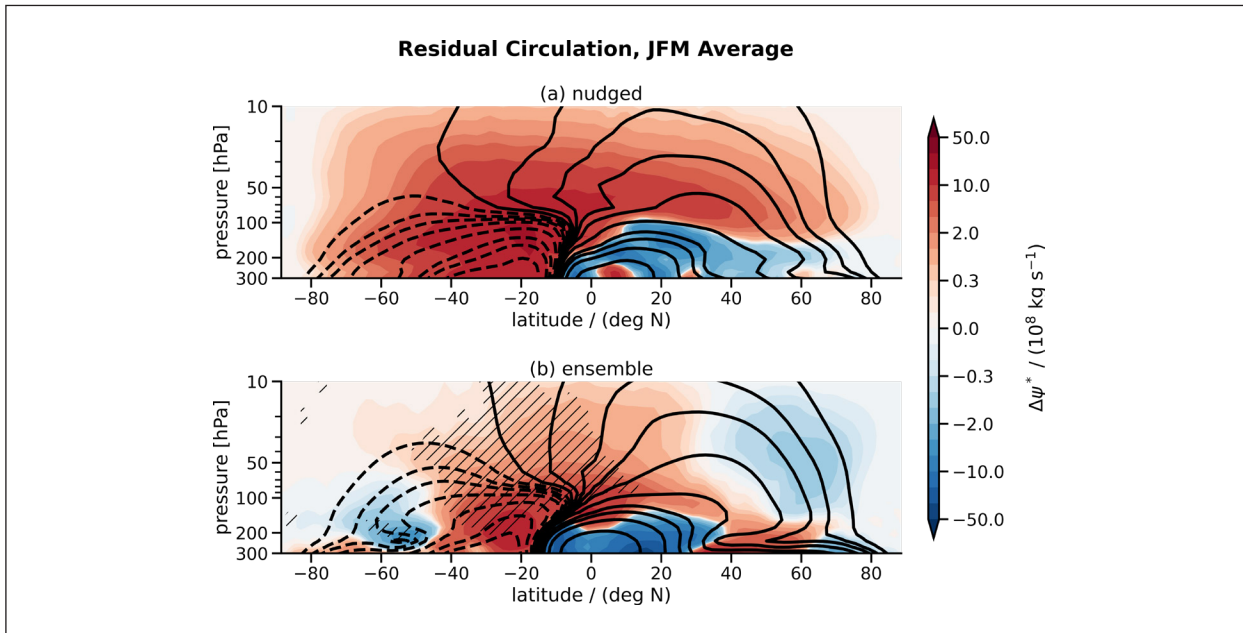


Fig. 2: Average perturbations in residual circulation for (a) nudged simulations and (b) ensemble simulation as a function of latitude and height. Contour lines indicate the state of the reference simulation of a no-fire case with solid lines for positive values and dashed lines for negative values. Perturbations of the residual circulation for the Australian fire case are presented in colored shading. Both contours and shading have logarithmic spacing. Hatching represents areas in which the ensemble mean perturbations are different from zero at the 95 % confidence level.

tropical upward motion, leading to changes in adiabatic cooling in the tropics.

In summary, we showed in *Senf et al. [2023]* that high-reaching smoke plumes from pyroconvection can cause modifications in the stratospheric circulation. The consequences of such large-scale circulation changes due to stratospheric smoke and potential impacts on

the troposphere are not yet fully understood, and further research is needed to disentangle the complex interaction and coupling mechanisms. As rapid climate change, affecting the atmosphere and vegetation, increases the risk and intensity of wildfires [*Jain et al., 2022*], the representation of deep pyroconvective events and associated transport of absorbing aerosols into the stratosphere have to be improved in global climate models.

References

- Butchart, N. (2014). The Brewer-Dobson circulation, *Rev. Geophys.*, 52, 157–184, doi: <https://doi.org/10.1002/2013RG000448>.
- Forster, P., Storelvmo, T., Armour, K., Collins, W., Dufresne, J.-L., Frame, D., Lunt, D., Mauritsen, T., Palmer, M., Watanabe, M., Wild, M., and Zhang, H. (2021). The Earth's Energy Budget, Climate Feedbacks, and Climate Sensitivity, pp. 923–1054, Cambridge University Press, Cambridge, United Kingdom and New York, NY, USA, doi: <https://doi.org/10.1017/9781009157896.009>.
- Heinold, B., Baars, H., Barja, B., Christensen, M., Kubin, A., Ohneiser, K., Schepanski, K., Schutgens, N., Senf, F., Schrödner, R., Villanueva, D., and Tegen, I. (2022). Important role of stratospheric injection height for the distribution and radiative forcing of smoke aerosol from the 2019–2020 Australian wildfires, *Atmos. Chem. Phys.*, 22, 9969–9985, doi: <https://doi.org/10.5194/acp-22-9969-2022>.
- Hirsch, E. and Koren, I. (2021). Record-breaking aerosol levels explained by smoke injection into the stratosphere, *Science*, 371, 1269–1274, doi: <https://doi.org/10.1126/science.abe1415>.
- Jain, P., Castellanos-Acuna, D., Coogan, S. C. P., Abatzoglou, J. T., and Flannigan, M. D. (2022). Observed increases in extreme fire weather driven by atmospheric humidity and temperature, *Nature Clim. Change*, 12, 63–70, doi: <https://doi.org/10.1038/s41558-021-01224-1>.
- Kablick, G., Allen, D. R., Fromm, M., and Nedoluha, G. (2020). Australian PyroCb Smoke Generates Synoptic-Scale Stratospheric Anticyclones, *Geophys. Res. Lett.*, 47, e2020GL088101, doi: <https://doi.org/10.1029/2020GL088101>.
- Khaykin, S., Legras, B., Bucci, S., Sellitto, P., Isaksen, L., Tencé, F., Bekki, S., Bourassa, A., Rieger, L., Zawada, D., Jumelet, J., and Godin-Beekmann, S. (2020). The 2019/20 Australian wildfires generated a persistent smoke-charged vortex rising up to 35 km altitude, *Commun. Earth Environ.*, 1, 22, doi: <https://doi.org/10.1038/s43247-020-00022-5>.
- Koch, D. and Del Genio, A. D. (2010). Black carbon semi-direct effects on cloud cover: review and synthesis, *Atmos. Chem. Phys.*, 10, 7685–7696, doi: <https://doi.org/10.5194/acp-10-7685-2010>.
- Liu, C.-C., Portmann, R. W., Liu, S., Rosenlof, K. H., Peng, Y., and Yu, P.: Significant Effective Radiative Forcing of Stratospheric Wildfire Smoke, *Geophys. Res. Lett.*, 49, e2022GL100175, [<https://doi.org/10.1029/2022GL100175>] (https://doi.org/10.1029/2022GL100175), 2022, doi: <https://doi.org/10.1029/2022GL100175>.

- Ohneiser, K., Ansmann, A., Kaifler, B., Chudnovsky, A., Barja, B., Knopf, D. A., Kaifler, N., Baars, H., Seifert, P., Villanueva, D., Jimenez, C., Radenz, M., Engelmann, R., Veselovskii, I., and Zamorano, F. (2022). Australian wildfire smoke in the stratosphere: the decay phase in 2020/2021 and impact on ozone depletion, *Atmos. Chem. Phys.*, 22, 7417–7442, doi: <https://doi.org/10.5194/acp-22-7417-2022>.
- Sellitto, P., Belhadji, R., Kloss, C., and Legras, B. (2022). Radiative impacts of the Australian bushfires 2019–2020 – Part 1: Large-scale radiative forcing, *Atmos. Chem. Phys.*, 22, 9299–9311, doi: <https://doi.org/10.5194/acp-22-9299-2022>.
- Senf, F., Heinold, B., Kubin, A., Müller, J., Schrödner, R., and Tegen, I. (2023). How the extreme 2019–2020 Australian wildfires affected global circulation and adjustments, *Atmos. Chem. Phys.*, 23, 8939–8958, doi: <https://doi.org/10.5194/acp-23-8939-2023>.
- Sherwood, S., Bony, S., Boucher, O., Bretherton, C., Forster, P., Gregory, J. and Stevens, B. (2015). Adjustments in the Forcing-Feedback Framework for Understanding Climate Change, B.
- Am. Meteor. Soc., 96(2) pp. 217-228, doi: <https://doi.org/10.1175/BAMS-D-13-00167.1>.
- Thornhill, G. D., Collins, W. J., Kramer, R. J., Olivié, D., Skeie, R. B., O'Connor, F. M., Abraham, N. L., Checa-Garcia, R., Bauer, S. E., Deushi, M., Emmons, L. K., Forster, P. M., Horowitz, L. W., Johnson, B., Keeble, J., Lamarque, J.-F., Michou, M., Mills, M. J., Mulcahy, J. P., Myhre, G., Nabat, P., Naik, V., Oshima, N., Schulz, M., Smith, C. J., Takemura, T., Tilmes, S., Wu, T., Zeng, G., and Zhang, J. (2021). Effective radiative forcing from emissions of reactive gases and aerosols – a multi-model comparison, *Atmos. Chem. Phys.*, 21, 853–874, doi: <https://doi.org/10.5194/acp-21-853-2021>.
- Yu, P., Davis, S. M., Toon, O. B., Portmann, R. W., Bardeen, C. G., Barnes, J. E., Telg, H., Maloney, C., and Rosenlof, K. H. (2021). Persistent Stratospheric Warming Due to 2019–2020 Australian Wildfire Smoke, *Geophys. Res. Lett.*, 48, e2021GL092609, doi: <https://doi.org/10.1029/2021GL092609>.

Funding

The study was internally funded by TROPOS. The ECHAM–HAMMOZ model was developed by a consortium composed of ETH Zürich, the Max Planck Institute for Meteorology, Forschungszentrum Jülich, the University of Oxford, the Finnish Meteorological Institute, and the Leibniz Institute for Tropospheric Research (TROPOS) and is managed by the Center for Climate Systems Modelling (C2SM) at ETH Zürich. Computational support for conducting the experiments and storing the data was provided by the Deutsches Klimarechenzentrum (DKRZ) within the compute projects bb1174, bb1262, bb1004, and bb1191. The publication of the article was funded by the Open Access Publishing Fund of the Leibniz Association.

Peroxyl radicals in the atmospheric aqueous phase

Thomas Schaefer, Yimu Zhang, Hartmut Herrmann

In der Atmosphäre haben sekundäre organische Aerosole (SOA) einen erheblichen Einfluss auf die Luftqualität. Die Reaktionen in der wässrigen Phase, die durch freie Radikale in Aerosolen und Wolken-tropfchen angetrieben werden, können erheblich zu den Bildungsprozessen von SOA beitragen. Diese Radikalreaktionen sind komplex und werden von vielen Faktoren beeinflusst, wie zum Beispiel der Struktur der organischen Spezies, dem pH-Wert und der Temperatur der wässrigen Phase, welche in der Atmosphäre einer Änderung unterliegen. Als wichtige Produkte radikal-initiiender Reaktionen spielen organische Peroxylradikale (RO_2^\cdot) bei der SOA-Bildung eine wichtige Rolle. Ziel der vorliegenden Studie ist es, die Reaktionskinetik und -mechanismen von RO_2^\cdot -Radikalen in der wässrigen Phase sowohl experimentell als auch mittels der Methoden der theoretischen Chemie zu untersuchen. Hierfür wurden die Energiebarrieren für die Bildungsreaktionen der Peroxylradikalspezies berechnet als auch die Konzentrations-Zeit-Verläufe in wässriger Lösung bestimmt. Mit diesen Berechnungen und den Absorptionsmessungen in der Laserphotolyse-Langwegabsorptionsapparatur wurden die Spektren der Hydroxymethyl-, Hydroxyethyl- und 2-Propanoylperoxyradikale wässriger Lösung ermittelt.

Introduction

In the atmosphere, secondary organic aerosols (SOA) have a significant impact on air quality variability [Shiraiwa *et al.*, 2017]. The reactions in the aqueous phase driven by radicals in atmospheric aerosols and cloud droplets can contribute significantly to the formation processes of SOA. Free radical reactions are complex and are influenced by many factors, such as the structure of the organic species, the pH and the temperature of the aqueous phase, all of which change frequently in the real atmosphere. [Herrmann *et al.*, 2015] As important products of radical-initiating reactions, organic peroxy radicals (RO_2^\cdot) play an important role in SOA formation. These RO_2^\cdot radicals behave differently depending on their structure, either by unimolecular decomposition or by a recombination reaction. [Herrmann *et al.*, 2015].

The aim of the present study is to investigate the reaction kinetics and mechanisms of RO_2^\cdot radicals in the aqueous phase both experimentally and using theoretical chemistry.

Methods

Spectroscopic studies. The RO_2^\cdot radicals were formed by the reaction of the organic precursor compound with OH radicals, which originated from the photolysis of hydrogen peroxide (H_2O_2). The alkyl radical is then formed by a hydrogen atom abstraction followed by an O_2 addition reaction resulting in RO_2^\cdot formation. The experimental studies of the peroxy radicals and their properties were performed by the laser photolysis - long path absorption (LP-LPA) setup. Briefly, this setup includes a cuboid reaction flow cell (3.5 cm long, 4 cm wide, 2 cm high), an

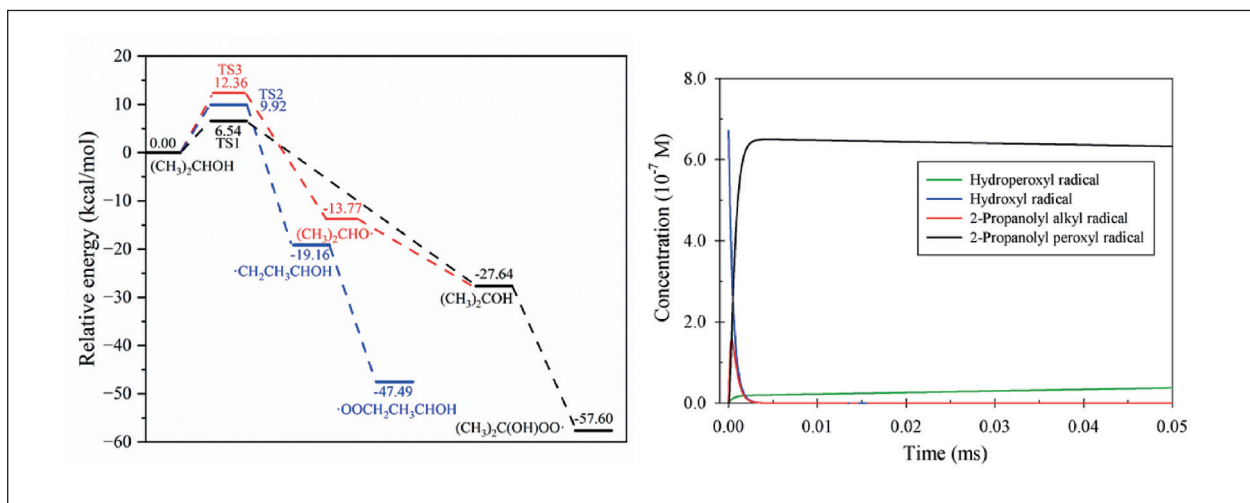


Fig. 1: The energy barriers for the 2-propanoyl peroxy radical formation are shown on the left side (A) of the figure. On the right side (B) the modelled concentration-time profiles of the different radical species in the aqueous phase are depicted.

excimer laser as photolysis light source at $\lambda = 248$ nm, a light source, a White cell mirror configuration in order to increase the absorption path length, and a detector. In case of the spectroscopic studies a deuterium lamp was used in combination with an intensified charge-coupled device (ICCD) camera. The concentration of O₂ in the aqueous solution was measured after the flow cell using a Clark electrode.

Theoretical studies. A COmplex PAthway SImulator (COPASI) model was used to calculate peroxy radical concentration-time profiles based on kinetic data.

Density-functional theory (DFT) calculations were carried out to determine reaction energy barriers using the Gaussian 16 package. The geometrical optimizations of reactants, transition states, and products were performed at the level of M06 2X and 6-311++G(d,p) basis set. In order to obtain more accurate energies, single point energies were calculated using a more flexible level of M06-2X/6-311++G(3df,2p) based on an optimized structure.

Results and Discussion

The reaction energy barriers for the formation of the following peroxy radical species were determined: Hydroxymethyl peroxy radical, hydroxyethyl peroxy radical and 2-propanoyl peroxy radical. Fig. 1a shows the different energy barriers of 2-propanoyl peroxy radical formation via the transition states (TS) and the corresponding alkyl radicals with subsequent barrier-less oxygen addition. The following trend of the reaction barriers of the hydrogen atom abstraction reaction at the position -CH < -CH₃ < -OH with the corresponding transition states TS1 < TS2 < TS3 was

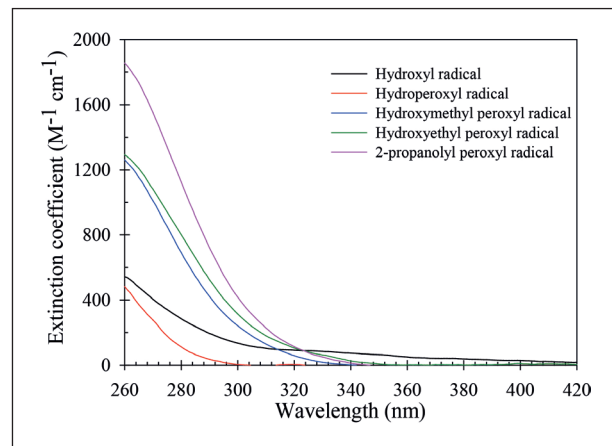


Fig. 2: Peroxyl radical spectra of this study, measured with the (LP-LPA) setup at the concentration maximum.

calculated, which reflects the formation of the different alkyl radical species.

Figure 1b shows the modelled concentration-time profiles of the different radical species for the reaction of 2-propanol with OH radicals in the (LP-LPA) setup obtained from the kinetic modelling. Using these approaches and the yielding data in combination with the absorption measurements in the (LP-LPA) setup the following spectra were derived (Fig. 2).

Figure 2 shows the molar extinction coefficient of the OH radical, the HO₂ radical (the simplest peroxy radical) and the organic peroxy radicals resulting from the oxidation of methanol, ethanol and 2-propanol in the aqueous phase. These measurements form the foundation for further experiments on the kinetics of the decay of peroxy radicals and their reactions with inorganic sulphur(IV) compounds such as SO₃²⁻/HSO₃⁻ species.

References

- Shiraiwa, M., Li, Y., Tsimpidi, A. P., Karydis, V. A., Berkemeier, T., Pandis, S. N., Lelieveld, J., Koop, T., and Pöschl, U.: Global distribution of particle phase state in atmospheric secondary organic aerosols, *Nat. Commun.*, 2017, 8, 15002, doi: <https://doi.org/10.1038/ncomms15002>.
- Herrmann, H., Schaefer, T., Tilgner, A., Styler, S. A., Weller, C., Teich, M., and Otto, T.: Tropospheric aqueous-phase chemistry: kinetics, mechanisms, and its coupling to a changing gas phase, *Chemical Reviews*, 2015, 115, 4259-4334, doi: <https://doi.org/10.1021/cr500447k>.

Funding

CSC research project: Kinetic and model simulation studies of aqueous phase peroxy radical reactions in the formation of secondary organic aerosol (SOA) in the atmosphere (grant number 202206220053) funded by the CSC (China Scholarship Council).

Modelling of heterogeneous chemistry on dust aerosol particles

Marvel B. E. Aiyuk, Erik H. Hoffmann, Andreas Tilgner, Hartmut Herrmann

Der Multiphasenchemiemechanismus MCM–CAPRAM wurde um ein Modul zur Beschreibung heterogener Reaktionen auf atmosphärischem Mineralstaubpartikeln erweitert. Anschließend wurden verschiedene Simulationen mit dem Boxmodell SPACCIM für den urbanen Hintergrund mit und ohne heterogene Reaktionen an Mineralstaubpartikeln durchgeführt. Unter Modellbedingungen mit niedrigen Staubkonzentrationen werden nur sehr geringe Änderungen in der Konzentration von Gasen simuliert. Anders verhält es sich unter Modellbedingungen mit einer hohen Konzentration an Mineralstaubpartikeln. Die Simulationen zeigen eine starke Abnahme an NO_x ($\approx 30\%$) und signifikante Änderungen für Carbonylverbindungen. Durchgeführte Sensitivitätsstudien zeigen, dass die modellierten NO_x Effekte hauptsächlich auf die Reaktion von N_2O_5 an der Oberfläche der Mineralstaubpartikel zurückzuführen sind.

Introduction

Dust aerosols make up an important fraction of the particulate matter in the atmosphere [Huneeus *et al.*, 2011; Tëxtor *et al.*, 2006]. They play an important role in atmospheric chemistry by providing an active surface for heterogeneous reactions. Heterogeneous reactions affect the composition of the troposphere, by the creation of new sources and sinks of various important trace gases and modifying the chemical and physical properties of aerosol particles [Bian and Zender, 2003; Krueger *et al.*, 2004]. Several laboratory and modelling studies have demonstrated the importance of heterogeneous reactions, but some uncertainties still persist. For example, more detailed model-based investigations are needed to better understand the role of dust-related heterogeneous chemistry in the atmosphere. The multiphase MCM-CAPRAM mechanism allows a very detailed implementation, due to its large number of processes and inclusion of several key processes.

Methods

Mechanism development. For a better understanding on the impact of heterogeneous reactions of dust on tropospheric chemistry, a modelling study was performed using the existing Master Chemical Mechanism (MCM) mechanism (MCMv3.3.1) together with a new developed Chemical Aqueous Phase Radical mechanism (CAPRAM) module describing

heterogeneous chemistry at aerosol surfaces (CAPRAM-het). The developed CAPRAM-het contains 10 heterogeneous reactions based on recommended kinetic data from the International Union of Pure and Applied Chemistry (IUPAC) database [Crowley *et al.*, 2010]. Heterogenous conversions of inorganic trace gas species are considered in CAPRAM-het.

Model simulations. Several simulations were performed for an urban scenario and different dust aerosol surface area conditions. Here, only the model runs with a specific surface area of 1.2×10^{-5} , which corresponds to very high dust conditions, are presented (dust simulation case, VHD). The overall simulation time was three days with a relative humidity set at 70%, implying that the water on dust surfaces does not affect the surface reactions or induce bulk reactions. The model results were compared with a control simulation where no heterogeneous chemistry (ND) was simulated.

Results and Discussion

The performed model runs showed that heterogenous reactions on dust lead to a concentration decrease for most of the compounds. The most significant losses modelled were in HNO_3 and N_2O_5 (Fig. 1a), by 99% and 88% on average, respectively. Both compounds have a high uptake coefficient compared to the other compounds and relatively few gas-phase reactions. Thus, the main sink is the dust

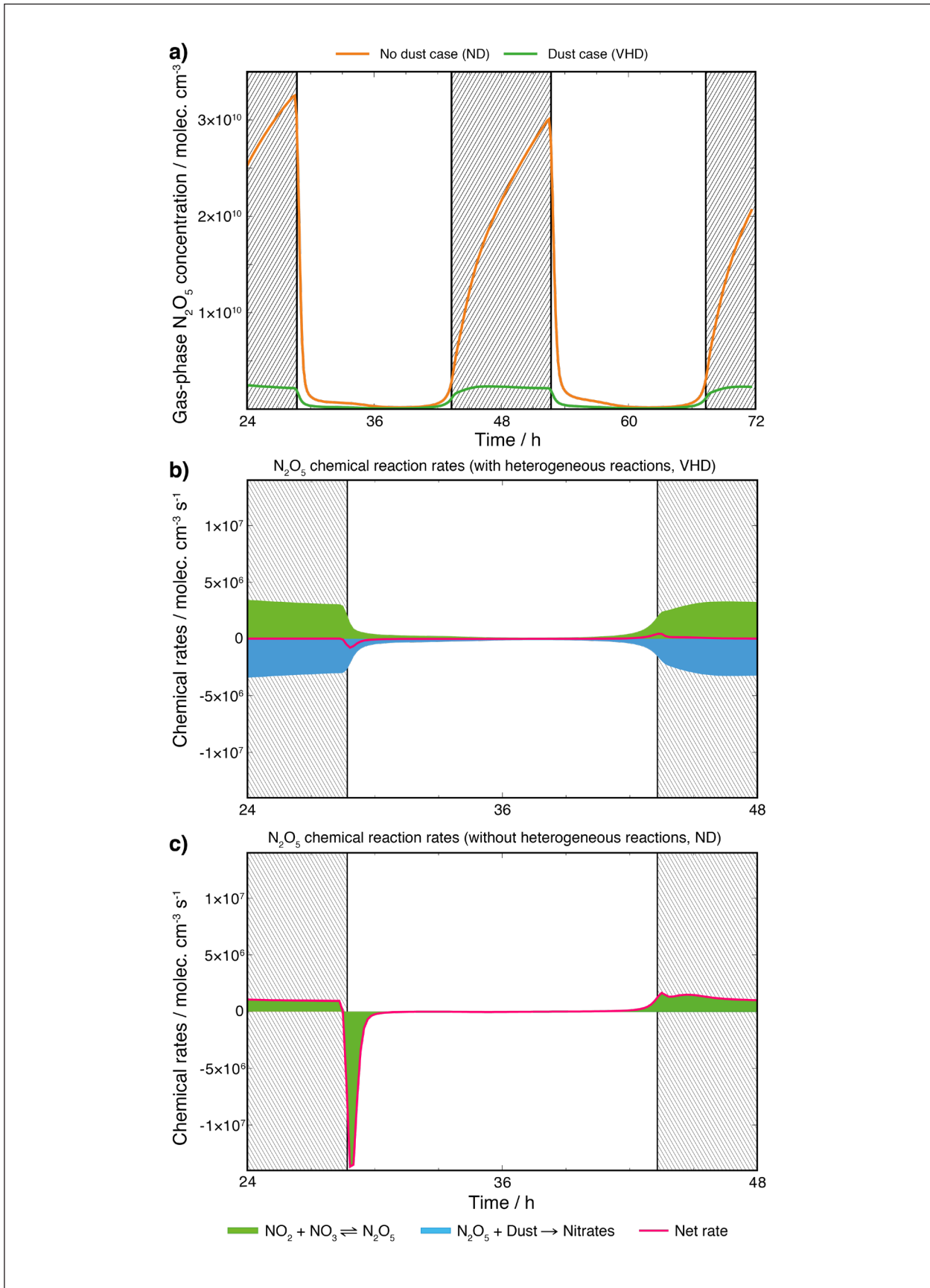


Fig. 1: a) Simulated N_2O_5 concentration profiles and N_2O_5 chemical rates b) with and c) without heterogenous dust chemistry considered.

uptake, contributing almost 100% to the total loss. For N_2O_5 , the heterogenous uptake on dust reduced the concentrations during the night, with the gas-phase reactions of N_2O_5 acting only as sources, while the dust reaction is the only sink. This effective uptake leads to an increased transfer of gaseous N_2O_5 onto the dust (Figure 1b and c). Other trace gases in which the dust uptake is the main sink include H_2O_2 (74%) and SO_2 (82%). For the other compounds, the changes are mostly caused by the loss of N_2O_5 , which affects the NO_x cycling. Under very high dust conditions, NO , NO_2 and NO_3 decrease by 27%, 28% and 79% on average, respectively. The changes in the HO_x are smaller, with OH and HO_2 decreasing by 7% and 4% on average, respectively.

The VOCs are also modelled to change, with the most significant changes modelled in the carbonyl compounds and in peroxyacetyl nitrate (PAN). Acetaldehyde and acetone decrease by 32% and 48%, respectively. The loss of acetaldehyde and NO results in a decrease in PAN by 25%. An increase in alkenes is also modelled, and this is due to the concentration decrease in oxidants such as OH and NO_3 . Accordingly, concentrations of emitted compounds such as ethene and propene increase by 5% and 13%, respectively.

In addition to the main simulations, a number of sensitivity studies were also performed. In the first sensitivity study, only one reaction was implemented. The results show that the uptake of only N_2O_5 results in even lower concentration in the NO_x species, with a concentration loss of 37% and 32% for NO and NO_2 , respectively. However, the concentration of oxidants, such HO_2 and H_2O_2 , increases by 8% and 18%, respectively. This indicates that the uptake of only N_2O_5 can predict the dust effects on NO_x well but is inadequate for $\text{HO}_{x,y}$. In subsequent sensitivity studies, the effect of the variation of the uptake coefficient was investigated, revealing that the higher uptake of O_3 acts as an indirect source of HONO , which increases by 183%. This is due to a reduction of the main NO sink, resulting in an increase in NO concentration by 140%.

Despite these important findings, there are still some limitations and more detailed processes like surface photocatalytic processes are being implemented in future CAPRAM-het modules for a better understanding of heterogeneous aerosol chemistry processes.

References

- Bian, H. S., and C. S. Zender (2003), Mineral dust and global tropospheric chemistry: Relative roles of photolysis and heterogeneous uptake, *J. Geophys. Res.-Atmos.*, 108(D21), 14, doi: <https://doi.org/10.1029/2002jd003143>.
- Crowley, J. N., M. Ammann, R. A. Cox, R. G. Hynes, M. E. Jenkin, A. Mellouki, M. J. Rossi, J. Troe, and T. J. Wallington (2010), Evaluated kinetic and photochemical data for atmospheric chemistry: Volume V - heterogeneous reactions on solid substrates, *Atmos. Chem. Phys.*, 10(18), 9059-9223, doi: <https://doi.org/10.5194/acp-10-9059-2010>.
- Huneeus, N., et al. (2011), Global dust model intercomparison in AeroCom phase I, *Atmos. Chem. Phys.*, 11(15), 7781-7816, doi: <https://doi.org/10.5194/acp-11-7781-2011>.
- Krueger, B. J., V. H. Grassian, J. P. Cowin, and A. Laskin (2004), Heterogeneous chemistry of individual mineral dust particles from different dust source regions: the importance of particle mineralogy, *Atmos. Environ.*, 38(36), 6253-6261.
- Textor, C., et al. (2006), Analysis and quantification of the diversities of aerosol life cycles within AeroCom, *Atmos. Chem. Phys.*, 6, 1777-1813, doi: <https://doi.org/10.5194/acp-6-1777-2006>.

Sources of particulate matter identified by labelled species in a chemical transport model and a complementary measurement campaign

Hanna Wiedenhaus, Roland Schrödner, Ralf Wolke, Shubhi Arora, Laurent Poulain, Hartmut Herrmann

Umfangreiche Messungen und Modellsimulationen mit COSMO-MUSCAT wurden durchgeführt, um ein besseres Verständnis der Feinstaubquellen und Transportprozesse in Mitteleuropa im Winter zu gewinnen. Ein neuer Ansatz zur Bestimmung der Anteile der verschiedenen Emissionsquellen wurde in einem Modell implementiert, um die Herkunft der primären Aerosole zu bestimmen. Diese Ergebnisse zeigen einen hohen Beitrag von Hausbrand, insbesondere in der Tschechischen Republik. Während das Modell die Konzentrationen von organischem Material an zwei der drei Messstationen gut wiedergibt, werden die gemessenen Konzentrationen an der Station in der Nähe von Prag stark unterschätzt. Da die modellierten primären Aerosole an allen Stationen gut mit den Messdaten übereinstimmen, vermuten wir eine Unterschätzung des sekundären organischen Aerosols (SOA) an dieser Station im Modell. Zu geringe Emissionen von flüchtigen organischen Verbindungen aus der Verbrennung von Holz und Kohle als Vorläufergase für die Bildung von SOA könnten hierfür einen Erklärungsansatz bieten.

Introduction

Much effort has been devoted to the reduction of mass concentrations of particulate matter (PM) in ambient air for the protection of human health. More detailed information on aerosol sources and transport processes is needed to effectively target the remaining air pollution with further mitigation strategies.

However, the complex system of multiple sources and dispersion of atmospheric aerosols is still not fully understood. Central Europe is characterised by a strong air pollution gradient with higher levels in the east. Transboundary transport during the inflow of eastern air masses can lead to a shift of these more polluted air masses. Previous studies in Germany have identified combustion processes as a major

contributor to regional background concentrations during periods with long-range transport from eastern Europe [van Pinxteren *et al.*, 2016] [van Pinxteren *et al.*, 2019].

This work is part of the TRACE project: Transport and transformation of atmospheric aerosol over Central Europe with emphasis on anthropogenic sources. Synergistic measurement methods and state-of-the-art modelling tools are combined to obtain a comprehensive picture of the contribution of transported anthropogenic aerosol compared to local emissions.

Method

A source attribution module has been developed within the multiscale modelling system

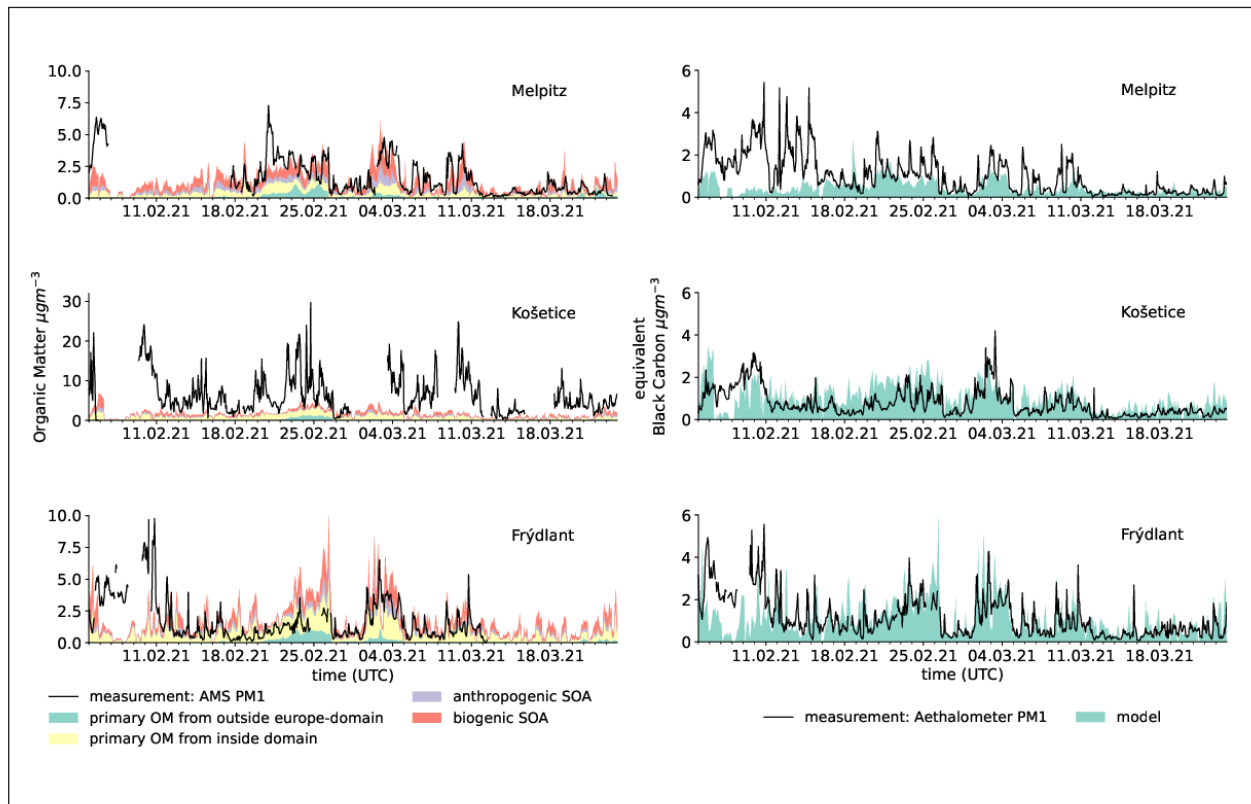


Fig. 1: Left: comparison of measured and modelled organic matter (OM) mass concentrations for the three sites. The modelled data are split into anthropogenic and biogenic secondary organic aerosols (SOA), primary OM concentration originating outside the outermost domain (*i.e.*, driving boundary data) and originating within the study domain. Right: comparison of measured equivalent black carbon and modelled elemental carbon mass concentration.

COSMO-MUSCAT (COSMO: Consortium for Small-scale Modelling [Schaettler et al., 2018]; MUSCAT: MultiScale Chemistry Aerosol Transport [Wolke et al., 2012]). The emitted species can be labelled and tracked during the model simulation. Transport processes (advection, diffusion, sedimentation) and removal processes (dry and wet deposition) are applied to the labelled tracers. However, gas phase chemistry and aerosol chemistry are not considered, limiting the approach to primary particles at present.

Focusing on winter combustion processes, this study tracks anthropogenic elemental carbon (EC) and organic matter (OM) emissions labelled by emission sector and country of origin. The domains for the simulations were chosen to cover the TRACE measurement sites in Germany and the Czech Republic. To reduce computational costs, the model is nested twice starting from an outermost domain covering most of Europe. The innermost domain covers 317×204 grid cells with a horizontal resolution of ~ 2 km.

Observational data are available from 05.02.2021 to 24.03.2021 for three sites: the two ACTRIS stations Melpitz (MPZ, DE) and Košetice (NAOK, CZ) and a third station in Frýdlant (FRY, CZ). The stations were chosen to represent the important transition area

between highly polluted and less polluted regions in Central Europe.

Highly time-resolved measurements of the concentrations of non-refractory PM1 (NR-PM1) aerosol species (organics, sulphate, nitrate, ammonium and chloride) were obtained using aerosol mass spectrometry. Continuous on-line measurement of equivalent black carbon (eBC) mass concentrations was performed using a multi-wavelength aethalometer (AE33). All measurements were conducted by our Czech collaborator and the Department of Atmospheric Chemistry, respectively.

Results and Discussion

In early February, an air mass boundary between cold air in the north and warm air in the south moved southward, bringing cold air to Central Europe. Clear nights with freezing temperatures and heavy snowfall occurred in the study region. During this period our model underestimates PM mass concentrations in all size classes.

From about 11 February, the weather pattern changed to a stationary, high-pressure system, leading to an increase in temperature. From then on,

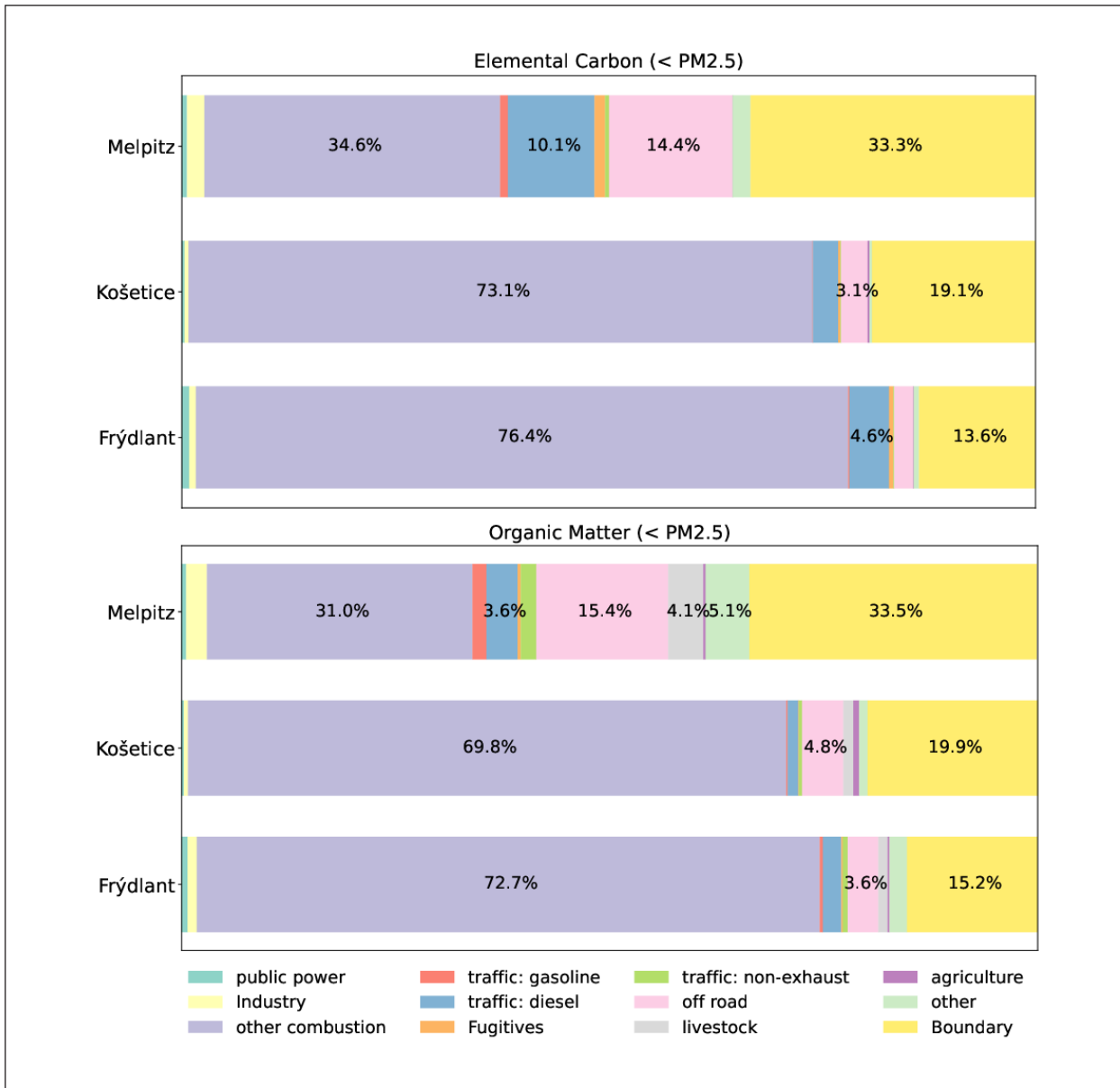


Fig. 2: Relative contribution of different source sectors to the total of EC (top) and OM (bottom) in PM2.5. ‘Boundary’ refers to all emissions from the outer domains into the inner domain (i.e., transport through the innermost domain boundary) that are not separated into different sectors.

the model reproduces the measured OM and EC concentrations well, with the exception of the Košetice station near Prague (Fig. 1).

The results of the labelling approach for primary EC and OM are shown in Fig. 2. The ‘other combustion’ sector is the largest single source sector within the model domain, which comprises stationary combustion processes in households (mainly domestic heating), small businesses, agriculture, forestry and fisheries. This sector accounts for more than half of the primary EC and OM in Košetice and Frýdlant.

As we can reproduce the elemental carbon concentrations at all stations reasonably well (Fig. 1,

right), we are confident that we are capturing the primary aerosols correctly. This leads to the conclusion that our model is not capturing the secondary organic aerosol (SOA) concentrations in Košetice. We assume an underestimation of anthropogenic volatile organic compound (AVOC) emissions from residential wood and coal burning, leading to an underestimation of SOA. Chamber studies analysing emissions from residential wood combustion have shown that at least 50% of the observed SOA is caused by non-traditional VOCs, which are not considered in models [Bruns et al., 2016]. This suggests that AVOC precursors could be a significant contributor to our SOA budget, which will be the subject of further work.

References

- Atkinson, R., and J. Arey (2003), Atmospheric degradation of volatile organic compounds, *Chem Rev*, 103(12), 4605-4638, doi: <https://doi.org/10.1021/cr0206420>.
- Bruns, E. A., I. El Haddad, J. G. Slowik, D. Kilic, F. Klein, U. Baltensperger, and A. S. Prevot (2016), Identification of significant precursor gases of secondary organic aerosols from residential wood combustion, *Sci Rep*, 6, 27881, doi: <https://doi.org/10.1038/srep27881>.
- Schättler, U., G. Doms, and C. Schraff (2018), COSMO-Model Version 5.05: A Description of the Nonhydrostatic Regional COSMO-Model - Part VII: User's Guide, Deutscher Wetterdienst, doi: https://doi.org/10.5676/DWD_pub/nww/cosmo-doc_5.05_VII.
- van Pinxteren, D., K. W. Fomba, G. Spindler, K. Muller, L. Poulain, Y. Linuma, G. Loschau, A. Hausmann, and H. Herrmann (2016), Regional air quality in Leipzig, Germany: detailed source apportionment of size-resolved aerosol particles and comparison with the year 2000, *Faraday Discuss*, 189, 291-315, doi: <https://doi.org/10.1039/c5fd00228a>.
- van Pinxteren, D., F. Mothes, G. Spindler, K. W. Fomba, and H. Herrmann (2019), Trans-boundary PM10: Quantifying impact and sources during winter 2016/17 in eastern Germany, *Atmospheric Environment*, 200, 119-130, doi: <https://doi.org/10.1016/j.atmosenv.2018.11.061>.
- Wolke, R., W. Schröder, R. Schrödner, and E. Renner (2012), Influence of grid resolution and meteorological forcing on simulated European air quality: A sensitivity study with the modeling system COSMO-MUSCAT, *Atmospheric Environment*, 53, 110-130, doi: <https://doi.org/10.1016/j.atmosenv.2012.02.085>.

Funding

German Research Foundation (DFG), Bonn, Germany (grant 431895563)
The Czech Science Foundation (GACR), Prague, Czech Republic (grant 20-08304J).

Cooperation

Department of Aerosol Chemistry and Physics, Institute of Chemical Process Fundamentals, Czech Academy of Sciences

The Small-Scale Variability of Solar Radiation Campaign – Overview and First Results

Hartwig Deneke¹, Jonas Witthuhn¹, Connor Flynn², Jens Redemann², Michael Ritsche³, Andreas Macke¹

¹ Leibniz Institute for Tropospheric Research, Leipzig, Germany

² School of Meteorology, University of Oklahoma, Norman, OK, US

³ Argonne National Laboratory, Lemont, IL, US

Ein am TROPOS entwickeltes Sensornetzwerk aus 60 autonomen Pyranometer-Stationen wurde im Sommer 2023 für einen Zeitraum von 12 Wochen am ARM (Atmospheric Radiation Measurement Program) Southern Great Plains (SGP) Observatorium in Oklahoma (USA) aufgestellt und betrieben. Die S2VSR-Kampagne (Small-Scale Variability of Solar Radiation) profitierte dabei von den Erfahrungen aus früheren Feldkampagnen, den spezifischen meteorologischen Bedingungen und der umfangreichen Instrumentierung des dortigen Observatoriums. Das Ergebnis ist ein einzigartiger Datensatz über die kleinskalige raumzeitliche Variabilität der globalen Sonnenstrahlung, die durch Wolken verursacht wird. In diesem Text wird ein Überblick über die Kampagne einschließlich ihrer Motivation und erster Ergebnisse gegeben.

A unique sensor network consisting of 60 autonomous pyranometer stations designed by TROPOS was deployed and operated for a 12-week period at the ARM (Atmospheric Radiation Measurement Program) Southern Great Plains (SGP) observatory in Oklahoma(US) in summer 2023. Benefiting from the experience gained during previous field campaigns, the specific meteorological conditions, and the extensive instrumentation at the observatory, the Small-Scale Variability of Solar Radiation (S2VSR) campaign offers an unprecedented data set on the small-scale spatiotemporal variability of global solar radiation as introduced by clouds. An overview of the campaign including its motivation and a look at some preliminary results is given here.

Motivation

Clouds introduce significant variability in solar radiation in particular for shallow cumulus and other convective cloud types. Variability at small spatio-temporal scales (e.g. below 1-min and 1-km) is however not sufficiently resolved by current satellite observations nor atmospheric models. Additionally, 3D photon transport is commonly neglected and causes significant deviations in 1D radiative transfer simulations at such small scales.

A specific challenge is to account for the point-like nature of traditional surface radiation measurements in comparison to spatially averaged quantities such as satellite pixels or model grid-boxes. The pyranometer network (PyrNet) was initially designed and built at TROPOS for the HDCP(2) project to help better characterize and understand this small-scale variability [Madhavan et al., 2016; Macke et al., 2017].

While several campaigns have been previously conducted with this network, the S2VSR campaign was planned specifically to benefit from past experience, the specific meteorological conditions in the Southern Great Plains featuring frequent shallow cumulus, and the availability of complementary instruments. Specifically, high-quality reference observations of global radiation are readily available for calibration, a camera network offers a 4D stereo-photogrammetric reconstruction of shallow cumulus, the so-called Clouds Optically Gridded by Stereo [COGS, Romps et al., 2018], and the GOES-R satellite can serve as proxy for the capabilities of the upcoming European Meteosat Third Generation.

Methods and Logistic Aspects

60 autonomous pyranometer stations were deployed and operated for a 12-week period at

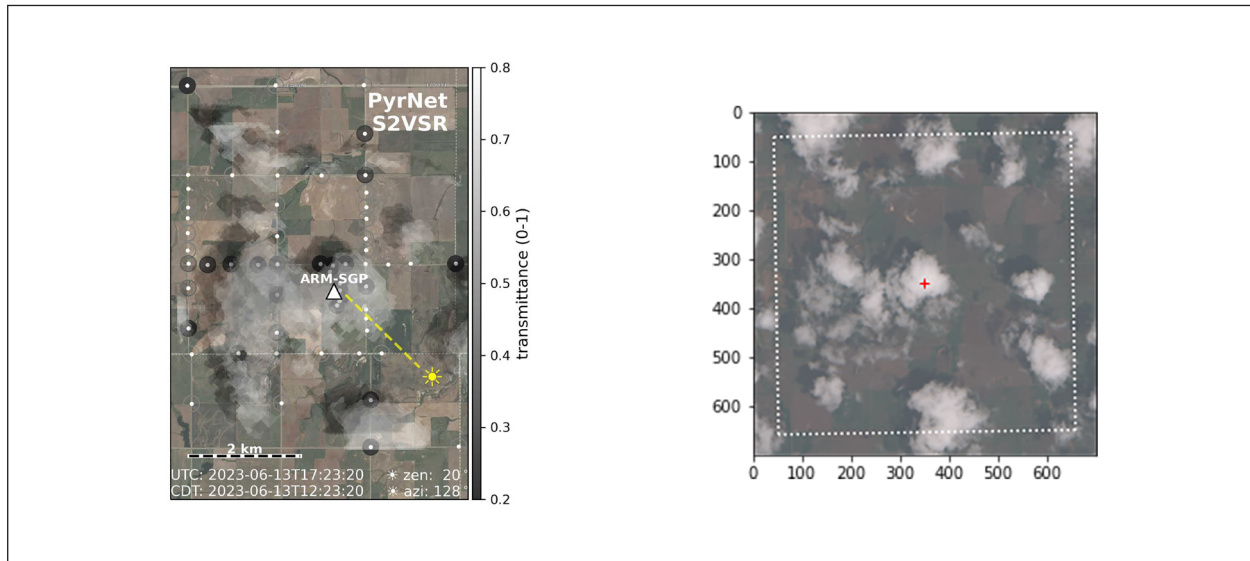


Fig. 1: (left) Map of the S2VSR station layout. Transmittance measured by PyrNet stations (dots) is shown by the tone of the circles marking the station positions. The COGS 3D cloud mask is displayed as white transparent layer, and the associated cloud shadows by a black layer. (right) The same cloud field as viewed by the Copernicus Sentinel-2 satellite.

the ARM Southern Great Plains site in Oklahoma distributed across a 6x6 km² domain centred on the Central Facility. Each station recorded global radiation together with air temperature and relative humidity at a sampling frequency of 1-Hz. In addition, 26 stations also recorded tilted solar irradiance using a second pyranometer. A map of the station layout is show in Fig. 1. Prior to the field deployment, all stations were setup on the ARM radiation platform in close vicinity to a reference measurement of global radiation to enable their in-field calibration.

The great support by ARM and the close co-operation with the school of Meteorology at the University of Oklahoma (OU) were essential for the

success of the campaign. In particular, OU students carried out the time-consuming weekly maintenance of stations, including visual inspection, cleaning, data download and replacement of batteries. While three stations were damaged – likely by agricultural activities – overall data quality and availability has been found to be excellent.

First Results and Perspective

Data quality has been closely monitored throughout the campaign by a student assistant at TROPOS. As part of the post-campaign activities and data analysis, a review and update of the established

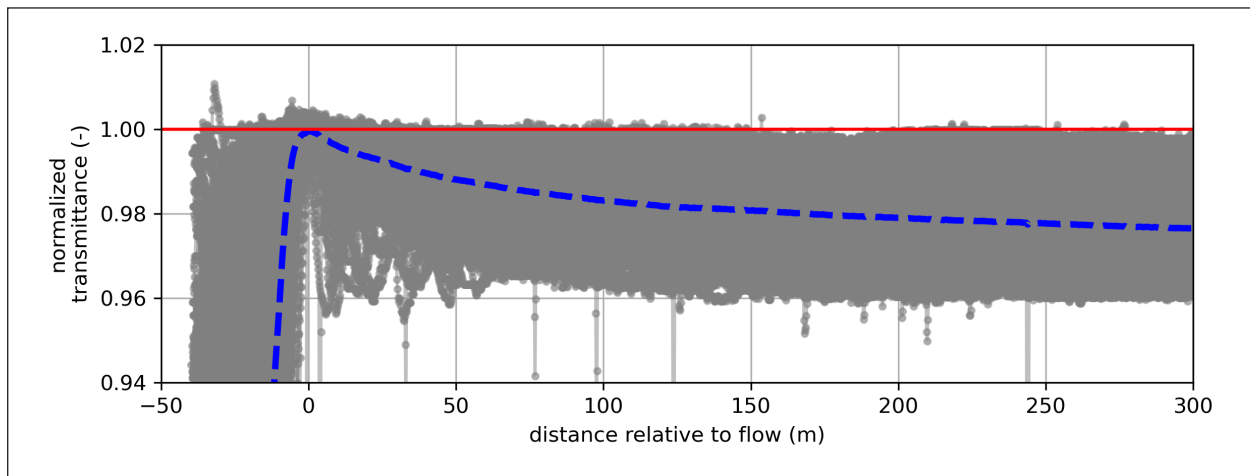


Fig. 2: Cloud shadow transition signatures of the measured transmittance, normalized and aligned to the time of the transmittance maximum, and aggregated for two case days (2023-06-13&2023-06-18). The mean signature is drawn as blue dashed line. The distance relative to the maximum is used as abscissa, and is calculated from the cloud motion estimated from the COGS product.

quality control procedures and the data format of PyrNet has been carried out and is nearing completion. This update will be used as basis for an open access publication of the S2VSR measurements. It also planned to reprocess and republish observations from prior campaigns both to benefit from the improved quality control and for consistency.

The published data will also be used as basis for several ongoing and planned science activities. Currently, further efforts are directed to the automatic identification of clear-sky periods in the global radiation time series based on the method of Reno et al. [2015]. These periods will be used to quantify the measurement uncertainty by comparing different stations, and to identify mis-aligned stations and other station anomalies. A further goal is to establish and demonstrate a method to infer the alignment of the tilted pyranometers using the difference of horizontal and tilted observations during sunshine, including an assessment of its uncertainty. As practical application,

such a method would enable the estimation of the tilt of photovoltaic modules based on their yield.

The combination of PyrNet observations and the COGS product enables a detailed characterization of the transition between sunshine and cloud shadow in global radiation time series (Fig. 2). Due to the large number of stations, such composites can be created and used to better understand this twilight zone, which is influenced by ambient aerosol conditions, cloud properties and mixing at the cloud edges, as well as strong 3D radiative effects [Calbó et al., 2017].

A comparison with satellite-derived solar irradiance has also been started to quantify the improvements by a novel 500-m resolution satellite product, and to investigate and improve upon existing parallax correction strategies. Finally, we hope that these data can also serve as basis for an in-depth investigation of 3D radiative effects and as reference for 3D radiative transfer simulations for shallow cumulus cloud cases.

References

- Calbó, J., C. N. Long, J.-A. González, J. Augustine, and A. McComiskey (2017), The thin border between cloud and aerosol: Sensitivity of several ground based observation techniques, *Atmos. Res.*, 196, 248-260, doi: <https://doi.org/10.1016/j.atmosres.2017.06.010>.
- Macke, A., P. Seifert, H. Baars, C. Barthlott, C. Beekmans, A. Behrendt, B. Bohn, M. Brueck, J. Bühl, S. Crewell, T. Damian, H. Deneke, S. Düsing, A. Foth, P. Di Girolamo, E. Hammann, R. Heinze, A. Hirvikko, J. Kalisch, N. Kalthoff, S. Kinne, M. Kohler, U. Löhnert, B. L. Madhavan, V. Maurer, S. K. Muppa, J. Schween, I. Serikov, H. Siebert, C. Simmer, F. Späth, S. Steinke, K. Träumner, S. Trömel, B. Wehner, A. Wieser, V. Wulfmeyer, and X. Xie (2017), The HD(CP)² Observational Prototype Experiment (HOPE) – an overview, *Atmos. Chem. and Phys.*, 17(7), 4887-4914, doi: <https://doi.org/10.5194/acp-17-4887-2017>.
- Madhavan, B. L., J. Kalisch, and A. Macke (2016), Shortwave surface radiation network for observing small-scale cloud inhomogeneity fields, *Atmos. Meas. Tech.*, 9(3), 1153-1166, doi: <https://doi.org/10.5194/amt-9-1153-2016>.
- Reno, M. J., and C. W. Hansen (2016), Identification of periods of clear sky irradiance in time series of GHI measurements, *Renewable Energy*, 90, 520-531, doi: <https://doi.org/10.1016/j.renene.2015.12.031>.
- Romps, D. M., and R. Öktem (2018), Observing Clouds in 4D with Multiview Stereophotogrammetry, *Bull. Am. Meteorol. Soc.*, 99(12), 2575-2586, doi: <https://doi.org/10.1175/bams-d-18-0029>.

Funding

The S2VSR campaign has been funded by TROPOS.

Cooperation

School of Meteorology, University of Oklahoma

Atmospheric Radiation Measurement (ARM) User Facility, U.S. Department of Energy

Particle deliquescence in a turbulent humidity field

Dennis Niedermeier, Rasmus Hoffmann, Silvio Schmalfuß, Wiebke Frey*, Fabian Senf, Olaf Hellmuth, Mira Pöhlker, and Frank Stratmann
 Leibniz Institute for Tropospheric Research, Leipzig, Germany
 *now at: Wageningen University & Research, Wageningen, Netherlands

Die turbulente Atmosphäre ist mit Aerosolpartikeln gefüllt, von denen ein Teil hygrokopischer Natur ist. Diese Partikel allein haben bereits direkte und indirekte Auswirkungen auf das Wetter und Klima. Darüber hinaus ist Turbulenz allgegenwärtig, die u.a. zu starken Schwankungen der Temperatur, des Wasserdampfgehalts und damit der relativen Feuchte führt. Diese Schwankungen wiederum beeinflussen möglicherweise den Phasenübergang hygrokopischer Partikel von einem festen Partikel zu einem Lösungströpfchen, bekannt als Partikeldeliquescenz. Dieser Prozess tritt bei einer bestimmten relativen Feuchte auf, der sogenannten Deliqueszenzfeuchte, welche wiederum von der Partikelsubstanz abhängt. In dieser Studie wurde der Einfluss von turbulenten Feuchteschwankungen auf das Deliqueszenzverhalten von Natriumchloridpartikeln und insbesondere auf die Anzahl der deliqueszierten Partikel untersucht. Dafür wurde der turbulente Feuchtluft-Windkanal LACIS-T (Turbulent Leipzig Aerosol Cloud Interaction Simulator) verwendet. Wir fanden heraus, dass die Turbulenz die Anzahl der deliqueszierten Partikel beeinflusst und dass diese Anzahl von einer Kombination aus mittlerer relativer Feuchte, Stärke der Feuchteschwankungen sowie Verweilzeit der Partikel im turbulenten Feuchtfeld abhängt. Eine Schlussfolgerung dieser Studie ist, dass die mittlere relative Feuchte allein nicht ausreicht, um den Phasenzustand einer deliqueszierenden Partikelspezies in der Atmosphäre bestimmen zu können. Sowohl die Feuchteschwankungen als auch die Geschichte der Partikel müssen ebenfalls berücksichtigt werden.

Introduction

The atmospheric aerosol contains hygroscopic particles of different sizes and in different phase states. The size of a particle has a strong effect on its ability to act as a cloud condensation nucleus (CCN) and on its likelihood to function as a Giant CCN. The phase state of particles affects their radiative properties, as wet particles have different angular scattering properties and refractive indices than the corresponding dry particles [Titos *et al.*, 2016]. The presence of water also allows for multiphase chemical reactions, such as solution-phase reactions with atmospheric pollutants [Bahadur and Russell, 2008].

One process of interest in this sense is particle deliquescence, which is the phase transition from a soluble solid particle to a solution droplet. It occurs at a specific relative humidity (RH), called the deliquescence RH (DRH). DRH is specific for each particle substance and depends on e.g., temperature.

However, the recrystallization or particle efflorescence does not occur at the DRH but at a lower RH, called efflorescence RH (ERH). The curve describing the deliquescent aerosol state is a hysteresis loop. Deliquescence itself is a well-studied process, both theoretically and experimentally [e.g., Shchekin *et al.*, 2013, Peng *et al.*, 2022]. Most of experimental investigations have focused on the process itself using various techniques [Tang *et al.*, 2019], with few experiments being performed under laminar flow conditions [e.g., Wex *et al.*, 2007]. However, the atmosphere is turbulent. Turbulent mixing, for example, leads to strong fluctuations in temperature, water vapour, and consequently RH [Bodenschatz *et al.*, 2010], which could affect the phase state of deliquescent particles. The behaviour of deliquescence in turbulent humidity fields, however, has not been investigated so far. The question is whether and how turbulent RH fluctuations affect the number of deliquesced particles in such a turbulent field and whether or not a time dependence

of the number of deliquesced particles is present due to the hysteresis effect.

With the turbulent moist-air wind tunnel LACIS-T (Turbulent Leipzig Aerosol Cloud Interaction Simulator, Niedermeier et al. [2020]), we want to address these fundamental questions. To do so, we adjust precisely controlled turbulent water vapour fields, so as to achieve conditions that allow for a detailed investigation of particle deliquescence–turbulence interaction. We use sodium chloride, as its DRH has a weak temperature dependence. The DRH is about 75.5% at 15°C [Seinfeld and Pandis, 2006], the temperature used for our investigations.

Experimental setup

The left part of Figure 1 shows the layout of LACIS-T. The tunnel is designed as a closed loop, in which the air circulates continuously. A total flow rate of 9.000 l/min is used in this study. The actual measurement section of LACIS-T is 2 m long, 80 cm wide and 20 cm deep. Two particle-free airflows, conditioned to the same temperature (by means of heat exchangers) but with different RH values, are turbulently mixed inside the measurement section. The turbulence hereby is generated by two passive planar grids in the air streams (4.500 l/min each). The amount of water vapour and consequently the RH in each air stream is set by means of a humidification system. For the different experiments, specific mean RH values are established in the mixing zone with different RH fluctuation strengths. Size-selected, monodisperse NaCl particles with a mobility diameter of 400 nm and a number concentration of

approx. 1.500 #/cm³ are introduced at a flow rate of 1.5 l/min into the mixing zone of the measurement section.

In the measurement section, the characterization of the respective fluid and thermodynamic states, as well as the microphysical properties is carried out. For the investigations presented here, we placed a welas 2300 optical system (from Palas GmbH) inside the measurement section to obtain the particle size distributions as shown on the right-hand side of Fig. 1. The position of the welas 2300 sensor was variable to study the effect of residence time on the number of deliquesced particles.

Results

Figure 1b shows the obtained size distributions for three different experiments. In all cases, the inlet of welas 2300 was placed 30 cm below the aerosol inlet of LACIS-T. In the first set, the mean RH was $RH_{mean} = 72.5\%$ and the strength of the RH fluctuations in terms of a standard deviation is $\sigma_{RH} = 6\%$. Solid NaCl particles were fed into the measurement section and a bimodal size distribution is obtained (solid brown curve). The left mode reflects solid, non-deliqesced NaCl particles while the right mode originates from deliquesced particles as is proven through the other two experiments looking on the size distribution of solid NaCl particles (red curve) and fully deliquesced NaCl particles (green curve) independently. By fitting both modes (dashed black curve), we could determine both the solid and the deliquesced particles fractions. This kind of experiment had been performed for various combinations

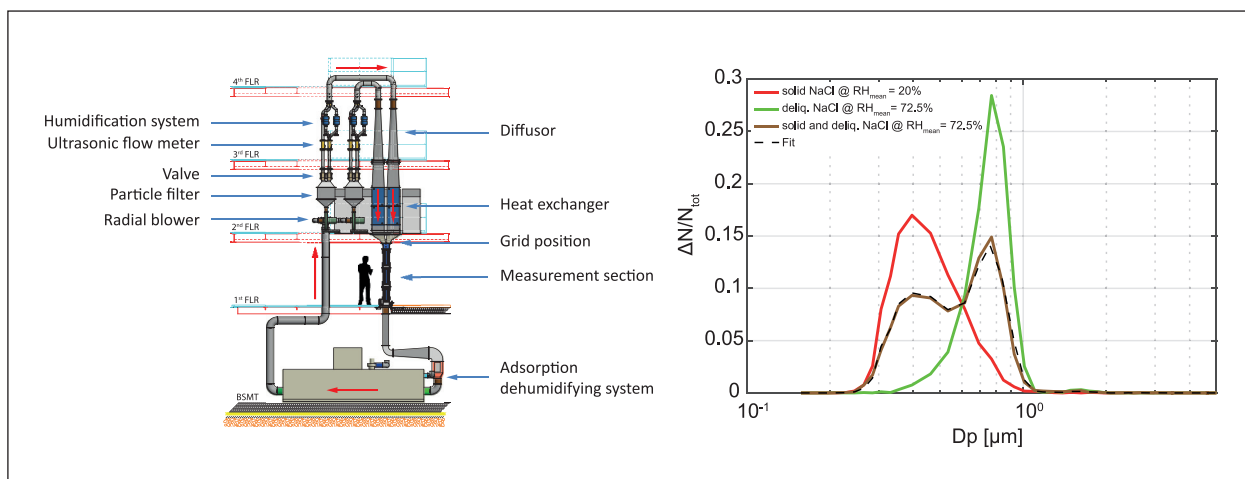


Fig 1: Left part: Schematic of LACIS-T. The red arrows indicate the flow direction; Right part: Normalized particle size distributions for three different conditions: (1) solid NaCl particles @ $RH_{mean} = 20\%$, $\sigma_{RH} = 0\%$ (red curve), (2) deliquesced NaCl particles @ $RH_{mean} = 72.5\%$, $\sigma_{RH} = 6\%$ (green curve, note that the particles were already deliquesced before entering LACIS-T), (3) solid and deliquesced NaCl particles @ $RH_{mean} = 72.5\%$, $\sigma_{RH} = 6\%$ (brown curve, solid particles were fed into LACIS-T). The dashed black line represents a bimodal fit to determine the solid and deliquesced particle fractions.

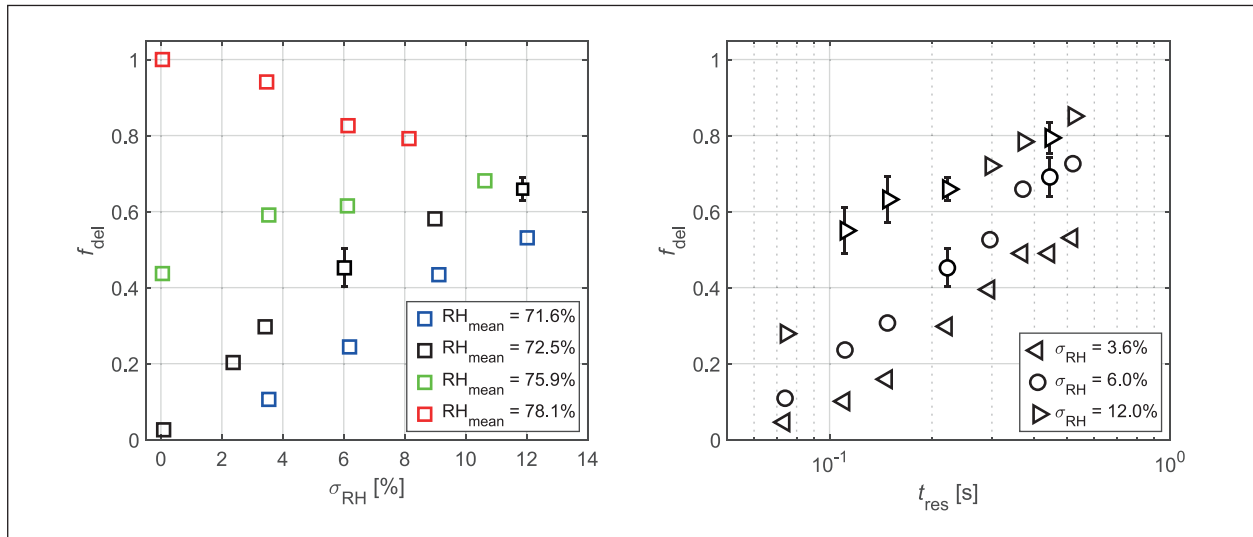


Fig 2: Left part: Deliquesced particle fraction f_{del} as a function of the standard deviation σ_{RH} of the RH fluctuations. RH_{mean} was varied, the position of welas 2300, and with that the residence time was fixed. Right part: Deliquesced particle fraction f_{del} as a function of particle residence time t_{res} . RH_{mean} was set to 72.5% and standard deviation σ_{RH} was varied.

of RH_{mean} and σ_{RH} as well as for different positions of welas 2300, i.e., different particle residence times.

The obtained deliquesced particle fractions f_{del} are presented in Fig. 2. In the first set of experiments (left part of the figure), the position of the welas 2300 sensor was again fixed to 30 cm below the aerosol inlet leading to a fixed residence time of the particles of approx. 0.22 s. For four different RH_{mean} values, the strength of the turbulent RH fluctuations was varied. It can be observed that humidity fluctuations influence the fraction of deliquesced particles, for example, leading to particle deliquescence although $RH_{\text{mean}} < DRH$. We detect an increase of the deliquesced particle fraction with increasing σ_{RH} as long as $RH_{\text{mean}} < DRH$. In this case, an increasing σ_{RH} increases the probability that solid NaCl particles are in a RH field with RH-values higher than DRH. The slope of f_{del} flattens for RH_{mean} getting close to DRH and becomes negative for $RH_{\text{mean}} > DRH$ as now the increasing σ_{RH} increases the probability that solid NaCl particles are in a RH field with RH-values lower than DRH and therefore do not deliquesce.

In the second set of experiments (shown in the right part of Fig. 2), the position of the welas 2300 sensor was varied leading to different residence times t_{res} of the particles in the measurement section. RH_{mean} was set to 72.5% and the strength of the turbulent RH fluctuations was varied. As can be seen, the fraction of deliquesced particles increases with increasing t_{res} for all three cases investigated, in other words, a clear time dependence of the deliquesced particle fraction is visible. The reason for this observation is that particles, once deliquesced, would not become solid again (i.e., effloresce) at DRH but at the ERH which is at

about ERH = 45% for 400 nm NaCl particles [Gao et al., 2007]. In our experiments, we did not reach this ERH.

Summary and Implication

We investigated the deliquescence behaviour of size-selected, monodisperse NaCl particles in a turbulent humidity field with LACIS-T. The mean RH, the strength of RH fluctuations and the residence time of the particles in the turbulent humidity field were varied. In general, we found that turbulence affects the number of deliquesced particles in a particle population and that this number depends on the combination of all three of these varied variables mentioned above. In particular, RH fluctuations can lead to particle deliquescence even though the mean RH is lower than the deliquescence RH. Furthermore, a solid NaCl particle population introduced into a fluctuating RH field, where the RH is always greater than the efflorescence RH, will deliquesce completely. The time scale to reach this fully deliquesced state depends on the mean RH (not shown here) and the strength of the fluctuations.

One implication of this study is that the mean RH alone is not sufficient to determine the phase state and size of a deliquescent particle species. RH variations must be taken into account, and with them the history of the deliquescent particles. This is particularly important as the optical properties of solid and deliquesced particles differ, which needs to be carefully considered, for example, in radiative transfer schemes in global atmospheric models [Haarig et al., 2017].

References

- Bodenschatz, E., S. P. Malinowski, R. A. Shaw, and F. Stratmann (2010), Can we understand clouds without turbulence?, *Science*, 327, 970–971, doi: <https://doi.org/10.1126/science.1185138>.
- Gao, Y., S. B. Chen, E. Y. Liya (2007), Efflorescence relative humidity of airborne sodium chloride particles: A theoretical investigation, *Atmos. Environ.*, 41(9), 2019–2023, doi: <https://doi.org/10.1016/j.atmosenv.2006.12.014>.
- Haarig, M., A. Ansmann, J. Gasteiger, K. Kandler, D. Althausen, H. Baars, M. Radenz, and D. A. Farrell (2017), Dry versus wet marine particle optical properties: RH dependence of depolarization ratio, backscatter, and extinction from multiwavelength lidar measurements during SALTRACE, *Atmos. Chem. Phys.*, 17, 14199–14217, doi: <https://doi.org/10.5194/acp-17-14199-2017>.
- Niedermeier, D., J. Voigtlander, S. Schmalfuß, D. Busch, J. Schumacher, R. A. Shaw, and F. Stratmann (2020), Characterization and first results from LACIS-T: A moist-air wind tunnel to study aerosol–cloud-turbulence interactions, *Atmos. Meas. Tech.*, 3, 2015–2033, doi: <https://doi.org/10.5194/amt-13-2015-2020>.
- Peng, C., L. Chen and M. Tang (2022), A database for deliquescence and efflorescence relative humidities of compounds with atmospheric relevance, *Fundam. Res.*, 2(4), 578–587, doi: <https://doi.org/10.1016/j.fmre.2021.11.021>.
- Seinfeld, J. H., and S. N. Pandis (2006), *Atmospheric Chemistry and Physics: From Air Pollution to Climate Change*, John Wiley & Sons: New York, 453f.
- Shchekin A. K., I. V. Shabaev, and O. Hellmuth (2013), Thermodynamic and kinetic theory of nucleation, deliquescence and efflorescence transitions in the ensemble of droplets on soluble particles, *J. Chem. Phys.*, 138, 054704, doi: <https://doi.org/10.1063/1.4789309>.
- Tang, M., C. K. Chan, Y. J. Li, H. Su, Q. Ma, Z. Wu, G. Zhang, Z. Wang, M. Ge, M. Hu, H. He, and X. Wang (2019), A review of experimental techniques for aerosol hygroscopicity studies, *Atmos. Chem. Phys.*, 19, 12631–12686, doi: <https://doi.org/10.5194/acp-19-12631-2019>.
- Titos, G., A. Cazorla, P. Zieger, E. Andrews, H. Lyamani, M. J. Granados-Muñoz, F. J. Olmo, L. Alados-Arboledas (2016), Effect of hygroscopic growth on the aerosol light-scattering coefficient: A review of measurements, techniques and error sources, *Atmos. Environ.*, 141, 494–507, doi: <http://dx.doi.org/10.1016/j.atmosenv.2016.07.021>.
- Wex, H., M. Ziese, A. Kiselev, S. Henning, and F. Stratmann (2007), Deliquescence and hygroscopic growth of succinic acid particles measured with LACIS, *Geophys. Res. Lett.*, 34, L17810, doi: <https://doi.org/10.1029/2007GL030185>.

Funding

ACTRIS-D is funded by the German Federal Ministry for Education and Research (BMBF) under grant agreements 01LK2001A-K & 01LK2002A-G.

BASS project: field campaigns

Olenka Jibaja Valderrama, Thomas Schaefer, Manuela van Pinxteren, Hartmut Herrmann

Die Vereinten Nationen haben die Jahre 2021 bis 2030 zum Jahrzehnt der Meeresforschung für nachhaltige Entwicklung erklärt. Ziel dieser Initiative ist es, das wissenschaftliche Verständnis unserer Ozeane zu verbessern und engere Verbindungen zwischen der Menschheit und den Ozeanen herzustellen. Es steht im Einklang mit dem SDG 14 der UN-Agenda 2030 für nachhaltige Entwicklung, das sich der Erhaltung und nachhaltigen Nutzung von Ozeanen, Meeren und Meeresressourcen widmet. In diesem Zusammenhang leistet TROPOS derzeit im Rahmen des BASS-Projekts einen Beitrag zur interdisziplinären Untersuchung des marinen Oberflächenfilms (Sea-Surface Microlayer: SML), einem entscheidenden Bestandteil der ozeanischen Dynamik und der Kopplung der Ozeane mit der Atmosphäre. Dieser Artikel stellt eine Einführung in das Gesamtprojekt und die Beteiligung von TROPOS an den Feldkampagnen vor.

Introduction

The SML is the boundary interface between the atmosphere and the ocean. It is a phenomenon of global relevance, as it covers 70% of the Earth's surface [Wurl *et al.*, 2011; Engel *et al.*, 2017]. The SML has different physical, chemical and biological properties compared to the sub-surface water, with an enrichment of organic matter that includes UV absorbing humic substances, fatty acids and many others [Ciuraru *et al.*, 2015]. Being rich in organic material and because of its exposure to strong UV radiation, the SML is expected to be photochemically active. Understanding such photochemical processes will strongly improve our ability to describe atmospheric chemistry in the marine environment because the SML will influence many ocean-atmosphere exchanges in both directions. SML chemistry is complex and the quantitative description of its chemical conversions is still in its infancy.

TROPOS ACD is actively involved in the interdisciplinary study of this research topic by taking part in the DFG research group BASS (Biogeochemical processes and Air-sea exchange in the Sea-Surface microlayer), which seeks to make conclusive statements regarding the role of the SML in climate-relevant processes, and to increase awareness of the importance of the SML in climate science.

BASS project

The BASS project aims to use an interdisciplinary approach to establish conclusive statements regarding the impact of the SML on climate-related processes globally. In comparison to the underlying bulk water, the SML exhibits higher concentrations of reactants. Furthermore, the SML is exposed to direct and strong UV solar radiation and is affected by oxidizing species from the atmosphere, such as the hydroxyl radical and ozone. Nevertheless, the extent to which SML-specific reactions contribute to overall organic matter transformation or the emission of volatile organic compounds into the atmosphere remains insufficiently understood, so does their integration into air-sea interaction models.

Field campaigns: Helgoland Island and Mesocosm study at the SURF facility

The BASS project seeks to gain a comprehensive understanding of the SML, and to quantify the processes regarding its reactivity, functional diversity, air-sea interaction, and dynamics. In order to accomplish these goals, a main field campaign in the Helgoland Island (North Sea) will be conducted in the summer of 2024, between July 9th and August 1st.

This above central joint field campaign will be complemented by mesocosm experiments that took

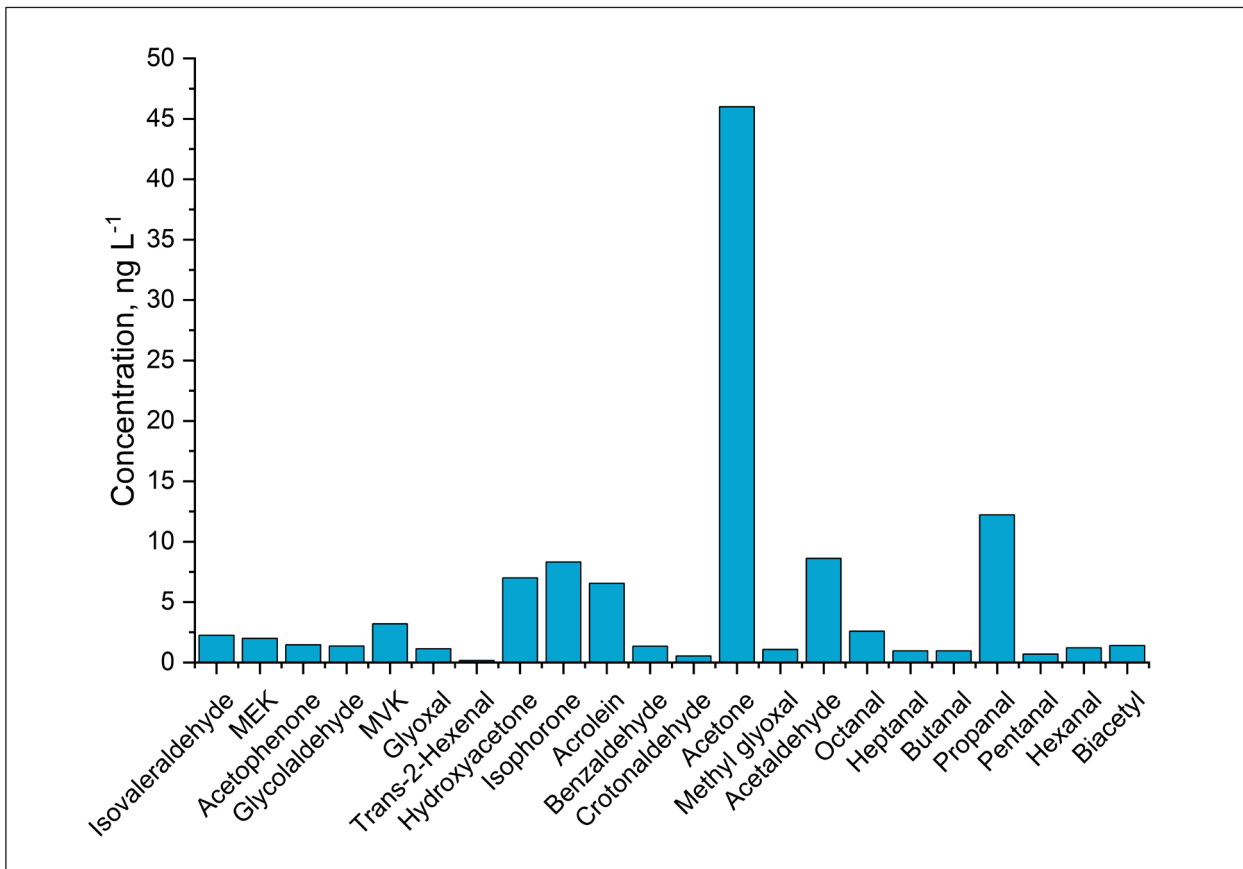


Fig 1: Concentration of carbonyl compounds present in an ambient sample collected during the mesocosm field study at the SURF facility.

place in 2023, from May 16th to June 16th, at the Sea-sURface Facility (SURF), located at ICBM in Wilhelmshaven. This facility provided controlled experimental conditions that allowed us to comprehend and measure SML processes under well-defined conditions such as wind, turbulent patterns, and biological productivity. SURF, situated in the outdoor area of the ICBM, is a one-meter-deep pool that can be filled with fresh seawater using a pumping system. For these reasons, SURF offers diverse possibilities for conducting scientific experiments concerning the sea surface.

Contribution of TROPOS in the field campaigns

The participation of TROPOS in the BASS project lies within SP1.4 – “Chemical and photochemical transformation of organic matter”. During the BASS field campaigns, the primary goal is to investigate the molecular details of abiotic SML-specific photochemical reactions, heterogeneous oxidation, and radical-driven reactions in ambient samples from the North Sea. In this context, carbonyl compounds are of special interest as they are products of photochemical reactions in the surface of

the ocean [Zhou and Mopper, 1997] and consequently, they may be involved in abiotic reactions and air-sea exchange. Fig. 1 shows the concentration of carbonyl compounds of an ambient bulk water sample collected during our field campaign at SURF. The analytical method developed and optimized at TROPOS was capable of identifying and quantifying a high variety of aldehydes and ketones. Future experiments will consist in the irradiation of bulk water and SML samples collected during the joint field campaigns with a light source mimicking the actinic radiation, and the investigation of the gas and bulk phase products making use of the established analytical technique for carbonyl compound speciation.

Our final goal is to provide a quantitative description of the formation of interfacial products and to better understand the differences in chemical conversion turnover and selectivity between the underlying bulk water and SML. To achieve this, we will combine advanced techniques such as photochemistry, laser-based kinetics, spectroscopy, and analytical methods. By integrating these approaches, we aim to increase our understanding of these processes at the molecular level within the complex marine SML reaction environment.

References

- Wurl, O., Wurl, E., Miller, L., Johnson, K. and Vagle, S. (2011). Formation and global distribution of sea-surface microlayers. *Biogeosciences*, 8(1), 121–135, doi: <https://doi.org/10.5194/bg-8-121-2011>, 2011.
- Engel, A., Bange, H., Cunliffe, M., Burrows, S., Friedrichs, G., Galgani, L., Herrmann, H., Hertkorn, N., Johnson, M., Liss, P., Quinn, P., Schartau, M., Soloviev, A., Stolle, C., Upstill-Goddard, R., van Pinxteren, M., and Zäncker, B.: The Ocean's Vital Skin: Toward an Integrated Understanding of the Sea Surface Microlayer, *Front. Mar. Sci.*, 4, doi: <https://doi.org/10.3389/fmars.2017.00165>, 2017.
- Ciuraru, R., Fine, L., van Pinxteren, M., D'Anna, B., Herrmann, H., and George, C. (2015). Unravelling New Processes at Interfaces: Photochemical Isoprene Production at the Sea Surface. *Environ. Sci. Technol.*, 49, 13199–13205, doi: <https://doi.org/10.1021/acs.est.5b02388>.
- Zhou, X., and Mopper, K. (1997). Photochemical production of low-molecular-weight carbonyl compounds in seawater and surface microlayer and their air-sea exchange. *Marine Chemistry*, 56(3-4), 201–213, doi: [https://doi.org/10.1016/S0304-4203\(96\)00076-X](https://doi.org/10.1016/S0304-4203(96)00076-X).

Funding

German Research Foundation (DFG), Bonn, Germany.

Cooperation

Institute for Chemistry and Biology of the Marine Environment (ICBM)
Carl von Ossietzky University of Oldenburg
Christian-Albrechts-University Kiel (CAU)
GEOMAR Helmholtz Centre for Ocean Research Kiel
Helmholtz-Centre Hereon
University of Hamburg
University of Vienna

Modeling the emission of marine organic aerosol based on a detailed biogeochemical model output

Anisbel Leon-Marcos⁽¹⁾, Brend Heinold⁽¹⁾, Manuela van Pinxteren⁽¹⁾, Moritz Zeising⁽²⁾, Sebastian Zeppenfeld⁽¹⁾

¹Leibniz-Institute for Tropospheric Research, 04318 Leipzig, Germany

²Alfred Wegener Institute, Helmholtz Center for Polar and Marine Research, Bremerhaven, Germany

Marine organisches Aerosol (MOA) trägt wesentlich zur Wolkenbildung über unberührten offenen Ozean- und Küstenregionen bei und hat daher einen wichtigen Einfluss auf das Klimasystem. Die in dieser Arbeit vorgestellte modellierte MOA-Emission folgt einem physikalisch basierten Schema, das ein detailliertes biogeochemisches Modell als Eingabedaten erfordert. Die berechnete Konzentration von MOA-Vorläufern im Meerwasser und der MOA-Massenanteil stimmen gut mit der Beobachtungen überein. In der Arktis sind der sommerliche Meereisverlust und der schnelle Eisrückgang entscheidende Faktoren, die seit 1990 den Massenanteil von MOA und ihren Vorläufersubstanzen im Meerwasser erhöht haben.

Introduction and Methodology

Air bubbles trapped in the water column in breaking waves burst at the water surface and release sea spray aerosols as a mixture of sea salt and marine organic aerosols (MOA) [Gantt and Meskhidze, 2013]. The nature of organics in marine aerosols reflects the abundance of their precursors in the topmost ocean surface layer [van Pinxteren et al., 2023].

Burrows et al. [2014] introduced a novel approach to represent the organic fraction in nascent aerosols (OCEANFILMS) based on a competitive Langmuir adsorption model on the bubble film. OCEANFILMS apportions the organic material in seawater into three to five classes of macromolecule groups with differing physicochemical characteristics. The surface ocean concentration of the biomolecules is one of these variables and is estimated from FESOM-RECoM (sea-ice Finite VolumE Sea-ice Ocean Model (FESOM) and Regulated Ecosystem Model (RECoM)) model output [*Gürses et al., 2023*]. The biogeochemical model data covers about 30 years (1990-2019) and the native model mesh is interpolated to a regular grid of approximately 28 km grid length.

To represent the organics in seawater, we focus on the modeled freshly produced dissolved organic carbon exuded by phytoplankton (DOC_exc) assuming that it is mostly formed by three groups: polar lipids (PL) dissolved combined amino acids (DCAA) and acidic polysaccharides (PCHO). Whereas PCHO is an additional tracer in the FESOM-RECoM model included by *Zeising et al. [2023]* (submitted to JGR), PL is considered to be a fraction of the DOC_exc and DCAA a fraction of PCHO.

Results

The surface concentration of PL, DCAA, and PCHO was compared against seawater samples (not shown) and, was in good agreement with the observations. After the evaluation, the macromolecular quantities served as input data for OCEANFILMS. The computed aerosol organic mass fraction (OMF) for the Arctic region (Fig. 1) presents a higher contribution of MOA during the seasonal phytoplankton blooms periods (with a maximum during spring and early summer) as a consequence of high productivity in daylight conditions and sea ice summer time loss. Among the macromolecules, PL contributes the majority of the organic aerosol (not shown) in

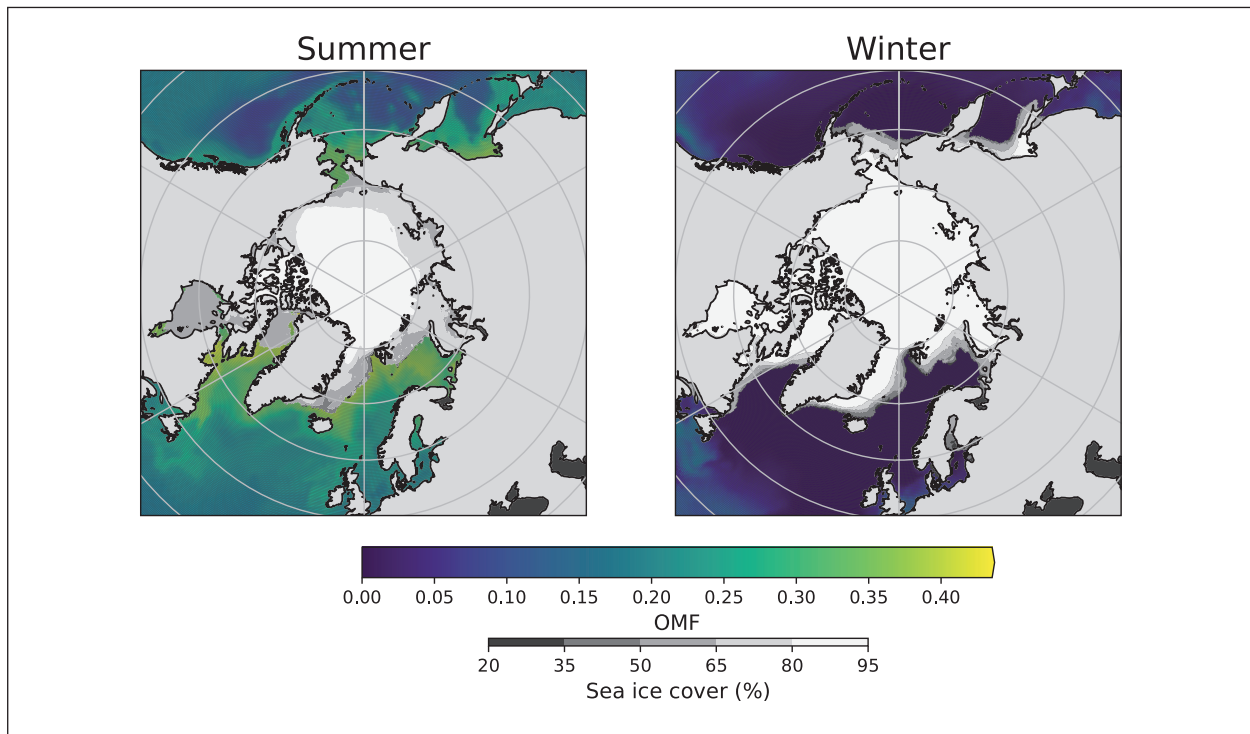


Fig. 1: Multiannual total mean of aerosol organic mass fraction from OCEANFILMS for the Arctic summer and winter.

this high-productivity region. This is due to the high surface affinity of lipids which facilitates their transfer to the atmosphere.

For a comprehensive overview of the interconnection between sea ice loss, marine productivity, and OMF over time, Fig. 2, shows the multiannual time series of sea ice, surface ocean concentration of biomolecules, and OMF for Arctic summer. Ocean surface concentration of the macromolecules and OMF peaked during a minimum of sea ice coverage

over the years. The negative trend in sea ice concentration during summer has conditioned a significant increase of marine biogenic aerosol precursors in Arctic Sea waters since 1990.

The positive trend in OMF has been enhanced in the last decade as a result of sea ice retreat. This indicates that marine local sources could predominate during summer over transported aerosol into the Arctic, potentially contributing to cloud formation.

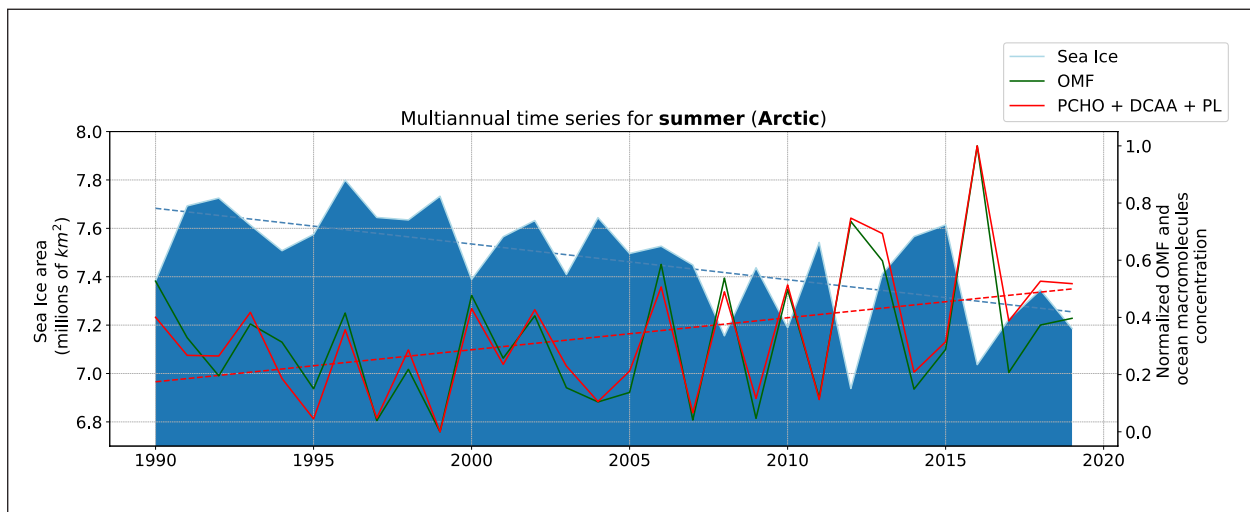


Fig. 2: Multiannual time series of sea ice area (blue), normalized OMF (green), and total surface ocean concentration of aerosol precursors over the Arctic (average over 60 to 90 degrees north) during the summer. Blue and red dashed lines show the trends of marine macromolecule concentration and sea ice area respectively.

References

- Burrows, S. M., Ogunro, O., Frossard, A. A., Russell, L. M., Rasch, P. J., and Elliott, S. M. (2014): A physically based framework for modeling the organic fractionation of sea spray aerosol from bubble film Langmuir equilibria, *Atmos. Chem. Phys.*, 14, 13601–13629, doi: <https://doi.org/10.5194/acp-14-13601-2014>.
- Gantt, B. and Meskhidze, N. (2013): The physical and chemical characteristics of marine primary organic aerosol: a review, *Atmos. Chem. Phys.*, 13, 3979–3996, doi: <https://doi.org/10.5194/acp-13-3979-2013>.
- Gürses, Ö., Oziel, L., Karaku^o, O., Sidorenko, D., Völker, C., Ye, Y., Zeising, M., Butzin, M., and Hauck, J. (2023): Ocean biogeochemistry in the coupled ocean–sea ice–biogeochemistry model FESOM2.1–REcoM3, *Geosci. Model Dev.*, 16, 4883–4936, doi: <https://doi.org/10.5194/gmd-16-4883-2023>.
- van Pinxteren, M., Zeppenfeld, S., Fomba, K. W., Triesch, N., Frka, S., and Herrmann, H. (2023): Amino acids, carbohydrates, and lipids in the tropical oligotrophic Atlantic Ocean: sea-to-air transfer and atmospheric in situ formation, *Atmos. Chem. Phys.*, 23, 6571–6590, doi: <https://doi.org/10.5194/acp-23-6571-2023>.
- Zeising, M., Oziel, L., Gürses, Ö., Hauck, J., Heinold, B., Losa, S., Thoms, S., van Pinxteren, M., Völker, C., Zeppenfeld, S., Bracher, A. (2023): Wide-spread Occurrence and Increasing Trend of Biogenic Aerosol Precursors in the Arctic Ocean Simulated by an Ocean Biogeochemical Model. ESS Open Archive, submitted to JGR: Biogeoscience, doi: <https://doi.org/10.22541/essoar.168332181.16821948/v1>.

Funding

We acknowledge the funding by the Deutsche Forschungsgemeinschaft (DFG; German Research Foundation; project number 268020496; TRR 172) within the Transregional Collaborative Research Centre “ArctiC Amplification: Climate Relevant Atmospheric and SurfaCe Processes, and Feedback Mechanisms (AC)³”.

Mineralogy in COSMO5.05-MUSCAT: implications and comparison with in-situ measurements

Sofía Gómez Maqueo Anaya¹, Kerstin Schepanski², Dietrich Althausen¹, Matthias Faust¹, Bernd Heinold¹, Ina Tegen¹

¹Leibniz Institute for Tropospheric Research (TROPOS), Leipzig, Germany

²Free University of Berlin, Berlin, Germany

Eine mineralogische Datenbank wurde zur Simulation des atmosphärischen Lebenszyklus von Mineralstaub zum Chemie- und Transportmodell COSMO5.05-MUSCAT hinzugefügt. Ein Vergleich mit Messergebnissen verdeutlicht den aktuellen Stand der mineralogischen Staubverteilung, der durch die Simulationen erzielt werden kann. Dieser weist auf Verbesserungspotenziale hin, einschließlich der Möglichkeit der Validierung durch Fernerkundungsmethoden. Durch die Simulation mineralogischer Informationen ist eine präzisere Untersuchung der Wechselwirkungen von Mineralstaub mit der Atmosphäre möglich, ebenso wie die Identifizierung möglicher Staubquellregionen.

Introduction

The majority of atmospheric models consider mineral dust as homogeneous regarding their composition, disregarding regional variations in mineralogy [Formenti *et al.*, 2011, 2014]. Differences in mineralogy alter the interaction between dust and other aerosols, and the atmospheric radiation budget since distinct minerals interact with different parts of the radiation spectrum [DiBiagio *et al.*, 2017, 2019]. In Gómez Maqueo Anaya *et al.* [2024] we describe the implementation of mineralogy to the mineral dust emission code contained in the regional chemistry and transport model COSMO-MUSCAT (COSMO: COnsortium for Small-scale Modelling; MUSCAT: MultiScale Chemistry Aerosol Transport Model). This implementation enables comparisons with mineral mass dust aerosol in-situ measurements and showcases both the ability of the model of representing mineralogy and areas of improvement.

Method

GMINER30 is a worldwide mineralogical database focusing on the fractions of eight minerals (quartz, feldspar, calcite, gypsum, illite, kaolinite, smectite and hematite) present in the silt and clay

soil size classes. Mineral fractions are exclusively reported for these sizes due to their higher likelihood of becoming aerosols [Nickovic *et al.*, 2012]. This database serves as an input for COSMO-MUSCAT's simulation of the mineral dust atmospheric life cycle, i.e., emission, transport, and deposition. The mineral fractions for each grid box of soil are directly considered in the dust aerosol description. For instance, if a grid box contains a fraction of 0.5 of quartz in its silt class size portion, the emitted mineral dust for that size class (i.e., 2 to 50 µm) will have a fraction of 0.5 of quartz content.

Simulation results are obtained from a model configuration specifically targeting the Sahara Desert region and are compared with in-situ measurements. This region is chosen due to its prominent role in mineral dust aerosol production and the availability of in-situ measurements related to dust aerosol mineralogy. Due to the scarcity of mineral-specific measurements, former in-situ aerosol mineral mass measurements were chosen for the comparison based on meteorological conditions. For instances where in-situ measurements represent one or two dust events, the meteorological conditions for these specific events were investigated through both archived meteorological data and satellite retrievals. Subsequently, dust aerosol transport conditions similar to the simulation

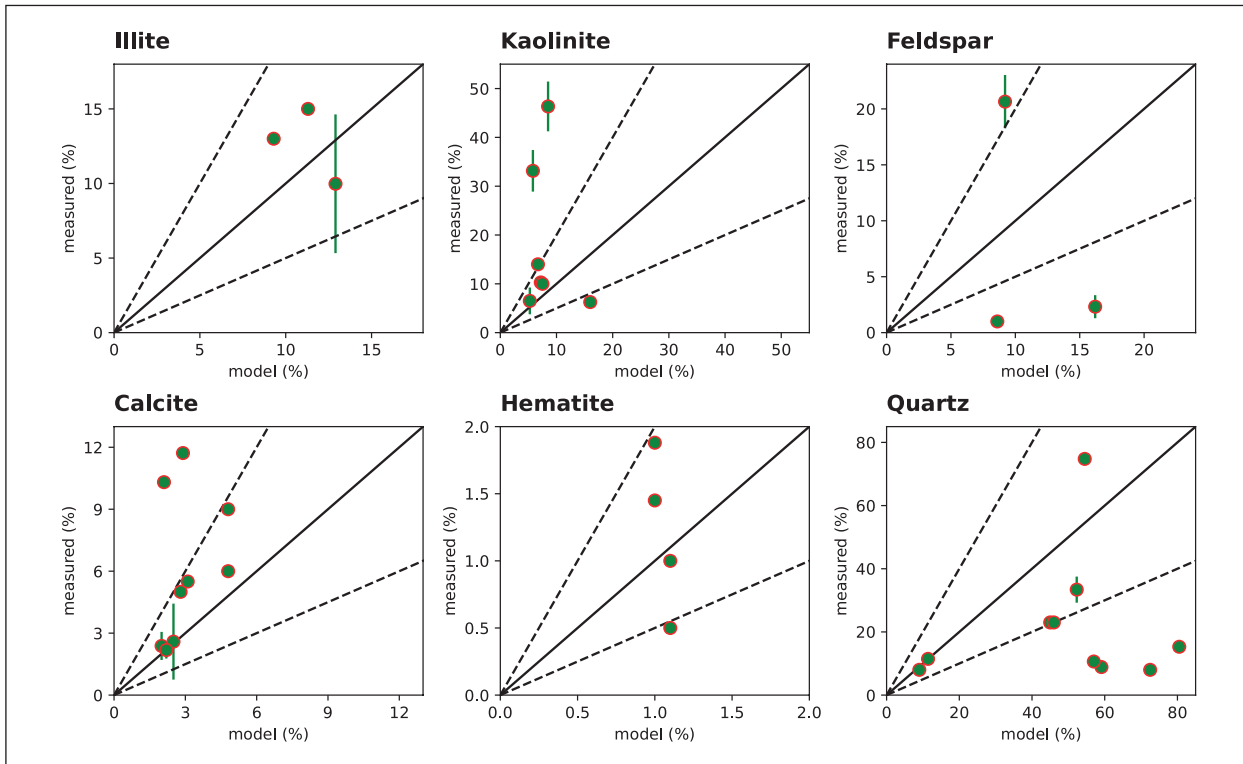


Fig. 1: Scatter plots of mineral mass fractions simulated by COSMO-MUSCAT vs measured. Dashed lines represent the ratios of 2:1 and 1:2 while the solid line represents the 1:1 comparison. The error bars are present when reported in the measurements.

period were selected for the comparison. For cases where in-situ measurements correspond to more than two dust events, the average results of the entire simulation period were used for comparison. The selected in-situ measurements can be found in Appendix A1 of Gómez Maqueo Anaya et al. [2024].

Results and implications

Figure 1 illustrates the results of the comparisons between in-situ dust aerosol mineral mass measurements and the COSMO-MUSCAT simulation. For some minerals, the comparison shows an overall good agreement with values being mostly inside the range of the 2:1 and 1:2 ratios. This is the case of illite, calcite and hematite. The comparisons for other minerals showcase an overrepresentation in the model simulation. This is the case for quartz; an underrepresentation in the model simulation is evident for kaolinite. Feldspar represents a special case, although not an uncommon one, in which the in-situ measurements represent different types of the same mineral (e.g., K-feldspar or other feldspar [Formenti et al., 2008; Jeong and Achterberg, 2014]).

The results are encouraging and highlight areas of opportunity. Similar model performances were achieved in previous works [Perlitz et al., 2015a,b], specifically, the underrepresentation of 'clay-only'

minerals (as defined in GMINER30) such as kaolinite and the overrepresentation of quartz have been characteristics in the earlier studies. They suggest to consider fractions of the 'clay-only' minerals into silt sizes and to calculate the size distribution changes for each mineral due to the emission process. These modifications result into increasing kaolinite mineral mass percentages while the quartz mineral mass percentages diminish. From the current state of the model, we consider that a similar approach would result in a more accurate mineralogical representation.

The implications of obtaining mineral specific mass fractions are the following: (1) the mineralogical aerosol content found in one place can be a fingerprint that points to certain dust source regions. This information is crucial to the investigation of which other biological and non-biological constituents could be travelling alongside dust from those regions. (2) The identification of distinct mineralogy due to their distinct responses to radiation opens up the possibility of remotely sensing minerals e.g., the hematite mineral absorbs in the UV part of the spectra. If it is possible to identify differences in mineral dust composition through remote sensing techniques, this would allow for both a further model validation approach and another way for monitoring dust transport pathways.

References

- Di Biagio, C., P. Formenti, Y. Balkanski, L. Caponi, M. Cazaunau, E. Pangui, E. Journet, S. Nowak, M. O. Andreae, K. Kandler, T. Saeed, S. Piketh, D. Seibert, E. Williams, and J. F. Doussin (2019), Complex refractive indices and single-scattering albedo of global dust aerosols in the shortwave spectrum and relationship to size and iron content, *Atmos. Chem. Phys.*, 19(24), 15503–15531, doi: <https://doi.org/10.5194/acp-19-15503-2019>.
- Di Biagio, C., P. Formenti, Y. Balkanski, L. Caponi, M. Cazaunau, E. Pangui, E. Journet, S. Nowak, S. Caquineau, M. O. Andreae, K. Kandler, T. Saeed, S. Piketh, D. Seibert, E. Williams, and J. F. Doussin (2017), Global scale variability of the mineral dust long-wave refractive index: a new dataset of in situ measurements for climate modeling and remote sensing, *Atmos. Chem. Phys.*, 17(3), 1901–1929, doi: <https://doi.org/10.5194/acp-17-1901-2017>.
- Formenti, P., S. Caquineau, K. Desboeufs, A. Klaver, S. Chevaillier, E. Journet, and J. L. Rajot (2014), Mapping the physico-chemical properties of mineral dust in western Africa: mineralogical composition, *Atmos. Chem. Phys.*, 14(19), 10663–10686, doi: <https://doi.org/10.5194/acp-14-10663-2014>.
- Formenti, P., J. L. Rajot, K. Desboeufs, S. Caquineau, S. Chevaillier, S. Nava, A. Gaudichet, E. Journet, S. Triquet, S. Alfaro, M. Chiari, J. Haywood, H. Coe, and E. Highwood (2008), Regional variability of the composition of mineral dust from western Africa: Results from the AMMA SOP0/DABEX and DODO field campaigns, *Journal of Geophysical Research: Atmospheres*, 113(D23), doi: <https://doi.org/10.1029/2008JD009903>.
- Formenti, P., L. Schütz, Y. Balkanski, K. Desboeufs, M. Ebert, K. Kandler, A. Petzold, D. Scheuvens, S. Weinbruch, and D. Zhang (2011), Recent progress in understanding physical and chemical properties of African and Asian mineral dust, *Atmos. Chem. Phys.*, 11(16), doi: <https://doi.org/8231-8256, 10.5194/acp-11-8231-2011>.
- Gómez Maqueo Anaya, S., Althausen, D., Faust, M., Baars, H., Heinold, B., Hofer, J., Tegen, I., Ansmann, A., Engelmann, R., Skupin, A., Heese, B., and Schepanski, K. (2024), The implementation of dust mineralogy in COSMO5.05-MUSCAT, *Geosci. Model Dev.*, 17, 1271–1295, doi: <https://doi.org/10.5194/gmd-17-1271-2024>.
- Jeong, G. Y., and E. P. Achterberg (2014), Chemistry and mineralogy of clay minerals in Asian and Saharan dusts and the implications for iron supply to the oceans, *Atmos. Chem. Phys.*, 14(22), 12415–12428, doi: <https://doi.org/10.5194/acp-14-12415-2014>.
- Nickovic, S., A. Vukovic, M. Vujiadinovic, V. Djurdjevic, and G. Pejanovic (2012), Technical Note: High-resolution mineralogical database of dust-productive soils for atmospheric dust modeling, *Atmos. Chem. Phys.*, 12(2), 845–855, doi: <https://doi.org/10.5194/acp-12-845-2012>.
- Perlitz, J. P., C. Pérez García-Pando, and R. L. Miller (2015), Predicting the mineral composition of dust aerosols – Part 2: Model evaluation and identification of key processes with observations, *Atmos. Chem. Phys.*, 15(20), 11629–11652, doi: <https://doi.org/10.5194/acp-15-11629-2015>.
- Perlitz, J. P., C. Pérez García-Pando, and R. L. Miller (2015), Predicting the mineral composition of dust aerosols – Part 1: Representing key processes, *Atmos. Chem. Phys.*, 15(20), 11593–11627, doi: <https://doi.org/10.5194/acp-15-11593-2015>.

Fluorescence lidar at TROPOS – the new MARTHA

Benedikt Gast, Cristofer Jimenez, Moritz Haarig, Albert Ansmann, Ronny Engelmann, Holger Baars, Ulla Wandinger

Im Jahr 2022 wurde ein neuer Detektionskanal zur Messung der Fluoreszenz atmosphärischer Aerosolpartikel in das Lidarsystem MARTHA eingebaut, der die eindeutige Identifikation von Waldbrand-aerosol ermöglicht. Bisherige Beobachtungen deuten darauf hin, dass Fluoreszenzmessungen die Detektion dünner Aerosolschichten verbessern. Eine grundlegende Modernisierung des MARTHA-Systems mit neuem Laser und Spektrometer soll Langzeitbeobachtungen troposphärischen und stratosphärischen Aerosols mit einem besonderen Fokus auf Rauch ermöglichen.

Introduction

Climate change is increasing the number and intensity of wildfires [Xu *et al.*, 2020]. Large amounts of biomass-burning aerosol are released into the troposphere and can even reach the stratosphere, influencing the Earth's radiation budget and cloud cover over long periods and large areas [Ansmann *et al.*, 2022]. To fully understand and quantify aerosol effects on climate, an accurate aerosol typing is crucial. Multiwavelength polarization lidars are powerful tools to detect and classify aerosol based on intensive quantities such as the lidar ratio, depolarization ratio and Ångström exponent [Floutsi *et al.*, 2023; Groß *et al.*, 2013; Burton *et al.*, 2012]. However, important limitations remain. In particular, it is difficult to distinguish between stratospheric smoke that has been transported into the stratosphere via a slow self-lofting pathway and volcanic sulfate aerosol, or to separate tropospheric smoke from urban pollution.

In recent years, a new lidar technique has emerged. Measuring the fluorescence of atmospheric aerosol particles induced by a UV laser opens a new door in aerosol characterization with lidar by exploiting the direct link between fluorescence and biogenic compounds in aerosol particles. Initial measurement reports suggest that the fluorescence backscattering coefficient, measured either spectrally resolved [Reichardt *et al.*, 2018] or via a broadband discrete detection channel [Veselovskii *et al.*, 2020], reliably indicates the presence of fluorescing aerosol – even inside clouds – while being about four orders of magnitude lower than its elastic counterparts. With the fluorescence capacity [Reichardt *et al.*,

2018], defined as the ratio of fluorescence to elastic backscattering coefficients, a new intensive aerosol property was derived. When this property is combined with the particle depolarization ratio, the separation between smoke and volcanic sulfate or between smoke and urban pollution appears to be a straightforward task [Veselovskii *et al.*, 2022].

Method

Motivated by these results, a discrete fluorescence channel was implemented in the Multiwavelength Atmospheric Raman Lidar for Temperature, Humidity and Aerosol Profiling (MARTHA) at TROPOS in 2022. A 44 nm broadband interference filter selects a portion of the aerosol fluorescence spectrum that is induced by excitation at the UV laser wavelength of 355 nm. Similarly, as proposed by Veselovskii *et al.* (2020), the particle fluorescence backscattering coefficient (β_{Fluo}) was derived by using the ratio of the fluorescence to the nitrogen Raman signal, which introduces a small effect of the transmission uncertainties into the retrieved information, similar to the traditional Raman method [Ansmann *et al.*, 1992]. To obtain the fluorescence capacity (G_F), β_{Fluo} is divided by the elastic backscattering coefficient at 532 nm.

The observations were performed manually and were only possible during the night, as the scattering of solar radiation during the day causes too much noise in the broadband fluorescence channel. Since the implementation of the new channel in 2022, about 50 measurements have been made, providing more than 250 hours of atmospheric aerosol fluorescence observations.

Results and discussion

Observations of Canadian wildfire smoke in 2023. In the spring and summer of 2023, huge wildfires raged across Canada, with unusual intensity in the provinces of Alberta and British Columbia. The prevailing westerly winds transported large amounts of wildfire aerosol towards Europe. From mid-May to mid-July, wildfire smoke layers were regularly observed with MARTHA over Leipzig. A total of 20 measurements allowed the analysis of the fluorescence of several smoke layers. For this aerosol type, G_F ranged from $1\text{--}15 \times 10^{-4}$, with values of $2\text{--}6.5 \times 10^{-4}$ being observed most frequently, in agreement with the results of Hu et al. (2022). The particle depolarization ratio at 532 nm was rather low (below 7 %) for most (95 %) of the investigated smoke layers.

Detection of thin aerosol layers. In addition to its clear potential to improve aerosol typing, other advantages of the new fluorescence technique have already become apparent. Several observations suggest that fluorescence measurements can improve the detection of thin aerosol layers. In particular, when optically thin, at high altitudes or present above cirrus clouds, smoke layers were sometimes missed by the elastic channels, but were clearly visible in the fluorescence signal. Figure 1 shows the height-time distributions of the range-corrected lidar signal at 1064 nm and the fluorescence backscattering coefficient for the night of 21–22 September 2022. Based on the elastic backscatter signal in panel (a), the upper troposphere appears rather clean. However, an enhanced β_{Fluo}

in panel (b) clearly shows two thin layers of wildfire smoke at about 9 and 9.75 km altitude. These layers became barely noticeable in the vertical profiles of the elastic backscattering coefficients after choosing a suitable averaging period. It can therefore be assumed that they would not have been detected without the new fluorescence channel.

A similar situation was observed during the night of 29–30 May 2023. Although there is no sign of aerosol presence in the elastic channels, a smoke layer at 10.5 to 12 km height was detected in the fluorescence backscattering, as shown in Fig. 2b). These thin layers may not have a relevant radiative effect, but their possible influence on cloud formation, especially in the case of cirrus clouds, is an aspect worth investigating. Indeed, a cirrus cloud formed directly below the smoke layer. At the beginning of the measurement, part of the cirrus cloud was even embedded in this layer. This suggests that smoke particles may have triggered the formation of cirrus by acting as ice-nucleating particles. Such data will enable the study of possible smoke-cirrus interactions in the upper troposphere and lower stratosphere (UTLS) region in the future.

Outlook – the new MARTHA

To perform such investigations at high altitudes up to the stratosphere, a high-performance lidar system is required. For this reason, the MARTHA system is currently undergoing a major upgrade. A new and powerful diode-pumped laser has been installed in December 2023. With a maximum energy

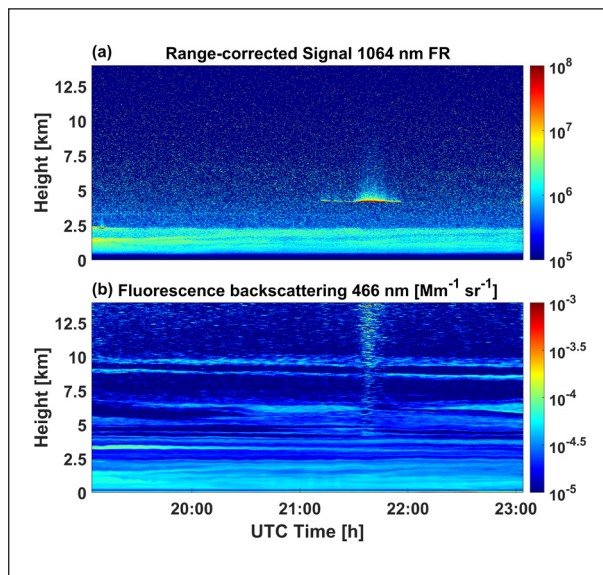


Fig. 1: Height-time distribution of (a) range-corrected lidar signal at 1064 nm and (b) fluorescence backscattering coefficient measured at Leipzig on 21 September 2022.

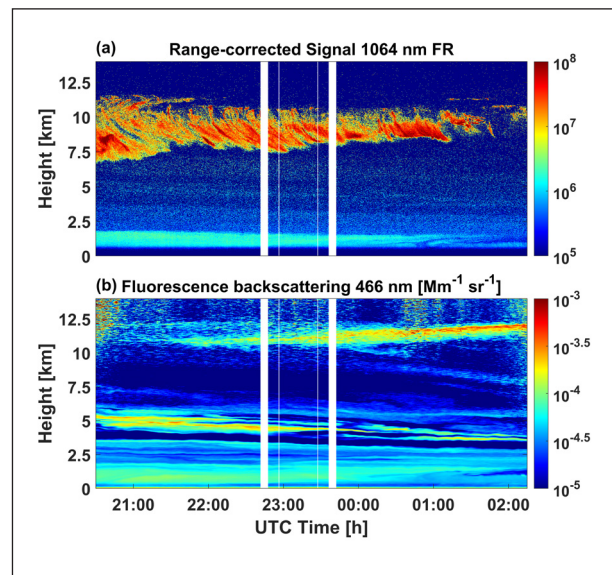


Fig. 2: Height-time distribution of (a) range-corrected lidar signal at 1064 nm and (b) fluorescence backscattering coefficient measured at Leipzig on 29 May 2023.

of about 1 J and a repetition rate of 100 Hz, the laser's power has doubled compared to its predecessor. Currently, the mounting of the near-range telescope and a new spectrometer telescope are under construction. The spectrometer will allow spectrally resolved measurements of aerosol fluorescence, which may help to better characterize aerosol mixtures and distinguish possible source regions. It is also planned to automate MARTHA to allow continuous measurements.

The laser and spectrometer were funded by the Saxon State Ministry for Science, Culture and Tourism (SMWK). In the framework of a PhD project, long-term monitoring of tropospheric and stratospheric aerosol layers with a focus on smoke occurrence is planned for the coming years. One of the objectives is to study the impact of wildfire smoke on ice nucleation in mixed-phase and ice clouds.

References

- Ansmann, A., K. Ohneiser, A. Chudnovsky, D.A. Knopf, E.W. Eloranta, D. Villanueva, P. Seifert, M. Radenz, B. Barja, F. Zamorano, C. Jimenez, R. Engelmann, H. Baars, H. Griesche, J. Hofer, D. Althausen, and U. Wandinger (2022): Ozone depletion in the Arctic and Antarctic stratosphere induced by wildfire smoke, *Atmos. Chem. Phys.*, 22(17), 11701–11726, doi: <https://doi.org/10.5194/acp-22-11701-2022>.
- Ansmann, A., U. Wandinger, M. Riebesell, C. Weitkamp, and W. Michaelis (1992): Independent measurement of extinction and backscatter profiles in cirrus clouds by using a combined Raman elastic-backscatter lidar, *Applied Optics*, 31(33), 7113-7131, doi: <https://doi.org/10.1364/AO.31.007113>.
- Burton, S. P., R. A. Ferrare, C. A. Hostetler, J. W. Hair, R. R. Rogers, M. D. Orlund, C. F. Butler, A. L. Cook, D. B. Harper, and K. D. Froyd (2012): Aerosol classification using airborne High Spectral Resolution Lidar measurements – methodology and examples, *Atmos. Meas. Tech.*, 5(1), 73-98, doi: <https://doi.org/10.5194/amt-5-73-2012>.
- Floutsi, A. A., H. Baars, R. Engelmann, D. Althausen, A. Ansmann, S. Bohlmann, B. Heese, J. Hofer, T. Kanitz, M. Haarig, K. Ohneiser, M. Radenz, P. Seifert, A. Skupin, Z. Yin, S. F. Abdullaev, M. Komppula, M. Filogiou, E. Giannakaki, I. S. Stachlewska, L. Janicka, D. Bortoli, E. Marinou, V. Amiridis, A. Gialitaki, R. E. Mamouri, B. Barja, and U. Wandinger (2023): DeLiAn – a growing collection of depolarization ratio, lidar ratio and Ångström exponent for different aerosol types and mixtures from ground-based lidar observations, *Atmos. Meas. Tech.*, 16(9), 2353-2379, doi: <https://doi.org/10.5194/amt-16-2353-2023>.
- Groß, S., M. Esselborn, B. Weinzierl, M. Wirth, A. Fix, and A. Petzold (2013): Aerosol classification by airborne high spectral resolution lidar observations, *Atmos. Chem. Phys.*, 13(5), 2487-2505, doi: <https://doi.org/10.5194/acp-13-2487-2013>.
- Hu, Q., P. Goloub, I. Veselovskii, and T. Podvin (2022): The characterization of long-range transported North American biomass burning plumes: what can a multi-wavelength Mie-Raman-polarization-fluorescence lidar provide?, *Atmos. Chem. Phys.*, 22(8), 5399-5414, doi: <https://doi.org/10.5194/acp-22-5399-2022>.
- Reichardt, J., R. Leinweber, and A. Schwebe (2018): Fluorescing aerosols and clouds: investigations of co-existence, *EPJ Web Conf.*, 176, 05010, doi: <https://doi.org/10.1051/epjconf/201817605010>.
- Veselovskii, I., Q. Hu, P. Goloub, T. Podvin, B. Barchunov, and M. Korenskii (2022): Combining Mie–Raman and fluorescence observations: a step forward in aerosol classification with lidar technology, *Atmos. Meas. Tech.*, 15(16), 4881-4900, doi: <https://doi.org/10.5194/amt-15-4881-2022>.
- Veselovskii, I., Q. Hu, P. Goloub, T. Podvin, M. Korenskii, O. Pujol, O. Dubovik, and A. Lopatin (2020): Combined use of Mie–Raman and fluorescence lidar observations for improving aerosol characterization: feasibility experiment, *Atmos. Meas. Tech.*, 13(12), 6691-6701, doi: <https://doi.org/10.5194/amt-13-6691-2020>.
- Xu, R., P. Yu, M. J. Abramson, F. H. Johnston, J. M. Samet, M. L. Bell, A. Haines, K. L. Ebi, S. Li, and Y. Guo (2020): Wildfires, Global Climate Change, and Human Health, *New England Journal of Medicine*, 383(22), 2173-2181, doi: <https://doi.org/10.1056/NEJMsr2028985>.

Funding

The Saxon State Ministry for Science, Culture and Tourism (SMWK), Dresden, Germany.

The Schmücke Cloud Observatory (SCO) and the Center for Cloud Water Chemistry (CCWaC)

Uwe Käfer, Dominik van Pinxteren, Silvia Henning, Mira Pöhler, Hartmut Herrmann

Für die langfristige und kontinuierliche Beobachtung und Erforschung von Aerosol-Wolken-Wechselwirkungen baut das TROPOS derzeit das Schmücke Cloud Observatory (SCO) im Thüringer Wald als nationale Einrichtung (NF) im Rahmen von ACTRIS auf. Das Observatorium wird aus insgesamt drei Stationen mit einem Messsturm auf dem Gipfel der Schmücke und zwei zusätzlichen Messstellen in den Tälern bei Goldlauter und Gehlberg bestehen. Zur umfassenden chemischen und physikalischen Charakterisierung der Luftmassen vor, während und nach dem Wolkendurchgang werden die drei Stationen mit modernster Instrumentierung zur Gas-, Partikel- und Wolken Analytik ausgestattet. Die konzeptionellen und vorbereitenden Arbeiten zum Bau des Observatoriums sind weitgehend abgeschlossen und der Start der ersten Baumaßnahmen wird für 2024 erwartet. In enger Verbindung zum SCO wurde das Zentrum für Wolkenwasserchemie (CCWaC) gegründet, das als zentrale ACTRIS TC Einrichtung hauptsächlich an der Etablierung und Harmonisierung von Methoden für die Beprobung von Wolkenwasser und nachfolgender chemischer Analyse arbeitet. Seit 2022 wurden in diesem Kontext erste Vergleichskampagnen für Wolkenwassersammler durchgeführt und Richtlinien erarbeitet.

Introduction

The interactions between aerosols and clouds play a key role in atmospheric chemistry and micro-physics and remain one of the largest uncertainties for our ability to understand and predict climate and air quality. Ground-based, Lagrangian-type cloud experiments in the past [*Herrmann et al., 2005; Tilgner et al., 2014*] showed great potential for detailed studies of these multiphase processes and provided important field data on e.g. aqueous phase processing, alteration of CCN activity and modification of particle size distribution. Therefore, a permanent observational site, the Schmücke Cloud Observatory (SCO) was proposed and is now being implemented as a national facility within the Aerosol, Cloud and Trace Gases Research Infrastructure (ACTRIS), for long-term, continuous, and all-season investigation of aerosol-cloud interactions.

Concept

The concept of the SCO follows decade-long developments at TROPOS ACD which included the very successful and strongly impactful combined field measurement and modelling studies FEBUKO

(2001/2) and HCCT-2010 (2010). The SCO features a setup unique for permanently operated field sites, consisting of three measurement sites often under connected air-flow conditions, distributed across a mountain ridge in the Thuringian Forest along the main wind direction path. The main site is located on the top of Mt. Schmücke (937 m asl), where ground-based clouds develop frequently (at about 200 days per year), providing ideal conditions for stationary in-cloud measurements. At the site will be a 20-meter-tall measurement tower with air-conditioned laboratory boxes to host state-of-the-art analytical instrumentation: Aerosol chemical speciation monitors (ACSMs), a proton-transfer-reaction mass spectrometer (PTR-MS), mobility particle size spectrometers (MPSSs), aethalometers, trace gas monitors, filter samplers, and more will be installed at gas-, interstitial and whole-air inlets while cloud water collectors will be mounted on the accessible rooftop for a comprehensive characterization of gas-, particle- and cloud phase.

The mountain site will be supplemented by two container-based valley stations with similar instrumentation in Goldlauter (upwind-site) and Gehlberg (downwind-site). This setup enables the characterization of air-masses before, during, and after cloud

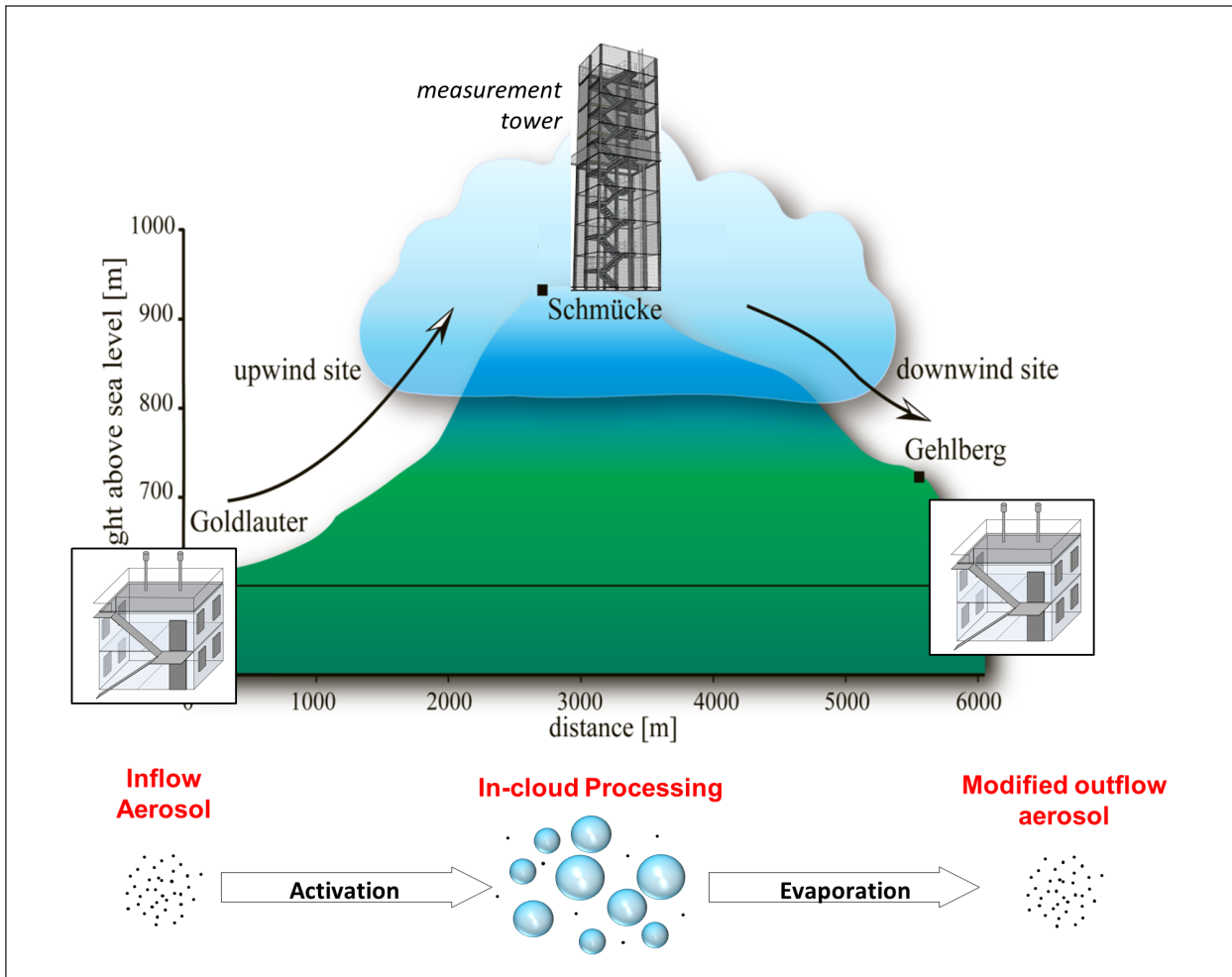


Fig. 1: Schematic representation of the concept and setup of the Schmücke Cloud Observatory (SCO) with three measurement sites.

passage to study chemical and physical differences, influenced by aerosol-cloud interactions. In addition to their role as permanent monitoring stations, all sites of the SCO are planned and dimensioned to host additional equipment and provide access for guest researchers for intensive measurement campaigns.

The infrastructure for the SCO field sites is currently being set up. Legal agreements with local authorities and station designs are in the final stages and the start of the construction works and delivery of the measurement containers is expected for summer 2024. Most of the analytical instrumentation is purchased, prepared and ready for the installation at their respective field sites. The SCO is expected to be fully operational in early 2026 and labeling is planned for cloud-in-situ and aerosol-in-situ ACTRIS components.

The Center for Cloud Water Chemistry

As an in-cloud observatory, the measurement tower of the SCO mountain station will also be an

important field site for the Center for Cloud Water Chemistry (CCWaC), a unit of the Cloud-in-situ topical center. Within the ACTRIS framework, the chemical composition of cloud water will be regularly analyzed at several observatories distributed over Europe. To ensure comparability and high data quality across the different facilities, CCWaC is currently developing guidelines and methods for the collection and offline chemical analysis of cloud water samples. In 2022 and 2023, first field campaigns were conducted for the characterization and intercomparison of commonly applied cloud water collectors in addition to laboratory experiments to test appropriate sample preparation protocols. After its full implementation in 2026, CCWaC will continue with operational support of ACTRIS national facilities for cloud water chemical composition variables and organize regular interlaboratory comparisons as well as collector intercomparisons at the SCO.

References

- Herrmann, H., R. Wolke, K. Müller, E. Brüggemann, T. Gnauk, P. Barzaghi, S. Mertes, K. Lehmann, A. Massling, W. Birmili, A. Wiedensohler, W. Wieprecht, K. Acker, W. Jaeschke, H. Kramberger, B. Svcina, K. Bächmann, J. L. Collett, D. Galgon, K. Schwirn, A. Nowak, D. van Pinxteren, A. Plewka, R. Chemnitzer, C. Rüd, D. Hofmann, A. Tilgner, K. Diehl, B. Heinold, D. Hinneburg, O. Knott, A. M. Sehili, M. Simmel, S. Wurzler, Z. Majdik, G. Mauersberger, and F. Müller (2005), FEBUKO and MODMEP: Field measurements and modelling of aerosol and cloud multiphase processes, *Atmospheric Environment*, 39(23-24), 4169-4183, doi: <https://doi.org/10.1016/j.atmosenv.2005.02.004>.
- Tilgner, A., L. Schöne, P. Bräuer, D. van Pinxteren, E. Hoffmann, G. Spindler, S. A. Styler, S. Mertes, W. Birmili, R. Otto, M. Merkel, K. Weinhold, A. Wiedensohler, H. Deneke, R. Schrödner, R. Wolke, J. Schneider, W. Haunold, A. Engel, A. Wéber, and H. Herrmann (2014), Comprehensive assessment of meteorological conditions and airflow connectivity during HCCT-2010, *Atmospheric Chemistry and Physics*, 14(17), 9105-9128, doi: <https://doi.org/10.5194/acp-14-9105-2014>.

Funding

German Federal Ministry of Education and Research (BMBF), Bonn, Germany.

Cooperation

German Weather Service (DWD)
German Environment Agency (UBA)

Algorithm development work for EarthCARE

Anja Hünerbein, Moritz Haarig, Ulla Wandinger, Sebastian Bley, Athena Augusta Floutsi

Die gemeinsame Wolken-, Aerosol- und Strahlungsmission EarthCARE der ESA und der japanischen Weltraumagentur JAXA wird 2024 gestartet. EarthCARE wird von einer einzigen Satellitenplattform aus aktive und passive Messungen ermöglichen. Diese Kombination erlaubt, die aus den aktiven Beobachtungen entlang des Tracks gewonnenen Produkte mittels aktiver/passiver Sensorsynergie in den Schwad auszudehnen, um die Wolken- und Aerosoleigenschaften zur Strahlungsschließung dreidimensional darzustellen. Das spektral hochauflösende Lidar (ATLID) und das Wolkenradar (CPR) werden vertikale Profile von Wolken- und Aerosolparametern mit hoher vertikaler Auflösung liefern. Ergänzend zu diesen aktiven Messungen liefert das abbildende Spektrometer (MSI) Messungen im Schwad auf einer Breite von 150 km und einer Pixelgröße von 500 m. Das Breitbandradiometer (BBR) misst die Strahlungsflussdichte am Oberrand der Atmosphäre [Abb. 1, Wehr et al., 2023]. TROPOS trägt zur Entwicklung der EarthCARE Level 2-Algorithmen maßgeblich bei und hat unter anderem drei wissenschaftliche Prozessoren entwickelt, um Wolkeneigenschaften aus MSI [Hünerbein et al., 2023, Hünerbein et al., 2024], Aerosol- und Wolkenschichtung aus ATLID [Wandinger et al., 2023a] sowie synergistische Wolken- und Aerosolprodukte von MSI und ATLID [Haarig et al., 2023] abzuleiten. Darüber hinaus dienen die Produkte als Input für synergistische Algorithmen, die Daten von ATLID und MSI nutzen. Ein wichtiger Punkt besteht darin, die Annahmen für Wolken- und Aerosoleigenschaften über die verschiedenen Instrumente hinweg konsistent zu halten. Zu diesem Zweck wurde ein Aerosolklassifizierungsmodell (HETEAC) als Grundlage für die Aerosoltypisierung entwickelt [Wandinger et al., 2023b]. Das Modell bietet eine konsistente End-to-End-Beschreibung der mikrophysikalischen, optischen und radiativen Eigenschaften der Aerosolpartikel.

Introduction

The joint ESA-JAXA cloud, aerosol, and radiation mission EarthCARE will be launched in 2024. EarthCARE will provide active profiling and passive imaging measurements from a single satellite platform. This combination will make it possible to extend the products obtained from the combined active/passive observations along the ground track into the swath by means of active/passive sensor synergy, to estimate the 3D fields of clouds and aerosol and to assess radiative closure. The high-spectral-resolution atmospheric lidar (ATLID) and the cloud profiling radar (CPR) provide vertical profiles of cloud and aerosol parameters with high vertical resolution. Complementing these active measurements, the passive multi-spectral imager (MSI) delivers visible

and infrared images for a swath width of 150 km and a pixel size of 500 m, and the broadband radiometer (BBR) measures the solar and thermal radiances [Fig. 1, Wehr et al., 2023]. TROPOS contributes to the development of the EarthCARE Level 2 algorithms and has developed three scientific processors to retrieve cloud properties from MSI [Hünerbein et al., 2023a, Hünerbein et al., 2024], aerosol and cloud layering from ATLID [Wandinger et al., 2023a], and synergistic cloud and aerosol products from MSI and ATLID [Haarig et al., 2023]. The MSI cloud processor combines visible to infrared MSI channels to determine cloud microphysical and macrophysical properties, which include cloud mask, cloud types, cloud phase, cloud optical thickness, cloud effective radius, and cloud top height. The ATLID layer product processor generates the upper cloud boundaries, the

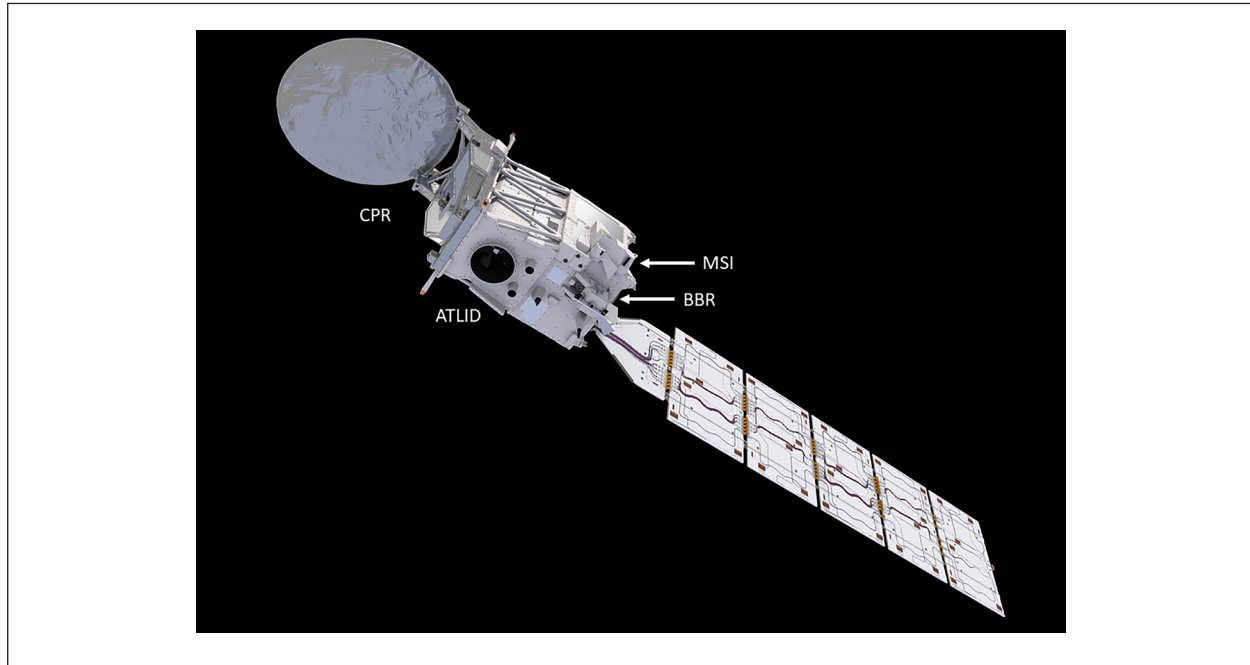


Fig. 1: Artist's impression of the EarthCARE satellite with the location of the four science instruments [ESA/ATG medialab, the Netherlands, Wehr et al. 2023].

cloud top height product, and aerosol layer descriptor products designed to continue the legacy of aerosol layer information available from the Cloud–Aerosol Lidar and Infrared Pathfinder Satellite Observations [CALIPSO, Vaughan et al., 2009]. The products are also used as input for synergistic algorithms.

An important issue is to keep the assumptions made for aerosol properties consistent across the range of different instruments. For this purpose, an aerosol classification model (HETEAC) has been developed as a basis for aerosol typing [Wandinger et al., 2023b]. The model provides a consistent end-to-end description of particle microphysical, optical, and radiative properties.

Results of the combination of active and passive remote sensing

EarthCARE offers the great opportunity to combine active and passive measurements. Figure 2 illustrates the combined view of ATLID and MSI using a synthetic EarthCARE scene with different cloud types. The vertical information from the ATLID Mie co-polar signal is shown along the track, with strong signals (white) indicating optically thick clouds; weaker signals (red to yellow) indicate optically thinner clouds or aerosol layers. The information across the track comes from the MSI brightness temperature at 10.8 μm . The high clouds in the center of the scene have low brightness temperature (blue) and the low broken clouds are visible in yellow. The

cloud top height retrieved from MSI is an infrared effective radiant height (M-CTH) located somewhere inside the cloud. The ATLID cloud top height (A-CTH) describes the physical boundaries of the clouds along the track and will be used to investigate the relationship between the effective and geometric cloud top heights. Figure 3 shows the A-CTH and M-CTH cloud top heights together with the cloud top height difference (AM-CTH) for the synthetic EarthCARE scene shown in Figure 2. The cloud top height difference is small for the scattered clouds in the south ($<32^\circ\text{N}$) and for the optically thick cirrus cloud at $36\text{--}39^\circ\text{N}$. However, the multi-layer cloud scenario in the center ($39\text{--}47^\circ\text{N}$) leads to large differences. MSI is sensitive to the optically thick liquid clouds at $5\text{--}7\text{ km}$ height, and ATLID detects the upper boundary of the thin cirrus cloud at 11 km height as cloud top height. Further north ($>50^\circ\text{N}$), nighttime conditions limit the ability of MSI to detect the cloud top height and lead to a larger scatter. Nevertheless, the agreement is mostly within 2 km , except for the high clouds north of 65°N . The differences in the cloud top height obtained with ATLID and MSI along the track are systematically investigated and classified as part of the ATLID–MSI column product processor [Haarig et al., 2023]. A scene classification scheme is developed to extrapolate the cloud top height difference to the MSI swath. This combination is an important step in the synergistic approach of EarthCARE, especially with respect to estimating the cloud top height of optically thin clouds for the entire scene [Haarig et al., 2023].

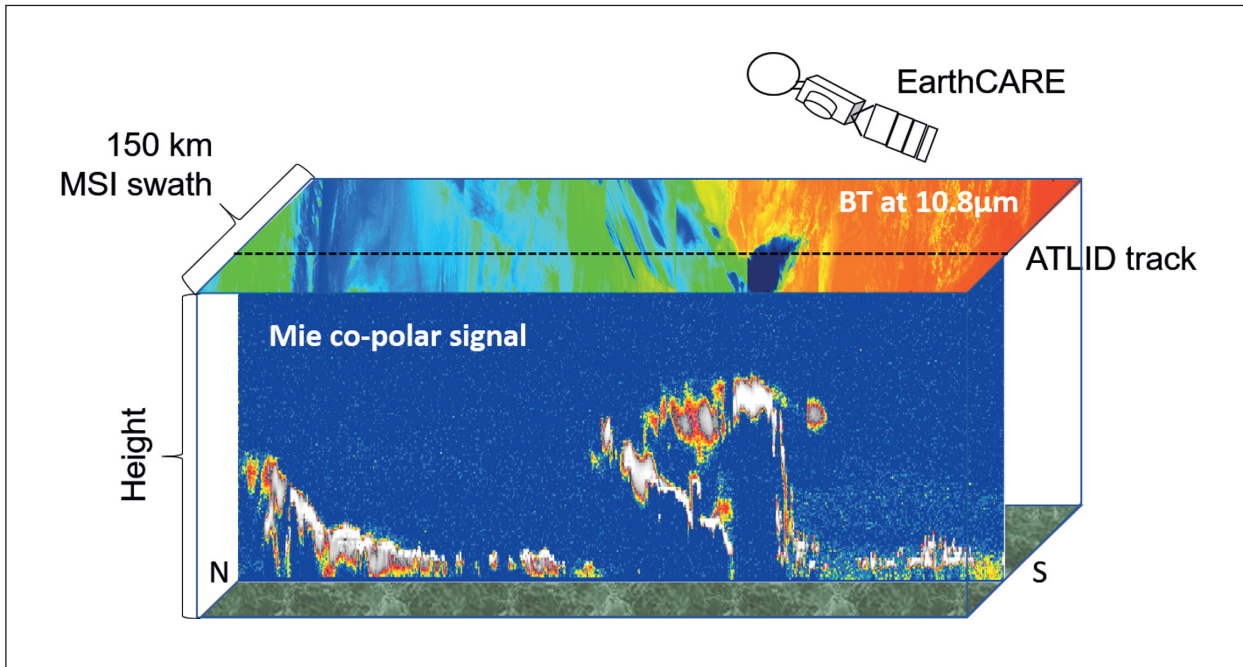


Fig. 1: Combined view of ATLID (curtain) and MSI (carpet) on the simulated so-called Halifax scene. A strong ATLID Mie co-polar signal (white) indicates optically thick clouds; weaker signals (red to yellow) indicate optically thinner clouds or aerosol layers. The high clouds in the center of the scene are detected by MSI on the basis of their low brightness temperature (BT; blue). The high brightness temperatures (red) on the MSI swath result from the surface return where the low broken clouds are visible in yellow.

Outlook

We are looking forward to the launch of EarthCARE, scheduled for May 2024. The satellite will fly in a sun-synchronous polar orbit with a descending node at 14:00 MLST (mean local solar time) at the equator. To date, algorithm verification has been based on synthetic test scenes and data from other satellite platforms. During the post-launch validation phase of EarthCARE, dedicated campaigns will be carried out using ground-based and airborne

instruments, providing the opportunity for a more comprehensive validation of the EarthCARE products. Geostationary satellites will also be used for the validation of MSI cloud products to support the selection of appropriate validation datasets and to provide complementary reference datasets on a global scale. Meteosat Third Generation (MTG) was launched into a geostationary orbit in 2022 [Holmlund et al., 2021]. Its Flexible Combined Imager (FCI) with 16 spectral channels and a spatial sampling of up to 500 m offers excellent opportunities for the validation of and syn-

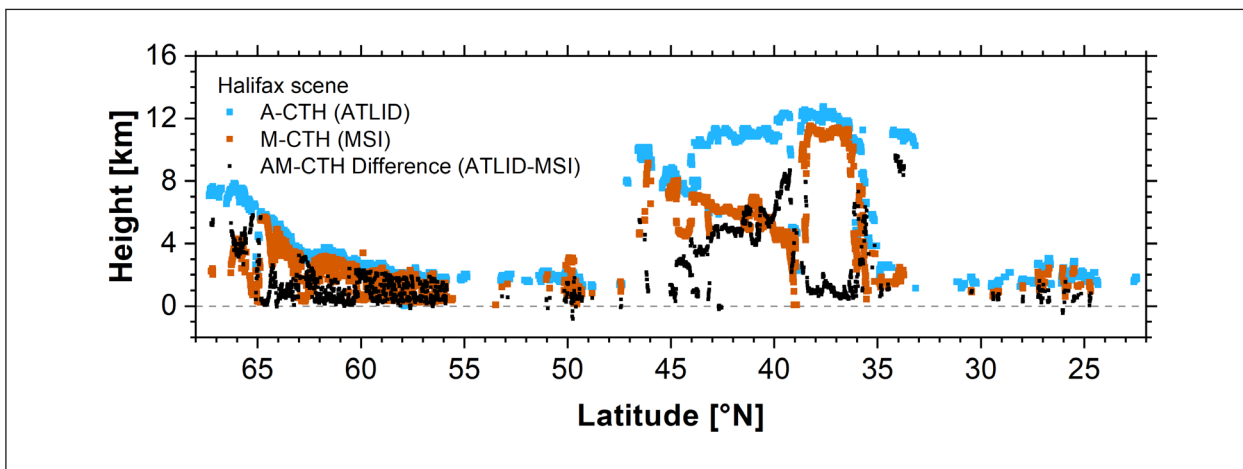


Fig. 3: Cloud top difference along the ATLID track derived from ATLID (A-CTH, blue dots) and MSI (M-CTH, orange dots). The AM-CTH algorithm calculates the difference (black dots) to transfer it to the MSI swath [Haarig et al., 2023].

ergies with the MSI products. The ground-based lidar network PollyNET [Baars et al., 2016], developed and managed by TROPOS, provides several sites from Cabo Verde to Leipzig and Dushanbe, Tajikistan, to validate the ATLID-derived aerosol and cloud products. Further ground-based devices complemented by

airborne remote sensing observations will contribute to a successful validation of the developed algorithms. Further improvements of EarthCARE products are expected when real observations become available, due to the flexible algorithm design.

References

- Baars, H., Kanitz, T., Engelmann, R., Althausen, D., Heese, B., Komppula, M., ... & Zamorano, F.: An overview of the first decade of Polly NET: an emerging network of automated Raman-polarization lidars for continuous aerosol profiling. *Atmospheric Chemistry and Physics*, 16(8), 5111–5137, 2016.
- Haarig, M., Hünerbein, A., Wandinger, U., Docter, N., Bley, S., Donovan, D., and van Zadelhoff, G.-J.: Cloud top heights and aerosol columnar properties from combined EarthCARE lidar and imager observations: the AM-CTH and AM-ACD products, *Atmos. Meas. Tech.*, 16, 5953–5975, doi: <https://doi.org/10.5194/amt-16-5953-2023>, 2023.
- Holmlund, K., Grandell, J., Schmetz, J., Stuhlmann, R., Bojkov, B., Munro, R., ... & Blythe, P.: Meteosat Third Generation (MTG): Continuation and innovation of observations from geostationary orbit. *Bulletin of the American Meteorological Society*, 1–71, 2021.
- Hünerbein, A., Bley, S., Horn, S., Deneke, H., and Walther, A.: Cloud mask algorithm from the EarthCARE Multi-Spectral Imager: the M-CM products, *Atmos. Meas. Tech.*, 16, 2821–2836, doi: <https://doi.org/10.5194/amt-16-2821-2023>, 2023a.
- Hünerbein, A., Bley, S., Deneke, H., Meirink, J. F., van Zadelhoff, G.-J., and Walther, A.: Cloud optical and physical properties retrieval from EarthCARE multi-spectral imager: the M-COP products, *Atmos. Meas. Tech.*, 17, 261–276, doi: <https://doi.org/10.5194/amt-17-261-2024>, 2024.
- Wandinger, U., Haarig, M., Baars, H., Donovan, D., and van Zadelhoff, G.-J.: Cloud top heights and aerosol layer properties from EarthCARE lidar observations: the A-CTH and A-ALD products, *Atmos. Meas. Tech.*, 16, 4031–4052, doi: <https://doi.org/10.5194/amt-16-4031-2023>, 2023a.
- Wandinger, U., Floutsi, A. A., Baars, H., Haarig, M., Ansmann, A., Hünerbein, A., Docter, N., Donovan, D., van Zadelhoff, G.-J., Mason, S., and Cole, J.: HETEAC – the Hybrid End-To-End Aerosol Classification model for EarthCARE, *Atmos. Meas. Tech.*, 16, 2485–2510, doi: <https://doi.org/10.5194/amt-16-2485-2023>, 2023b.
- Wehr, T., Kubota, T., Tzeremes, G., Wallace, K., Nakatsuka, H., Ohno, Y., Koopman, R., Rusli, S., Kikuchi, M., Eisinger, M., Tanaka, T., Taga, M., Deghaye, P., Tomita, E., and Bernaerts, D.: The EarthCARE mission – science and system overview, *Atmos. Meas. Tech.*, 16, 3581–3608, doi: <https://doi.org/10.5194/amt-16-3581-2023>, 2023.

Funding

This research has been supported by ESA under grant nos. 4000112018/14/NL/CT (APRIL) and 4000134661/21/NL/AD (CARDINAL).

Cooperation

Free University of Berlin (FUB)
 Royal Netherlands Meteorological Institute (KNMI)
 European Centre for Medium Range Weather Forecasts (ECMWF)
 Environment and Climate Change Canada (ECCC)

Aerosol properties of cloud particle residuals measured during CIRRUS-HL

Stephan Mertes, Bruno Wetzel, Sarah Grawe, Jonas Schaefer, Frank Stratmann

Im Rahmen der HALO Mission CIRRUS-HL wurden über den HALO-CVI Einlass des TROPOS die Eispartikelresiduen verschiedener Wolkentypen in der oberen Troposphäre in mittleren und hohen Breiten untersucht. Im Vorfeld der Mission konnte die Anbauposition des HALO-CVI an die für die Anströmung wesentlich günstigere Rumpfunterseite von HALO realisiert werden. Aus dem Vergleich zur gemessenen Eispartikelkonzentration und zum Eiszwassergehalt konnte nachgewiesen werden, dass Wolkenpartikel quantitativ gesammelt wurden. Die Form der Residuengrößenverteilungen zeigen trotz unterschiedlicher Entstehungsprozesse der Wolken (liquid-origin, in-situ) keine gravierenden Unterschiede und fallen ab 300 nm wesentlich flacher ab, als die Größenverteilungen der umgebenden Aerosolpartikel. Dies deutet auf den Beitrag eisnukleierender Partikel an der Zirrenbildung hin. In allen Wolkentypen konnte die Massenkonzentration von schwarzem Kohlenstoff detektiert werden, mit den höchsten Beiträgen pro Residuum in liquid-origin Zirren in mittleren und hohen Breiten. Die Auswertung der Residueneigenschaften der durchflogenen Eiswolken ist nicht abgeschlossen und wird in Zusammenarbeit mit anderen Projektpartnern mit der chemischen Zusammensetzung der Residuen zusammengebracht.

Introduction

The microphysical parameters of upper tropospheric (UT) clouds are mainly determined by the ice formation process (heterogeneous vs. homogeneous ice nucleation) and by the cloud formation pathway (in-situ vs. liquid-origin) [Krämer et al., 2016]. These classifications imply the participation of aerosol particles in the UT ice cloud formation. One approach to increase the knowledge of particles that are potentially involved in cloud formation is to measure the properties of ice particle residuals (IPR).

Therefore, a counterflow virtual impactor (HALO-CVI) was deployed aboard the research aircraft HALO during CIRRUS-HL in June/July 2021 for an IPR investigation.

Experimental setup of the HALO-CVI system

At the HALO-CVI inlet tip a controlled counter-flow is blown out, which allows only ice particles with a diameter larger than 5 µm [Mertes et al., 2005] to enter the sampling system [Ogren et al., 1985]. The

ice particles are impacted into a particle-free and dry sample flow, so that the ice water content (IWC) is completely driven into the gas phase, whereby the IPR are released for analysis. This includes the measurement of the number concentration, number size distribution (NSD), absorption coefficient, ice nucleating particle (INP) concentration, and IWC.



Fig. 1: The German research aircraft HALO with inlets and wing probes in the CIRRUS-HL configuration. The position of the HALO-CVI as the only inlet at the lower fuselage is marked by the red circle and its construction shown in the enlargement.

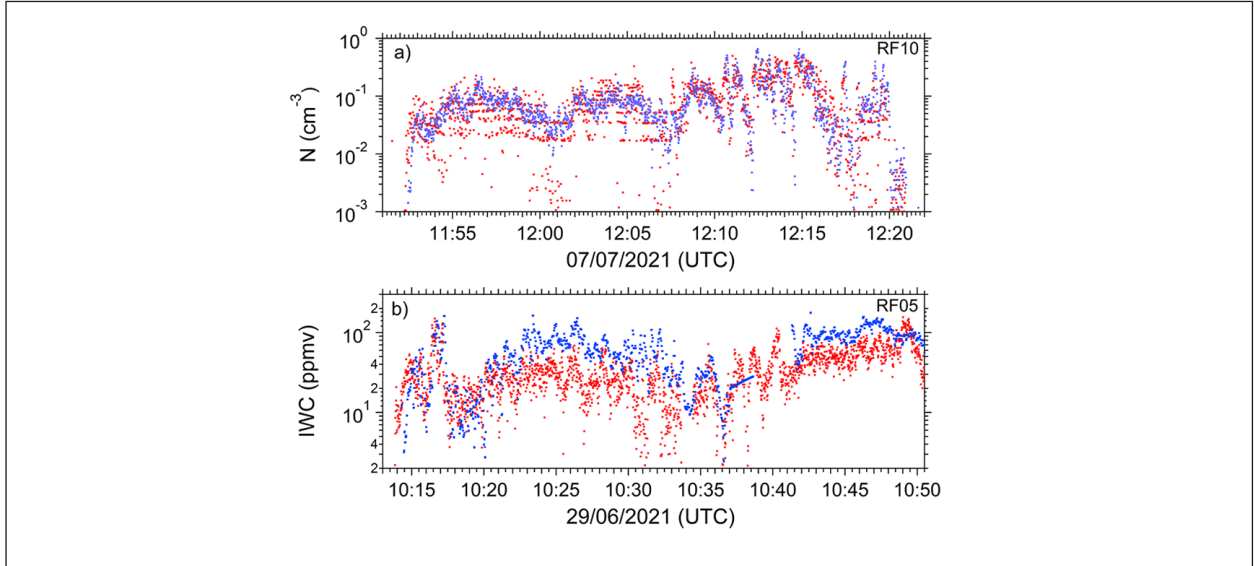


Fig. 2: Exemplary comparison of HALO-CVI (blue) measurements and the NIXE cloud probe (red). a) Ice particle (red) and IPR (blue) number concentration measured during research flight 10. b) In-situ measured (red) and sampled (blue) ice water content measured during research flight 05. NIXE data in courtesy of A. Afchine and M. Krämer (Research Centre Jülich).

Confirmation of a quantitative cloud particle sampling

Since CIRRUS-HL, the mounting position of the HALO-CVI inlet is optimized to the lower fuselage of HALO in order to sample cloud hydrometeors more quantitatively (Fig. 1). This could be confirmed by the comparison to in-situ measured ice particle concentration and IWC (Fig. 2). The good agreement with IPR concentration and sampled IWC illustrates the quantitative cloud particle sampling of the HALO-CVI.

Aerosol properties of ice particle residuals in the upper troposphere

Different cloud types have been encountered in the UT. Liquid-origin and in-situ cirrus could be studied in mid and high latitudes (ML and HL, separation at 60° N) according to *De La Torre Castro et al.* [2023], but high convective clouds, cumulonimbus (CB) outflow and contrails only in mid latitudes. Mean IPR NSDs are presented in Fig. 3a together with the mean NSD of cloud droplet residuals sampled in low

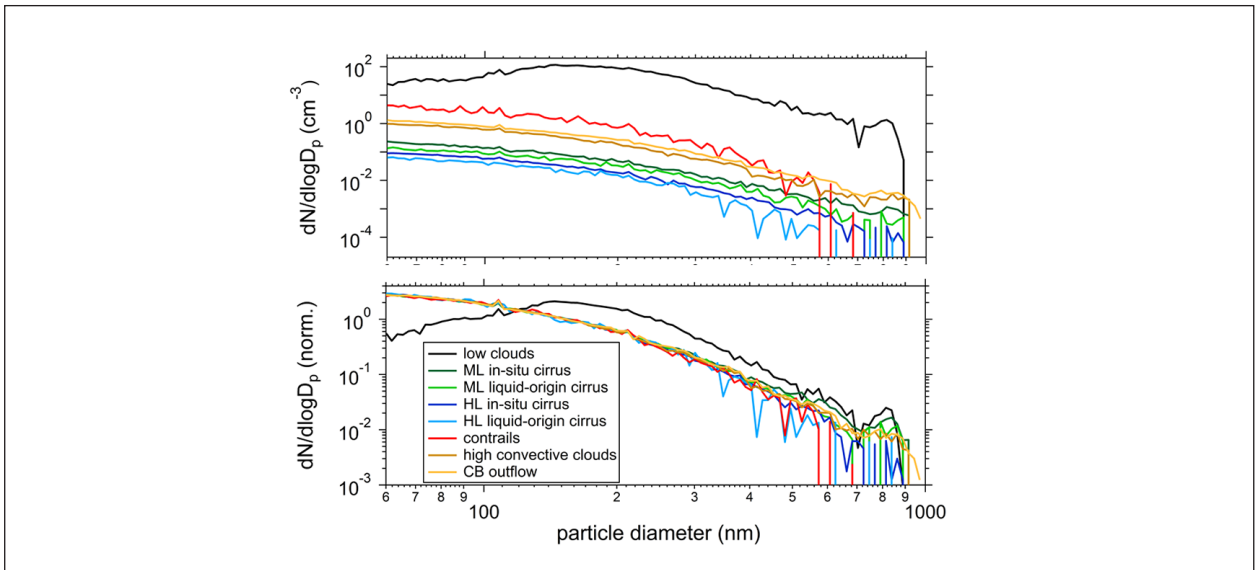


Fig. 3: a) Mean number size distributions of CDR (low clouds, black) and IPR from ML in-situ and liquid-origin cirrus (dark and light green), from HL in-situ and liquid-origin cirrus (dark and light blue), contrails (red), high convective clouds (ochre), and CB outflow (yellow). b) same as before, but the number size distributions are normalized by their respective number concentration. Contrail periods were gratefully provided by V. Hahn (DLR).

clouds as reference. The latter shows the presence of cloud condensation nuclei by the pronounced accumulation mode, while the IPR NSDs decrease only slightly from smaller to larger sizes. In general, these NSD shapes represent those of the UT aerosol particles up to 300 nm. For larger diameters the IPR NSDs fall off significantly flatter implying that INPs are involved in the UT ice cloud formation. Apart from the low level clouds, the corresponding median IPR number concentrations (Fig. 4a) indicate highest concentrations with more than 1 cm^{-3} for contrails followed by the convective clouds and CB outflow with several hundred L^{-1} . Several tens L^{-1} were observed for in-situ and liquid-origin cirrus with slightly higher numbers in mid latitudes. In-situ cirrus has higher concentrations than liquid-origin cirrus in both regions.

In order to look for differences in the shape of the NSDs they were normalized by their underlying IPR concentration (Fig. 3b). Only small differences are observed, which is reflected by the narrow range of the median mean diameter (Fig. 4b). However, systematic features are obvious. First, in-situ and liquid-origin cirrus in ML have larger mean diameters than in HL. Second, contrails possess the smallest mean diameters, with no IPR larger 600 nm seen in the NSD (Fig. 3a). Third, the IPR in the CB outflow are observed to be larger than in the convective clouds below the outflow.

Chemical information is inferred by inverting the absorption coefficient into a black carbon (BC) mass concentration using a mass absorption efficiency determined by *Mertes et al.* [2004]. Most of the BC was found in the low clouds and contrails and the fewest for HL cirrus (Fig. 4c). In order to make the BC measurements more comparable, the median BC mass was normalized by the respective median number concentration (Fig. 4d). Surprisingly, the highest BC content is seen in the liquid-origin cirrus of ML and HL and by far the lowest in the convective clouds and CB outflow. A more extensive analysis will be done for the BC particle number concentration which was measured by German Aerospace Centre. By means of the IPR chemical composition and supermicrometer NSD derived by the Max Planck Institute for Chemistry an even more comprehensive investigation will be carried out to complete this unique data set of UT IPR aerosol properties.

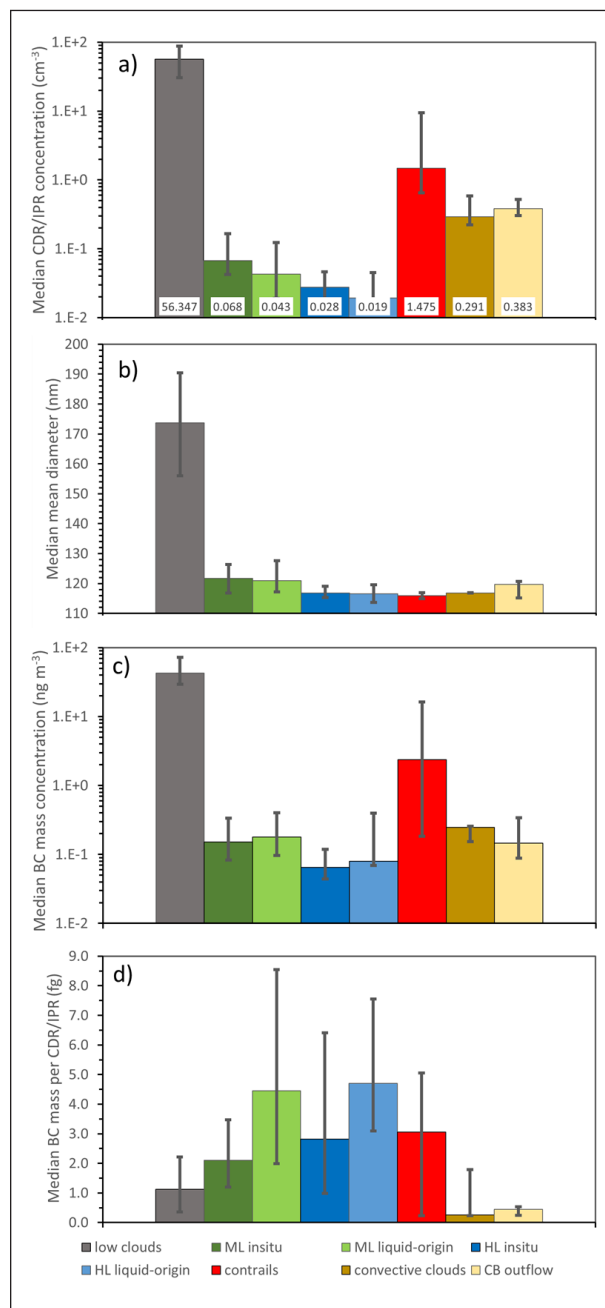


Fig. 4: Aerosol characterization of CDR (black) and IPR from ML in-situ and liquid-origin cirrus (dark and light green), from HL in-situ and liquid-origin cirrus (dark and light blue), contrails (red), high convective clouds (ochre), and CB outflow (yellow). a) median number concentration, b) median mean diameter, c) median BC mass concentration, d) median BC mass per residual particle. Error bars denote the 25th and 75th percentiles. Contrail periods were gratefully provided by V. Hahn (DLR).

References

- De La Torre Castro, E., T. Jurkat-Witschas, A. Afchine, V. Grewe, V. Hahn, S. Kirschler, M. Krämer, J. Lucke, N. Spelten, H. Wernli, M. Zöger, and C. Voigt (2023), Differences in microphysical properties of cirrus at high and mid-latitudes, *Atmos. Chem. Phys.*, 23, 13167-13189, doi: <https://doi.org/10.5194/acp-23-13167-2023>.
- Krämer, M., C. Rolf, A. Luebke, A. Afchine, N. Spelten, A. Costa, J. Meyer, M. Zöger, J. Smith, R. L. Herman, B. Buchholz, V. Ebert, D. Baumgardner, S. Borrmann, M. Klingebiel, and L. Avallone (2016), A microphysics guide to cirrus clouds – Part 1: Cirrus types, *Atmos. Chem. Phys.*, 16, 3463–3483, doi: <https://doi.org/10.5194/acp-16-3463-2016>.
- Mertes, S., B. Dippel, and A. Schwarzenböck (2004), Quantification of graphitic carbon in atmospheric aerosol particles by Raman spectroscopy and first application for the determination of mass absorption efficiencies, *J. Aerosol Sci.*, 35, 347-361, doi: <https://doi.org/10.1016/j.jaerosci.2003.10.002>.
- Mertes, S., K. Lehmann, A. Nowak, A. Massling, and A. Wiedensohler (2005), Link between aerosol hygroscopic growth and droplet activation observed for hill-capped clouds at connected flow conditions during FEBUKO, *Atmos. Environ.*, 39(23-24), 4247-4256, doi: <https://doi.org/10.1016/j.atmosenv.2005.02.010>.
- Ogren, J. A., J. Heintzenberg, and R. J. Charlson (1985), In-situ sampling of clouds with a droplet to aerosol converter, *Geophys. Res. Lett.*, 12(3), 121-124, doi: <https://doi.org/10.1029/GL012i003p00121>.

Funding

This work was supported by the German Research Foundation (DFG) – project numbers 48902976 and 442648163 within the priority program 1294 ‘Atmospheric and Earth System Research with the Research Aircraft HALO (High Altitude and Long Range Research Aircraft)’.

The technical realization and certification of the HALO-CVI inlet at the lower fuselage of HALO have been funded by the Max Planck Society.

Cooperation

Max Planck Institute for Chemistry Mainz (MPI-C)
Research Centre Jülich (FZJ)
German Aerospace Centre Oberpfaffenhofen (DLR-IPA)

DeLiAn – a new aerosol climatology based on PollyXT lidars

Athena A. Floutsi, Henriette Gebauer, Holger Baars, Ronny Engelmann, Moritz Haarig, Annett Skupin, Ulla Wandinger

Zum Zweck der Aerosolcharakterisierung ist die Nutzung intensiver optischer Aerosoleigenschaften weit verbreitet. Deshalb präsentieren wir an dieser Stelle DeLiAn, eine Datensammlung intensiver optischer Aerosoleigenschaften, welche auf Langzeitmessungen mit bodengebundenen Mehrwellenlängen-Raman- und Polarisationslidaren beruht. Diese Messungen wurden hauptsächlich mit am Leibniz-Institut für Troposphärenforschung (TROPOS) entwickelten Lidaren durchgeführt. Die Datensammlung bot die Grundlage für die Entwicklung des Hybrid End-To-End Aerosol Classification (HETEAC) Model für die Weltraum-Mission EarthCARE und von HETEAC-Flex, eines auf optimaler Schätzung beruhenden Aerosolcharakterisierungsschemas. Neben bereits bekannten Aerosoltypen werden in DeLiAn auch neue Aerosoltypen und -mischungen berücksichtigt, wie z.B. das kürzlich über Mindelo, Cabo Verde, beobachtete Sulfat-Aerosol, welches vom Ausbruch des Vulkans Cumbre Vieja auf La Palma stammte.

Introduction

Lidar-derived intensive, i.e., concentration-independent, optical parameters can be effectively used for aerosol typing, as they provide information on the size, shape and absorption efficiency of the aerosol particles. In addition, a climatology of ground-based intensive optical properties of different aerosol is of great importance for the harmonization of spaceborne lidar observations. The PollyXT lidars [Engelmann *et al.*, 2016] are ideal for building such a data collection as they are globally distributed within international lidar networks [e.g., PollyNET, Baars *et al.*, 2016; EARLINET, Pappalardo *et al.*, 2014] and have been used in several international campaigns [e.g., MOSAiC, Shupe *et al.*, 2022; ASKOS, Marinou *et al.*, 2023].

DeLiAn and aerosol-typing developments

Based on globally distributed ground-based PollyXT lidar measurements (Fig. 1), a collection of lidar-derived intensive optical properties for several aerosol types has been produced, namely the particle linear depolarization ratio, the extinction-to-backscatter ratio (lidar ratio), and the Ångström exponent [DeLiAn, Floutsi *et al.*, 2023]. The intensive optical properties are available at two wavelengths, 355 and 532 nm, for 13 aerosol categories (Fig. 2). The categories cover not only the basic aerosol types (i.e., marine, pollution, continental European background,

volcanic ash, smoke, mineral dust), as well as the most frequently observed mixtures they form, but also more peculiar aerosol types that are rarely observed, such as dried marine aerosol and stratospheric smoke. The DeLiAn climatology will be regularly updated to provide up-to-date information on the intensive aerosol optical properties for the existing aerosol types, but also to include new aerosol types and mixtures not previously considered, e.g., sulfate aerosol.

Particles originating from the volcanic eruptions that took place at the Cumbre Vieja ridge, La Palma, Canary Islands from 19 September to 13 December 2021 were recorded by the PollyXT lidar located at Mindelo, in Cabo Verde [Gebauer *et al.*, 2023]. Usually, typical aerosol conditions over Mindelo are a clean marine planetary boundary layer (PBL) and a Saharan dust layer just above the PBL. In contrast, during the time of the volcanic eruptions, a highly polluted PBL with extinction coefficient values up to 600 Mm^{-1} was observed for several days, starting four days after the first eruption on 23 September 2021. An example is shown in Fig. 3, where a volcanically influenced day (24 September) is contrasted with a typical day before the eruption (16 September 2021). Clear differences are obvious for the PBL. Due to the low depolarization ratio, volcanic ash occurrence in the PBL can be excluded. While volcanic aerosol, in particular volcanic ash, have been frequently observed with lidars [e.g., Ansmann *et al.*, 2010; Groß *et al.*, 2012], measurements of sulfate aerosol and sulfate-based aerosol

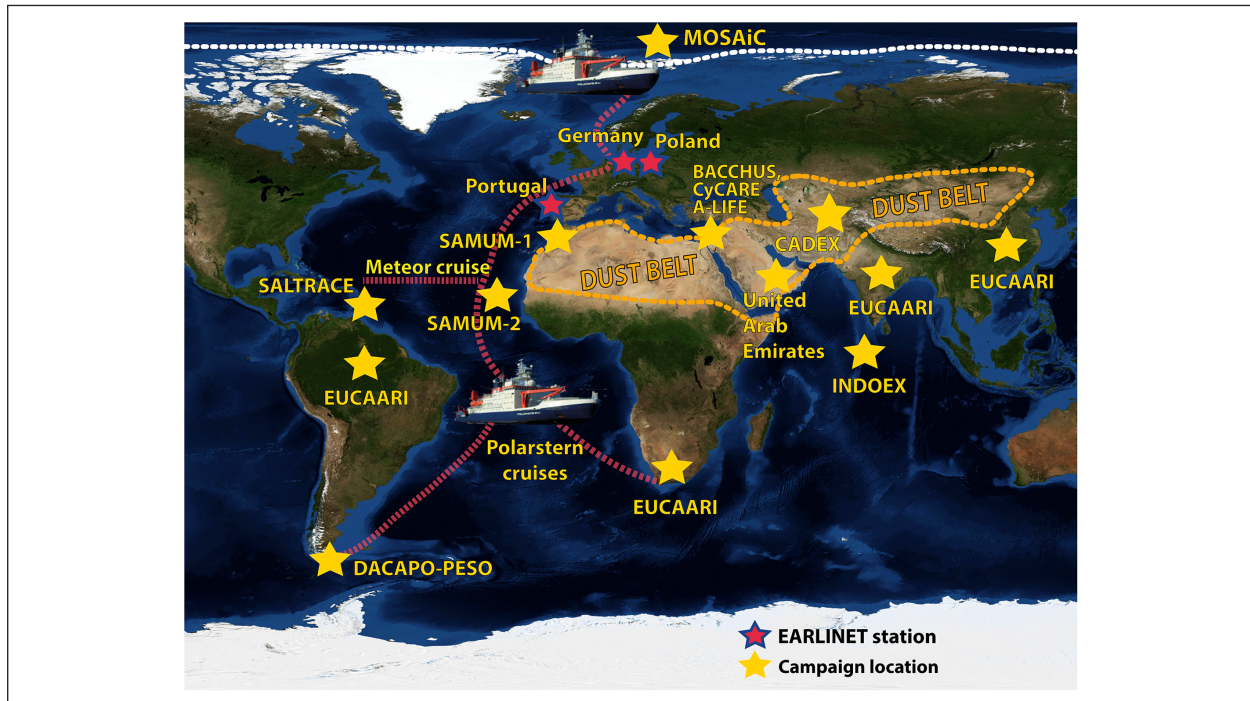


Fig. 1: Locations of measurement campaigns (yellow stars) or permanent stations (red and blue stars) from which data for DeLiAn were used. Map source: NASA Earth Observatory.

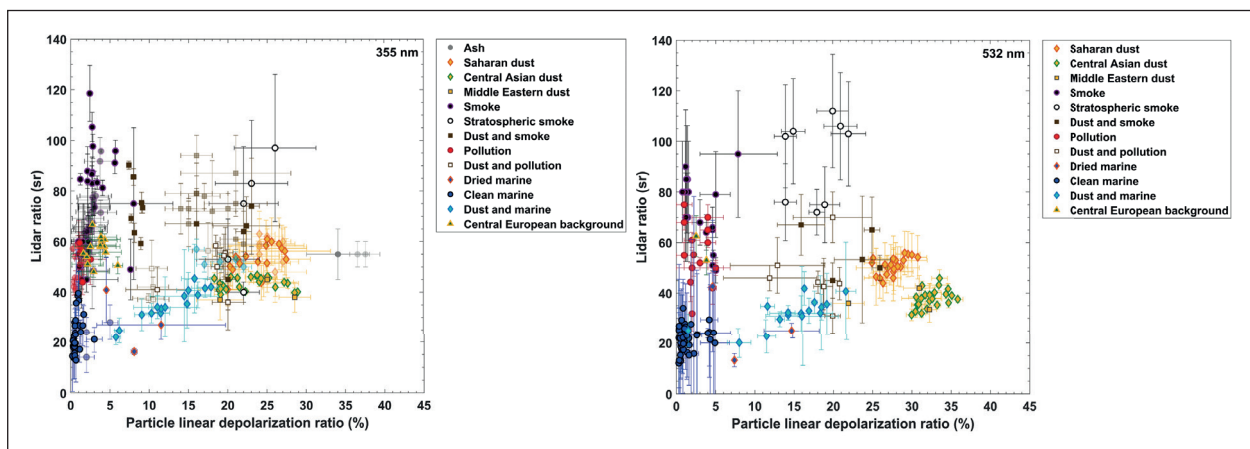


Fig. 2: Intensive optical properties of different aerosol types measured at 355 nm (left) and 532 nm (right).

mixtures are rare and thus provide a valuable contribution to the data collection.

DeLiAn has successfully provided a solid basis for the development of two typing schemes, the HETEAC model for the upcoming EarthCARE mission [Wandinger et al., 2023] and HETEAC-Flex, a novel aerosol-typing approach [Floutsi et al., 2024], which will serve as a ground-based validation scheme for EarthCARE. In particular, HETEAC-Flex is an optimal-estimation-based typing scheme (Fig. 4) that allows the identification of up to four different aerosol components of an aerosol mixture and the quantification of their contribution to the aerosol mixture in terms of relative particle volume. Similar to HETEAC,

the four aerosol components adequately reflect the most commonly observed aerosol types in the atmosphere: combustion- and pollution-related aerosol, sea salt and desert dust. The lidar-derived optical parameters used are the lidar ratio and the particle linear depolarization ratio at two distinct wavelengths (355 and 532 nm), the backscatter-related color ratio for the wavelength pair of 532/1064 nm and the extinction-related Ångström exponent for the wavelength pair of 355/532 nm. These intensive optical properties can be combined in different ways, making the method flexible and allowing it to be applied to lidar systems with different configurations.

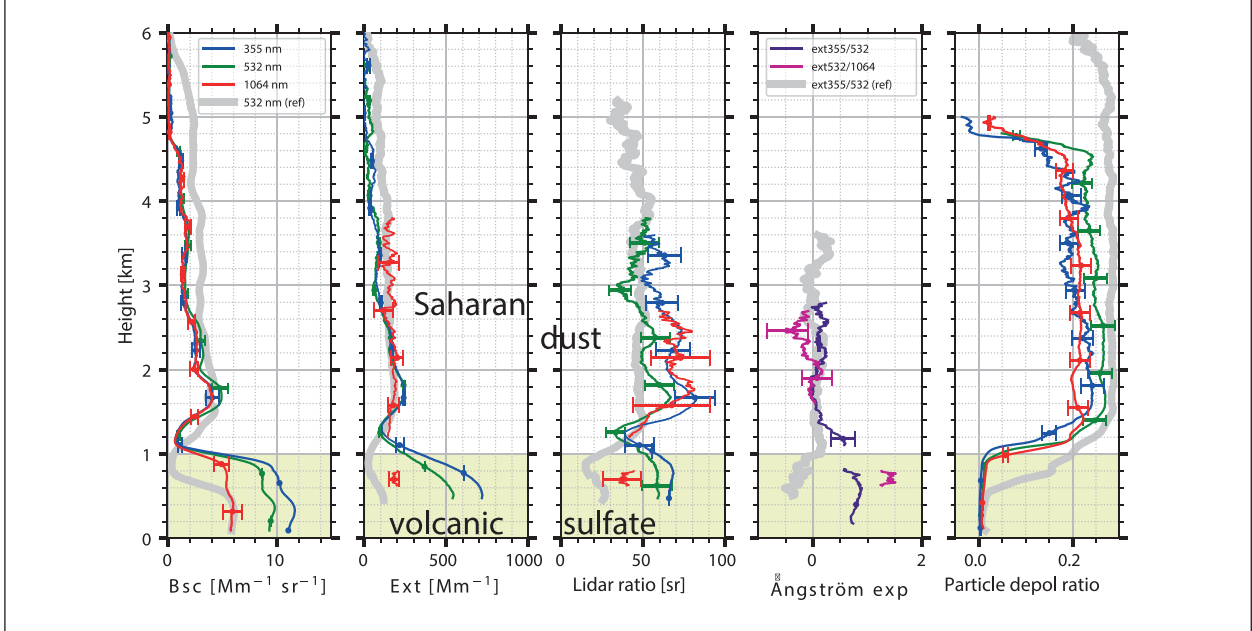


Fig. 3: From left to right: vertical profiles of the particle backscatter coefficient, the particle extinction coefficient, the lidar ratio, the Ångström exponent, and the particle linear depolarization ratio measured with a PollyXT lidar at Mindelo, Cabo Verde, on 24 September 2021, between 04:38 and 05:57 UTC. Thick grey lines correspond to measurements (at 532 nm) prior to the eruption, on 16 September 2021, and represent the typical aerosol conditions over Mindelo.

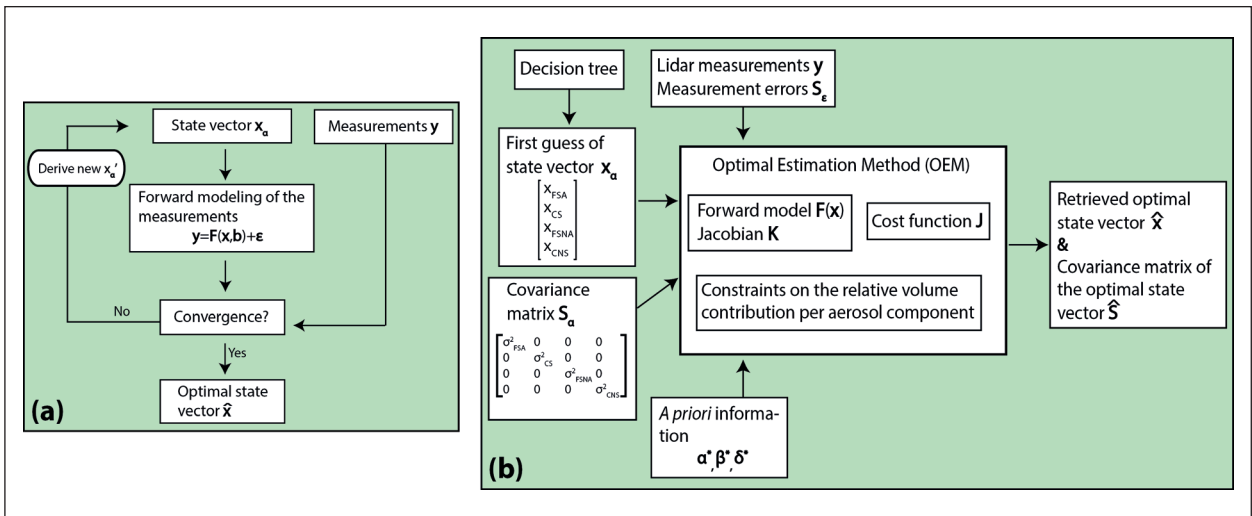


Fig. 4: (a) Generalized concept of the optimal estimation method and (b) detailed illustration of the workflow of HETEAC-Flex. Two aerosol components represent absorbing and less absorbing fine-mode particles (FSA and FSNA, respectively) and the other two spherical and non-spherical coarse-mode particles (CS and CNS, respectively).

Conclusion

DeLiAn is a data collection of lidar-derived optical properties covering a wide range of different aerosol types and mixtures, and will be continuously updated with the most recent measurements. The collection has multiple uses and is of great importance for the development and improvement of existing and new

aerosol-typing schemes and for data harmonization between lidar networks and satellites. In particular, the functionality of DeLiAn has been demonstrated by its use in the development of HETEAC and HETEAC-Flex. The forthcoming launch of EarthCARE will provide a great opportunity for spectral harmonization of long-term ground-based and spaceborne lidar data sets.

References

- Ansmann, A., M. Tesche, S. Groß, V. Freudenthaler, P. Seifert, A. Hiebsch, J. Schmidt, U. Wandinger, I. Mattis, D. Müller, and M. Wiegner (2010), The 16 April 2010 major volcanic ash plume over central Europe: EARLINET lidar and AERONET photometer observations at Leipzig and Munich, Germany, *Geophysical Research Letters*, 37(13), doi: <https://doi.org/10.1029/2010GL043809>.
- Baars, H., T. Kanitz, R. Engelmann, D. Althausen, B. Heese, M. Komppula, J. Preißler, M. Tesche, A. Ansmann, U. Wandinger, J. H. Lim, J. Y. Ahn, I. S. Stachlewska, V. Amiridis, E. Marinou, P. Seifert, J. Hofer, A. Skupin, F. Schneider, S. Bohlmann, A. Foth, S. Bley, A. Pfüller, E. Giannakaki, H. Lihavainen, Y. Viisanen, R. K. Hooda, S. N. Pereira, D. Bortoli, F. Wagner, I. Mattis, L. Janicka, K. M. Markowicz, P. Achtert, P. Artaxo, T. Pauliquevis, R. A. F. Souza, V. P. Sharma, P. G. van Zyl, J. P. Beukes, J. Sun, E. G. Rohwer, R. Deng, R. E. Mamouri, and F. Zamorano (2016), An overview of the first decade of PollyNET: an emerging network of automated Raman-polarization lidars for continuous aerosol profiling, *Atmos. Chem. Phys.*, 16(8), 5111–5137, doi: <https://doi.org/10.5194/acp-16-5111-2016>.
- Engelmann, R., T. Kanitz, H. Baars, B. Heese, D. Althausen, A. Skupin, U. Wandinger, M. Komppula, I. S. Stachlewska, V. Amiridis, E. Marinou, I. Mattis, H. Linné, and A. Ansmann (2016), The automated multiwavelength Raman polarization and water-vapor lidar PollyXT: the neXT generation, *Atmos. Meas. Tech.*, 9(4), 1767–1784, doi: <https://doi.org/10.5194/amt-9-1767-2016>.
- Floutsi, A. A., Baars, H., and Wandinger, U. (2024), HETEAC-Flex: an optimal estimation method for aerosol typing based on lidar-derived intensive optical properties, *Atmos. Meas. Tech.*, 17, 693–714, doi: <https://doi.org/10.5194/amt-17-693-2024>.
- Floutsi, A. A., H. Baars, R. Engelmann, D. Althausen, A. Ansmann, S. Bohlmann, B. Heese, J. Hofer, T. Kanitz, M. Haarig, K. Ohneiser, M. Radenz, P. Seifert, A. Skupin, Z. Yin, S. F. Abdullaev, M. Komppula, M. Filioglou, E. Giannakaki, I. S. Stachlewska, L. Janicka, D. Bortoli, E. Marinou, V. Amiridis, A. Gialitaki, R. E. Mamouri, B. Barja, and U. Wandinger (2023), DeLiAn – a growing collection of depolarization ratio, lidar ratio and Ångström exponent for different aerosol types and mixtures from ground-based lidar observations, *Atmos. Meas. Tech.*, 16(9), 2353–2379, doi: <https://doi.org/10.5194/amt-16-2353-2023>.
- Gebauer, H., A. A. Floutsi, M. Haarig, M. Radenz, R. Engelmann, D. Althausen, A. Skupin, A. Ansmann, C. Zenk, and H. Baars (2023), Tropospheric sulfate from Cumbre Vieja volcano at Las Palmas, transported towards Cabo Verde - lidar measurements of aerosol extinction, backscatter and depolarization at 355, 532 and 1064 nm, *EGUphere*, 2023, 1–25, doi: <https://doi.org/10.5194/egusphere-2023-2305>.
- Gross, S., V. Freudenthaler, M. Wiegner, J. Gasteiger, A. Geiss, and F. Schnell (2012), Dual-wavelength linear depolarization ratio of volcanic aerosols: Lidar measurements of the Eyjafjallajökull plume over Maisach, Germany, *Atmospheric Environment*, 48, 85–96.
- Marinou, E., P. Paschou, I. Tsikoudi, A. Tsekeri, V. Daskalopoulou, D. Kouklaki, N. Siomos, V. Spanakis-Misirlis, K. A. Voudouri, T. Georgiou, E. Drakaki, A. Kampouri, K. Papachristopoulou, I. Mavropoulou, S. Mallios, E. Proestakis, A. Gkikas, I. Koutsoupi, I. P. Raptis, S. Kazadzis, H. Baars, A. Floutsi, R. Pirloaga, A. Nemuc, F. Marencu, M. Kezoudi, A. Papetta, G. Močnik, J. Y. Díez, C. L. Ryder, N. Ratcliffe, K. Kandler, A. Sudharaj, and V. Amiridis (2023), An Overview of the ASKOS Campaign in Cabo Verde, *Environmental Sciences Proceedings*, 26(1), 200.
- Pappalardo, G., A. Amodeo, A. Apituley, A. Comeron, V. Freudenthaler, H. Linné, A. Ansmann, J. Bösenberg, G. D'Amico, I. Mattis, L. Mona, U. Wandinger, V. Amiridis, L. Alados-Arboledas, D. Nicolae, and M. Wiegner (2014), EARLINET: towards an advanced sustainable European aerosol lidar network, *Atmos. Meas. Tech.*, 7(8), 2389–2409, doi: <https://doi.org/10.5194/amt-7-2389-2014>.
- Shupe, M. D., M. Rex, B. Blomquist, P. O. G. Persson, J. Schmale, T. Uttal, D. Althausen, H. Angot, S. Archer, and L. Bariteau (2022), Overview of the MOSAiC expedition: Atmosphere, *Elem Sci Anth.*, 10(1), 00060.
- Wandinger, U., A. A. Floutsi, H. Baars, M. Haarig, A. Ansmann, A. Hünerbein, N. Docter, D. Donovan, G. J. van Zadelhoff, S. Mason, and J. Cole (2023a), HETEAC – the Hybrid End-To-End Aerosol Classification model for EarthCARE, *Atmos. Meas. Tech.*, 16(10), 2485–2510, doi: <https://doi.org/10.5194/amt-16-2485-2023>.

Funding

Parts of this research have been supported by the German Federal Ministry for Economic Affairs and Energy (BMWi) under grant no. 50EE1721C, by European Union's Horizon 2020 research and innovation program through ACTRIS-2 under grant agreement no. 654109, by the German Federal Ministry of Education and Research (BMBF) through PoLiCyTa under grant no. 01LK1603A and by the European Space Agency under the L2A+ project, contract no. 4000139424/22/I-NS among many other projects for which the measurements were acquired.

Cooperation

European Space Agency (ESA)
 Ocean Science Centre Mindelo (OSCM)
 GEOMAR
 PollyNET consortium (NOA, FMI, UW, CGE, EcoE, TAU, DWD, NAST)

Ultra-fine dust pollution from airports in Berlin (ULTRAFLEB) – the results of the stationary UFP measurements

Ulf Winkler, Kay Weinhold, Maik Merkel, Alfred Wiedensohler

Im Rahmen des Projekts „Ultrafeinstaubbelastung durch Flughäfen in Berlin“ (ULTRAFLEB) beauftragt vom Umweltbundesamt (UBA) und koordiniert von TROPOS, wurden in den Jahren 2020-2022 stationäre und mobile Feldmessungen von Ultrafeinpartikeln (UFP) im Umfeld der Berliner Flughäfen durchgeführt. Bei Flughafen-Wind tragen Luftverkehrs-Emissionen auch in mehreren Kilometern Entfernung signifikant zur UFP-Konzentration bei oder dominieren diese sogar, vor allem im Durchmesser-Bereich 10-20 nm. Wenn nur nichtflüchtige Partikel betrachtet werden, ergibt sich allerdings ein wesentlich geringerer Luftverkehrs-Einfluss - dies ist eine wesentliche Erkenntnis von ULTRAFLEB. Flugzeugemissionen werden demnach von flüchtigen Partikeln dominiert.

Air traffic produces considerable amounts of ultrafine particles (UFP). The project “Ultrafine dust pollution from airports in Berlin” (ULTRAFLEB), commissioned by the Umweltbundesamt (German Federal Environment Agency, UBA), was the first large-scale UFP monitoring project around the Berlin airports.

ULTRAFLEB [TROPOS, 2024] started in November 2020 and will end on 31 May 2025. The



Fig. 1: The TROPOS trailer station at Eichwalde primary school under the BER approach path.

measurements were terminated in November 2022, the remainder of the project is dedicated to data evaluation, modelling, and model validation. TROPOS is in charge of the management of ULTRAFLEB and carried out most of the measurements; other contributors are the Technical Universities of Braunschweig (TU BS) and Berlin (TUB) and the environmental department of the airport operator Flughafen Berlin Brandenburg GmbH (FBB). The modelling tasks lie in the hands of TNO (Netherlands), Ingenieurbüro Janicke GbR (Überlingen, Lake Constance) and IVU Umwelt GmbH (Freiburg im Breisgau). ULTRAFLEB collaborates with the Berlin-Brandenburg Air Study (BEAR), an epidemiological study on possible health effects of aircraft emissions, especially UFP, on elementary school children. BEAR is a joint project by Charité – Universitätsmedizin Berlin, the University of Düsseldorf and Helmholtz Munich [Soppa et al., 2023, Charité, 2024].

Methods

Several monitoring stations were installed around the Berlin airports. From July 2020 (before the official start of ULTRAFLEB), a TROPOS station was deployed in Berlin-Reinickendorf, about 4 km east of the terminal of the Berlin Tegel (TXL) airport. TXL was shut down on 8 November 2020 (since then, the entire Berlin air traffic is handled at BER airport), the Reinickendorf station however kept monitoring the air at this inner-city location until July 2021. Around the

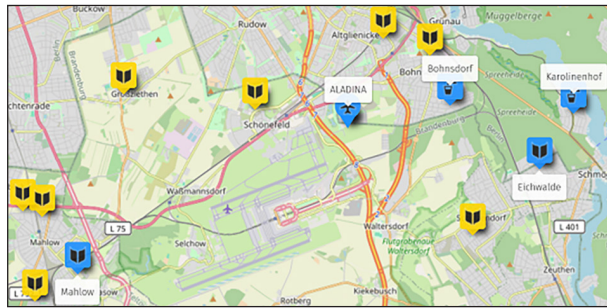


Fig. 2: Map of the area around the BER airport, showing the locations (light blue) of the ULTRAFLEB monitoring stations at Mahlow, Bohnsdorf, Eichwalde and Karolinenhof, and of the ALADINA drone launch site. Yellow symbols mark primary schools around the BER taking part in the epidemiological BEAR study.

BER airport (see map Fig. 2), UFP monitoring was conducted both northeast (Berlin-Bohnsdorf, station operated by FBB, 2021-22) and west (Blankenfelde-Mahlow, TROPOS, July 2021 to November 2022) of the BER airport. Additionally, special campaigns took place east of the BER in autumn 2021 and summer/autumn 2022: TROPOS deployed a trailer station (Fig. 1) at two locations (Eichwalde and Berlin-Karolinenhof), and TU BS conducted mobile measurements using a car [Gerling & Weber, 2023], a cargo bike and (in October 2021) the drone ALADINA.

At all stations, particle number size distributions were monitored using a TROPOS-made mobility particle size spectrometer (MPSS). A novelty of ULTRAFLEB (with regard to measurements in an airport environment) was an alteration between monitoring all particles (AMB=ambient) and non-volatile particle only (TD=thermodenuder): Before reaching the MPSS, the sample air passes through a thermodenuder which was alternately switched on or off for 5 minutes. When the TD is switched on, only non-volatile particles can pass to the MPSS.

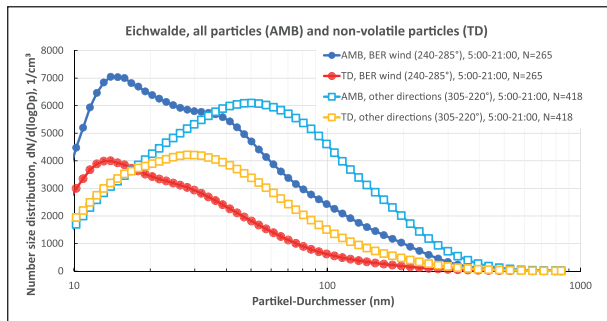


Fig. 3: Particle number size distributions measured at the Eichwalde monitoring station. Median of all hourly mean distributions. Only measurements between 5:00 and 21:00 local time were considered. Separate distributions for all (AMB) and non-volatile (TD) particles, and for hours with wind from the BER airport (240-285°) or from other directions (305-220°; a 20° gap to airport winds was left). The legend mentions the number N of hourly means contributing to each distribution.

Results

When the monitoring stations were exposed to airport wind, high particle concentrations were frequently registered in the diameter range up to about 40 nm (see AMB distributions for Eichwalde, Fig. 3). This confirms similar findings from previous measurements at other airports worldwide. For larger particles, the airport contribution is insignificant: at Eichwalde (located east of the BER) the average AMB concentrations above 40 nm were even lower at airport wind than at other wind directions. This is a consequence of long-range transport which leads to higher particle concentrations with easterly winds.

When only non-volatile particles are considered (TD in Fig. 3 and Fig. 4), an increase in the concentration at airport wind is only apparent for particle diameters up to about 20 nm, and is clearly less significant than for all particles (AMB). ULTRAFLEB thus revealed that UFP generated by air traffic are dominated by volatile particles.

Figure 4 shows polar plots for particle concentrations (diameter range 10-20 nm) at Reinickendorf, averaged for the time before and after the TXL shutdown. For all particles (AMB), the airport signature is very distinct even at this Berlin inner-city location, about 4 km away from the airport. Meanwhile in the TD data (i.e. non-volatile particles only), air-traffic contributions hardly stand out from the background. This finding may be highly relevant for research into health effects of aircraft emissions.

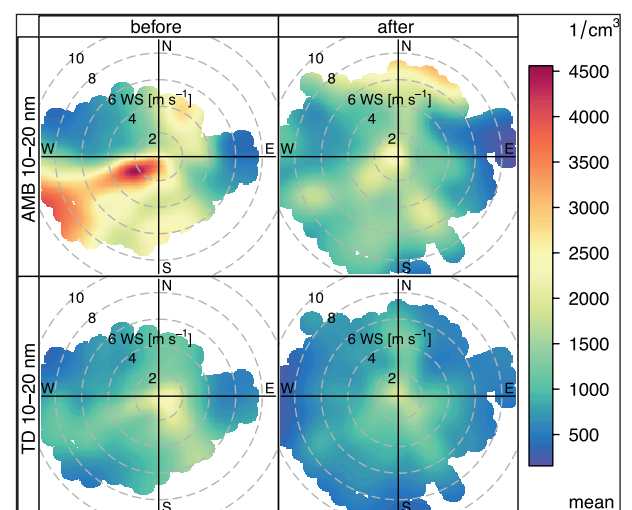


Fig. 4: Fig. 4: Polar plot: mean particle concentrations in the diameter range 10-20 nm as a function of wind direction and wind speed, Produced by openair [Carslaw & Ropkins, 2012] for Reinickendorf. Separate plots for all (AMB) and non-volatile (TD) particles, including all measurements either before (left) or after (right) the shutdown of the TXL airport (located at 230-260°) on 8 November 2020. Only measurements between 5:00 and 21:00 local time were included.

References

- Carslaw, D. C., K. Ropkins (2012), openair — An R package for air quality data analysis. *Environmental Modelling & Software* 27–28 (0), 52–61, doi: <https://doi.org/10.1016/j.envsoft.2011.09.008>.
- Charité (2024), Berlin Brandenburg Air Study (BEAR), https://hygiene.charite.de/forschung/berlin_brandenburg_air_study_bear, URL: https://hygiene.charite.de/forschung/berlin_brandenburg_air_study_bear.
- Gerling, L., S. Weber (2023), Mobile measurements of atmospheric pollutant concentrations in the pollutant plume of BER airport, *Atmospheric Environment*, 304, 119770, doi: <https://doi.org/10.1016/j.atmosenv.2023.119770>.
- Soppa, V., S. Lucht, Ogurtsova, A. Buschka, M. López-Vicente, M. Guxens, K. Weinhold, U. Winkler, A. Wiedensohler, A. Held, S. Lüchtrath, J. Cyrys, S. Kecorius, P. Gastmeier, M. Wiese-Posselt, B. Hoffmann (2023), The Berlin-Brandenburg Air Study—A Methodological Study Paper of a Natural Experiment Investigating Health Effects Related to Changes in Airport-Related Exposures, *Int J Public Health*, 17 November 2023, doi: <https://doi.org/10.3389/ijph.2023.1606096>.
- TROPOS (2024), <https://www.tropos.de/en/research/projects-infrastructures-technology/joint-research-projects/ultrafleb>, URL: <https://www.tropos.de/en/research/projects-infrastructures-technology/joint-research-projects/ultrafleb>.

Funding

Umweltbundesamt (German Federal Environment Agency, UBA) grant FKZ 3720522010

Assessing Mineral Dust Toxic Potency Using the Oxidative Potential Assays

Eduardo J. dos S. Souza, Khanneh Wadinga Fomba, and Hartmut Herrmann

Das oxidative Potenzial (OP) von Mineralstaubpartikeln kann Informationen über die Toxizität der Partikel und das damit verbundene Expositionsrisiko liefern, wenn es auf die PM-Masse und das Expositionsvolumen normiert wird. Dazu werden verschiedene chemische Assays auf Staubpartikel angewandt, z. B. der Dithiothreitol (DTT)-Assay. Während der DUSTRISK-Kampagne im 10. Januar und 20. Februar 2022 wurde der DTT-Assay für die Untersuchung der OP-Verteilung an zwei Probenahmestellen in ländlichen und städtischen Gebieten in Cabo Verde, Afrika, verwendet. Während bei Staubereignissen ein höheres Expositionsrisiko gegenüber Feinstaub-OP beobachtet wurde, war die Toxizität der Partikel in staubarmen Zeiten nicht sehr hoch. Bei groben Partikeln waren sowohl die toxische Wirkung als auch das Expositionsrisiko während Staubereignissen um mehr als 50 % höher als in staubarmen Zeiten. Die Studie zeigt, dass Staubereignisse die Exposition gegenüber chemischen reaktiven Spezies in Partikeln und die damit verbundenen Gesundheitseffekte deutlich erhöhen.

Introduction

In recent years, mineral dust (MD) pollution is becoming one of the biggest health concerns worldwide [Francis *et al.*, 2023; Soleimani-Sardo *et al.*, 2023; Zheng *et al.*, 2023]. Exposure to MD has been linked to numerous diseases, including respiratory, cardiovascular, eye, and allergic diseases, diabetes, and hypertension [Grasso *et al.*, 2023; Kok *et al.*, 2018]. As sand dust storm (SDS) events generally influence the long-range transport of chemical and biological species, this study investigates the effects of dust chemical composition on human health. To identify potential chemical species that can cause oxidative stress in the body, routine oxidative potential (OP) assays are used to link the chemical composition of particulate matter (PM) to toxicity. OP assays monitor the ability of aerosol particles to produce reactive oxygen species (ROS) that can cause adverse health and help explain the health effects of people exposed to PM [Daellenbach *et al.*, 2020]. Despite reports of OP levels in different regions and testing routines, little research has been done on the effects of Saharan dust events on PM exposure

and the possible influence of the mineral dust OP on public health.

The DUSTRISK (A risk index for health effects of mineral dust and associated microbes) project focuses on this important subject to investigate and highlight amongst others, the effects of dust composition on human health. The project is funded under the Leibniz SAW competition as a Collaborative Excellence initiative involving five institutions in Cabo Verde, including the local hospitals and the National Institute of Public Health, as well as three other Leibniz institutions in Germany with further Portuguese and American scientists. The core of the project involved a field campaign at two islands of the Cape Verde islands at both rural and urban sites on 10 January and 20 February 2022. Herein, advanced studies on the effects of dust chemical composition were carried out including the evaluation of their OP as an effective chemical analytical tool to predict the toxicity of the particles. The chemical content of PM_{10} and $PM_{2.5}$ samples, including OP drivers and their overall impact, was investigated using the dithiothreitol (DTT) assay.

Methods

The DTT assay (OP^{DTT}) was investigated by monitoring the 2-nitro-5-thiobenzoic acid (TNB^{2-}) formation using absorbance measurements with a UV-VIS-spectrophotometer. About 6.1 cm^2 of the PM filter was extracted using 10 mL of phosphate buffer solution (PBS) and 3 mL of PM extraction was incubated with $30\text{ }\mu\text{L}$ of 10 mM DTT in PBS. The TNB^{2-} formation was monitored at 412 nm under the addition of $50\text{ }\mu\text{L}$ of 10 mM 5,50-dithiobis-2-nitrobenzoic acid (DTNB) at $0, 5, 10, 20$, and 30 min of incubation using a 1 cm cuvette. The obtained OP^{DTT} (analog to the TNB^{2-} formation rate) was normalized by the incubated PM mass (DTT_M , $\text{nmol min}^{-1}\text{ }\mu\text{g}^{-1}$) and sampled air volume (DTT_V , $\text{nmol min}^{-1}\text{ m}^{-3}$) to determine the association with PM toxicity and human exposure [Pietrogrande et al., 2018]. In total 60 PM samples collected at the rural (countryside) and urban sites in Mindelo, Cabo Verde were investigated.

Results and Discussion

The observed DTT_M and DTT_V activities indicated significant effects on ROS formation at elevated PM levels during dust events and are shown in Fig. 1.

Significant DTT_M activities were observed for $PM_{2.5}$ during non-dust events, indicating a contribution

of toxic components significantly driving $PM_{2.5}$ OP. These components could include organic compounds originating from long-range transport as well as local combustion activities in the city. However, $PM_{2.5}$ DTT_V activities were significantly higher during dust events, indicating an increased exposure to MD-loaded PM catalyst that can generate high OP. In other words, there is a significant increase in the reactions that promote the formation of ROS in the body during dust events as PM mass increases significantly. Higher DTT_M activities were observed in PM_{10} , suggesting that coarse particulate matter could also transport significant redox-active PM species that can increase PM toxicity, even those released by anthropogenic emissions. This indicates that long-range transport of MD, which is rich in coarse particles, markedly increases chemical species that trigger oxidative stress. Likewise, DTT_V activities in PM_{10} were about four times higher during dust episodes than non-dust periods, reiterating the greater human health effects associated with PM exposure to coarse dust particles.

The DTT_V activity of fine particles is strongly correlated with PM mass during both dust (0.71) and non-dust events (0.80), suggesting that DTT_V activity increases at higher $PM_{2.5}$ concentrations. However, the exposure to OP redox-active species increased during dust events together with the potential toxicity of the PM_{10} particles. These results together with

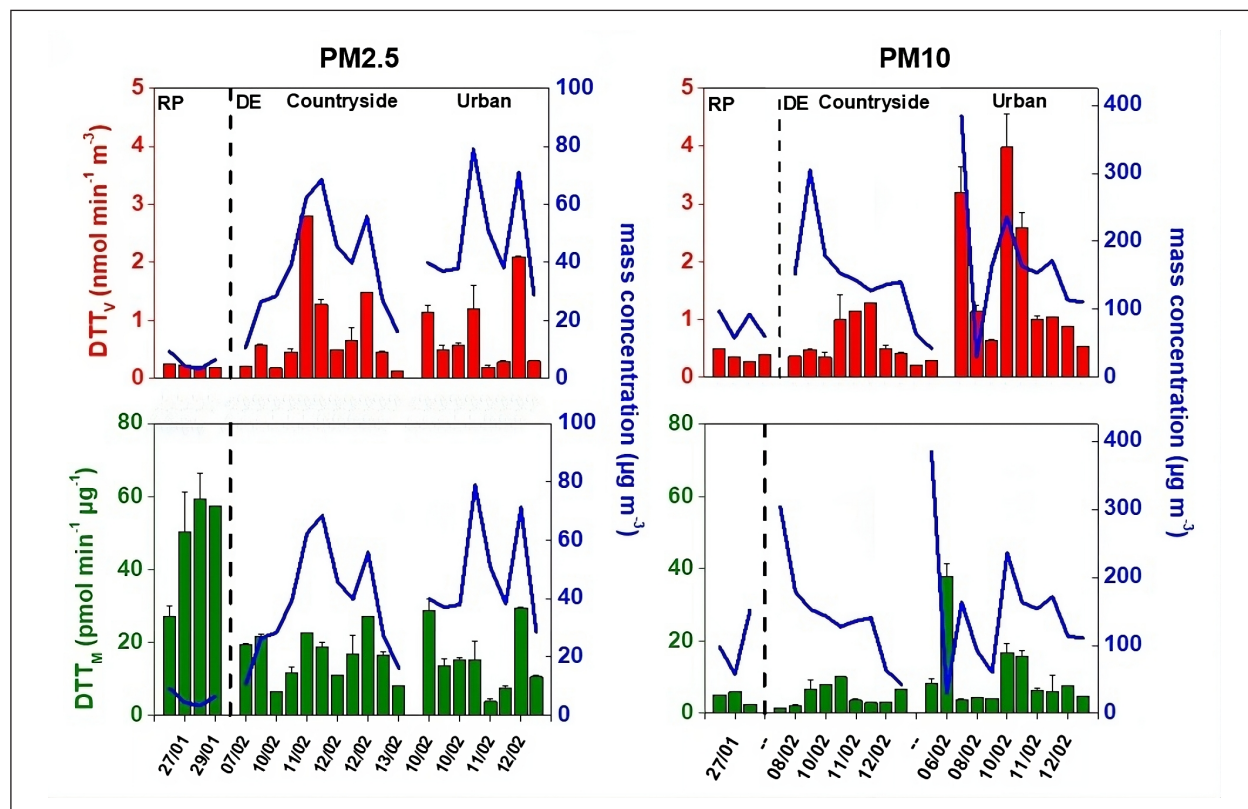


Fig. 1. DTT_V and DTT_M activities for $PM_{2.5}$ and PM_{10} for countryside and urban sites during dust (DE) and non-dust events (RP) in Mindelo, Cabo Verde.

other studies from cellular assays from project partner institutions highlight the potential toxic effects of coarse mode particles, which are often considered less relevant in health assessment studies, and suggest the necessity of further investigations on the exact coarse mode chemical components responsible

for the elevated OP, and associated risks. Potential human health effects can also be associated with high PM_{2.5} OPs, as exposure to toxic PM_{2.5} components also contributes to the formation of ROS and oxidative stress that affect human health.

References

- Francis, D., Fonseca, R., Nelli, N., Bozkurt, D., Cuesta, J., & Bosc, E. (2023), On the Middle East's severe dust storms in spring 2022: Triggers and impacts. *Atm. Envi.*, 296, doi: <https://doi.org/10.1016/j.atmosenv.2022.119539>.
- Soleimani-Sardo, M., Shirani, M., & Strezov, V. (2023), Heavy metal pollution levels and health risk assessment of dust storms in Jazmurian region, Iran. *Scientific Reports*, 13(1), doi: <https://doi.org/10.1038/s41598-023-34318-1>.
- Zheng, K., Zeng, Z., Lin, Y., Wang, Q., Tian, Q., & Huo, X. (2023), Current status of indoor dust PBDE pollution and its physical burden and health effects on children. *Env. Sci. and Pol. Res.*, 30, 8, pp. 19642–19661, doi: <https://doi.org/10.1007/s11356-022-24723-w>.
- Grasso, C., Giacchero, F., Crivellari, S., Bertolotti, M., & Maconi, A. (2023), A Review on The Role of Environmental Exposures in IgG4-Related Diseases. *Curr. Environ. Health Rep.*, pp 1-9, doi: <https://doi.org/10.1007/s40572-023-00401-y>.
- Kok, J. F., Ward, D. S., Mahowald, N. M., & Evan, A. T. (2018), Global and regional importance of the direct dust-climate feedback. *Nat. Com.*, 9(1), doi: <https://doi.org/10.1038/s41467-017-02620-y>.
- Daellenbach, K.R., Uzu, G., Jiang, J., Cassagnes, L.E., Leni, Z., Vlachou, A., Stefenelli, G., Canonaco, F., Weber, S., Segers, A. and Kuenen, J.J., (2020), Sources of particulate-matter air pollution and its oxidative potential in Europe, *Nature*, 587(7834), pp.414-419, doi: <https://doi.org/10.1038/s41586-020-2902-8>.
- Pietrogrande, M. C., Cristina D., Rossana D., Paolo L., Francesco M., Marco V., and Gabriele T., (2018), Chemical composition and oxidative potential of atmospheric coarse particles at an industrial and urban background site in the alpine region of northern Italy." *Atmospheric Environment* 191: 340-350, doi: <https://doi.org/10.1016/j.atmosenv.2018.08.022>.

Funding

We gratefully acknowledge the Leibniz Collaborative Excellence Programme for funding the Dustrisk project K225/2019.

Urban modelling at the grey zone

Michael Weger and Bernd Heinold

Die Repräsentation von urbanen Luftschadstoff-Hotspots mittels mikroskaliger Modelle ist aufgrund der benötigten Rechenressourcen immer noch mit Einschränkungen verbunden. Eine geringere Modellauflösung ermöglicht signifikante Kosteneinsparungen, führt jedoch zum Problem der expliziten Gebäudedarstellung im Bereich der urbanen Grauzone. Das am TROPOS entwickelte Luftqualitätsmodell CAIRDIO verwendet einen diffusen Gebäudeansatz, welcher eine hohe Flexibilität in der Wahl der räumlichen Auflösung ermöglicht. Damit ist es möglich ganze Städte numerisch effizient und dennoch mit ausreichender Genauigkeit zu simulieren, um auch verkehrsnahe Belastungs-Hotspots mit dem Modell abbilden zu können.

In diesem Beitrag werden Ergebnisse zweier Anwendungsstudien mit CAIRDIO zur Ausbreitungssimulation von Ruß und Feinstaub in den Städten Leipzig und Dresden gezeigt. Während in der ersten Anwendungsstudie auf die Stadt Leipzig Gebäudeeffekte auf die urbane Meteorologie und Luftschadstoffausbreitung untersucht wurden, spielten in der zweiten Anwendungsstudie auf die Stadt Dresden orographische Effekte eine übergeordnete Rolle.

The grey zone model CAIRDIO

The urban grey zone is the transition range from the urban microscale (up to a few meters) to the mesoscale. It is characterized by the difficulty in representing building effects in models by the two contrasting approaches of explicit representation vs. parameterization [Barlow *et al.*, 2017]. The City-scale AIR dispersion model with DIffuse Obstacles (CAIRDIO) allows for a seamless transition of sharply defined explicit building boundaries at the microscale to diffuse building boundaries at the urban grey zone. This is accomplished by introducing flow-permeability fields in the discrete conservation laws governing fluid flow and tracer transport. Terrain-following coordinates can additionally represent the large-scale natural topography. For realistic simulations, initial and boundary conditions for meteorology and air pollution fields are inferred from mesoscale host simulations, and spatially detailed and temporally varying urban emissions are prescribed in the model. A detailed model description of CAIRDIO can be found in Weger *et al.* [2021], Weger *et al.* [2022], and Weger *et al.* [2023].

Case study 1: Intra-urban air pollution variability in Leipzig

In a first simulation case study, the model CAIRDIO is applied to simulate the dispersion of black carbon (BC) and particulate matter (PM10) within the city of Leipzig during the period from 1 March to 3 March 2020 [Weger *et al.*, 2022]. One study objective is to validate the model representation of the intra-urban air pollution variability at 40 m horizontal grid spacing using measurements from operational air monitoring stations covering urban background and high-traffic sites. Figure 1 shows the spatial distribution of near-surface BC and PM10 on 2 March at 12:30 UTC as simulated with CAIRDIO and complemented with observations. During this time, a convective boundary layer led to a rapid vertical mixing of BC emitted by the traffic and therefore to a large intra-urban variability as evidenced by the sharp concentration gradients. Compared to BC, the PM10 distribution is also more significantly influenced by industrial emissions. The model results are in generally good agreement with the available measurements, especially when considering the concentration differences between urban background (e.g., LT in Fig. 1) and high-traffic sites (e.g., LC in Fig. 1).

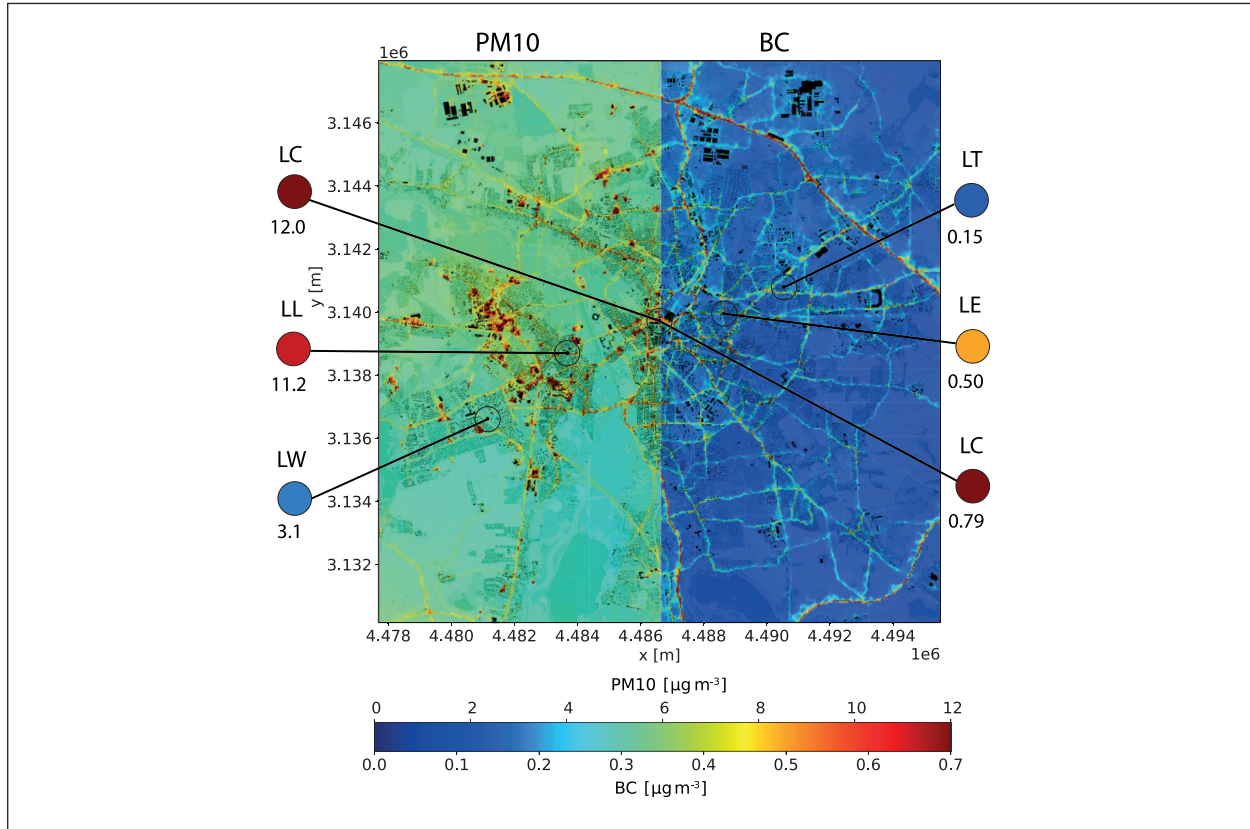


Fig. 1: Modeled BC (right half domain) and PM10 (left half domain) concentrations in Leipzig on 2 March 2020 at 12:30 UTC. Observations are additionally displayed by colour-filled circles and numeric values in units of $\mu\text{g m}^{-3}$. Label LW refers to station Leipzig West, LL to Leipzig Lütznerstr., LC to Leipzig Center, LE to Leipzig Eisenbahnstr., and LT to Leipzig TROPOS, respectively.

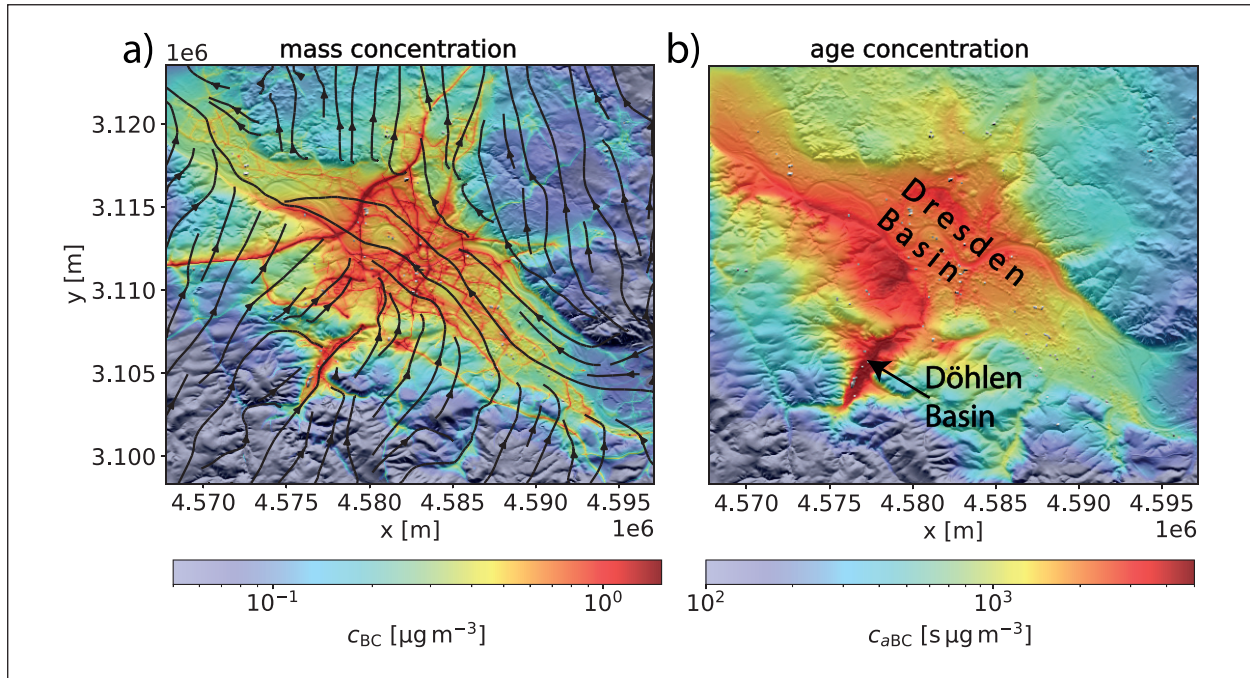


Fig. 2: (a) BC distribution pattern in the Dresden Basin during stable boundary layer conditions and an associated down-valley wind within the Elbe Valley (indicated by the streamlines). (b) Corresponding age concentration pattern showing the areas most prone to air-pollution trapping.

Case study 2: Orographic air-pollution effects in Dresden

With extensive urban simulation domains, it becomes important to consider also effects of the larger-scale surface topography in addition to the urban topography (buildings) and interactions between the two types of topographies. The city of Dresden situated within the Elbe Valley was selected for a second simulation case study [Weger *et al.*, 2023]. The entire region of the Dresden Basin (ca. 29 km x 25 km) was simulated with CAIRDIO using a horizontal grid spacing of 60 m.

Meteorological conditions during the simulation period (27 February to 10 March 2021) were dominated by high-pressure weather and a stably stratified boundary layer, favouring the trapping of urban air pollution within orographic depressions. A statistical analysis showed that high urban background BC concentrations in the Dresden Basin are associated with a cold-air stream flowing in down-valley direction during strong nocturnal inversion layers. Orographic

hot-spots are revealed by modeling the so-called age concentration [Deleersnijder *et al.*, 2020] of BC, which temporally accumulates in stagnating or recirculating air flows. Figure 2 shows the spatial BC concentration and age concentration distributions during periods of a down-valley oriented cold air stream.

Conclusion

Urban grey zone resolutions make spatially extensive model domains computationally feasible. As a result, entire cities can be modeled with sufficient accuracy to explicitly represent many aspects of meteorological interactions driving the intra-urban air-pollutant transport. The urban grey zone scale proved further to be particularly suitable for also including the effects of the larger-scale natural topography, which makes it possible to study additional meteorological interactions important for air pollution transport (e.g., orographic winds) that cannot be extensively considered in microscale simulations.

References

- Barlow, J., Best, M., Bohnenstengel, S. I., Clark, P., Grimmond, S., Lean, H., Christen, A., Emeis, S., Haeffelin, M., Harman, I. N., Lemonsu, A., Martilli, A., Pardyjak, E., Rotach, M. W., Ballard, S., Boutle, I., Brown, A., Cai, X., Carpentieri, M., Coceal, O., Crawford, B., Sabatino, S. D., Dou, J., Drew, D. R., Edwards, J. M., Fallmann, J., Fortuniak, K., Gornall, J., Gronemeier, T., Haliotis, C. H., Hertwig, D., Hirano, K., Holtlag, A. A. M., Luo, Z., Mills, G., Nakayoshi, M., Pain, K., Schlünzen, K.H., Smith, S., So ulhac, L., Steeneveld, G.-J., Sun, T., Theeuwes, N.E., Thomson, D., Voogt, J. A., Ward, H. C., Xie, Z.-T., and Zhong, J.: Developing a research strategy to better understand, observe, and simulate urban atmospheric processes at kilometer to subkilometer scales, *Bulletin of the American Meteorological Society*, 98, 261 – 264, doi: <https://doi.org/10.1175/BAMS-D-17-0106.1>, 2017.
- Deleersnijder, E., Draoui, I., Lambrechts, J., Legat, V., and Mouchet, A.: Consistent boundary conditions for age calculations, *Water*, 12, 1–29, doi: <https://doi.org/10.3390/w12051274>, 2020
- Weger, M., Knoth, O., and Heinold, B.: An urban large-eddy-simulation-based dispersion model for marginal grid resolutions: CAIRDIO v1.0, *Geoscientific Model Development*, 14, 1469–1492, doi: <https://doi.org/10.5194/gmd-14-1469-2021>, 2021.
- Weger, M., Baars, H., Gebauer, H., Merkel, M., Wiedensohler, A., and Heinold, B.: On the application and grid-size sensitivity of the urban dispersion model CAIRDIO v2.0 under real city weather conditions, *Geoscientific Model Development*, 15, 3315–3345, doi: <https://doi.org/10.5194/gmd-15-3315-2022>, 2022.
- Weger, M. and Heinold, B.: Air pollution trapping in the Dresden Basin from gray-zone scale urban modeling, *Atmospheric Chemistry and Physics*, 23, 13769–13790, doi: <https://doi.org/10.5194/acp-23-13769-2023>, 2023.

Appendices



Publications

Publication statistics

	2022	2023
Total number of publications	325	329
Books (author, editor) *	-	1
Book sections *	3	2
Contributions to collected editions *	-	1
Articles in peer reviewed journals *	102	90
Articles (others)	44	48
Presentations (invited)	5	11
Presentations (others)	142	143
Reports/Datasets/Software *	29	33

Publications *

- Abdullah, N. A., Latif, M. T., Juneng, L., Uning, R., Hassan, H., Azhari, A., **Tuch, T.** and **Wiedensohler, A.** 2022. Aerosol particle properties at a remote tropical rainforest in Borneo. *Atmos. Pollut. Res.*, **13**, 101383. <https://www.sciencedirect.com/science/article/pii/S1309104222000691>.
- Ahlawat, A.**, Mishra, S. K., **Herrmann, H.**, Rajeev, P., Gupta, T., Goel, V., Sun, Y. and **Wiedensohler, A.** 2022. Impact of chemical properties of human respiratory droplets and aerosol particles on airborne viruses' viability and indoor transmission. *Viruses*, **14**, 1497. <https://doi.org/10.3390/v14071497>.
- Akansu, E. F.**, **Siebert, H.**, Dahlke, S., Graeser, J., Jaiser, R. and Sommerfeld, A. 2022. Energy dissipation rate profiles derived from tethered balloon-borne measurements during the MOSAiC expedition from December 2019 to May 2020. *Data from: Arctic Amplification (AC3); Multidisciplinary drifting Observatory for the Study of Arctic Climate (MOSAiC). PANGAEA*, <https://doi.org/10.1594/PANGAEA.948546>.
- Andrés Hernández, M. D., Hilboll, A., Ziereis, H., Förster, E., Krüger, O. O., Kaiser, K., Schneider, J., Barnaba, F., Vrekoussis, M., Schmidt, J., Huntrieser, H., Blechschmidt, A.-M., George, M., Nenakhov, V., Harlass, T., Holanda, B. A., Wolf, J., Eirenschmalz, L., Krebsbach, M., **Pöhlker, M. L.**, Hedegaard, A. B. K., Mei, L., Pfeilsticker, K., Liu, Y., Koppmann, R., Schlager, H., Bohn, B., Schumann, U., Richter, A., Schreiner, B., Sauer, D., Baumann, R., Mertens, M., Jöckel, P., Kilian, M., Stratmann, G., Pöhlker, C., Campanelli, M., Pandolfi, M., Sicard, M., Gómez-Amo, J. L., Pujadas, M., Bigge, K., Kluge, F., Schwarz, A., Daskalakis, N., Walter, D., Zahn, A., Pöschl, U., Bönisch, H., Borrmann, S., Platt, U. and Burrows, J. P. 2022. Overview: On the transport and transformation of pollutants in the outflow of major population centres – observational data from the EMeRGe European intensive operational period in summer 2017. *Atmos. Chem. Phys.*, **22**, 5877-5924. <https://doi.org/10.5194/acp-22-5877-2022>.
- Ansmann, A.**, **Ohneiser, K.**, Chudnovsky, A., Knopf, D. A., Eloranta, E. W., Villanueva, D., **Seifert, P.**, **Radenz, M.**, Barja, B., Zamorano, F., **Jimenez, C.**, **Engelmann, R.**, **Baars, H.**, **Griesche, H.**, **Hofer, J.**, **Althausen, D.** and **Wandinger, U.** 2022. Ozone depletion in the Arctic and Antarctic stratosphere induced by wildfire smoke. *Atmos. Chem. Phys.*, **22**, 11701-11726. <https://doi.org/10.5194/acp-22-11701-2022>.
- Aregahegn, K. Z., **Felber, T.**, **Tilgner, A.**, **Hoffmann, E. H.**, **Schaefer, T.** and **Herrmann, H.** 2022. Kinetics and mechanisms of aqueous-phase reactions of triplet-state imidazole-2-carboxaldehyde and 3,4-dimethoxybenzaldehyde with α,β-unsaturated carbonyl compounds. *J. Phys. Chem. A*, **126**, 8727-8740. <https://doi.org/10.1021/acs.jpca.2c05015>.

Appendices: Publications

Artaxo, P., Hansson, H.-C., Andreae, M. O., Bäck, J., Alves, E. G., Barbosa, H. M. J., Bender, F., Bourtsoukidis, E., Carbone, S., Chi, J., Decesari, S., Després, V. R., Ditas, F., Ezhova, E., Fuzzi, S., Hasselquist, N. J., **Heintzenberg, J.**, Holanda, B. A., Guenther, A., Hakola, H., Heikkinen, L., Kerminen, V.-M., Kontkanen, J., Krejci, R., Kulmala, M., Lavric, J. V., de Leeuw, G., Lehtipalo, K., Machado, L. A. T., McFiggans, G., Franco, M. A. M., Meller, B. B., Morais, F. G., Mohr, C., Morgan, W., Nilsson, M. B., Peichl, M., Petäjä, T., Praß, M., Pöhlker, C., Pöhlker, M. L., Pöschl, U., Von Randow, C., Riipinen, I., Rinne, J., Rizzo, L. V., Rosenfeld, D., Silva Dias, M. A. F., Sogacheva, L., Stier, P., Swietlicki, E., Sörgel, M., Tunved, P., Virkkula, A., Wang, J., Weber, B., Yáñez-Serrano, A. M., Zieger, P., Mikhailov, E., Smith, J. N. and Kesselmeier, J. 2022. Tropical and Boreal Forest – Atmosphere Interactions: A Review. Tellus B: Chemical and Physical Meteorology, **74**, 24-163. <http://doi.org/10.16993/tellusb.34>.

Banks, J., Heinold, B. and Schepanski, K. 2022. Impacts of the desiccation of the Aral Sea on the Central Asian dust life-cycle. J. Geophys. Res. - Atmos., **127**, e2022JD036618. <https://doi.org/10.1029/2022JD036618>.

Banks, J., Heinold, B. and Schepanski, K. 2022. Dataset associated with Banks et al. (2022): Impacts of the desiccation of the Aral Sea on the Central Asian dust life-cycle [Dataset]. Data from: Zenodo, <https://doi.org/10.5281/zenodo.6022747>.

Barrientos-Velasco, C., Deneke, H., Hünerbein, A., Griesche, H. J., Seifert, P. and Macke, A. 2022. Radiative closure and cloud effects on the radiation budget based on satellite and shipborne observations during the Arctic summer research cruise, PS106. Atmos. Chem. Phys., **22**, 9313–9348. <https://doi.org/10.5194/acp-22-9313-2022>.

Becagli, S., Barbaro, E., Bonamano, S., Caiazzo, L., di Sarra, A., Feltracco, M., Grigioni, P., **Heintzenberg, J.**, Lazzara, L., Legrand, M., Madonia, A., Marcelli, M., Melillo, C., Meloni, D., Nuccio, C., Pace, G., Park, K.-T., Preunkert, S., Severi, M., Vecchiato, M., Zangrando, R. and Traversi, R. 2022. Factors controlling atmospheric DMS and its oxidation products (MSA and nssSO₄²⁻) in the aerosol at Terra Nova Bay, Antarctica. Atmos. Chem. Phys., **22**, 9245-9263. <https://doi.org/10.5194/acp-22-9245-2022>.

Beck, J., Brüggemann, M., van Pinxteren, D. and Herrmann, H. 2022. Nontarget approach to identify complexing agents in atmospheric aerosol and rainwater samples. Anal. Chem., **94**, 8966-8974. <https://doi.org/10.1021/acs.analchem.2c00815>.

Bergman, T., Makkonen, R., **Schrödner, R.**, Swietlicki, E., Phillips, V. T. J., Le Sager, P. and van Noije, T. 2022. Description and evaluation of a secondary organic aerosol and new particle formation scheme within TM5-MP v1.2. Geosci. Model Dev., **15**, 683-713. <https://doi.org/10.5194/gmd-15-683-2022>.

Berndt, T. 2022. Peroxy radical and product formation in the gas-phase ozonolysis of α -pinene under near-atmospheric conditions: Occurrence of an additional series of peroxy radicals $O_2O-C_{10}H_{15}O(O_2)_yO_2$ with $y = 1-3$. J. Phys. Chem. A, **126**, 6526-6537. <https://doi.org/10.1021/acs.jpca.2c05094>.

Berndt, T., Chen, J., Kjærgaard, E. R., Møller, K. H., **Tilgner, A.**, Hoffmann, E. H., **Herrmann, H.**, Crounse, J. D., Wenneberg, P. O. and Kjaergaard, H. G. 2022. Hydrotrioxide (ROOOH) formation in the atmosphere. Science, **376**, 979-982. <https://www.science.org/doi/abs/10.1126/science.abn6012>.

Bley, S., Rennie, M., Žagar, N., Pinol Sole, M., Straume, A. G., Antifaev, J., Candido, S., Carver, R., Fehr, T., von Bismarck, J., **Hünerbein, A.** and **Deneke, H.** 2022. Validation of the Aeolus L2B Rayleigh winds and ECMWF short-range forecasts in the upper troposphere and lower stratosphere using Loon super pressure balloon observations. Q. J. Roy. Meteor. Soc., **148**, 3852-3868. <https://doi.org/10.1002/qj.4391>.

Braga, R. C., Rosenfeld, D., Andreae, M. O., Pöhlker, C., Pöschl, U., Voigt, C., Weinzierl, B., Wendisch, M., **Pöhlker, M. L.** and Harrison, D. 2022. Detrainment Dominates CCN Concentrations Around Non-Precipitating Convective Clouds Over the Amazon. Geophys. Res. Lett., **49**, e2022GL100411. <https://doi.org/10.1029/2022GL100411>.

Bretschneider, L., Schlerf, A., Baum, A., Bohlius, H., Buchholz, M., **Düsing, S.**, Ebert, V., Erraji, H., Frost, P., **Käthner, R.**, Krüger, T., Lange, A. C., Langner, M., Nowak, A., Pätzold, F., Rüdiger, J., Saturno, J., Scholz, H., Schuldt, T., Seldschopf, R., Sobotta, A., Tillmann, R., **Wehner, B.**, Wesolek, C., Wolf, K. and Lampert, A. 2022. MesSBAR—multicopter and instrumentation for air quality research. Atmosphere, **13**, 629. <https://doi.org/10.3390/atmos13040629>.

Cai, D., Wang, X., George, C., Cheng, T., **Herrmann, H.**, Li, X. and Chen, J. 2022. Formation of secondary nitroaromatic compounds in polluted urban environments. J. Geophys. Res. - Atmos., **127**, e2021JD036167. <https://doi.org/10.1029/2021JD036167>.

Chen, G., Canonaco, F., Tobler, A., Aas, W., Alastuey, A., Allan, J., **Atabakhsh, S.**, Aurela, M., Baltensperger, U., Bougiatioti, A., De Brito, J. F., Ceburnis, D., Chazeau, B., Chebaicheb, H., Daellenbach, K. R., Ehn, M., El Haddad, I., Eleftheriadis, K., Favez, O., Flentje, H., Font, A., Fossum, K., Freney, E., Gini, M., Green, D.

Appendices: Publications

- C., Heikkinen, L., **Herrmann, H.**, Kalogridis, A. C., Keernik, H., Lhotka, R., Lin, C., Lunder, C., Maasikmets, M., Manousakas, M. I., Marchand, N., Marin, C., Marmureanu, L., Mihalopoulos, N., Močnik, G., Nęcki, J., O'Dowd, C., Ovadnevaite, J., Peter, T., J., P., Pikridas, M., Platt, S. M., Pokorná, P., **Poulain, L.**, Priestman, M., Riffault, V., **Rinaldi, M.**, Różański, K., Schwarz, J., Sciare, J., Simon, L., Skiba, A., Slowik, J. G., Sosedova, Y., Stavroulas, I., Styszko, K., Teinemaa, E., Timonen, H., Tremper, A., Vasilescu, J., Via, M., Vodička, P., **Wiedensohler, A.**, Zografou, O., Minguillón, M. C. and Prévôt, A. S. H. 2022. European aerosol phenomenology - 8: Harmonised source apportionment of organic aerosol using 22 Year-long ACSM/AMS datasets. *Environ. Internat.*, **166**, 107325. <https://doi.org/10.1016/j.envint.2022.107325>.
- Cheng, Z., Morgenstern, M., Zhang, B., Fraund, M., Lata, N. N., Brimberry, R., Marcus, M. A., Mazzoleni, L., Fialho, P., **Henning, S.**, **Wehner, B.**, Mazzoleni, C. and China, S. 2022. Particle phase-state variability in the North Atlantic free troposphere during summertime is determined by atmospheric transport patterns and sources. *Atmos. Chem. Phys.*, **22**, 9033-9057. <https://doi.org/10.5194/acp-22-9033-2022>.
- Choudhury, G., **Ansmann, A.** and Tesche, M. 2022. Evaluation of aerosol number concentrations from CALIPSO with ATom airborne in situ measurements. *Atmos. Chem. Phys.*, **22**, 7143-7161. <https://doi.org/10.5194/acp-22-7143-2022>.
- Christensen, M., Gettelman, A., Cermak, J., Dagan, G., Diamond, M., Douglas, A., Feingold, G., Glassmeier, F., Goren, T., Grosvenor, D., Gryspeerdt, E., Kahn, R., Li, Z., Ma, P.-L., Malavelle, F., McCoy, I. L., McCoy, D. T., McFarquhar, G., Mülmenstädt, J., Pal, S., Possner, A., Povey, A., Quaas, J., Rosenfeld, D., Schmidt, A., **Schrödner, R.**, Sorooshian, A., Stier, P., Toll, V., Watson-Parris, D., Wood, R., Yang, M. and Yuan, T. 2022. Opportunistic experiments to constrain aerosol effective radiative forcing. *Atmos. Chem. Phys.*, **22**, 641-674. <https://doi.org/10.5194/acp-22-641-2022>.
- Curtius, J., **Hermann, M.**, Karl, M., Lauenburg, M., **van Pinxteren, D.**, Schikowski, T., Schins, R., **Tuch, T.** and Vogel, A. 2022. *Detailliertes Konzept „Belastungsstudie Frankfurt Flughafen und Region“*. Goethe-Universität Frankfurt (GUF), Frankfurt/Main; Leibniz-Institut für Troposphärenforschung (TROPOS), Leipzig; Helmholtz-Zentrum hereon (HEREON), Geestacht; Leibniz-Institut für Umweltmedizinische Forschung (IUF), Düsseldorf. 58 pp.
- Dada, L., Angot, H., Beck, I., Baccarini, A., Quéléver, L. L. J., Boyer, M., Laurila, T., Brasseur, Z., Jozef, G., de Boer, G., Shupe, M. D., **Henning, S.**, Bucci, S., Dütsch, M., Stohl, A., Petäjä, T., Daellenbach, K. R., Jokinen, T. and Schmale, J. 2022. A central arctic extreme aerosol event triggered by a warm air-mass intrusion. *Nat. Commun.*, **13**, 5290. <https://doi.org/10.1038/s41467-022-32872-2>.
- Dall'Osto, M., Sotomayor-Garcia, A., Cabrera-Brufau, M., Berdalet, E., Vaqué, D., **Zeppenfeld, S.**, **van Pinxteren, M.**, **Herrmann, H.**, **Wex, H.**, Rinaldi, M., Paglione, M., Beddows, D., Harrison, R., Avila, C., Martin-Martin, R. P., Park, J. and Barbosa, A. 2022. Leaching material from Antarctic seaweeds and penguin guano effects cloud-relevant aerosol production. *Sci. Total Environ.*, **831**, 154772. <https://doi.org/10.1016/j.scitotenv.2022.154772>.
- Dall'Osto, M., Vaqué, D., Sotomayor, D. V. A., Cabrera-Brufau, M., Estrada, M., Buchaca, T., Soler, M., Nunes, S., **Zeppenfeld, S.**, **van Pinxteren, M.**, **Herrmann, H.**, **Wex, H.**, Rinaldi, M., Paglione, M., Beddows, D. C. S., Harrison, R. M. and Berdalet, E. 2022. Sea ice microbiota in the Antarctic Peninsula modulates cloud-relevant sea spray aerosol production. *Front. Mar. Sci.*, **9**, 827061. <https://doi.org/10.3389/fmars.2022.827061>.
- di Biagio, C., **Banks, J. R.** and Gaetani, M. 2022. Dust atmospheric transport over long distances. In: *J. F. Shroder (Ed.) Treatise on geomorphology*. Academic Press, London, p. 259-300. <https://doi.org/10.1016/B978-0-12-818234-5.12001-2>.
- Döscher, R., Acosta, M., Alessandri, A., Anthoni, P., Arsouze, T., Bergman, T., Bernardello, R., Boussetta, S., Caron, L. P., Carver, G., Castrillo, M., Catalano, F., Cvijanovic, I., Davini, P., Dekker, E., Doblas-Reyes, F. J., Docquier, D., Echevarria, P., Fladrich, U., Fuentes-Franco, R., Gröger, M., v. Hardenberg, J., Hieronymus, J., Karami, M. P., Keskinen, J. P., Koenigk, T., Makkonen, R., Massonnet, F., Ménégoz, M., Miller, P. A., Moreno-Chamarro, E., Nieradzik, L., van Noije, T., Nolan, P., O'Donnell, D., Ollinaho, P., van den Oord, G., Ortega, P., Prims, O. T., Ramos, A., Reerink, T., Rousset, C., Ruprich-Robert, Y., Le Sager, P., Schmith, T., **Schrödner, R.**, Serva, F., Sicardi, V., Sloth Madsen, M., Smith, B., Tian, T., Tourigny, E., Uotila, P., Vancoppenolle, M., Wang, S., Wårldin, D., Willén, U., Wyser, K., Yang, S., Yepes-Arbós, X. and Zhang, Q. 2022. The EC-Earth3 Earth system model for the Coupled Model Intercomparison Project 6. *Geosci. Model Dev.*, **15**, 2973-3020. <https://doi.org/10.5194/gmd-15-2973-2022>.
- Dragoneas, A., Molleker, S., Appel, O., Hüning, A., Böttger, T., **Hermann, M.**, Drewnick, F., Schneider, J., Weigel, R. and Borrmann, S. 2022. The realization of autonomous, aircraft-based, real-time aerosol mass

Appendices: Publications

- spectrometry in the upper troposphere and lower stratosphere. *Atmos. Meas. Tech.*, **15**, 5719-5742. <https://doi.org/10.5194/amt-15-5719-2022>.
- Drinovec, L., Jagodič, U., Pirker, L., Škarabot, M., Kurtjak, M., Vidović, K., Ferrero, L., Visser, B., Röhrbein, J., Weingartner, E., Kalbermatter, D. M., Vasilatou, K., Bühlmann, T., Pascale, C., Müller, T., Wiedensohler, A. and Močnik, G. 2022. A dual-wavelength photo-thermal aerosol absorption monitor: Design, calibration and performance. *Atmos. Meas. Tech.*, **15**, 3805–3825. <https://doi.org/10.5194/amt-15-3805-2022>.
- Dunker, S., Boyd, M., Durka, W., Erler, S., Harpole, W. S., Henning, S., Herzschuh, U., Hornick, T., Knight, T., Lips, S., Mäder, P., Švara, E. M., Mozarowski, S., Rakosy, D., Römermann, C., Schmitt-Jansen, M., Stoop-Leichsenring, K., Stratmann, F., Treudler, R., Virtanen, R., Wendt-Pothoff, K. and Wilhelm, C. 2022. The potential of multispectral imaging flow cytometry for environmental monitoring. *Cytometry A*, **101**, 782–799. <https://doi.org/10.1002/cyto.a.24658>.
- Ebell, K., Walbröl, A., Engelmann, R., Griesche, H., Radenz, M., Hofer, J. and Althausen, D. 2022. Temperature and humidity profiles, integrated water vapour and liquid water path derived from the HATPRO microwave radiometer onboard the Polarstern during the MOSAiC expedition. *Data from: Arctic Amplification (AC3), Multidisciplinary drifting Observatory for the Study of Arctic Climate (MOSAiC)*, PS122/1_1-38, PS122/2_14-18, PS122/3_28-6, PS122/4_43-11, PS122/4_43-145, PS122/5_58-3. PANGAEA, <https://doi.org/10.1594/PANGAEA.952139>.
- Efraim, A., Lauer, O., Rosenfeld, D., Braga, R. C., Franco, M. A., Kremer, L. A., Zhu, Y., Pöschl, U., Pöhlker, C., Andreae, M. O., Artaxo, P., de Araújo, A. C. and Pöhlker, M. L. 2022. Satellite-based detection of secondary droplet activation in convective clouds. *J. Geophys. Res. - Atmos.*, **127**, e2022JD036519. <https://doi.org/10.1029/2022JD036519>.
- Ehlers, F., Flament, T., Dabas, A., Trapón, D., Lacour, A., Baars, H. and Straume-Lindner, A. G. 2022. Optimization of Aeolus' aerosol optical properties by maximum-likelihood estimation. *Atmos. Meas. Tech.*, **15**, 185–203. <https://doi.org/10.5194/amt-15-185-2022>.
- Engelhardt, V., Pérez, T., Donoso, L., Müller, T. and Wiedensohler, A. 2022. Black carbon and particulate matter mass concentrations in the Metropolitan District of Caracas, Venezuela: An assessment of temporal variation and contributing sources. *Elem. Sci. Anth.*, **10**, 00024. <https://doi.org/10.1525/elementa.2022.00024>.
- Engelmann, R., Griesche, H., Radenz, M., Hofer, J., Althausen, D., Macke, A. and Hengst, R. 2022. Total Sky Imager observations during POLARSTERN cruise PS122/1 on 2019-10-01. *Data from: Multidisciplinary drifting Observatory for the Study of Arctic Climate (MOSAiC) / PS122/1_1-38*. PANGAEA, <https://doi.org/10.1594/PANGAEA.952139>.
- Escribano, J., Di Tomaso, E., Jorba, O., Klose, M., Ageitos, M. G., Macchia, F., Amiridis, V., Baars, H., Marinou, E., Proestakis, E., Urbanneck, C., Althausen, D., Bühl, J., Mamouri, R.-E. and García-Pando, C. P. 2022. Assimilating spaceborne lidar dust extinction can improve dust forecasts. *Atmos. Chem. Phys.*, **22**, 535–560. <https://doi.org/10.5194/acp-22-535-2022>.
- Feistel, R., Hellmuth, O. and Lovell-Smith, J. W. 2022. Defining relative humidity in terms of water activity: III. Relations to dew-point and frost-point temperatures. *Metrologia*, **59**, 045013. <https://doi.org/10.1088/1681-7575/ac7185>.
- Feldner, J., Ramacher, M. O. P., Karl, M., Quante, M. and Luttkus, M. L. 2022. Analysis of the effect of abiotic stressors on BVOC emissions from urban green infrastructure in northern Germany. *Environ. Sci.: Atmos.*, **2**, 1132-1151. <https://doi.org/10.1039/D2EA00038E>.
- Franke, S., Eckstaller, A., Heitland, T., Schaefer, T. and Asseng, J. 2022. The role of Antarctic overwintering teams and their significance for German polar research. *Polarforschung*, **90**, 65-79. <https://doi.org/10.5194/polf-90-65-2022>.
- Glojek, K., Gregorič, A., Mocnik, G., Drinovec, L., Alas, H. D. C., Cuesta-Mosquera, A., Weinhold, K., Merkel, M., Müller, T., Ristorini, M., van Pinxteren, D., Herrmann, H., Wiedensohler, A. and Ogrin, M. 2022. Onesnaženost zraka z delci in s črnim ogljikom. In: M. Ogrin (Ed.) *Geografski oris občine Loški Potok*. Univerza v Ljubljani, Filozofska fakulteta Ljubljana, p. 195-206 (Chapter 9). (GeograFF ; 25). <https://doi.org/10.4312/9789610605584>.

Appendices: Publications

- Glojek, K., Močnik, G., **Alas, H. D. C.**, Cuesta-Mosquera, A., Drinovec, L., Gregorić, A., Ogrin, M., **Weinhold, K.**, Ježek, I., Müller, T., Rigler, M., Remškar, M., van Pinxteren, D., Herrmann, H., Ristorini, M., Merkel, M., Markelj, M. and **Wiedensohler, A.** 2022. The impact of temperature inversions on black carbon and particle mass concentrations in a mountainous area. *Atmospheric Chemistry and Physics* **22**, 5577–5601. <https://doi.org/10.5194/acp-22-5577-2022>.
- Gong, X., Radenz, M., Wex, H., Seifert, P., Ataei, F., Henning, S., Baars, H., Barja, B., Ansmann, A. and Stratmann, F. 2022. Significant continental source of ice-nucleating particles at the tip of Chile's southernmost Patagonia region. *Atmos. Chem. Phys.*, **22**, 10505-10525. <https://doi.org/10.5194/acp-22-10505-2022>.
- Gong, X., Wex, H., Müller, T., Henning, S., Voigtlander, J., Wiedensohler, A. and Stratmann, F. 2022. Understanding aerosol microphysical properties from 10 years of data collected at Cabo Verde based on an unsupervised machine learning classification. *Atmos. Chem. Phys.*, **22**, 5175-5194. <https://doi.org/10.5194/acp-22-5175-2022>.
- Haarig, M., Ansmann, A., Engelmann, R., Baars, H., Toledoano, C., Torres, B., Althausen, D., Radenz, M. and Wandinger, U. 2022. First triple-wavelength lidar observations of depolarization and extinction-to-backscatter ratios of Saharan dust. *Atmos. Chem. Phys.*, **22**, 355-369. <https://doi.org/10.5194/acp-22-355-2022>.
- Hamilton, D. S., Perron, M. M. G., Bond, T. C., Bowie, A. R., Buchholz, R. R., Guieu, C., Ito, A., Maenhaut, W., Myriokefalitakis, S., Olgun, N., Rathod, S. D., Schepanski, K., Tagliabue, A., **Wagner, R.** and Mahowald, N. M. 2022. Earth, wind, fire, and pollution: Aerosol nutrient sources and impacts on ocean biogeochemistry. *Ann. Rev. Mar. Sci.*, **14**, 303-330. <https://doi.org/10.1146/annurev-marine-031921-013612>.
- Hartmann, S., Ling, M. L., Dreyer, L. S. A., Zipori, A., Finster, K., **Grave, S.**, Jensen, L. Z., Borck, S., Reicher, N., Drace, T., **Niedermeier, D.**, Jones, N. C., Hoffmann, S. V., **Wex, H.**, Rudich, Y., Boesen, T. and Šantl-Temkiv, T. 2022. Structure and protein-protein interactions of ice nucleation proteins drive their activity. *Front. Microbiol.*, **13**, 872306. <https://doi.org/10.3389/fmicb.2022.872306>.
- Heese, B., Floutsi, A. A., Baars, H., Althausen, D., Hofer, J., Herzog, A., Mewes, S., Radenz, M. and Schechner, Y. Y. 2022. The vertical aerosol type distribution above Israel – 2 years of lidar observations at the coastal city of Haifa. *Atmos. Chem. Phys.*, **22**, 1633-1648. <https://doi.org/10.5194/acp-22-1633-2022>.
- Heikenfeld, M., Freeman, S., Jones, W., Kukulies, J., **Senf, F.** and galexsky 2022. tobac-project/tobac: tobac 1.3.1 (v1.3.1). Zenodo, <https://doi.org/10.5281/zenodo.6761978>.
- Heikenfeld, M., Freeman, S., Jones, W., Kukulies, J., **Senf, F.** and galexsky 2022. tobac-project/tobac: tobac 1.3 (v1.3). Zenodo, <https://doi.org/10.5281/zenodo.6454129>.
- Heikenfeld, M., Freeman, S., Jones, W., Kukulies, J., **Senf, F.**, Pfeifer, N. and galexsky 2022. tobac-project/tobac: tobac 1.3.3 (v1.3.3). Zenodo, <https://doi.org/10.5281/zenodo.7062841>.
- Heikenfeld, M., Freeman, S., Jones, W., Kukulies, J., **Senf, F.**, Pfeifer, N. and galexsky 2022. tobac-project/tobac: tobac 1.3.2 (v1.3.2). Zenodo, <https://doi.org/10.5281/zenodo.6857618>.
- Heinold, B., Baars, H., Barja, B., Christensen, M., Kubin, A., Ohneiser, K., Schepanski, K., Schutgens, N., **Senf, F.**, Schrödner, R., Villanueva, D. and Tegen, I. 2022. Important role of stratospheric injection height for the distribution and radiative forcing of smoke aerosol from the 2019–2020 Australian wildfires. *Atmos. Chem. Phys.*, **22**, 9969-9985. <https://doi.org/10.5194/acp-22-9969-2022>.
- Hengst, R., Ohneiser, K., Hajipour, M., Witthuhn, J. and Engelmann, R. 2022. Total Sky Imager observations during POLARSTERN cruise PS127, Bremerhaven - Cape Town. Data from: PS127-track. PANGAEA, <https://doi.org/10.1594/PANGAEA.951342>.
- Henning, S. 2022. *Final Report on project STR 453/12-1: Study of cloud condensation nuclei and ice nucleating particles during the Antarctic Circumnavigation Expedition (ACE)*.
- Henning, S. 2022. *Final Report on project HE 6770/2-1: Vertical distribution of cloud condensation nuclei in marine and continental air masses over Europe and their connection to the cloud droplet number distribution in warm clouds*.
- Henning, S., Orth, L. M., Keck, H., Weller, R. and Stratmann, F. 2022. VACCINE (*Variation in Antarctic Cloud Condensation Nuclei (CCN) and Ice Nucleating Particle (INP) Concentrations at Neumayer Station III*). C. Wesche and J. Regnery (Ed.), In: *Expeditions to Antarctica: ANT-Land 2021/22 Neumayer Station III, Kohnen Station, Flight Operations and Field Campaigns*. Alfred-Wegener-Institut, Helmholtz-Zentrum für Polar- und Meeresforschung. Bremerhaven. **Berichte zur Polar- und Meeresforschung = Reports on Polar and Marine Research** ; **767**. 60-63 pp. https://doi.org/10.57738/BzPM_0767_2022.

Appendices: Publications

- Hernández Pardo, L., Morrison, H., Lauritzen, P. H. and **Pöhlker, M. L.** 2022. Impact of advection schemes on tracer interrelationships in large-eddy simulations of deep convection. *Mon. Wea. Rev.*, **150**, 2765-2785. <https://doi.org/10.1175/MWR-D-22-0025.1>.
- Hornick, T., Richter, A., Harpole, W. S., Bastl, M., Bohlmann, S., Bonn, A., Bumberger, J., Dietrich, P., Gemeinholzer, B., Grote, R., **Heinold, B.**, Keller, A., **Luttkus, M. L.**, Mäder, P., Motivans Švara, E., Passonneau, S., Punyasena, S. W., Rakosy, D., Richter, R., Sickel, W., Steffan-Dewenter, I., Theodorou, P., Treudler, R., Werchan, B., Werchan, M., **Wolke, R.** and Dunker, S. 2022. An integrative environmental pollen diversity assessment and its importance for the sustainable development goals. *Plants People Planet*, **4**, 110-121. <https://doi.org/10.1002/ppp3.10234>.
- Huang, S., Wu, Z., Wang, Y., **Poulain, L.**, Höpner, F., **Merkel, M.**, **Herrmann, H.** and **Wiedensohler, A.** 2022. Aerosol hygroscopicity and its link to chemical composition in a remote marine environment based on three transatlantic measurements. *Environ. Sci. Technol.*, **56**, 9613-9622. <https://doi.org/10.1021/acs.est.2c00785>.
- Janicke, U., **Gatzsche, K.**, **Wolke, R.**, **Tilgner, A.**, Lorentz, H. and Düring, I. 2022. *Chemische Umwandlungen in der anlagenbezogenen Ausbreitungsrechnung nach TA Luft (ChemTAL) (Zwischenbericht 2022-04)*. **UBA FKZ 3719 51 203 0 / Z 1.5 - 50 131-1/26**. 14 pp.
- Janicke, U., **Gatzsche, K.**, **Wolke, R.**, **Tilgner, A.**, Lorentz, H. and Düring, I. 2022. *Chemische Umwandlungen in der anlagenbezogenen Ausbreitungsrechnung nach TA Luft (ChemTAL) (Zwischenbericht 2022-10)*. **UBA FKZ 3719 51 203 0 / Z 1.5 - 50 131-1/26**. 36 pp.
- Kalesse-Los, H., Schimmel, W., Luke, E. and **Seifert, P.** 2022. Evaluating cloud liquid detection against Cloudnet using cloud radar Doppler spectra in a pre-trained artificial neural network. *Atmos. Meas. Tech.*, **15**, 279-295. <https://doi.org/10.5194/amt-15-279-2022>.
- Ke, J., Sun, Y., Dong, C., Zhang, X., Wang, Z., Lyu, L., Zhu, W., **Ansmann, A.**, Su, L., Bu, L., Xiao, D., Wang, S., Chen, S., Liu, J., Chen, W. and Liu, D. 2022. Development of China's first space-borne aerosol-cloud high-spectral-resolution lidar: retrieval algorithm and airborne demonstration. *PhotonX*, **3**, 17 (20 pp.). <https://doi.org/10.1186/s43074-022-00063-3>.
- Leinonen, V., Kokkola, H., Yli-Juuti, T., Mielonen, T., Kühn, T., Nieminen, T., Heikkinen, S., Miinalainen, T., Bergman, T., Carslaw, K., Decesari, S., Fiebig, M., Hussein, T., Kivekäs, N., Krejci, R., Kulmala, M., Leskinen, A., Massling, A., Mihalopoulos, N., Mulcahy, J. P., Noe, S. M., van Noije, T., O'Connor, F. M., O'Dowd, C., Olivie, D., Pernov, J. B., Petäjä, T., Selander, Ø., Schulz, M., Scott, C. E., Skov, H., Swietlicki, E., **Tuch, T.**, **Wiedensohler, A.**, Virtanen, A. and Mikkonen, S. 2022. Comparison of particle number size distribution trends in ground measurements and climate models. *Atmos. Chem. Phys.*, **22**, 12873-12905. <https://doi.org/10.5194/acp-22-12873-2022>.
- Lonardi, M., **Pilz, C.**, **Akansu, E. F.**, Dahlke, S., **Egerer, U.**, Ehrlich, A., **Griesche, H.**, Heymsfield, A. J., Kirbus, B., Schmitt, C. G., Shupe, M. D., **Siebert, H.**, **Wehner, B.** and Wendisch, M. 2022. Tethered balloon-borne profile measurements of atmospheric properties in the cloudy atmospheric boundary layer over the Arctic sea ice during MOSAiC: Overview and first results. *Elem. Sci. Anth.*, **10**, 000120. <https://doi.org/10.1525/elementa.2021.000120>.
- Lücke, J., Held, A., **Siebert, H.**, **Michalkow, M.** and **Wehner, B.** 2022. Vertical aerosol particle exchange in the marine boundary layer estimated from helicopter-borne measurements in the Azores region. *Atmos. Chem. Phys.*, **22**, 10007-10021. <https://doi.org/10.5194/acp-22-10007-2022>.
- Luttkus, M. L.**, Hoffmann, E., **Poulain, L.**, **Tilgner, A.** and **Wolke, R.** 2022. The effect of land use classification on the gas-phase and particle composition of the troposphere: Tree species versus forest type information. *J. Geophys. Res. - Atmos.*, **127**, e2021JD035305. <https://doi.org/10.1029/2021JD035305>.
- Madueño, L.**, **Kecorius, S.**, Löndahl, J., Schnelle-Kreis, J., **Wiedensohler, A.** and **Pöhlker, M.** 2022. A novel in-situ method to determine the respiratory tract deposition of carbonaceous particles reveals dangers of public commuting in highly polluted megacity. *Part. Fibre Toxicol.*, **19**, 61. <https://doi.org/10.1186/s12989-022-00501-x>.
- Man, R., Wu, Z., Zong, T., Voliotis, A., Qiu, Y., **Größ, J.**, **van Pinxteren, D.**, Zeng, L., **Herrmann, H.**, **Wiedensohler, A.** and Hu, M. 2022. Impact of water uptake and mixing state on submicron particle deposition in the human respiratory tract (HRT) based on explicit hygroscopicity measurements at HRT-like conditions. *Atmos. Chem. Phys.*, **22**, 12387-12399. <https://doi.org/10.5194/acp-22-12387-2022>.
- Mateus-Fontech, L., Vargas-Burbano, A., Jimenez, R., Rojas, N. Y., Rueda-Saa, G., **van Pinxteren, D.**, **van Pinxteren, M.**, **Fomba, K. W.** and **Herrmann, H.** 2022. Understanding aerosol composition in a tropical

Appendices: Publications

- inter-Andean valley impacted by agro-industrial and urban emissions. *Atmos. Chem. Phys.*, **22**, 8473-8495. <https://doi.org/10.5194/acp-22-8473-2022>.
- Mertes, S.** and **Wetzel, B.** 2022. Aerosol particle number concentration, size distribution, absorption coefficient and water vapor concentration measured during the HALO-mission CIRRUS-HL. *Data from: HALO database, German Aerospace Center*.
- Mettke, P., Mutzel, A., Böge, O. and Herrmann, H.** 2022. Synthesis and characterization of atmospherically relevant hydroxy hydroperoxides. *Atmosphere*, **13**, 507. <https://doi.org/10.3390/atmos13040507>.
- Nowak, J. L., Grosz, R., Frey, W., Niedermeier, D., Mijas, J., Malinowski, S. P., Ort, L., Schmalfuß, S., Stratmann, F., Voigtlander, J. and Stacewicz, T. 2022. Contactless optical hygrometry in LACIS-T. *Atmos. Meas. Tech.*, **15**, 4075-4089. <https://doi.org/10.5194/amt-15-4075-2022>.
- Ohneiser, K., Ansmann, A., Kaifler, B., Chudnovsky, A., Barja, B., Knopf, D. A., Kaifler, N., Baars, H., Seifert, P., Villanueva, D., Jimenez, C., Radenz, M., Engelmann, R., Veselovskii, I. and Zamorano, F.** 2022. Australian wildfire smoke in the stratosphere: The decay phase in 2020/2021 and impact on ozone depletion. *Atmos. Chem. Phys.*, **22**, 7417-7442. <https://doi.org/10.5194/acp-22-7417-2022>.
- Peng, X., Wang, T., Wang, W., Ravishankara, A. R., George, C., Xia, M., Cai, M., Li, Q., Salvador, C. M., Lau, C., Lyu, X., Poon, C. N., Mellouki, A., Mu, Y., Hallquist, M., Saiz-Lopez, A., Guo, H., Herrmann, H., Yu, C., Dai, J., Wang, Y., Wang, X., Yu, A., Leung, K., Lee, S. and Chen, J. 2022. Photodissociation of particulate nitrate as a source of daytime tropospheric Cl₂. *Nat. Commun.*, **13**, 939. <https://doi.org/10.1038/s41467-022-28383-9>.
- Pilz, C., Düsing, S., Wehner, B., Müller, T., Siebert, H., Voigtlander, J. and Lonardi, M.** 2022. CAMP: An instrumented platform for balloon-borne aerosol particle studies in the lower atmosphere. *Atmos. Meas. Tech.*, **15**, 6889-6905. <https://doi.org/10.5194/amt-15-6889-2022>.
- Pilz, C., Lonardi, M., Siebert, H. and Wehner, B.** 2022. Tethered balloon-borne measurements of aerosol particle microphysics during the MOSAiC expedition from June to July 2020. Leibniz-Institut für Troposphärenforschung e.V., Leipzig. *Data from: Arctic Amplification (AC3); Multidisciplinary drifting Observatory for the Study of Arctic Climate (MOSAiC). PANGAEA*, <https://doi.org/10.1594/PANGAEA.943907>.
- Pilz, C., Siebert, H. and Lonardi, M.** 2022. Tethered balloon-borne measurements of meteorological parameters during MOSAiC leg 4 in June and July 2020. *Data from: Arctic Amplification (AC3); Multidisciplinary drifting Observatory for the Study of Arctic Climate (MOSAiC). PANGAEA*, <https://doi.org/10.1594/PANGAEA.952341>.
- Platt, S. M., Hov, Ø., Berg, T., Breivik, K., Eckhardt, S., Eleftheriadis, K., Evangelou, N., Fiebig, M., Fisher, R., Hansen, G., Hansson, H.-C., Heintzenberg, J., Hermansen, O., Heslin-Rees, D., Holmén, K., Hudson, S., Kallenborn, R., Krejci, R., Krognes, T., Larssen, S., Lowry, D., Myhre, C. L., Lunder, C., Nisbet, E., Nizzetto, P. B., Park, K.-T., Pedersen, C. A., Pfaffhuber, K. A., Röckmann, T., Schmidbauer, N., Solberg, S., Stohl, A., Ström, J., Svendby, T., Tunved, P., Tørnvist, K., van der Veen, C., Vratolis, S., Yoon, Y. J., Yttri, K. E., Zieger, P., Aas, W. and Tørseth, K. 2022. Atmospheric composition in the European Arctic and 30 years of the Zeppelin Observatory, Ny-Ålesund. *Atmos. Chem. Phys.*, **22**, 3321-3369. <https://doi.org/10.5194/acp-22-3321-2022>.
- Poulain, L., Tilgner, A., Brüggemann, M., Mettke, P., He, L., Anders, J., Böge, O., Mutzel, A. and Herrmann, H.** 2022. Particle-phase uptake and chemistry of highly oxygenated organic molecules (HOMs) from α-pinene OH oxidation. *J. Geophys. Res. - Atmos.*, **127**, e2021JD036414. <https://doi.org/10.1029/2021JD036414>.
- Reifenberg, S. F., Martin, A., Kohl, M., Hamryszczak, Z., Tadic, I., Röder, L., Crowley, D. J., Fischer, H., Kaiser, K., Schneider, J., Dörich, R., Crowley, J. N., Tomsche, L., Marsing, A., Voigt, C., Zahn, A., Pöhlker, C., Holanda, B., Krüger, O., Pöschl, U., Pöhlker, M., Jöckel, P., Dorf, M., Schumann, U., Williams, J., Bohn, B., Curtius, J., Harder, H., Schlager, H., Lelieveld, J. and Pozzer, A. 2022. Numerical simulation of the impact of COVID-19 lockdown on tropospheric composition and aerosol radiative forcing in Europe. *Atmos. Chem. Phys.*, **22**, 10901-10917. <https://doi.org/10.5194/acp-22-10901-2022>.
- Richter, P., Palm, M., Weinzierl, C., Griesche, H., Rowe, P. M. and Notholt, J. 2022. A dataset of microphysical cloud parameters, retrieved from Fourier-transform infrared (FTIR) emission spectra measured in Arctic summer 2017. *Earth Syst. Sci. Data*, **14**, 2767-2784. <https://doi.org/10.5194/essd-14-2767-2022>.
- Rodriguez-Caballero, E., Stanelle, T., Egerer, S., Cheng, Y., Su, H., Canton, Y., Belnap, J., Andreae, M. O., Tegen, I., Reick, C. H., Pöschl, U. and Weber, B. 2022. Global cycling and climate effects of aeolian dust controlled by biological soil crusts. *Nat. Geosci.*, **15**, 458-463. <https://doi.org/10.1038/s41561-022-00942-1>.
- Romshoo, B., Pöhlker, M., Wiedensohler, A., Pfeifer, S., Saturno, J., Nowak, A., Ciupek, K., Quincey, P., Vasilatou, K., Ess, M. N., Gini, M., Eleftheriadis, K., Robins, C., Gaie-Levrel, F. and Müller, T.** 2022.

Appendices: Publications

- Importance of size representation and morphology in modelling optical properties of black carbon: comparison between laboratory measurements and model simulations. *Atmos. Meas. Tech.*, **15**, 6965-6989. <https://doi.org/10.5194/amt-15-6965-2022>.
- Salzmann, M., Ferrachat, S., Tully, C., Münch, S., Watson-Parris, D., Neubauer, D., Siegenthaler-Le Drian, C., Rast, S., **Heinold, B.**, Crueger, T., Brokopf, R., Mühlstädt, J., Quaas, J., Wan, H., Zhang, K., Lohmann, U., Stier, P. and **Tegen, I.** 2022. The global atmosphere-aerosol model ICON-A-HAM2.3—Initial model evaluation and effects of radiation balance tuning on aerosol optical thickness. *Journal of Advances in Modeling Earth Systems*, **14**, e2021MS002699. <https://doi.org/10.1029/2021MS002699>.
- Sartelet, K., Kim, Y., Couvidat, F., **Merkel, M.**, Petäjä, T., Sciare, J. and **Wiedensohler, A.** 2022. Influence of emission size distribution and nucleation on number concentrations over Greater Paris. *Atmos. Chem. Phys.*, **22**, 8579–8596. <https://doi.org/10.5194/acp-22-8579-2022>.
- Schaefer, J.**, **Grawe, S.** and **Stratmann, F.** 2022. Ice nucleating particle concentrations measured during the HALO mission CIRRUS-HL. *Data from: HALO database, German Aerospace Center*.
- Schimmel, W., Kalesse-Los, H., Maahn, M., Vogl, T., Foth, A., Saavedra Garfias, P. and **Seifert, P.** 2022. Identifying cloud droplets beyond lidar attenuation from vertically pointing cloud radar observations using artificial neural networks. *Atmos. Meas. Tech.*, **15**, 5343–5366. <https://doi.org/10.5194/amt-15-5343-2022>.
- Scholz, W., Mentler, B., Fischer, L., **Berndt, T.** and Hansel, A. 2022. The INNpinJeR: A new wall-free reactor for studying gas-phase reactions. *Environ. Sci.: Atmos.*, **2**, 73–84. <https://doi.org/10.1039/D1EA00072A>.
- Schulz, H., Franke, H., Quaglia, I., Stolla, K., **Engelmann, R.**, Lehmke, J., Ruhtz, T., **Skupin, A.** and Windmiller, J. 2022. Sounding data of SO284 (v1.0.0) [Data set]. *Data from: Zenodo*, <https://doi.org/10.5281/zenodo.7051674>.
- Shang, X., **Baars, H.**, Stachlewska, I. S., Mattis, I. and Komppula, M. 2022. Pollen observations at four EARLINET stations during the ACTRIS-COVID-19 campaign. *Atmos. Chem. Phys.*, **22**, 3931–3944. <https://doi.org/10.5194/acp-22-3931-2022>.
- Shupe, M. D., Rex, M., Blomquist, B., Persson, P. O. G., Schmale, J., Uttal, T., **Althausen, D.**, Angot, H., Archer, S., Bariteau, L., Beck, I., Bilberry, J., Bucci, S., Buck, C., Boyer, M., Brasseur, Z., Brooks, I. M., Calmer, R., Cassano, J., Castro, V., Chu, D., Costa, D., Cox, C. J., Creamean, J., Crewell, S., Dahlke, S., Damm, E., de Boer, G., Deckelmann, H., Dethloff, K., Dütsch, M., Eboll, K., Ehrlich, A., Ellis, J., **Engelmann, R.**, Fong, A. A., Frey, M. M., Gallagher, M. R., Ganzeveld, L., Gradinger, R., Graeser, J., Greenamyer, V., **Griesche, H.**, Griffiths, S., Hamilton, J., Heinemann, G., Helmig, D., Herber, A., Heuzé, C., **Hofer, J.**, Houchens, T., Howard, D., Inoue, J., Jacobi, H.-W., Jaiser, R., Jokinen, T., Jourdan, O., Jozef, G., King, W., Kirchgaessner, A., Klingebiel, M., Krassovski, M., Krumpen, T., Lampert, A., Landing, W., Laurila, T., Lawrence, D., Lonardi, M., Loose, B., Lüpkes, C., Maahn, M., **Macke, A.**, Maslowski, W., Marsay, C., Maturilli, M., Mech, M., Morris, S., Moser, M., Nicolaus, M., Ortega, P., Osborn, J., Pätzold, F., Perovich, D. K., Petäjä, T., **Pilz, C.**, Pirazzini, R., Posman, K., Powers, H., Pratt, K. A., Preußer, A., Quéléver, L., **Radenz, M.**, Rabe, B., Rinke, A., Sachs, T., Schulz, A., **Siebert, H.**, Silva, T., Solomon, A., Sommerfeld, A., Spreen, G., Stephens, M., Stohl, A., Svensson, G., Uin, J., Viegas, J., Voigt, C., von der Gathen, P., **Wehner, B.**, Welker, J. M., Wendisch, M., Werner, M., Xie, Z. Q. and Yue, F. 2022. Overview of the MOSAiC expedition: Atmosphere. *Elem. Sci. Anth.*, **10**, 00060. <https://doi.org/10.1525/elementa.2021.00060>.
- Sicard, M., Córdoba-Jabonero, C., López-Cayuela, M.-Á., **Ansmann, A.**, Comerón, A., Zorzano, M.-P., Rodríguez-Gómez, A. and Muñoz-Porcar, C. 2022. Aerosol radiative impact during the summer 2019 heatwave produced partly by an inter-continental Saharan dust outbreak – Part 2: Long-wave and net dust direct radiative effect. *Atmos. Chem. Phys.*, **22**, 1921–1937. <https://doi.org/10.5194/acp-22-1921-2022>.
- Skupin, A.**, **Engelmann, R.** and **Baars, H.** 2022. Lidar für die Atmosphärenforschung. *Gefahrst. Reinhalt. L.*, **82**, 253–254. <https://doi.org/10.37544/0949-8036-2022-09-10-31>.
- Snijders-Leijonmalm, P., Flores, H., Sakinan, S., Hildebrandt, N., Svenson, A., Castellani, G., Vane, K., Mark, F. C., Heuzé, C., Tippenhauer, S., Niehoff, B., Hjelm, J., Hentati Sundberg, J., Schaafsma, F. L., **Engelmann, R.** and EFICA-MOSAiC-TEAM 2022. Unexpected fish and squid in the central Arctic deep scattering layer. *Sci. Adv.*, **8**, 17 pp (18 February 2022). <https://www.science.org/doi/full/10.1126/sciadv.abj7536>.
- Spänkuch, D., **Hellmuth, O.** and Görsdorf, U. 2022. What is a cloud? Toward a more precise definition. *Bull. Amer. Meteor. Soc.*, **103**, E1894–E1929. <https://doi.org/10.1175/BAMS-D-21-0032.1>.
- Tatzelt, C.**, **Henning, S.**, Welti, A., Baccarini, A., **Hartmann, M.**, Gysel-Beer, M., **van Pinxteren, M.**, Modini, R. L., Schmale, J. and **Stratmann, F.** 2022. Circum-Antarctic abundance and properties of CCN and INPs. *Atmos. Chem. Phys.*, **22**, 9721–9745. <https://doi.org/10.5194/acp-22-9721-2022>.

Appendices: Publications

- Teri, M., Müller, T., Gasteiger, J., Valentini, S., Horvath, H., Vecchi, R., Bauer, P., Walser, A. and Weinzierl, B. 2022. Impact of particle size, refractive index, and shape on the determination of the particle scattering coefficient – an optical closure study evaluating different nephelometer angular truncation and illumination corrections. *Atmos. Meas. Tech.*, **15**, 3161. <https://doi.org/10.5194/amt-15-3161-2022>.
- Timmermans, R., van Pinxteren, D., Kranenburg, K., Hendriks, C., Fomba, K. W., Herrmann, H. and Schaap, M. 2022. Evaluation of modelled LOTOS-EUROS with observational based PM10 source attribution. *Atmos. Environ.*: X, **14**, 100173. <https://doi.org/10.1016/j.aeaoa.2022.100173>.
- Tzallas, V., Hünerbein, A., Deneke, H., Stengel, M., Meirink, J. F., Benas, N., Trentmann, J. and Macke, A. 2022. CRAAS: Cloud Regime dAtAset based on the CLAAS-2.1 climate data record [Data set]. *Data from: Zenodo*, <https://doi.org/10.5281/zenodo.7120267>.
- Tzallas, V., Hünerbein, A., Deneke, H., Stengel, M., Meirink, J. F., Benas, N., Trentmann, J. and Macke, A. 2022. CRAAS: A European Cloud Regime dAtAset Based on the CLAAS-2.1 Climate Data Record. *Remote Sens.*, **14**, 5548. <https://doi.org/10.3390/rs14215548>.
- Ungeheuer, F., Caudillo, L., Ditas, F., Simon, M., van Pinxteren, D., Kılıç, D., Rose, D., Jacobi, S., Kürten, A., Curtius, J. and Vogel, A. L. 2022. Nucleation of jet engine oil vapours is a large source of aviation-related ultrafine particles. *Commun. Earth Environ.*, **3**, 319. <https://doi.org/10.1038/s43247-022-00653-w>.
- Vainiger, A., Shubi, O., Schechner, Y. Y., Zhenping, Y., Baars, H., Heese, B. and Althausen, D. 2022. ALiDAn: Spatiotemporal and multiwavelength atmospheric lidar data augmentation. *IEEE T. Geosci. Remote*, **60**, 1-17, Art no. 5705517. <https://ieeexplore.ieee.org/document/9870174/>.
- van Pinxteren, D., Fuchs, S. and Herrmann, H. 2022. Bereitstellung einer Methode zur Bestimmung von Levoglucosan und weiteren Tracersubstanzen in Filterproben für das UBA-Luftmessnetz (Abschlussbericht). Umweltbundesamt, Vorhaben Z 1.5 - 54 550-4/16; Projekt-Nr. 133383.
- van Pinxteren, D. and Herrmann, H. 2022. Einfluss der Trockenheit auf die PM10-Konzentrationen (Abschlussbericht). Landesamt für Umwelt, Landwirtschaft und Geologie (LfULG), Vorhaben 51-Z1017/21.
- van Pinxteren, D., Wang, Y., Engelhardt, V., Heinold, B., Schacht, J., Stoll, J., Wolke, R. and Herrmann, H. 2022. Tendenzen, Verursacher und Auswirkungen der Ozonbelastung in Sachsen (Abschlussbericht). LfULG-Projekt.
- van Pinxteren, M., Robinson, T.-B., Zeppenfeld, S., Gong, X., Bahlmann, E., Fomba, K. W., Triesch, N., Stratmann, F., Wurl, O., Engel, A., Wex, H. and Herrmann, H. 2022. High number concentrations of transparent exopolymer particles in ambient aerosol particles and cloud water – A case study at the tropical Atlantic Ocean. *Atmos. Chem. Phys.*, **22**, 5725-5742. <https://doi.org/10.5194/acp-22-5725-2022>.
- van Zadelhoff, G.-J., Barker, H. W., Baudrez, E., Bley, S., Clerbaux, N., Cole, J. N. S., de Kloe, J., Docter, N., Domenech, C., Donovan, D. P., Dufresne, J.-L., Eisinger, M., Fischer, J., García-Marañón, R., Haarig, M., Hogan, R. J., Hünerbein, A., Kollias, P., Koopman, R., Madenach, N., Mason, S. L., Preusker, R., Puigdomènech Treserras, B., Qu, Z., Ruiz-Saldaña, M., Shephard, M., Velázquez-Blazquez, A., Villefranque, N., Wandinger, U., Wang, P. and Wehr, T. 2022. EarthCARE level-2 demonstration products from simulated scenes (09.01) [Data set]. *Data from: Zenodo*, <https://doi.org/10.5281/zenodo.7117116>.
- van Zadelhoff, G.-J., Barker, H. W., Baudrez, E., Bley, S., Clerbaux, N., Cole, J. N. S., de Kloe, J., Docter, N., Domenech, C., Donovan, D. P., Dufresne, J.-L., Eisinger, M., Fischer, J., García-Marañón, R., Haarig, M., Hogan, R. J., Hünerbein, A., Kollias, P., Koopman, R., Madenach, N., Mason, S. L., Preusker, R., Puigdomènech Treserras, B., Qu, Z., Ruiz-Saldaña, M., Shephard, M., Velázquez-Blazquez, A., Villefranque, N., Wandinger, U., Wang, P. and Wehr, T. 2022. EarthCARE level-2 demonstration products from simulated scenes (10.01) [Data set]. *Data from: Zenodo*, <https://doi.org/10.5281/zenodo.7311704>.
- Vernooij, R., Winiger, P., Wooster, M., Strydom, T., Poulain, L., Dusek, U., Grosvenor, M., Roberts, G. J., Schutgens, N. and van der Werf, G. R. 2022. A quadcopter unmanned aerial system (UAS)-based methodology for measuring biomass burning emission factors. *Atmos. Meas. Tech.*, **15**, 4271-4294. <https://doi.org/10.5194/amt-15-4271-2022>.
- Veselovskii, I., Hu, Q., Ansmann, A., Goloub, P., Podvin, T. and Korenskiy, M. 2022. Fluorescence lidar observations of wildfire smoke inside cirrus: a contribution to smoke–cirrus interaction research. *Atmos. Chem. Phys.*, **22**, 5209-5221. <https://doi.org/10.5194/acp-22-5209-2022>.
- Vogel, D. and Knoth, O. 2022. High-order polynomial recovery in finite element advection schemes. In: D. Zeidan, J. Merker, E. G. Da Silva, and L. T. Zhang (Eds.), *Numerical fluid dynamics : Methods and computations*. Springer, Singapore, p. 93-120. (Forum for Interdisciplinary Mathematics (FFIM)). <https://doi.org/10.1007/978-981-16-9665-7>.

Appendices: Publications

- Voigt, C., Lelieveld, J., Schlager, H., Schneider, J., Curtius, J., Meerkötter, R., Sauer, D., Bugliaro, L., Bohn, B., Crowley, J. N., Erbertseder, T., Groß, S., Hahn, V., Li, Q., Mertens, M., **Pöhlker, M. L.**, Pozzer, A., Schumann, U., Tomsche, L., Williams, J., Zahn, A., Andreae, M., Borrmann, S., Bräuer, T., Dörich, R., Dörnbrack, A., Edtbauer, A., Ernle, L., Fischer, H., Giez, A., Granzin, M., Grewe, V., Harder, H., Heinritzi, M., Holanda, B. A., Jöckel, P., Kaiser, K., Krüger, O. O., Lucke, J., Marsing, A., Martin, A., Matthes, S., Pöhlker, C., Pöschl, U., Reifenberg, S., Ringsdorf, A., Scheibe, M., Tadic, I., Zauner-Wieczorek, M., Henke, R. and Rapp, M. 2022. Cleaner skies during the COVID-19 lockdown. Bull. Amer. Meteor. Soc., **103**, E1796-E1827. <https://doi.org/10.1175/BAMS-D-21-0012.1>
- Waclawczyk, M., Nowak, J. L., **Siebert, H.** and Malinowski, S. P. 2022. Detecting nonequilibrium states in atmospheric turbulence. J. Atmos. Sci., **79**, 2757–2772 <https://doi.org/10.1175/JAS-D-22-0028.1>.
- Walbröl, A., Crewell, S., **Engelmann, R.**, Orlandi, E., **Griesche, H.**, **Radenz, M.**, **Hofer, J.**, **Althausen, D.**, Maturilli, M. and Ebelt, K. 2022. Atmospheric temperature, water vapour and liquid water path from two microwave radiometers during MOSAiC. Sci. Data, **9**, 534. <https://doi.org/10.1038/s41597-022-01504-1>.
- Wang, Y., Amodeo, A., O'Connor, E. J., **Baars, H.**, Bortoli, D., Hu, Q., Sun, D. and D'Amico, G. 2022. Numerical weather predictions and re-analysis as input for lidar inversions: Assessment of the impact on optical products Remote Sens., **14**, 2342. <https://doi.org/10.3390/rs14102342>.
- Wang, Y., Henning, S., Poulain, L., Lu, C., Stratmann, F., Wang, Y., Niu, S., Pöhlker, M. L., Herrmann, H. and Wiedensohler, A.** 2022. Aerosol activation characteristics and prediction at the central European ACTRIS research station of Melpitz, Germany. Atmos. Chem. Phys., **22**, 15943-15962. <https://doi.org/10.5194/acp-22-15943-2022>.
- Weger, M., **Baars, H.**, Gebauer, H., Merkel, M., **Wiedensohler, A.** and **Heinold, B.** 2022. On the application and grid-size sensitivity of the urban dispersion model CAIRDIO v2.0 under real city weather conditions. Geosci. Model Dev., **15**, 3315–3345. <https://doi.org/10.5194/gmd-15-3315-2022>.
- Weger, M., **Heinold, B.** and **Knoth, O.** 2022. CAIRDIO City-Scale Air Dispersion Model with Diffusive Obstacles (Version 2.1). Zenodo, <http://doi.org/10.5281/zenodo.7409604>.
- Weger, M., **Heinold, B.** and **Knoth, O.** 2022. CAIRDIO City-Scale Air Dispersion Model with Diffusive Obstacles (Version 2.0). Zenodo, <http://doi.org/10.5281/zenodo.6075354>.
- Wen, L., Schaefer, T., Zhang, Y., He, L., Ventura, O. N. and Herrmann, H. 2022. T- and pH-dependent OH radical reaction kinetics with glycine, alanine, serine, and threonine in the aqueous phase. Phys. Chem. Chem. Phys., **24**, 11054-11065. <https://doi.org/10.1039/D1CP05186E>
- Wieder, J., Ihn, N., Mignani, C., **Haarig, M.**, Bühl, J., Seifert, P., **Engelmann, R.**, Ramelli, F., Kanji, Z. A., Lohmann, U. and Henneberger, J. 2022. Retrieving ice-nucleating particle concentration and ice multiplication factors using active remote sensing validated by in situ observations. Atmos. Chem. Phys., **22**, 9767-9797. <https://doi.org/10.5194/acp-22-9767-2022>.
- Winkler, U.** 2022. *Bewertende Literaturstudie zum Auftreten, zur Ausbreitung und zu gesundheitlichen Auswirkungen von ionisierten Schadstoffpartikeln in der Umgebung von Starkstromleitungen - Vorhaben 3618S82453. Bundesamt für Strahlenschutz (BfS) 2022, Ressortforschungsberichte zum Strahlenschutz, BfS-RESFOR-195/22.* 309 pp. <https://www.emf-portal.org/de/article/47588>.
- Xavier, C., Baykara, M., Wollesen de Jonge, R., Altstädter, B., Clusius, P., Vakkari, V., Thakur, R., Beck, L., Becagli, S., Severi, M., Traversi, R., Krejci, R., Tunved, P., Mazzola, M., **Wehner, B.**, Sipilä, M., Kulmala, M., Boy, M. and Roldin, P. 2022. Secondary aerosol formation in marine Arctic environments: A model measurement comparison at Ny-Ålesund. Atmos. Chem. Phys., **22**, 10023-10043. <https://doi.org/10.5194/acp-22-10023-2022>.
- Yáñez-Serrano, A. M., Aguilos, M., Barbosa, C., Bolaño-Ortiz, T. R., Carbone, S., Díaz-López, S., Diez, S., Dominutti, P., **Engelhardt, V.**, Gomes Alves, E., Pedraza, J., Saturno, J. and Tzompa-Sosa, Z. A. 2022. The Latin America Early Career Earth System Scientist Network (LAECCESS): Addressing present and future challenges of the upcoming generations of scientists in the region. npj Clim. Atmos. Sci., **5**, Article number 79. <https://doi.org/10.1038/s41612-022-00300-3>.
- Yang, D., Schaefer, T., Wen, L. and Herrmann, H. 2022. Temperature- and pH- dependent OH radical reaction kinetics of tartaric and mucic acids in the aqueous phase. J. Phys. Chem. A, **126**, 6244-6252. <https://doi.org/10.1021/acs.jpca.2c03044>.
- Zhang, Y., He, L., Sun, X., Ventura, O. N. and Herrmann, H. 2022. Theoretical investigation on the oligomerization of methylglyoxal and glyoxal in aqueous atmospheric aerosol particles. ACS Earth Space Chem., Online first. <https://doi.org/10.1021/acsearthspacechem.1c00422>.

Appendices: Publications

- Zhang, Z., Jiang, J., Lu, B., Meng, X., **Herrmann, H.**, Cheng, J. and Li, X. 2022. Attributing increases in ozone to accelerated oxidation of volatile organic compounds at reduced nitrogen oxides concentrations. PNAS Nexus, **1**, 1-10. <https://doi.org/10.1093/pnasnexus/pgac266>.
- Zhi, M., Zhang, K., Zhang, X. C., **Herrmann, H.**, Gao, J., **Fomba, K. W.**, Tang, W., Luo, Y., Li, H. and Meng, F. 2022. A statistic comparison of multi-element analysis of low atmospheric fine particles ($PM_{2.5}$) using different spectroscopy techniques. J. Environ. Sci. (China), **114**, 194-203. <https://doi.org/10.1016/j.jes.2021.08.034>.
- Zhu, Y., Tilgner, A., Hoffmann, E. H., Herrmann, H.**, Kawamura, K., Xue, L., Yang, L. and Wang, W. 2022. Molecular distributions of dicarboxylic acids, oxocarboxylic acids, and α -dicarbonyls in aerosols over Tuoji Island in the Bohai Sea: Effects of East Asian continental outflow. Atmos. Res., **272**, 106154. <https://doi.org/10.1016/j.atmosres.2022.106154>.
- Zong, T., Wang, H., Wu, Z., Lu, K., Wang, Y., Zhu, Y., Shang, D., Fang, X., Huang, X., He, L., Ma, N., **Größ, J.**, Huang, S., Guo, S., Zeng, L., **Herrmann, H.**, **Wiedensohler, A.**, Zhang, Y. and Hu, M. 2022. Particle hygroscopicity inhomogeneity and its impact on reactive uptake. Sci. Total Environ., **811**, 151364. <https://doi.org/10.1016/j.scitotenv.2021.151364>.

2023

- Adebiyi, A., Kok, J. F., Murray, B. J., Ryder, C. L., Stuut, J.-B. W., Kahn, R. A., Knippertz, P., Formenti, P., Mahowald, N. M., Garcia-Pando, C. P., Klose, M., **Ansmann, A.**, Samset, B. H., Ito, A., Balkanski, Y., Di Bagio, C., Romanias, M. N., Huang, Y. and Meng, J. 2023. A review of coarse mineral dust in the Earth system. Aeolian Res., **60**, 100849. <https://doi.org/10.1016/j.aeolia.2022.100849>.
- Akansu, E. F.**, Dahlke, S., **Siebert, H.** and Wendisch, M. 2023. Evaluation of methods to determine the surface mixing layer height of the atmospheric boundary layer in the central Arctic during polar night and transition to polar day in cloudless and cloudy conditions. Atmos. Chem. Phys., **23**, 15473-15489. <https://doi.org/10.5194/acp-23-15473-2023>.
- Akansu, E. F.**, Egerer, U. and **Siebert, H.** 2023. Energy Dissipation Rate calculation algorithm for tethered balloon-borne turbulence observations during MOSAiC Legs 1, 2, and 3. Zenodo, <https://doi.org/10.5281/zenodo.8116420>.
- Akansu, E. F., Siebert, H.**, Dahlke, S., Graeser, J., Jaiser, R. and Sommerfeld, A. 2023. Tethered balloon-borne turbulence measurements in winter and spring during the MOSAiC expedition. Sci. Data, **10**, 723. <https://doi.org/10.1038/s41597-023-02582-5>.
- Akansu, E. F., Siebert, H.**, Dahlke, S., Graeser, J., Jaiser, R. and Sommerfeld, A. 2023. Tethered balloon-borne measurements of turbulence during the MOSAiC expedition from December 2019 to May 2020. *Data from: Arctic Amplification (AC3); Multidisciplinary drifting Observatory for the Study of Arctic Climate (MOSAiC)*. PANGAEA, <https://doi.org/10.1594/PANGAEA.962309>.
- Alpert, P. A., Bernard, F., Connolly, P., Crabeck, O., George, C., Kaiser, J., Möhler, O., **Niedermeier, D.**, Nowak, J., Perrier, S., Seakins, P., **Stratmann, F.** and Thomas, M. 2023. Application of simulation chambers to investigate interfacial processes. In: *J.-F. Doussin, H. Fuchs, A. Kiendler-Scharr, P. Seakins, and J. Wenger (Eds.), A practical guide to atmospheric simulation chambers*. Springer, Cham, Switzerland, p. 293-330 (Chapter 8). <https://doi.org/10.1007/978-3-031-22277-1>.
- Althausen, D.** 2023. VDI-Richtlinie VDI 3786 Blatt 23 - Entwurf : Umweltmeteorologie - Bodengebundene Fernmessung meteorologischer Parameter - Mikrowellenradiometer / Environmental meteorology - Ground-based remote sensing of meteorological parameters - Microwave radiometers. VDI-Verl., Düsseldorf, 36 pp. (Auch enthalten in: VDI/DIN-Handbuch Reinhaltung der Luft - Band 1a: Maximale Immissions-Werte; Band 1B: Umweltmeteorologie). <https://www.vdi.de/richtlinien/details/vdi-3786-blatt-23-umweltmeteorologie-bodengebundene-fernmessung-meteorologischer-parameter-mikrowellenradiometer>.
- Amiridis, V., Marinou, E., Paschou, P., **Baars, H.**, Pirloaga, R., **Engelmann, R.**, Tsakiri, A., Tsikoudi, I., Daskalopoulou, V., Kazadzis, S., **Skupin, A.**, Marenco, F., Kezoudi, M., Kouklaki, D., Siomos, N., **Floutsi, A. A.**, Metallinos, S., Spanakis Misirlis, V., Raptis, P., **Althausen, D.**, **Seifert, P.**, Nemuc, A., Antonescu, B., Alkritis, P. and **Wandinger, U.** 2023. ASKOS Campaign Dataset. *Data from: ESA Atmospheric Validation Data Centre (EVDC)*, <https://doi.org/10.60621/jatac.campaign.2021.2022.caboverde>.
- Ansmann, A., Ohneiser, K., Engelmann, R., Radenz, M., Griesche, H., Hofer, J., Althausen, D.**, Creamean, J. M., Boyer, M. C., Knopf, D. A., Dahlke, S., Maturilli, M., **Gebauer, H.**, Bühl, J., Jimenez, C., **Seifert, P.** and **Wandinger, U.** 2023. Annual cycle of aerosol properties over the central Arctic during MOSAiC

Appendices: Publications

- 2019–2020 — light-extinction, CCN, and INP levels from the boundary layer to the tropopause. *Atmos. Chem. Phys.*, **23**, 12821–12849. <https://doi.org/10.5194/acp-23-12821-2023>.
- Atabakhsh, S., Poulain, L., Chen, G., Canonaco, F., Prévôt, A. S. H., Pöhlker, M., Wiedensohler, A. and Herrmann, H.** 2023. A 1-year aerosol chemical speciation monitor (ACSM) source analysis of organic aerosol particle contributions from anthropogenic sources after long-range transport at the TROPOS research station Melpitz. *Atmos. Chem. Phys.*, **23**, 6963–6988. <https://doi.org/10.5194/acp-23-6963-2023>.
- Baars, H., Engelmann, R., Seifert, P. and Wandinger, U.** 2023. *EVAA: Experimentelle Validierung und Assimilation von Aeolus Beobachtungen - Validierung der Wind- und Aerosolprodukte der europäischen Satellitenmission Aeolus und Assimilationsexperimente mit numerischen Modellen zur Wettervorhersage : Teilprojekt 5: Validierung der Aerosol- und Windprodukte durch bodengebundene Instrumente des TROPOS (Schlussbericht)*. DLR-Förderkennzeichen: 50EE1721C. 14 pp.
- Baars, H., Walchester, J., Basharova, E., Gebauer, H., Radenz, M., Bühl, J., Barja, B., Wandinger, U. and Seifert, P.** 2023. Long-term validation of Aeolus L2B wind products at Punta Arenas, Chile and Leipzig, Germany. *Atmos. Meas. Tech.*, **16**, 3809–3834. <https://doi.org/10.5194/amt-16-3809-2023>.
- Bagheri, G., Schlenczek, O., Turco, L., Thiede, B., Stieger, K., Kosub, J. M., Clauberg, S., Pöhlker, M. L., Pöhlker, C., Moláček, J., Scheithauer, S. and Bodenschatz, E. 2023. Size, concentration, and origin of human exhaled particles and their dependence on human factors with implications on infection transmission. *J. Aerosol Sci.*, **168**, 106102. <https://doi.org/10.1016/j.jaerosci.2022.106102>.
- Banks, J., Heinold, B. and Schepanski, K.** 2023. Dataset associated with Banks et al. (2023): “Radiative cooling and atmospheric perturbation effects of dust aerosol from the Aralkum Desert in Central Asia” [Dataset]. Data from: Zenodo, <https://doi.org/10.5281/zenodo.10143872>.
- Banks, J., Heinold, B. and Schepanski, K.** 2023. Python code associated with Banks et al. (2023): “Radiative cooling and atmospheric perturbation effects of dust aerosol from the Aralkum Desert in Central Asia” [Software]. Zenodo, <https://doi.org/10.5281/zenodo.10160848>.
- Berndt, T., Hoffmann, E. H., Tilgner, A., Stratmann, F. and Herrmann, H.** 2023. Direct sulfuric acid formation from the gas-phase oxidation of reduced-sulfur compounds. *Nat. Commun.*, **14**, 4849. <https://doi.org/10.1038/s41467-023-40586-2>.
- Borrás, E., Herrmann, H., Kalberer, M., Muñoz, A., Mutzel, A., Vera, T. and Wenger, J. 2023. Sampling for offline analysis. In: J.-F. Doussin, H. Fuchs, A. Kiendler-Scharr, P. Seakins, and J. Wenger (Eds.), *A practical guide to atmospheric simulation chambers*. Springer, Cham, Switzerland, p. 207–240 (Chapter 6). <https://doi.org/10.1007/978-3-031-22277-1>.
- Boyer, M., Aliaga, D., Pernov, J. B., Angot, H., Quéléver, L. L. J., Dada, L., Heutte, B., Dall’Osto, M., Beddows, D. C. S., Brasseur, Z., Beck, I., Bucci, S., Duetsch, M., Stohl, A., Laurila, T., Asmi, E., Massling, A., Thomas, D. C., Nøjgaard, J. K., Chan, T., Sharma, S., Tunved, P., Krejci, R., Hansson, H. C., Bianchi, F., Lehtipalo, K., Wiedensohler, A., Weinhold, K., Kulmala, M., Petäjä, T., Sipilä, M., Schmale, J. and Jokinen, T. 2023. A full year of aerosol size distribution data from the central Arctic under an extreme positive Arctic Oscillation: insights from the Multidisciplinary drifting Observatory for the Study of Arctic Climate (MOSAiC) expedition. *Atmos. Chem. Phys.*, **23**, 389–415. <https://doi.org/10.5194/acp-23-389-2023>.
- Bredeck, G., Busch, M., Rossi, A., Stahlmecke, B., Fomba, K. W., Herrmann, H. and Schins, R. P. F. 2023. Inhalable Saharan dust induces oxidative stress, NLRP3 inflammasome activation, and inflammatory cytokine release. *Environ. Internat.*, **172**, 107732. <https://doi.org/10.1016/j.envint.2023.107732>.
- Chappell, A., Webb, N. P., Hennen, M., Schepanski, K., Ciais, P., Balkanski, Y., Zender, C. S., Tegen, I., Zeng, Z., Tong, D., Baker, B., Ekström, M., Baddock, M., Eckardt, F. D., Kandakji, T., Lee, J. A., Nobakht, M., von Holdt, J. and Leys, J. F. 2023. Satellites reveal Earth’s seasonally shifting dust emission sources. *Sci. Total Environ.*, **883**, 163452. <https://doi.org/10.1016/j.scitotenv.2023.163452>.
- Cheng, Z., Morgenstern, M., Henning, S., Zhang, B., Roberts, G. C., Fraund, M., Marcus, M. A., Lata, N. N., Fialho, P., Mazzoleni, L., Wehner, B., Mazzoleni, C. and China, S. 2023. Cloud condensation nuclei activity of internally mixed particle populations at a remote marine free troposphere site in the North Atlantic Ocean. *Sci. Total Environ.*, **904**, 166865. <https://doi.org/10.1016/j.scitotenv.2023.166865>.
- Chylik, J., Chechin, D., Dupuy, R., Kulla, B. S., Lüpkes, C., Mertes, S., Mech, M. and Neggers, R. A. J. 2023. Aerosol impacts on the entrainment efficiency of Arctic mixed-phase convection in a simulated air mass over open water. *Atmos. Chem. Phys.*, **23**, 4903–4929. <https://doi.org/10.5194/acp-23-4903-2023>.
- Dalton, E. Z., Hoffmann, E. H., Schaefer, T., Tilgner, A., Herrmann, H. and Raff, J. D. 2023. Daytime atmospheric halogen cycling through aqueous-phase oxygen atom chemistry. *J. Amer. Chem. Soc.*, **145**, 15652–15657. <https://doi.org/10.1021/jacs.3c03112>.

Appendices: Publications

- Dinoi, A., Gullì, D., **Weinhold, K.**, Ammoscato, I., Calidonna, C. R., **Wiedensohler, A.** and Contini, D. 2023. Characterization of ultrafine particles and the occurrence of new particle formation events in an urban and coastal site of the Mediterranean area. *Atmos. Chem. Phys.*, **23**, 2167-2181. <https://doi.org/10.5194/acp-23-2167-2023>.
- Egerer, U., Cassano, J. J., Shupe, M. D., de Boer, G., Lawrence, D., Doddi, A., **Siebert, H.**, Jozef, G., Calmer, R., Hamilton, J., **Pilz, C.** and Lonardi, M. 2023. Estimating turbulent energy flux vertical profiles from uncrewed aircraft system measurements: Exemplary results for the MOSAiC campaign. *Atmos. Meas. Tech.*, **16**, 2297-2317. <https://doi.org/10.5194/amt-16-2297-2023>.
- Egerer, U., Siebert, H., Hellmuth, O.** and Sorensen, L. L. 2023. The role of a low-level jet for stirring the stable atmospheric surface layer in the Arctic. *Atmos. Chem. Phys.*, **23**, 15365-15373. <https://doi.org/10.5194/acp-23-15365-2023>.
- Engelmann, R., Griesche, H., Radenz, M., Hofer, J., Althausen, D., Macke, A.** and **Hengst, R.** 2023. Total Sky Imager observations during POLARSTERN cruise PS122/2 on 2019-12-13. *Data from: Multidisciplinary drifting Observatory for the Study of Arctic Climate (MOSAiC) / PS122/2_14-18. PANGAEA*, <https://doi.org/10.1594/PANGAEA.954037>.
- Engelmann, R., Griesche, H., Radenz, M., Hofer, J., Althausen, D., Macke, A.** and **Hengst, R.** 2023. Total Sky Imager observations during POLARSTERN cruise PS122/3 on 2020-03-01. *Data from: Multidisciplinary drifting Observatory for the Study of Arctic Climate (MOSAiC) / PS122/3_28-6. PANGAEA*, <https://doi.org/10.1594/PANGAEA.954363>.
- Engelmann, R., Griesche, H., Radenz, M., Hofer, J., Althausen, D., Macke, A.** and **Hengst, R.** 2023. Total Sky Imager observations during POLARSTERN cruise PS122/4, Longyearbyen - Arctic Ocean. *Data from: Multidisciplinary drifting Observatory for the Study of Arctic Climate (MOSAiC) / PS122/4_43-11, PS122/4_43-145. PANGAEA*, <https://doi.org/10.1594/PANGAEA.955483>.
- Engelmann, R., Griesche, H., Radenz, M., Hofer, J., Althausen, D., Macke, A.** and **Hengst, R.** 2023. Total Sky Imager observations during POLARSTERN cruise PS122/5, Arctic Ocean - Bremerhaven. *Data from: Multidisciplinary drifting Observatory for the Study of Arctic Climate (MOSAiC) / PS122/5_58-3. PANGAEA*, <https://doi.org/10.1594/PANGAEA.955618>.
- Engelmann, R., Griesche, H., Radenz, M., Hofer, J., Althausen, D., Seidel, C., Baars, H., Klamt, A.** and **Hengst, R.** 2023. Water vapor profiles retrieved during the POLARSTERN cruises PS122/1, PS122/2 and PS122/3, 28 September 2019 – 29 February 2020, Arctic Ocean. *Data from: Multidisciplinary drifting Observatory for the Study of Arctic Climate (MOSAiC)/PS122/1_1-38, PS122/2_14-18, PS122/3_28-6. PANGAEA*, <https://doi.org/10.1594/PANGAEA.957158>.
- Fadnavis, S., **Heinold, B.**, Sabin, T. P., **Kubin, A.**, Huang, K., Rap, A. and Müller, R. 2023. Air pollution reductions caused by the COVID-19 lockdown open up a way to preserve the Himalayan glaciers. *Atmos. Chem. Phys.*, **23**, 10439-10449. <https://doi.org/10.5194/acp-23-10439-2023>.
- Feistel, R. and **Hellmuth, O.** 2023. Thermodynamics of evaporation from the ocean surface. *Atmosphere*, **14**, 560 (32 pp.). <https://doi.org/10.3390/atmos14030560>.
- Floutsi, A. A., Baars, H., Engelmann, R., Althausen, D., Ansmann, A., Bohlmann, S., Heese, B., Hofer, J., Kanitz, T., Haarig, M., Ohneiser, K., Radenz, M., Seifert, P., Skupin, A., Yin, Z., Abdulajev, S. F., Komppula, M., Filioglou, M., Giannakaki, E., Stachlewska, I. S., Janicka, L., Bortoli, D., Marinou, E., Amiridis, V., Gialitaki, A., Mamouri, R.-E., Barja, B. and Wandinger, U.** 2023. DeLiAn – a growing collection of depolarization ratio, lidar ratio and Ångström exponent for different aerosol types and mixtures from ground-based lidar observations. *Atmos. Meas. Tech.*, **16**, 2353-2379. <https://doi.org/10.5194/amt-16-2353-2023>.
- Floutsi, A. A., Baars, H., Engelmann, R., Althausen, D., Ansmann, A., Bohlmann, S., Heese, B., Hofer, J., Kanitz, T., Haarig, M., Ohneiser, K., Radenz, M., Seifert, P., Skupin, A., Yin, Z., Abdulajev, S. F., Komppula, M., Filioglou, M., Giannakaki, E., Stachlewska, I. S., Janicka, L., Bortoli, D., Marinou, E., Amiridis, V., Gialitaki, A., Mamouri, R.-E., Barja, B. and Wandinger, U.** 2023. DeLiAn – a growing collection of depolarization ratio, lidar ratio and Ångström exponent for different aerosol types and mixtures from ground-based lidar observations. *Data from: Zenodo*, <https://doi.org/10.5281/zenodo.7751752>.
- Floutsi, A. A., Baars, H., Haarig, M. and Wandinger, U.** 2023. Aerosol typing and space-borne lidars: Potentials and limitations. In: J. T. Sullivan, T. Leblanc, S. Tucker, B. Demoz, E. Eloranta, C. Hostetler, S. Ishii, L. Mona, F. Moshary, A. Papayannis, and K. Rupavatharam (Eds.), *Proceedings of the 30th International Laser Radar Conference (ILRC-30) [Big Sky, Montana, USA (Online), 26 June - 1 July 2022]*. Springer, Cham, Switzerland, p. 683-689. (Springer Atmospheric Sciences). https://doi.org/10.1007/978-3-031-37818-8_88.

Appendices: Publications

- Gkikas, A., Gialitaki, A., Binietoglou, I., Marinou, E., Tsichla, M., Siomos, N., Paschou, P., Kampouri, A., Voudouri, K. A., Proestakis, E., Mylonaki, M., Papanikolaou, C.-A., Michailidis, K., **Baars, H.**, Straume, A. G., Balis, D., Papayannis, A., Parrinello, T. and Amiridis, V. 2023. First assessment of Aeolus Standard Correct Algorithm particle backscatter coefficient retrievals in the eastern Mediterranean. *Atmos. Meas. Tech.*, **16**, 1017-1042. <https://doi.org/10.5194/amt-16-1017-2023>.
- Gómez Maqueo Anaya, S., Faust, M., Heinold, B., Schepanski, K. and Tegen, I.** 2023. Dustonly/Dustonly: v1.0 (v1.0). Zenodo, <http://doi.org/10.5281/zenodo.8321174>.
- Gong, K., Ao, J., Li, K., Liu, L., Liu, Y., Xu, G., Wang, T., Cheng, H., Wang, Z., Zhang, X., Wei, H., George, C., Mellouki, A., **Herrmann, H.**, Wang, L., Chen, J., Ji, M., Zhang, L. and Francisco, J. S. 2023. Imaging of pH distribution inside individual microdroplet by stimulated Raman microscopy. *Proc. Nat. Acad. Sci. (PNAS)*, **120**, e2219588120. <https://doi.org/10.1073/pnas.2219588120>.
- Gong, X., Wang, Y., Xie, H., Zhang, J., Lu, Z., Wood, R., **Stratmann, F., Wex, H.**, Liu, X. and Wang, J. 2023. Maximum supersaturation in the marine boundary layer clouds over the North Atlantic. *AGU Advances*, **4**, e2022AV000855. <https://doi.org/10.1029/2022AV000855>.
- Grawe, S., Jentzsch, C., Schaefer, J., Wex, H., Mertes, S. and Stratmann, F.** 2023. Next-generation ice-nucleating particle sampling on board aircraft: Characterization of the High-volume flow aERosol particle filter sAmpler (HERA). *Atmos. Meas. Tech.*, **16**, 4551-4570. <https://doi.org/10.5194/amt-16-4551-2023>.
- Griesche, H.** 2023. Single column 1D radiative transfer simulations during PS106 including low-level-stratus clouds in the central Arctic (v1.0) [Data set]. *Data from: Zenodo*, <https://doi.org/10.5281/zenodo.10209707>.
- Griesche, H. J. and Seifert, P.** 2023. MOSAiC Cloudnet issue data set [Data set]. *Data from: Zenodo*, <https://doi.org/10.5281/zenodo.7120267>.
- Griesche, H. J., Seifert, P., Engelmann, R., Radenz, M., Hofer, J. and Althausen, D.** 2023. Cloud profiling products from RV Polarstern during MOSAiC, ACTRIS Cloud remote sensing data centre unit (CLU). *Data from: Cloudnet*, <https://hdl.handle.net/21.12132/2.7159000f643348a6>.
- Guo, J., Zhang, X., Gao, Y., Wang, Z., Zhang, M., Xue, W., **Herrmann, H.**, Brasseur, G. P., Wang, T. and Wang, Z. 2023. Evolution of ozone pollution in China: What track will it follow? *Environ. Sci. Technol.*, **57**, 109-117. <https://doi.org/10.1021/acs.est.2c08205>.
- Haarig, M., Hünerbein, A., Wandinger, U., Docter, N., Bley, S., Donovan, D. and van Zadelhoff, G.-J.** 2023. Cloud top heights and aerosol columnar properties from combined EarthCARE lidar and imager observations: The AM-CTH and AM-ACD products. *Atmos. Meas. Tech.*, **16**, 5953-5975. <https://doi.org/10.5194/amt-16-5953-2023>.
- Harm-Altstädtter, B., Bärfuss, K., Bretschneider, L., Schön, M., Bange, J., **Kähner, R.**, Krejci, R., Mazzola, M., Park, K., Pätzold, F., Peuker, A., Traversi, R., **Wehner, B.** and Lampert, A. 2023. Spatial distribution and variability of boundary layer aerosol particles observed in Ny-Ålesund during late spring in 2018. *Aerosol Research*, **1**, 39-64. <https://doi.org/10.5194/ar-1-39-2023>.
- Heintzenberg, J., Legrand, M., Gao, Y., Hara, K., Huang, S., Humphries, R. S., Kamra, A. K., Keywood, M. D. and Sakerin, S. M.** 2023. Spatio-temporal distributions of the natural non-sea-salt aerosol over the Southern Ocean and coastal Antarctica and its potential source regions. *Tellus B: Chemical and Physical Meteorology*, **75**, 47-64. <http://doi.org/10.16993/tellusb.1869>.
- Hell, M., van Pinxteren, D. and Herrmann, H.** 2023. Aussagekraft kontinuierlicher Messungen von kohlenstoffhaltigen Ozon-Vorläuferstoffen (4. Zwischenbericht). **Landesamt für Umwelt, Landwirtschaft und Geologie (LfULG), Projekt „Ozon-Vorläuferstoffe“**.
- Hellmuth, O., Egerer, U., Siebert, H. and Sørensen, L. L.** 2023. PAMARCMIP Contribution: An analytic model companion based on observations: The role of low-level jets in the advection of passive tracers in the high Arctic. Technical note, Zenodo, 55 pp. <https://doi.org/10.5281/zenodo.7689308>.
- Henneberger, J., Ramelli, F., Spirig, R., Omanovic, N., Miller, A. J., Fuchs, C., Zhang, H., **Bühl, J.**, Hervo, M., Kanji, Z. A., **Ohneiser, K., Radenz, M., Rösch, M., Seifert, P.** and Lohmann, U. 2023. Seeding of supercooled low stratus clouds with a UAV to study microphysical ice processes: An introduction to the CLOUDLAB project *Bull. Amer. Meteor. Soc.*, **104**, E1962-E1979. <https://doi.org/10.1175/BAMS-D-22-0178.1>.
- Henning, S., Weller, R. and Wex, H.** 2023. VACCINE - Variation in Antarctic Cloud Condensation Nuclei (CCN) and Ice Nucleating Particle (INP) concentrations at NEumayer Station III. C. Wesche and J. Regnery (Ed.), In: *Expeditions to Antarctica: ANT-Land 2022/23 Neumayer Station III, Kohnen Station, Flight Operations and Field Campaigns*. Alfred-Wegener-Institut, Helmholtz-Zentrum für Polar- und Meeresforschung. Bremerhaven. **Berichte zur Polar- und Meeresforschung = Reports on Polar and Marine Research**.

Appendices: Publications

- Heutte, B., Bergner, N., Beck, I., Angot, H., Dada, L., Quéléver, L. L. J., Laurila, T., Boyer, M., Brasseur, Z., Daellenbach, K. R., **Henning, S.**, Kuang, C., Kulmala, M., Lampilahti, J., Lampimäki, M., Petäjä, T., Shupe, M. D., Sipilä, M., Uin, J., Jokinen, T. and Schmale, J. 2023. Measurements of aerosol microphysical and chemical properties in the central Arctic atmosphere during MOSAiC. *Sci. Data*, **10**, 690. <https://doi.org/10.1038/s41597-023-02586-1>.
- Holanda, B. A., Franco, M. A., Walter, D., Artaxo, P., Carbone, S., Cheng, Y., Chowdhury, S., Ditas, F., Gysel-Beer, M., Klimach, T., Kremer, L. A., Krüger, O. O., Lavric, J. V., Lelieveld, J., Ma, C., Machado, L. A. T., Modini, R., Morais, F. G., Pozzer, A., Saturno, J., Su, H., Wendisch, M., Wolff, S., **Pöhlker, M. L.**, Andreae, M. O., Pöschl, U. and Pöhlker, C. 2023. African biomass burning affects aerosol cycling over the Amazon. *Commun. Earth Environ.*, **4**, 154. <https://doi.org/10.1038/s43247-023-00795-5>.
- Hünerbein, A., Bley, S., Horn, S., Deneke, H.** and Walther, A. 2023. Cloud mask algorithm from the EarthCARE Multi-Spectral Imager: The M-CM products. *Atmos. Meas. Tech.*, **16**, 2821-2836. <https://doi.org/10.5194/amt-16-2821-2023>.
- Ioannidis, E., Law, K. S., Raut, J.-C., Marelle, L., Onishi, T., Kirpes, R. M., Upchurch, L. M., **Tuch, T., Wiedensohler, A.**, Massling, A., Skov, H., Quinn, P. K. and Pratt, K. A. 2023. Modelling wintertime sea-spray aerosols under Arctic haze conditions. *Atmos. Chem. Phys.*, **23**, 5641-5678. <https://doi.org/10.5194/acp-23-5641-2023>.
- Jiang, Y., Hoffmann, E. H., Tilgner, A., Aiyuk, M. B. E., Andersen, S. T., Wen, L., van Pinxteren, M., Shen, H., Xue, L., Wang, W. and Herrmann, H.** 2023. Insights into NO_x and HONO chemistry in the tropical marine boundary layer at Cape Verde during the MarParCloud campaign. *J. Geophys. Res. - Atmos.*, **128**, e2023JD038865. <https://doi.org/10.1029/2023JD038865>.
- Kalesse-Los, H., Kötsche, A., Foth, A., Röttenbacher, J., Vogl, T. and **Witthuhn, J.** 2023. The Virga-Sniffer – a new tool to identify precipitation evaporation using ground-based remote-sensing observations. *Atmos. Meas. Tech.*, **16**, 1683-1704. <https://doi.org/10.5194/amt-16-1683-2023>.
- Kecorius, S., Hoffmann, E. H., Tilgner, A., Barrientos-Velasco, C., van Pinxteren, M., Zeppenfeld, S., Vogl, T., Madueño, L., Lovrić, M., Wiedensohler, A., Kulmala, M., Paasonen, P. and Herrmann, H.** 2023. Rapid growth of Aitken-mode particles during Arctic summer by fog chemical processing and its implication. *PNAS Nexus*, **2**, 1-11 (pgad 124). <https://doi.org/10.1093/pnasnexus/pgad124>.
- Kirbus, B., Tiedeck, S., Camplani, A., Chylik, J., Crewell, S., Dahlke, S., Ebelt, K., Gorodetskaya, I., **Griesche, H., Handorf, D., Höschel, I., Lauer, M., Neggers, R., Rückert, J., Shupe, M. D., Spreen, G., Walbröl, A., Wendisch, M. and Rinke, A.** 2023. Surface impacts and associated mechanisms of a moisture intrusion into the Arctic observed in mid-April 2020 during MOSAiC. *Front. Earth Sci.*, **11**, 1147848. <https://doi.org/10.3389/feart.2023.1147848>.
- Kjærgaard, E. R., Møller, K. H., **Berndt, T.** and Kjaergaard, H. G. 2023. Highly efficient autoxidation of triethylamine. *J. Phys. Chem. A*, <https://doi.org/10.1021/acs.jpca.3c04341>.
- Lei, T., Su, H., Ma, N., Pöschl, U., **Wiedensohler, A.** and Cheng, Y. 2023. Size-dependent hygroscopicity of levoglucosan and D-glucose aerosol nanoparticles. *Atmos. Chem. Phys.*, **23**, 4763-4774. <https://doi.org/10.5194/acp-23-4763-2023>.
- Li, T., Mao, H., Wang, Z., Zhen, J., Li, S., Nie, X., **Herrmann, H.** and Wang, Y. 2023. Field evidence for Asian outflow and fast depletion of total gaseous mercury in the polluted coastal atmosphere. *Environ. Sci. Technol.*, **57**, 4101-4112. <https://doi.org/10.1021/acs.est.2c07551>.
- Lin, C.-Y., Chen, W.-C., Chien, Y.-Y., Chou, C. C. K., Liu, C.-Y., Ziereis, H., Schlager, H., Förster, E., Obersteiner, F., Krüger, O. O., Holanda, B. A., **Pöhlker, M. L.**, Kaiser, K., Schneider, J., Bohn, B., Pfeilsticker, K., Weyland, B., Andrés Hernández, M. D. and Burrows, J. P. 2023. Effects of transport on a biomass burning plume from Indochina during EMeRGe-Asia identified by WRF-Chem. *Atmos. Chem. Phys.*, **23**, 2627–2647. <https://doi.org/10.5194/acp-23-2627-2023>.
- Liu, X., Hadiatullah, H., Zhang, X., Trechera, P., Savadkoohi, M., Garcia-Marlès, M., Reche, C., Pérez, N., Beddows, D. C. S., Salma, I., Thén, W., Kalkavouras, P., Mihalopoulos, N., Hueglin, C., Green, D. C., Tremper, A. H., Chazeau, B., Gille, G., Marchand, N., Niemi, J. V., Manninen, H. E., Portin, H., Zikova, N., Ondracek, J., Norman, M., Gerwig, H., Bastian, S., **Merkel, M., Weinhold, K.**, Casans, A., Casquero-Vera, J. A., Gómez-Moreno, F. J., Artíñano, B., Gini, M., Diapouli, E., Crumeyrolle, S., Riffault, V., Petit, J.-E., Favez, O., Putaud, J.-P., Dos Santos, S. M., Timonen, H., Aalto, P. P., Hussein, T., Lampilahti, J., Hopke, P. K., **Wiedensohler, A.**, Harrison, R. M., Petäjä, T., Pandolfi, M., Alastuey, A. and Querol, X. 2023. Ambient air particulate total lung deposited surface area (LDSA) levels in urban Europe. *Sci. Total Environ.*, **898**, 165466. <https://doi.org/10.1016/j.scitotenv.2023.165466>.

Appendices: Publications

- Liu, Y., Su, H., Wang, S., Wei, C., Tao, W., **Pöhlker, M. L.**, Pöhlker, C., Holanda, B. A., Krüger, O. O., Hoffmann, T., Wendisch, M., Artaxo, P., Pöschl, U., Andreae, M. O. and Cheng, Y. 2023. Strong particle production and condensational growth in the upper troposphere sustained by biogenic VOCs from the canopy of the Amazon Basin. *Atmos. Chem. Phys.*, **23**, 251-272. <https://doi.org/10.5194/acp-23-6963-2023>.
- Lu, B., Liu, C., Meng, X., Zhang, Z., **Herrmann, H.** and Li, X. 2023. High-resolution mapping of regional NMVOCs using the fast space-time Light Gradient Boosting Machine (LightGBM). *J. Geophys. Res. - Atmos.*, **128**, e2023JD039591. <https://doi.org/10.1029/2023JD039591>.
- Lu, B., Meng, X., Dong, S., Zhang, Z., Liu, C., Jiang, J., **Herrmann, H.** and Li, X. 2023. High-resolution mapping of regional VOCs using the enhanced space-time extreme gradient boosting machine (XGBoost) in Shanghai. *Sci. Total Environ.*, **905**, 167054. <https://doi.org/10.1016/j.scitotenv.2023.167054>.
- Lu, B., Zhang, Z., Jiang, J., Meng, X., Liu, C., **Herrmann, H.**, Chen, J., Xue, L. and Li, X. 2023. Unraveling the O_3 - NO_x -VOCs relationships induced by anomalous ozone in industrial regions during COVID-19 in Shanghai. *Atmos. Environ.*, **308**, 119864. <https://doi.org/10.1016/j.atmosenv.2023.119864>.
- Mallet, M. D., Humphries, R. S., Fiddes, S. L., Alexander, S. P., Altieri, K., Angot, H., Anilkumar, N., Bartels-Rausch, T., Creamean, J., Dall'Osto, M., Dommergue, A., Frey, M., **Henning, S.**, Lannuzel, D., Lapere, R., Mace, G. G., Mahajan, A. S., McFarquhar, G. M., Meiners, K. M., Miljevic, B., Peeken, I., Protat, A., Schmale, J., Steiner, N., Sellegri, K., Simó, R., Thomas, J. L., Willis, M. D., Winton, V. H. L. and Woodhouse, M. T. 2023. Untangling the influence of Antarctic and Southern Ocean life on clouds. *Elem. Sci. Anth.*, **11**, 000130. <https://doi.org/10.1525/elementa.2022.000130>.
- Mamouri, R.-E., **Ansmann, A.**, **Ohneiser, K.**, Knopf, D. A., Nisantzi, A., **Bühl, J.**, **Engelmann, R.**, **Skupin, A.**, **Seifert, P.**, **Baars, H.**, Ene, D., **Wandinger, U.** and Hadjimitsis, D. 2023. Wildfire smoke triggers cirrus formation: Lidar observations over the eastern Mediterranean. *Atmos. Chem. Phys.*, **23**, 14097-14114. <https://doi.org/10.5194/acp-23-14097-2023>.
- Mardoñez, V., Pandolfi, M., Borlaza, L. J. S., Jaffrezo, J.-L., Alastuey, A., Besombes, J.-L., Moreno, I., Perez, N., Močnik, G., Ginot, P., Krejci, R., Chrastny, V., **Wiedensohler, A.**, Laj, P., Andrade, M. and Uzu, G. 2023. Source apportionment study on particulate air pollution in two high-altitude Bolivian cities: La Paz and El Alto. *Atmos. Chem. Phys.*, **23**, 10325-10347. <https://doi.org/10.5194/acp-23-10325-2023>.
- Mekic, M.**, **Schaefer, T.**, **Hoffmann, E. H.**, **Aiyuk, M. B. E.**, **Tilgner, A.** and **Herrmann, H.** 2023. Temperature-dependent oxidation of hydroxylated aldehydes by ·OH, SO_4^{2-} , and NO_3^- radicals in the atmospheric aqueous phase. *J. Phys. Chem. A*, **127**, 6495-6508. <https://doi.org/10.1021/acs.jpca.3c00700>.
- Meng, X., Jiang, J., Chen, T., Zhang, Z., Lu, B., Liu, C., Xue, L., Chen, J., **Herrmann, H.** and Li, X. 2023. Chemical drivers of ozone change in extreme temperatures in eastern China. *Sci. Total Environ.*, **874**, 162424. <http://dx.doi.org/10.1016/j.scitotenv.2023.162424>.
- Meng, X., Lu, B., Liu, C., Zhang, Z., Chen, J. and **Herrmann, H.** 2023. Abrupt exacerbation in air quality over Europe after the outbreak of Russia-Ukraine war. *Environ. Internat.*, **178**, 108120. <https://doi.org/10.1016/j.envint.2023.108120>.
- Mertes, S.** and **Wetzel, B.** 2023. Airborne in-situ measurements of aerosol properties of cloud particle residuals / ambient particles and of the cloud water content / water vapor during the HALO-AC3 campaign in March and April 2022. *Data from: Arctic Amplification (AC3). PANGAEA*, <https://doi.pangaea.de/10.1594/PANGAEA.963771>.
- Mettke, P.**, **Brüggemann, M.**, **Mutzel, A.**, **Gräfe, R.** and **Herrmann, H.** 2023. Secondary Organic Aerosol (SOA) through Uptake of Isoprene Hydroxy Hydroperoxides (ISOPOOH) and its oxidation products. *ACS Earth Space Chem.*, **7**, 1025-1037. <https://doi.org/10.1021/acsearthspacechem.2c00385>.
- Michailidis, K., Koukouli, M. E., Balis, D., Veefkind, J. P., de Graaf, M., Mona, L., Papagianopoulos, N., Pappalardo, G., Tsikoudi, I., Amiridis, V., Marinou, E., Gialitaki, A., Mamouri, R. E., Nisantzi, A., Bortoli, D., João Costa, M., Salgueiro, V., Papayannis, A., Mylonaki, M., Alados-Arboledas, L., Romano, S., Perrone, M. R. and **Baars, H.** 2023. Validation of the TROPOMI/S5P aerosol layer height using EARLINET lidars. *Atmos. Chem. Phys.*, **23**, 1919-1940. <https://doi.org/10.5194/acp-23-1919-2023>.
- Min, N., Yao, J., Li, H., Chen, Z., Pang, W., Zhu, J., Kümmel, S., **Schaefer, T.**, **Herrmann, H.** and Richnow, H. H. 2023. Humic substance photosensitized degradation of phthalate esters characterized by 2H and ^{13}C isotope fractionation. *Environ. Sci. Technol.*, **57**, 1930-1939. <https://doi.org/10.1021/acs.est.2c06783>.
- Min, N., Yao, J., Li, H., Zhu, J., Kümmel, S., Lechtenfeld, O. J., **Schaefer, T.**, **Herrmann, H.** and Richnow, H.-H. 2023. Carbon and hydrogen isotope fractionation of phthalates during photocatalysis reactions in aqueous solution containing Fe(III) complexes or iron minerals. *Water Res.*, **247**, 120740. <https://doi.org/10.1016/j.watres.2023.120740>.

Appendices: Publications

- Min, N., Yao, J., Li, H., Zhu, J., Kümmel, S., **Schaefer, T.**, **Herrmann, H.** and Richnow, H. H. 2023. Carbon isotope fractionation of di-(2-ethylhexyl)-phthalate during photosensitized degradation by •OH and SO₄•- for characterization of reaction mechanisms. *Chem. Eng. J.*, **475**, 145950. <https://doi.org/10.1016/j.cej.2023.145950>.
- Mothes, F.**, **Hoffmann, E. H.** and **Herrmann, H.** 2023. Urban grime photochemistry and its interaction with air pollutants NO, NO₂, and O₃: A source for HONO and NO₂ impacting OH in urban areas. *ACS Earth Space Chem.*, **7**, 2263-2274. <https://doi.org/10.1021/acsearthspacechem.3c00184>.
- Ochei, M.**, Oluleye, A., **Wolke, R.**, Pratt, D. and Njie, T. 2023. Aerosols' variability and their relationship with climatic parameters over West Africa. *Environ. Monit. Assess.*, **195**, 672. <https://doi.org/10.1007/s10661-023-11204-x>.
- Ohneiser, K.**, **Ansmann, A.**, **Withuhn, J.**, **Deneke, H.**, Chudnovsky, A., **Walter, G.** and **Senf, F.** 2023. Self-lofting of wildfire smoke in the troposphere and stratosphere: Simulations and space lidar observations. *Atmos. Chem. Phys.*, **23**, 2901-2925. <https://doi.org/10.5194/acp-23-2901-2023>.
- Peräkylä, O., **Berndt, T.**, Franzon, L., Hasan, G., Meder, M., Valiev, R. R., Daub, C. D., Varelas, J. G., Geiger, F. M., Thomson, R. J., Rissanen, M., Kurtén, T. and Ehn, M. 2023. Large gas-phase source of esters and other accretion products in the atmosphere. *J. Amer. Chem. Soc.*, **145**, 7780-7790. <https://doi.org/10.1021/jacs.2c10398>.
- Pilz, C.**, Lonardi, M., **Egerer, U.**, **Siebert, H.**, Ehrlich, A., Heymsfield, A. J., Schmitt, C. G., Shupe, M. D., **Wehner, B.** and Wendisch, M. 2023. Profile observations of the Arctic atmospheric boundary layer with the BELUGA tethered balloon during MOSAiC. *Sci. Data*, **10**, 534. <https://doi.org/10.1038/s41597-023-02423-5>.
- Pöhlker, M. L.**, Pöhlker, C., Krüger, O. O., **Förster, J.-D.**, Berkemeier, T., Elbert, W., Fröhlich-Nowoisky, J., Pöschl, U., Bagheri, G., Bodenschatz, E., Huffman, J. A., Scheithauer, S. and Mikhailov, E. 2023. Respiratory aerosols and droplets in the transmission of infectious diseases. *Rev. Mod. Phys.*, **95**, 045001. <https://link.aps.org/doi/10.1103/RevModPhys.95.045001>.
- Pöhlker, M. L.**, Pöhlker, C., Quaas, J., Mülmenstädt, J., Pozzer, A., Andreae, M. O., Artaxo, P., Block, K., Coe, H., Ervens, B., Gallimore, P., Gaston, C. J., Gunthe, S. S., **Henning, S.**, **Herrmann, H.**, Krüger, O. O., McFiggans, G., **Poulain, L.**, Raj, S. S., Reyes-Villegas, E., Royer, H. M., Walter, D., Wang, Y. and Pöschl, U. 2023. Global organic and inorganic aerosol hygroscopicity and its effect on radiative forcing. *Nat. Commun.*, **14**, 6139. <https://doi.org/10.1038/s41467-023-41695-8>.
- Putaud, J.-P., Pisoni, E., Mangold, A., Hueglin, C., Sciare, J., Pikridas, M., Savvides, C., Ondracek, J., Mbengue, S., **Wiedensohler, A.**, **Weinhold, K.**, **Merkel, M.**, **Poulain, L.**, **van Pinxteren, D.**, **Herrmann, H.**, Massling, A., Nordstrøm, C., Alastuey, A., Reche, C., Pérez, N., Castillo, S., Sorribas, M., Adame, J. A., Petaja, T., Lehtipalo, K., Niemi, J., Riffault, V., de Brito, J. F., Colette, A., Favez, O., Petit, J.-E., Gros, V., Gini, M. I., Vratolis, S., Eleftheriadis, K., Diapouli, E., van der Gon, H. D., Yttri, K. E. and Aas, W. 2023. Impact of 2020 COVID-19 lockdowns on particulate air pollution across Europe. *Atmos. Chem. Phys.*, **23**, 10145-10161. <https://doi.org/10.5194/acp-23-10145-2023>.
- Rahlf, J., Esser, S. P., Plewka, J., Heinrichs, M. E., Soares, A., Scarchilli, C., Grigioni, P., **Wex, H.**, Giebel, H.-A. and Probst, A. J. 2023. Marine viruses disperse bidirectionally along the natural water cycle. *Nat. Commun.*, **14**, 6354. <https://doi.org/10.1038/s41467-023-42125-5>.
- Rogozovsky, I., **Ohneiser, K.**, Lyapustin, A., **Ansmann, A.** and Chudnovsky, A. 2023. The impact of different aerosol layering conditions on the high-resolution MODIS/MAIAC AOD retrieval bias: The uncertainty analysis. *Atmos. Environ.*, **309**, 119930. <https://doi.org/10.1016/j.atmosenv.2023.119930>.
- Royer, H. M., **Pöhlker, M. L.**, Krüger, O., Blades, E., Sealy, P., Lata, N. N., Cheng, Z., China, S., Ault, A. P., Quinn, P. K., Zuidema, P., Pöhlker, C., Pöschl, U., Andreae, M. and Gaston, C. J. 2023. African smoke particles act as cloud condensation nuclei in the wintertime tropical North Atlantic boundary layer over Barbados. *Atmos. Chem. Phys.*, **23**, 981-998. <https://doi.org/10.5194/acp-23-981-2023>.
- Sanaei, A., **Herrmann, H.**, **Alshaabi, L.**, **Beck, J.**, Ferlian, O., **Fomba, K. W.**, **Haferkorn, S.**, **van Pinxteren, M.**, Quaas, J., Quosh, J., **Rabe, R.**, Wirth, C., Eisenhauer, N. and Weigelt, A. 2023. Changes in biodiversity impact atmospheric chemistry and climate through plant volatiles and particles. *Commun. Earth Environ.*, **4**, 445. <https://doi.org/10.1038/s43247-023-01113-9>.
- Sarang, K., **Otto, T.**, Gagan, S., Rudzinski, K., **Schaefer, T.**, **Brüggemann, M.**, Grgić, I., Kubas, A., **Herrmann, H.** and Szmigelski, R. 2023. Aqueous-phase photo-oxidation of selected green leaf volatiles initiated by •OH radicals: Products and atmospheric implications. *Sci. Total Environ.*, **879**, 162622. <http://dx.doi.org/10.1016/j.scitotenv.2023.162622>.

Appendices: Publications

- Savadkoohi, M., Pandolfi, M., Reche, C., Niemi, J. V., Mooibroek, D., Titos, G., Green, D. C., Tremper, A. H., Hueglin, C., Liakakou, E., Mihalopoulos, N., Stavroulas, I., Artiñano, B., Coz, E., Alados-Arboledas, L., Beddows, D., Riffault, V., de Brito, J. F., Bastian, S., Baudic, A., Colombi, C., Costabile, F., Chazeau, B., Marchand, N., Gómez-Amo, J. L., Estellés, V., Matos, V., van der Gaag, E., Gille, G., Luoma, K., Manninen, H. E., Norman, M., Silvergren, S., Petit, J.-E., Putaud, J.-P., Rattigan, O. V., Timonen, H., **Tuch, T.**, **Merkel, M.**, **Weinhold, K.**, Vratolis, S., Vasilescu, J., Favez, O., Harrison, R. M., Laj, P., **Wiedensohler, A.**, Hopke, P. K., Petäjä, T., Alastuey, A. and Querol, X. 2023. The variability of mass concentrations and source apportionment analysis of equivalent black carbon across urban Europe. *Environ. Internat.*, **178**, 108081. <https://doi.org/10.1016/j.envint.2023.108081>.
- Scholz, W., Shen, J., Aliaga, D., Wu, C., Carbone, S., Moreno, I., Zha, Q., Huang, W., Heikkinen, L., Jaffrezo, J. L., Uzu, G., Partoll, E., Leiminger, M., Velarde, F., Laj, P., Ginot, P., Artaxo, P., **Wiedensohler, A.**, Kulmala, M., Mohr, C., Andrade, M., Sinclair, V., Bianchi, F. and Hansel, A. 2023. Measurement Report: Long-range transport and the fate of dimethyl sulfide oxidation products in the free troposphere derived from observations at the high-altitude research station Chacaltaya (5240 m a.s.l.) in the Bolivian Andes. *Atmos. Chem. Phys.*, **23**, 895-920. <https://doi.org/10.5194/acp-23-895-2023>.
- Senf, F.** 2023. Jupyter Notebooks for Plotting and Analysis of the “Circulation Responses for WiFi-AUS” study, Revision1 Release (v1.2_revision 1). Zenodo, <https://doi.org/10.5281/zenodo.7957666>.
- Senf, F.** 2023. An illustrative example for cloud-radiation coupling in ICON-LEM v2.6.5 (v1.0). Zenodo, <https://doi.org/10.5281/zenodo.7780733>.
- Senf, F., Heinold, B., Kubin, A., Müller, J., Schrödner, R. and Tegen, I.** 2023. How the extreme 2019–2020 Australian wildfires affected global circulation and adjustments. *Atmos. Chem. Phys.*, **23**, 8939-8958. <https://doi.org/10.5194/acp-23-8939-2023>.
- Senf, F., Heinold, B., Kubin, A., Müller, J., Schrödner, R. and Tegen, I.** 2023. Dataset associated with Senf et al. (2023): “How the extreme 2019-2020 Australian wildfire affected global circulation and adjustments” (Version v1.0.submission) [Data set]. *Data from: Zenodo*, <http://doi.org/10.5281/zenodo.7568466>.
- Senf, F., Heinold, B., Tegen, I. and Villanueva, D.** 2023. Course material for “ComputerLab - Atmospheric models: Scales and parameterizations”, University Leipzig (Version v2023,1) [Data set]. *Data from: Zenodo*, <http://doi.org/10.5281/zenodo.8282872>.
- Senf, F., Schrödner, R., Stoll, J., Schimmel, W., Simmel, M., Knoth, O., Wolke, R., Lieber, M., Diehl, K. and Grützun, V.** 2023. COSMO-SPECS: A spectrally-resolved cloud microphysics framework coupled to the weather model COSMO (v0.9_cycare). Zenodo, <https://doi.org/10.5281/zenodo.8325230>.
- Senf, F., Schrödner, R., Stoll, J., Schimmel, W., Simmel, M., Knoth, O., Wolke, R., Lieber, M., Diehl, K. and Grützun, V.** 2023. COSMO-SPECS: A spectrally-resolved cloud microphysics framework coupled to the weather model COSMO (v0.9.1_flare). Zenodo, <https://doi.org/10.5281/zenodo.8325255>.
- Soppa, V., Lucht, S., Ogurtsova, K., Buschka, A., López-Vicente, M., Guxens, M., **Weinhold, K.**, **Winkler, U.**, **Wiedensohler, A.**, Held, A., Lüchtrath, S., Cyrys, J., Kecorius, S., Gastmeier, P., Wiese-Posselt, M. and Hoffmann, B. 2023. The Berlin-Brandenburg Air Study — A methodological study paper of a natural experiment investigating health effects related to changes in airport-related exposures. *Int. J. Public Health*, **68**, 1606096. <https://doi.org/10.3389/ijph.2023.1606096>.
- Souza, A. N., He, J., Bischoff, T., Waruszewski, M., Novak, L., Barra, V., Gibson, T., Sridhar, A., Kandala, S., Byrne, S., Wilcox, L. C., Kozdon, J., Giraldo, F. X., **Knoth, O.**, Marshall, J., Ferrari, R. and Schneider, T. 2023. The flux-differencing discontinuous Galerkin method applied to an idealized fully compressible nonhydrostatic dry atmosphere. *Journal of Advances in Modeling Earth Systems*, **15**, e2022MS003527. <https://doi.org/10.1029/2022MS003527>.
- Sze, K. C. H., Wex, H., Hartmann, M., Skov, H., Massling, A. and Stratmann, F.** 2023. Two years of data on Ice Nucleating Particles (INP) from Villum Research Station (VRS) in Northern Greenland. *Data from: Arctic Amplification (AC3); Station_Nord (Villum Research Station)*. *PANGAEA*, <https://doi.org/10.1594/PANGAEA.953838>.
- Sze, K. C. H., Wex, H., Hartmann, M., Skov, H., Massling, A. and Stratmann, F.** 2023. Sample and droplet volume information of Ice Nucleating Particles (INP) including original files, from Villum Research Station (VRS) in Northern Greenland. *Data from: Arctic Amplification (AC3); Station_Nord (Villum Research Station)*. *PANGAEA*, <https://doi.org/10.1594/PANGAEA.953839>.
- Sze, K. C. H., Wex, H., Hartmann, M., Skov, H., Massling, A., Villanueva, D. and Stratmann, F.** 2023. Ice-nucleating particles in northern Greenland: Annual cycles, biological contribution and parameterizations. *Atmos. Chem. Phys.*, **23**, 4741-4761. <https://doi.org/10.5194/acp-23-4741-2023>.

Appendices: Publications

- tobac-Community, Brunner, K., Freeman, S. W., Jones, W. K., Kukulies, J., **Senf, F.**, Bruning, E., Stier, P., van den Heever, S. C., Heikenfeld, M., Marinescu, P. J., Collis, S. M., **Lettl, K.**, **Pfeifer, N.**, Raut, B. A., Zhang, X. and Sokolowsky, G. A. 2023. tobac - Tracking and Object-based Analysis of Clouds (v1.5.0). Zenodo, <https://doi.org/10.5281/zenodo.8164675>.
- Trechera, P., Garcia-Marlès, M., Liu, X., Reche, C., Pérez, N., Savadkoohi, M., Beddows, D., Salma, I., Vörösmarty, M., Casans, A., Casquero-Vera, J. A., Hueglin, C., Marchand, N., Chazeau, B., Gille, G., Kalkavouras, P., Mihalopoulos, N., Ondracek, J., Zikova, N., Niemi, J. V., Manninen, H. E., Green, D. C., Tremper, A. H., Norman, M., Vratolis, S., Eleftheriadis, K., Gómez-Moreno, F. J., Alonso-Blanco, E., Gerwig, H., **Wiedensohler, A.**, **Weinhold, K.**, **Merkel, M.**, Bastian, S., Petit, J.-E., Favez, O., Crumeyrolle, S., Ferlay, N., Martins Dos Santos, S., Putaud, J.-P., Timonen, H., Lampilahti, J., Asbach, C., Wolf, C., Kaminski, H., Altug, H., Hoffmann, B., Rich, D. Q., Pandolfi, M., Harrison, R. M., Hopke, P. K., Petäjä, T., Alastuey, A. and Querol, X. 2023. Phenomenology of ultrafine particle concentrations and size distribution across urban Europe. *Environ. Internat.*, **172**, 107744. <https://doi.org/10.1016/j.envint.2023.107744>.
- Tsekeli, A., Gialitaki, A., Di Paolantonio, M., Dionisi, D., Liberti, G. L., Fernandes, A., Szkop, A., Pietruczuk, A., Pérez-Ramírez, D., Granados Muñoz, M. J., Guerrero-Rascado, J. L., Alados-Arboledas, L., Pantaleón, D. B., Bravo-Aranda, J. A., Kampouri, A., Marinou, E., Amiridis, V., Sicard, M., Comerón, A., Muñoz-Porcar, C., Rodríguez-Gómez, A., Romano, S., Perrone, M. R., Shang, X., Komppula, M., Mamouri, R.-E., Nisantzi, A., Hadjimitsis, D., Navas-Guzmán, F., Haeffele, A., Szczepanik, D., Tomczak, A., Stachiewska, I. S., Belegante, L., Nicolae, D., Voudouri, K. A., Balis, D., **Floutsi, A. A.**, **Baars, H.**, Miladi, L., Pascal, N., Dubovik, O. and Lopatin, A. 2023. Combined sun-photometer–lidar inversion: Lessons learned during the EARLINET/ACTRIS COVID-19 campaign. *Atmos. Meas. Tech.*, **16**, 6025-6050. <https://doi.org/10.5194/amt-16-6025-2023>.
- Tukainen, S., O'Connor, E., Anniina, K. and **Griesche, H. J.** 2023. CloudnetPy for MOSAiC (v1.0.0) [Software]. Zenodo, <https://doi.org/10.5281/zenodo.7801660>.
- Twigg, M. M., Di Marco, C. F., McGhee, E. A., Braban, C. F., Nemitz, E., Brown, R. J. C., Blakley, K. C., Leeson, S. R., Sanocka, A., Green, D. C., Priestman, M., Riffault, V., Bourin, A., Minguillón, M. C., Via, M., Ovadnevaite, J., Ceburnis, D., O'Dowd, C., **Poulain, L.**, **Stieger, B.**, Makkonen, U., Rumsey, I. C., Beachley, G., Walker, J. T. and Butterfield, D. M. 2023. The potential of high temporal resolution automatic measurements of PM_{2.5} composition as an alternative to the filter-based manual method used in routine monitoring. *Atmos. Environ.*, **315**, 120148. <https://doi.org/10.1016/j.atmosenv.2023.120148>.
- van Pinxteren, D.**, **Zeppenfeld, S.** and **Herrmann, H.** 2023. *Trenduntersuchung der Levoglucosan-Konzentration in der Außenluft am Standort Melpitz unter Berücksichtigung der Witterungsbedingungen (Abschlussbericht). UBA-Projekt.*
- van Pinxteren, M.**, **Zeppenfeld, S.**, **Fomba, K. W.**, **Triesch, N.**, Frka, S. and **Herrmann, H.** 2023. Amino acids, carbohydrates, and lipids in the tropical oligotrophic Atlantic Ocean: Sea-to-air transfer and atmospheric in situ formation. *Atmos. Chem. Phys.*, **23**, 6571-6590. <https://doi.org/10.5194/acp-23-6571-2023>.
- Wandinger, U.**, **Floutsi, A. A.**, **Baars, H.**, **Haarig, M.**, **Ansmann, A.**, **Hünerbein, A.**, Docter, N., Donovan, D., van Zadelhoff, G.-J., Mason, S. and Cole, J. 2023. HETEAC – The Hybrid End-To-End Aerosol Classification model for EarthCARE: Look-Up Table (LUT) for aerosol mixtures. *Data from: Zenodo*, <https://doi.org/10.5281/zenodo.7732338>.
- Wandinger, U.**, **Floutsi, A. A.**, **Baars, H.**, **Haarig, M.**, **Ansmann, A.**, **Hünerbein, A.**, Docter, N., Donovan, D., van Zadelhoff, G.-J., Mason, S. and Cole, J. 2023. HETEAC – The Hybrid End-To-End Aerosol Classification model for EarthCARE. *Atmos. Meas. Tech.*, **16**, 2485-2510. <https://doi.org/10.5194/amt-16-2485-2023>.
- Wandinger, U.**, **Haarig, M.**, **Baars, H.**, Donovan, D. and van Zadelhoff, G.-J. 2023. Cloud top heights and aerosol layer properties from EarthCARE lidar observations: the A-CTH and A-ALD products. *Atmos. Meas. Tech.*, **16**, 4032-4052. <https://doi.org/10.5194/amt-16-4032-2023>.
- Weger, M.** and **Heinold, B.** 2023. CAIRDIO simulation results and observational data for Dresden (Version 1.0) [Data set]. *Data from: Zenodo*, <http://doi.org/10.5281/zenodo.8388993>.
- Weger, M.** and **Heinold, B.** 2023. Air pollution trapping in the Dresden Basin from gray-zone scale urban modeling. *Atmos. Chem. Phys.*, **23**, 13769-13790. <https://doi.org/10.5194/acp-23-13769-2023>.
- Wen, L., Xue, L., Dong, C., Wang, X., Chen, T., Jiang, Y., Gu, R., Zheng, P., Li, H., Shan, Y., Zhu, Y., Zhao, Y., Yin, X., Liu, H., Gao, J., Wu, Z., Wang, T., **Herrmann, H.** and Wang, W. 2023. Reduced atmospheric sulfate enhances fine particulate nitrate formation in eastern China. *Sci. Total Environ.*, **898**, 165303. <http://dx.doi.org/10.1016/j.scitotenv.2023.165303>.

Appendices: Publications

Wendisch, M., Brückner, M., Crewell, S., Ehrlich, A., Notholt, J., Lüpkes, C., **Macke, A.**, Burrows, J. P., Rinke, A., Quaas, J., Maturilli, M., Schemann, V., Shupe, M. D., **Akansu, E. F.**, **Barrientos-Velasco, C.**, Bärfuss, K., Blechschmidt, A.-M., Block, K., Bougoudis, I., Bozem, H., Böckmann, C., Bracher, A., Bresson, H., Bretschneider, L., Buschmann, M., Chechin, D. G., Chylik, J., Dahlke, S., **Deneke, H.**, Dethloff, K., Donth, T., Dorn, W., Dupuy, R., Eboll, K., **Egerer, U.**, **Engelmann, R.**, Eppers, O., Gerdes, R., Gierens, R., Gorodetskaya, I. V., Gottschalk, M., **Griesche, H.**, Gryanik, V. M., Handorf, D., Harm-Altstädtter, B., Hartmann, J., **Hartmann, M.**, **Heinold, B.**, Herber, A., **Herrmann, H.**, Heygster, G., Höschel, I., Hofmann, Z., Hölemann, J., **Hünerbein, A.**, Jafariserajehlou, S., Jäkel, E., Jacobi, C., Janout, M., Jansen, F., Jourdan, O., Jurányi, Z., Kalesse-Los, H., Kanzow, T., Kähnner, R., Kliesch, L. L., Klingebiel, M., Knudsen, E. M., Kovács, T., Körtke, W., Krampe, D., Kretzschmar, J., Kreyling, D., Kulla, B., Kunkel, D., Lampert, A., Lauer, M., Lelli, L., von Lerber, A., Linke, O., Lohnert, U., Lonardi, M., Losa, S. N., Losch, M., Maahn, M., Mech, M., Mei, L., **Mertes, S.**, Metzner, E., Mewes, S., Michaelis, J., Mioche, G., Moser, M., Nakoudi, K., Neggers, R., Neuber, R., Nomokonova, T., Oelker, J., Papakonstantinou-Presvelou, I., Pätzold, F., Pefanis, V., Pohl, C., **van Pinxteren, M.**, Radovan, A., Rhein, M., Rex, M., Richter, A., Risse, N., Ritter, C., Rostosky, P., Rozanov, V. V., Ruiz Donoso, E., Saavedra Garfias, P., Salzmann, M., **Schacht, J.**, Schäfer, M., Schneider, J., Schnierstein, N., **Seifert, P.**, Seo, S., **Siebert, H.**, Soppa, M. A., Spreen, G., Stachlewska, I. S., Stapf, J., **Stratmann, F.**, **Tegen, I.**, Viceto, C., Voigt, C., Vountas, M., Walbröl, A., Walter, M., **Wehner, B.**, **Wex, H.**, Willmes, S., Zanatta, M. and **Zeppenfeld, S.** 2023. Atmospheric and surface processes, and feedback mechanisms determining arctic amplification: A review of first results and prospects of the (AC)3 Project. Bull. Amer. Meteor. Soc., **104**, E208-E242. <https://doi.org/10.1175/BAMS-D-21-0218.1>.

Zanatta, M., **Mertes, S.**, Jourdan, O., Dupuy, R., Järvinen, E., Schnaiter, M., Eppers, O., Schneider, J., Jurányi, Z. and Herber, A. 2023. Airborne investigation of black carbon interaction with low-level, persistent, mixed-phase clouds in the Arctic summer. Atmos. Chem. Phys., **23**, 7955-7973. <https://doi.org/10.5194/acp-23-7955-2023>.

Zeppenfeld, S., **van Pinxteren, M.**, **Hartmann, M.**, Zeising, M., Bracher, A. and **Herrmann, H.** 2023. Marine carbohydrates in Arctic aerosol particles and fog – diversity of oceanic sources and atmospheric transformations. Atmos. Chem. Phys., **23**, 15561-15587. <https://doi.org/10.5194/acp-23-15561-2023>.

Zhang, C., Lu, M., Ma, N., Yang, Y., Wang, Y., **Größ, J.**, Fan, Z., Wang, M. and **Wiedensohler, A.** 2023. Hygroscopicity of aerosol particles composed of surfactant SDS and its internal mixture with ammonium sulfate at relative humidities up to 99.9%. Atmos. Environ., **298**, 119625. <https://doi.org/10.1016/j.atmosenv.2023.119625>.

Zhang, Q., Liu, P., Wang, Y., George, C., Chen, T., Ma, S., Ren, Y., Mu, Y., Song, M., **Herrmann, H.**, Mellouki, A., Chen, J., Yue, Y., Zhao, X., Wang, S. and Zeng, Y. 2023. Unveiling the underestimated direct emissions of nitrous acid (HONO). Proc. Nat. Acad. Sci. (PNAS), **120**, e2302048120. <https://doi.org/10.1073/pnas.2302048120>.

Zhang, Y., Su, H., **Kecorius, S.**, Ma, N., Wang, Z., Sun, Y., Zhang, Q., Pöschl, U., **Wiedensohler, A.**, Andreae, M. O. and Cheng, Y. 2023. Extremely low-volatility organic coating leads to underestimation of black carbon climate impact. One Earth, **6**, 158-166. <https://doi.org/10.1016/j.oneear.2023.01.009>.

Appendices: University courses

University courses

Lecturer	Course	WS 2021/ 2022	SS 2022	WS 2022/ 2023	SS 2023	WS 2023/ 2024
Ansmann, A. Althausen, D. Baars, H. Engelmann, R. Seifert, P.	Active Remote Sensing with Lidar (2 sh)	x		x		x
Ansmann, A. Althausen,D. Baars, H. Engelmann, R.	Seminar Active Remote Sensing with Lidar (2 sh)	x		x		x
Beck, J. Tilgner, A. van Pinxteren, D.	Advanced Studies: Analytics and Spektroscopy (Atmospheric Chemistry)		x		x	
Beck, J. Hell, M. Arora, S. Poschart, S.	seminar: "Chemistry for Medical Students" (1 sh) + Praktikum (2.5 sh)	x		x x x		
Deneke, H. Macke, A.	Leipzig Graduate School Clouds, Aerosols and Radiation (LGS-CAR) Advanced Training Module LGS-CAR 16 – Remote Sensing of Cloud Development					x
Heinold, B.	Integrated Research Training Group (IRTG)-Arctic Amplification (AC) ³ TR 172, online lecture 20: "The challenge of modelling the Arctic aerosol-climate impact"		x			
	Retreat DFG Research Training Group 2624, lecture: "Introduction to Air Pollution Modelling"				x	
Hartmann, S. Henning, S.	LIM Meteorological Seminar	x				
Henning, S.	Guest lecture: M7 Cloud Condensation Nuclei Counter				x	
Herrmann, H.	Basic Atmospheric Chemistry and Exercises (3 sh)		x		x	
	Atmospheric Chemistry, the Multiphase System and exercises (3 sh)	x		x		x
	Atmospheric Chemistry Seminar (1 sh)	x	x	x	x	x
	Atmospheric Chemistry Lab Course (1 sh)	x	x	x	x	x
	Course of Atmospheric Chemistry, Shanding University	x		x		x

Appendices: University courses

Lecturer	Course	WS 2021/ 2022	SS 2022	WS 2022/ 2023	SS 2023	WS 2023/ 2024
Herrmann, H. Tilgner, A. Hoffmann, E. H. Schaefer, T. Mettke, P. Schrödner, R. Fomba, W. van Pinxteren, D.	Leipzig Graduate School Clouds, Aerosols and Radiation (LGS-CAR) Advanced Training Module LGS-CAR 15 – Atmospheric Multiphase Chemistry		x			
Macke, A.	Atmospheric Radiation (1 sh)		x		x	
Macke, A. Deneke, H. Hünerbein, A. Bley, S.	Satellite Remote Sensing and Exercises (2 sh)		x		x	
Macke, A. Hartmann, S. Wex, H. Stratmann, F.	Cloud Physics and Exercises (3 sh)		x		x	
Mothes, F.	OGTAC-CC training on Organic Tracers and Aerosol Constituents			x		x
	ACTRIS CAIS-ECAC Aerosol In-Situ Course: Fundamentals & Methods for Aerosol Sampling and Physical & Chemical In-Situ Measurements				x	
	Dust in the Atmosphere Seminar (1sh)					
Seifert, P.	Microwave Remote Sensing	x		x		x
Tegen, I.	Modeling of Atmospheric Trace Substances (2 sh)	x		x		x
	Seminar Modeling of Atmospheric Trace Substances (1 sh)	x		x		x
	Modelling of the Atmosphere (1sh)		x			
	Contribution to modul SQ15 “Energy and Environment,” University of Leipzig: “Transport of Atmospheric Pollutants”			x		x
Tegen, I. Senf, F. B. Heinold Schrödner, R. Kubin, A.	Atmospheric Models: Scales and Parameterizations and Exercises (3 sh)				x	
Wandinger, U.	Scattering and Atmospheric Optics (2 sh)	x		x		x
	Seminar Applied Scattering Theory (1 sh)	x		x		x

Appendices: University courses

Lecturer	Course	WS 2021/ 2022	SS 2022	WS 2022/ 2023	SS 2023	WS 2023/ 2024
Stratmann, F. Müller, T. Pöhlker, M. Wiedensohler, A. Hartmann, S.	Atmospheric Aerosols (2 sh) Master	x	x		x	
	Seminar Atmospheric Aerosols (1 sh)	x				
Pöhlker, M.	Aerosol Physics (2 sh)		x	x		
	Exercises Aerorol Measurements		x	x		
	Lecture at the Autumn School 2023 of Helmholtz Zentrum Potsdam, German Research Centre for Geosciences "Africa in Focus"					x
van Pinxteren, M.	Guest lecture: Analysis and Spectroscopy: Gas Chromatography, lecture in an one week course	x		x		x
	Lecturer at the Sino-European Summer School on Atmospheric Chemistry (SESAC 4)					
	Lecturer at the SOLAS Summer School		x		x	
	Lecturer at the SOLAS Master Programme			x		

* did not take place, but was offered

Appendices: Academic degrees

Academic degrees

Completed academic qualifications 2022/2023

Academic degree*	Name	Title	Faculty	Year
Ph.D.	Alas, H.D.	Mobile measurements of black carbon and PM: optimization of techniques and data analysis for pedestrian exposure	University Leipzig, Faculty of Physics and Earth Sciences	2022
	Barrientos-Velasco, C.	Radiative effects of clouds in the Arctic	University Leipzig, Faculty of Physics and Earth Sciences	2022
	Düsing, S.	Investigation of physio-optical aerosol properties with in-situ and remote-sensing techniques	University Leipzig, Faculty of Physics and Earth Sciences	2022
	Faust, M.	Modelling dust emissions from agricultural sources in Europe	University Leipzig, Faculty of Physics and Earth Sciences	2023
	Floutsi, A.A.	Development and application of an automatic lidar-based aerosol typing algorithm	University Leipzig, Faculty of Physics and Earth Sciences	2022
	Griesche, H.	Arctic low-level mixed-phase clouds and their complex interactions with aerosol and radiation - Remote sensing of the Arctic troposphere with the shipborne supersite OCEANET-Atmosphere	University Leipzig, Faculty of Physics and Earth Sciences	2022
	Ohneiser, K.	Lidar Observations of Record-breaking Stratospheric Wildfire Smoke Events in 2019-2021: Siberian Smoke over the Central Arctic and Australian Smoke over South America	University Leipzig, Faculty of Physics and Earth Sciences	2023
	Radenz, M.	Hemispheric contrasts of ice formation in stratiform supercooled liquid clouds	University Leipzig, Faculty of Physics and Earth Sciences	2022
	Tatzelt, C.	Cloud condensation nuclei and ice-nucleating particles over the Southern Ocean: Abundance and properties during the Antarctic circum-navigation expedition	University Leipzig, Faculty of Physics and Earth Sciences	2023
	Tzallas, V.	Development and applications of a cloud regime dataset over Europe using satellite observations	University Leipzig, Faculty of Physics and Earth Sciences	2023
	Witthuhn, J.	Aerosol - remote sensing, characterization and aerosol-radiation interaction	University Leipzig, Faculty of Physics and Earth Sciences	2022
Dipl. Ing. FH	Claes, M.	Entwicklung einer neuen Schneide zur optimierten Strömungsführung im Forschungswindkanal LACIS-T	Faculty of Automotive and Mechanical Engineering at the West Saxon University of Applied Sciences Zwickau	2022

Appendices: Academic degrees

Academic degree*	Name	Title	Faculty	Year
M.Sc.	Alshaabi, L.	Untersuchung der biogenen organischen Partikelphase in Baumkronen von Laubbäumen bei unterschiedlicher Biodiversität im MyDiv Bad Lauchstädt mittels IC/HR-MS Analytik	University of Leipzig, Faculty of Chemistry and Mineralogy	2023
	Bader, N.	Can Convective Initiation provide Indicators for Convective Severity?	University Leipzig, Faculty of Physics and Earth Sciences	2022
	Gast, B.	Implementation of a fluorescence channel in a multiwavelength lidar system to measure biological particles in the atmosphere	University Leipzig, Faculty of Physics and Earth Sciences	2023
	Hoffmann, R.	Particle deliquescence in a turbulent humidity field	University Leipzig, Faculty of Physics and Earth Sciences	2023
	Käplinger, H.	Simulation of rapid adjustments to aerosol-radiation interactions over land with ICON	University Leipzig, Faculty of Physics and Earth Sciences	2023
	Kula, C.	Ionic strength dependency of Fenton reactions in the presence of sulfate and acidic pH	University of Leipzig, Faculty of Chemistry and Mineralogy	2023
	Le, S.	Charakterisierung eines Aerospektrometers mSEMS 904 sowie Integration in eine mobile Messbox	Leipzig University of Applied Sciences	2022
	Löbel, S.	Biological ice nuclei in air and rainwater samples: studies on ice nucleating potential, macromolecular composition and morphology	University Leipzig, Faculty of Physics and Earth Sciences	2023
	Mahesh, M.	BBCOMP: Analysis of Biomass Burning Molecular Composition in Twin Sites in Melpitz	Indian Institute of Science Education and Research Mohali	2023
	Müller, J.	Global Adjustments and Circulation Responses to Smoke Aerosol Forcing from Australian Wildfires	Faculty of Physics and Earth Sciences, University Leipzig	2022
	Nibert, P:	Compaction and application of the CAPRAM biomass burning module BBM 1.0	Claude Bernard University Lyon 1 (UCBL1)	2023
	Nongma, K.	Fluxes of Atmospheric Nutrients During Dust events to the Atlantic Ocean and their impact on regional ocean productivity	Atlantic University of Technology	2023
	Oehlke, P.	Konzipierung und Aufbau eines Messsystems für die Abschätzung von Aerosolpartikelflüssen über der Meeresoberfläche des arktischen Ozeans	Leipzig University of Applied Sciences	2022
	Ritter, O.	Characterisation of the properties of trade wind cumulus clouds with Sentinel-2 observations	University Leipzig, Faculty of Physics and Earth Sciences	2022

Appendices: Academic degrees

Academic degree*	Name	Title	Faculty	Year
M.Sc.	Saxena, M.	Investigation into the composition and characteristics of burn chamber generated biomass burning aerosol exposed to different atmospherically relevant conditions	University of Leipzig, Faculty of Chemistry and Mineralogy	2023
	Schaefer, J.T.	Investigation of stratospheric ice nucleating particle concentrations for background conditions and in a biomass burning plume	University Leipzig, Faculty of Physics and Earth Sciences	2022
	Seidel, C.	Analysis of water vapour mixing ratio profiles in the Arctic from Raman lidar measurements during the MOSAiC-campaign profiles of two atmospheric models	University Leipzig, Faculty of Physics and Earth Sciences	2022
	Seidel, J. S.	Is secondary ice production as consequence of collisions between supercooled droplets and ice particles a relevant process? - A laboratory investigation	University Leipzig, Faculty of Physics and Earth Sciences	2023
	Weikert, H.	Non-Parametric Supervised Machine Learning for Classification and Analysis of Simulated Cloud Distributions	University Leipzig, Faculty of Physics and Earth Sciences	2023
B.Sc.	Baumer, F.	Comparison of radiosonde data from Leipzig to meteorological profiles of two atmospheric models	University Leipzig, Faculty of Physics and Earth Sciences	2022
	Gaußmann, D.	Laser-Doppler- und Phase-Doppler-Anemometrie am turbulenten Windkanal LACIS-T: Konstruktion eines Rahmens für die Positionierung der Anemometer am Windkanal und Bestimmung der Geschwindigkeit und Größe von Wolkenpartikeln	Leipzig University of Applied Sciences	2023
	Gundlach, J.	Temperaturempfindlichkeit biogener und arktischer Eiskeime	University Leipzig, Faculty of Physics and Earth Sciences	2022
	Hartmann, R.	Boundary layer aerosol and ice formation	University Leipzig, Faculty of Physics and Earth Sciences	2023
	Horn, C.	Untersuchung der räumlichen Struktur von simulierten konvektiven Ereignissen über Deutschland	University Leipzig, Faculty of Physics and Earth Sciences	2023
	Kellermann, M.	Examining aerosol properties during an Arctic Haze event in Ny-Ålesund (Svalbard) using tethered balloon and ground based measurements	University Leipzig, Faculty of Physics and Earth Sciences	2023
	Stallmach, A.	Analysis of the meteorological situation during the pyroCb outbreaks of the Australian New Year Wildfire 2019/20	University Leipzig, Faculty of Physics and Earth Sciences	2023
	Sührig, A.	Einfluss des Lockdowns im Frühjahr 2020 auf die Luftqualität in Deutschland	University Leipzig, Faculty of Physics and Earth Sciences	2023

Appendices: Academic degrees / Awards

Academic degree*	Name	Title	Faculty	Year
B.Sc.	Wimmer, A.	Untersuchung der Sättigungsdynamik von Einzelphotonenpulsen verschiedener Photomultiplier mit dem Ziel der Erhöhung der maximalen Zählrate für eine Lidardatenerfassung	University Leipzig, Faculty of Physics and Earth Sciences	2023
Großer Beleg (similar to B.Sc.)	Potts, H.	Implementierung von Eiskristallbildung und -wachstum in OpenFOAM und Simulation eines Testfalls anhand des Beispiels LACIS-T	TU Freiberg	2023

* Habil.: Habilitation, Ph. D.: Doctoral theses, Dipl.: Diploma, M.Sc.: Master of Science, B.Sc.: Bachelor of Science

Summary of completed academic qualifications

Academical degrees	Number		Total
	2022	2023	
Habilitation	0	0	0
Doctoral theses	7	4	11
Dipl.-Ing.	1	0	1
Master of Science	6	12	18
Bachelor of science	2	8	10

Awards

Name	Prize	Awarding institution	Comments/Description
Romshoo, B.	AMS Outstanding Student Oral/Poster Presentation Award (AMS 2023, Denver, Colorado)	AMS (American Meteorological Society)	presentation: “Black Carbon Physicochemical and Optical Properties Database : Numerical Simulations, Radiative Forcing Estimates, and Size-Resolved Parameterizations”
Romshoo, B.	EAC Best Poster Award (EAC 2023, Malaga, Spain)	EAA (European Aerosol Assembly)	Machine learning algorithm for predicting black carbon (BC) optical properties at various stages of aging

Appendices: Editorships

Editorships

Name	Journal
Deneke, H.	Section Editor "Atmospheric Remote Sensing"
Frey, W.	Associate Editor "Atmospheric Measurement Techniques"
Heinold, B.	Guest Editor "Frontiers Environmental Science"
Heinold, B.	Associate Editor "Atmosphere - MDPI"
Herrmann, H.	Associate Editor "Atmospheric Measurement Techniques"
	Editorial Board Member "Atmospheric Pollution Research"
	"Atmospheric Chemistry and Physics," Special Issue Editor (HCCT-2010)
	Editorial Board Member "Aerosol and Air Quality Research" (AAQR)
	"Science of the Total Environment" (STOTEN) - Special Issue Editor
	"Atmospheric Chemistry and Physics" (ACP) - EUROCHAMP-2020 Special Issue Editor
	"Journal of Geophysical Research" (JGR) Atmospheres - Associate Editor
	Associate Editor
	International Advisory Board "Environmental Science and Technology"
Macke, A.	Member of the Advisory Board "Meteorologische Zeitschrift"
	Associate Editor "Atmospheric Measurement Techniques"
	Member of Editing Committee "promet"
Seifert, P.	Guest Editor for an Atmospheric Chemistry and Physics and Atmospheric Measurement Techniques Special Issue (PROM)
Tegen, I.	Associate Editor "Journal of Geophysical Research"
Wandinger, U.	Editorial Board Member "Atmospheric Measurement Techniques"
van Pinxteren, D.	Scientific Advisory Board of the Journal "Gefahrstoffe, Reinhaltung der Luft"
Wehner, B.	Editorial Board Member "Atmospheric Chemistry and Physics"

Memberships

Name	Board
Althausen, D.	Commission on Air Pollution Prevention of VDI and DIN - Standards Committee KRdL, NA 134-02-01-22 UA "Ground-based remote sensing of meteorological parameters", Department II Environmental Meteorology
Baars, H.	Member and Speaker of the EARLINET Council
	Member of the ESA Aeolus Science Advisory Group
Deneke, H.	Member of the International Radiation Comission
	Member of the Convection Working Group
	Member of the International Cloud Working Group (ICWG)
Faust, M.	Member of the International Society for Aeolian Research (ISAR)
Fomba, K.W.	Member of the African Society of Air Quality
Heinold, B.	Member of the HAMMOZ Steering Committee
Hellmuth, O.	Membership in the International Association for the Properties of Water and Steam (IAPWS), Working Group Thermophysical Properties of Water and Steam (TPWS)
	Member of Leibniz-Sozietät der Wissenschaften zu Berlin e. V.
Henning, S.	Co-chair of the EAA Working Group: Atmospheric Aerosol Studies (AAS) for Aerosol-cloud-interaction in Warm, Mixed-Phase and Ice Clouds
Hermann, M.	Member of the HALO Board of Trusties
	Memebr of the VDI code of practice board NA 134-04-02-18 UA "Measurement of Particles in the Outdoor Air - Determination of Particle Number"
Herrmann, H.	Chairman of the working group "Atmospheric Chemistry" in the GDCh-division "Environmental Chemistry and Ecotoxicology (AKAC)"
	DECHEMA/GDCh/ (Bunsen Society), Community Committee "Chemistry of the Atmosphere"
	DECHEMA/GDCh/KRdL Division Particulate Matter - Co-Chair
	IUPAC Task Group on Atmospheric Chemical Kinetic Data Evaluation
	Advisory Board Member of ProcessNet-Fachgemeinschaft (Specialist Community) SuPER
	Fellow of International Union of Pure and Applied Chemistry (IUPAC)
	National Co-Representative "International Surface Ocean - Lower Atmosphere Study" (SOLAS)
	Membership of the American Chemical Society (AMC)
	Member of the Second International Indian Ocean Expedition (IIOE-2)

Appendices: Memberships

Name	Board
Herrmann, H.	Distinguished Visiting Professor for Environmental Sciences and Engineering at Shandong University, Qingdao, China
	Professor for Environmental Sciences and Engineering at Fudan University, Shanghai, China
	Member of the Evaluation Commission of the Czech Academy of Sciences
Macke, A.	Deputy Chair of Section E of the Leibniz Society
	Member of the Steering Committee Collaborative Research Cluster TR 172 "Arctic Amplification"
	Member of the Standing Commission for Scientific Infrastructure Facilities and Research Museums of the Leibniz Association
	Member of the Steering Committee of the Leibniz Research Network "Integrated Earth System Research"
Mertes, S.	Member of the Science Team of CIRRUS-HL: The airborne experiment on CIRRUS in High Latitudes with the highaltitude long-range research aircraft HALO
	Ordinary member of the DFG collaborative research center TR 172 "Arctic Amplification"
Müller, Ke.	Member of the German Library Association (dbv)
	Member of the Professional Association Information Library (BIB)
Niedermeier, D.	Member of the German Society of Humboldtians - Regional group Halle-Leipzig
Pöhlker, M.	HALO Scientific Steering Committee (WLA)
Seifert, P.	Ordinary member of the DFG Collaborative Research Center TR 172 "Arctic Amplification"
Stratmann, F.	Member of the Science Team of CIRRUS-HL: The Airborne Experiment on CIRRUS in High Latitudes with the Highaltitude Long-range Research Aircraft HALO
Tegen, I.	Member of the Steering Committee natESM (National Earth System Modelling) Initiative
	HAMMOZ Steering Committee member
Tilgner, A.	Member of the working group NA 134 VDI/DIN-Commission on Air Quality Control (KRdL) - Standards Committee NA 134-02-01-08 UA Subcommittee Environmental Meteorology - Deposition Parameters
van Pinxteren, D.	Member of the European working group CEN/TC 264/WG 44 "Source Apportionment"
	Member of the KRdL National Mirror Committee of CEN/TC 264/WG 44 "Source Apportionment"
Wandinger, U.	Member of the ESA-JAXA EarthCARE Joint Mission Advisory Group
	Member of the EARLINET Council
	Member of the ACTRIS "Research Infrastructure Committee"

Appendices: Memberships / Meetings

Name	Board
Wehner, B.	Member of VDI/DIN Commission "Clean Air" (KRdL) - subgroup Meteorological Measurements
	Secretary General of GAeF (Society for Aerosol Research)
Wex, H.	Vice President of the International Comission on Clouds and Precipitation (ICCP)

Meetings

Meetings	Date	national/international	number of participants
Hammox User Meeting (online)	3/31/2022	international	25
ACTRIS-D Annual Conference	20. - 22.06.2022	national	103
Dustrisk Project Meeting	7/10/2022	national/international	12
Arctic Amplification, PI Meeting	19. - 21.09.2022	national/international	40
First International Conference on Air Quality in Africa (ICAQ)	10. - 14.10.2022	International	160
Arctic Amplification (AC)3, General Assembly and Planning Phase III	21. - 25.11.2022	national/international	more than 100
Cloud Tracking Workshop	17. - 21.4.2023	international	172
EARLINET General Assembly (online)	14.12.2023	international	80
EarthCARE Cal/Val and Science Workshop	17.11.2023	international	150
SOURCE FFR Measurements Modelling Kick-Off Meeting	26. - 27.04.2023	national	40
Staubtag	14. - 15.09.2023	national/international	35
Workshop Arctic Aerosol, Focus Airborne Measurements	11. - 13.12.2023	international	25
BASS Meeting	16. - 18.10.2023	national/international	30
Arctic Amplification, Evaluation	27. - 28.06.2023	national/international	40
EarthCARE CARDINAL Meeting	18. - 19.09.2023	national/international	20

Appendices: Reviews / Guest scientists

Reviews

Reviews	Number	
	2022	2023
Journals	154	183
Projects	20	32
Statements, position papers	6	0
Others	24	100
Total	204	315

Guest scientists

Name	Period of stay	Institution
Jörss, A.-M.	03.01. - 07.01.22	Alfred Wegener Institute, Helmholtz Centre for Polar and Marine Research, Bremerhaven, Germany
Nozirov, D.	03.01. - 12.01.22	Academy of Sciences of Republic of Tajikistan, Dushanbe, Tadschikistan
Trapon, D.	01.08. - 31.12.22	Meteo-France, Toulouse, France
Trapon, D.	27.06. - 01.07.22	Meteo-France, Toulouse, France
Mies, J.	24.01. - 28.01.22	Umweltbundesamt Langen, Germany
Spinnler, K.	28.01. - 28.01.22	Umweltbundesamt Langen, Germany
Böing, S.	29.03. - 01.04.22	University of Leeds, UK
Nozirov, D.	28.04. - 25.07.22	Academy of Sciences of Republic of Tajikistan, Dushanbe, Tajikistan
Khodzhakhon, M.	28.04. - 30.06.22	Academy of Sciences of Republic of Tajikistan, Dushanbe, Tajikistan
Khalifaeva, S.	28.04. - 30.06.22	Academy of Sciences of Republic of Tajikistan, Dushanbe, Tajikistan
Malollari, G.	01.05. - 30.11.22	Agricultural University of Tirana, Albania
Persson, O.	01.05. - 03.05.22	University of Colorado, USA
Lüchtrath, S.	30.05. - 17.06.22	Technical University of Berlin, Germany
Wang, J.	31.05. - 30.06.23	School of Civil and Environmental Engineering Atlanta, USA
Raff, J. D.	01.06. - 31.08.22	Indiana University, USA

Appendices: Guest scientists

Name	Period of stay	Institution
Kiselev, A.	13.06. - 24.06.22	Karlsruhe Institute for Technology, Germany
Stolle, C.	15.06. - 16.06.22	Leibniz Institute for Atmospheric Physics, Kühlungsborn, Germany
Wittink, J.	27.06. - 01.07.22	Koninklijk Nederlands Meteorologisch Instituut, De Bilt, The Netherlands
Schimmel, W.	01.07. - 31.12.22	Leipzig Institute for Meteorology, Germany
Laksin, A.	11.07. - 15.07.22	Purdue University Chemistry Department, West Lafayette, USA
Avinash, K.	25.07. - 31.08.22	Tampere University, Finland
Rowell, A.	25.07. - 31.08.22	University of Birmingham, UK
Brean, J.	25.07. - 31.08.22	University of Birmingham, UK
Lopez Cayuela, M.A.	10.09. - 09.10.22	Instituto National de Técnica Aeroespacial, Madrid, Spain
Atabakhsh, S.	01.10. - 31.10.23	Yazd University, Iran
Ferron, G.	01.11.22 - 31.12.24	Helmholtz-Zentrum München, Germany
Karg, E.	01.11.22 - 31.12.24	Helmholtz-Zentrum München, Germany
Loulli, E.	23.11 - 17.12.22	Cyprus University of Technology, Limassol, Cyprus
Gligorovski, S.	23.11. - 25.11.22	Chinese Academy of Sciences, Beijing, China
Hu, Y.	01.12.21 - 31.06.22	Shandong University, China
Warnes, D.	16.01. - 24.01.23	Cambridge University, UK
Nozirov, D.	16.01. - 15.03.23	Academy of Sciences of Republic of Tajikistan, Dushanbe, Tajikistan
Kolodziejczyk, A.	23.01. - 10.02.23	Institute of Physical Chemistry Polish Academy of Sciences, Warsaw, Poland
Ervens, B.	25.01. - 27.01.2023	Institute of Chemistry, Université Clermont Auvergne, Clermont-Ferrand, France
Engel, A.	30.01. - 31.01.23	GEOMAR Helmholtz Centre for Ocean Research Kiel, Germany
Kalmbach, D.	30.01. - 04.02.23	Alfred Wegener Institute, Helmholtz Centre for Polar and Marine Research, Bremerhaven, Germany
Cremer, R.	01.02. - 31.07.23	Stockholm University, Sweden
Hartmann, M.	12.03. - 15.03.23	University of Gothenburg, Sweden
Opp, C.	20.03. - 02.04.23	Philipps-Universität Marburg, Germany
Idrissa, S. M.	28.03. - 29.04.22	Atlantic Technical University (UTA), Cabo Verde
Dembele, M.B.	14.04. - 07.05.23	Atlantic Technical University (UTA), Cabo Verde

Appendices: Guest scientists / Visits of TROPOS

Name	Period of stay	Institution
Baltensperger, U.	01.05. - 03.05.23	Paul Scherrer Institut, Villingen, Switzerland
Sharma, V.K.	04.05. - 06.05.23	School of Public Health, Texas A&M University, College Station, USA
Sommerfeld, M.	22.05. - 22.05.23	Otto-von-Guericke-Universität Magdeburg, Germany
Grgic, I.	23.05. - 25.05.23	National Institute of Chemistry Ljubljana, Slovenia
Morrish, D.	30.05. - 02.06.23	National Institute of Water & Atmospheric Research Ltd Auckland, New Zealand
Huang, C.H.	04.06. - 08.06.23	School of Civil and Environmental Engineering Atlanta, USA
Machado, Luiz	05.06. - 06.06.23	Max Planck Institute Mainz, Germany
Pizarro, R.J.	26.06. - 26.07.23	Universidad Nacianal de Colombia, Bogotá, Columbia
Mascumento, J.	03.07. - 05.07.23	Universität Colorado Boulder, USA
Shaw, R.	07.03. - 13.03.23	Michigan Technological University, USA
Makoric, P.	24.07. - 23.08.23	Universität Nova Gorica, Slovenia

Visits of TROPOS scientists

Name	Period of stay	Institution
Fomba, K. W.	01.11. - 09.11.22	Mohammed VI Polytechnic University, Ben Guierir, Marocco
Fomba, K. W.	06.01. - 10.01.22	University of Cabo Verde, Praia, Santiago, Kap Verde
Engelhardt, V.	06.06. - 16.07.22	Multidisciplinary Institute of Plant Biology, Cordoba, Argentina
Pöhlker, M.	27.07.2022	Karlsruhe Institute for Technology, Germany
Gebauer, H.	15.08. - 10.10.22	National Academy of Science, Dushanbe, Tajikistan
Gaudek, T.	15.08. - 10.10.22	National Academy of Science, Dushanbe, Tajikistan
Lipken, F.	15.08. - 10.10.22	National Academy of Science, Dushanbe, Tajikistan
Althausen, D.	15.08. - 10.10.22	National Academy of Science, Dushanbe, Tajikistan
Engelmann, R.	15.08. - 10.10.22	National Academy of Science, Dushanbe, Tajikistan
Hajipour, M.	21.11. - 25.11.22	Deutscher Wetterdienst, Hohenpeissenberg, Germany
Niedermeier, D.	28.11. - 02.12.22	Universität Hamburg, Germany
Goharian, K.	28.11. - 02.12.22	Universität Hamburg, Germany
Gómez M.A., S.	18.09 - 18.11.23	Laboratoire Inter-Universitaire des Systèmes Atmosphériques (LISA), Paris, France
Niedermeier, D.	25.09. - 13.10.23	Michigan Tech University, Houghton, USA

Appendices: International and national field campaigns

International and national field campaigns

Campaign	Project partner
9-Euro-Ticket Saxony, Hesse Effects of the 9-euro ticket on air quality TROPOS: AMP***	Leipziger Verkehrsbetriebe, WG Psychology University of Leipzig, Saxon State Office for Environment, Agriculture and Geology, Hessian State Office for Nature Conservation, Environment and Geology, Bielefeld University of Applied Sciences, Germany
ACROSS (Atmospheric ChemistRy Of the Suburban foreSt) TROPOS: ACD*, AMP	> 10 partners from France and USA
ACTRIS Cloud in-situ comparison campaign , Austria Comparison of different measuring devices for cloud liquid water content, effective drop radius and drop size distribution under high alpine conditions TROPOS: AMP, ACD	Central Institute for Meteorology and Geodynamics, Austria
Aerosol characterization in Southern Chile / Punta Arenas TROPOS: AMP	University de Magallanes (UMAG), Chile
APAICA (within ATWAIce) measurements on Polarstern (aerosol / turbulenz) in the Arctic TROPOS: ACD, AMP	Technische Universität Berlin, Alfred Wegener Institute, Helmholtz Center for Polar and Marine Research, Bremerhaven, Germany
BACSAM , Norway Investigation of the vertical distribution of aerosol particles, CCN and INP in the Arctic with the Polar 6 and the AWI's new T-Bird towed vehicle TROPOS: AMP	Alfred Wegener Institute, Helmholtz Centre for Polar and Marine Research, Germany
BELUGA@Ny-Alesund Tethered balloon measurements of the Arctic boundary layer to measure vertical profiles of temperature, stability, radiation and aerosol particles TROPOS: AMP	(AC) ³ consortium
CAFE-Brazil aircraft measurement campaign of (HALO) in combination with measurements at the ATTO tower to study the new particle formation in the upper troposphere of the amazonian rainforest. TROPOS: AMP	Max Planck Institute for Chemistry Mainz, Germany, ATTO and HALO consortium
CCN & INP in North Greenland / Villum Reseach Station TROPOS: AMP	Aarhus University, Denmark
CCWaC_INT23 Comparison of different cloud water collectors for ACTRIS on the Schmücke TROPOS: ACD	

Appendices: International and national field campaigns

Campaign	Project partner
CLOUDLAB Researching microphysical processes by using stratus clouds as natural laboratory TROPOS: RSD****	ETH Zurich, Switzerland
DUSTRISK (main campaign) Investigation of harmful aspects of mineral dusts in combination with adhering microbes TROPOS: ACD	Leibniz Institute DSMZ - German Collection of Microorganisms and Cell Cultures, Research Center Borstel Leibniz Lung Center, Leibniz Institute for Environmental Medical Research, Germany, institutions from Cabo Verde, including hospitals, universities and public health institutes
EARLINET (permanent experiment) European Aerosol Research Lidar Network Leipzig, Germany, Dushanbe, Tajikistan TROPOS: RSD	EARLINET consortium
GoAfrica measurements of cocking emissions in combination with lung function tests in Africa. TROPOS: AMP	(AC) ³ consortium
GoSouth measurements to better understand the aerosole population in the southern hemisphere TROPOS: ACD, AMP	TROPOS and New Zealand partner
GUAN German Ultrafine Aerosol Network TROPOS: ExAWoMp*****, ACD	German Federal Environmental Agency Langen; German Research Center for Environmental Health, Munich; Saxon State Ministry of the Environment and Agriculture, Dresden; Institute of Energy and Environmental Technology e.V., Duisburg; DWD Hohenpeissenberg, Germany; ISSEP, Liège, Belgium
HALO-AC3 Coordinated aircraft measurement campaign of three research aircrafts (HALO, Polar 5, Polar 6) to study Arctic clouds, the Arctic boundary layer and the Arctic free troposphere TROPOS: AMP	(AC) ³ and HALO consortium
IDEFIX-I Investigations of rime-splintering mechanism TROPOS: AMP	Karlsruhe Institute of Technology, Germany
JATAC Joint Aeolus Tropical Atlantic Campaign. Measruements at Cabo Verde for the validation of Aeolus TROPOS: RSD	9 partners from Germany, France, Greece, Slovenia, Cap Verde
Leipzig PM Composition (DFG project ARG-GER, Leipzig III) Size-resolved composition and source apportionment Leipzig TROPOS: ACD	

Appendices: International and national field campaigns

Campaign	Project partner
LoCo-PM Use of miniaturized low-cost PM2.5 and PM10 measurement devices in order to increase the spatial density in air quality networks, Application in Leipzig-Lindenau TROPOS: ACD, AMP	Dr. Födisch Umweltmesstechnik AG, Makranstädt, Germany
LOSTECCA Lidar Observations of SpatioTEmporal Contrasts in Clouds and Aerosols, Pahia, New Zealand TROPOS: RSD	National Institute of Water and Atmospheric Research, New Zealand
MESOCOSM Chemical reactions in the sea -surface microlayer, Wilhelmshaven TROPOS: ACD	
MiST , Bad Lauchstädt Influence of different foliage and thus biodiversity on solar radiation solar radiation and the microclimate using a pyranometer, among other things TROPOS: RSD	German Center for Integrative Biodiversity Research, University of Leipzig, CFE, Germany
ORIGAMY Exploring the atmospheric ORIGIN of Amines within the Marine boundary layer: A combined field modelling approach TROPOS: AMP	
Ozonvorläufer Kontinuierliche VOC-Messungen in Borna TROPOS: ACD	Saxon State Office for Environment, Agriculture and Geology, Germany
PARAMOUNT Laboratory studies for the production of aerosol particle organic matter in clouds at the CESAM cloud chamber in Paris TROPOS: ACD, AMP	Laboratoire Interuniversitaire des Systèmes Atmosphériques Paris, Laboratoire de Chimie de l'Environnement Marseille, France
PHILEAS Investigation of the export of air from the Asian summer monsoon to high latitudes in Alaska TROPOS: AMP	University of Mainz, Research Center Jülich, Germany
Polar Change Antarctic TROPOS: ACD	University Barcelona, Spain
PollyNet (permanent experiment) Network of institutions with a PollyXT TROPOS: RSD	PollyNet consortium
Polly Tirana , Albania Vertical aerosol distribution over Albania/Western Balkans using PollyXT TROPOS: RSD	Universiteti Bujqësor i Tiranës, Albania

Appendices: International and national field campaigns

Campaign	Project partner
PS 127 Polarstern cruise with OCEANET container on board from Bremerhaven to Cape Town TROPOS: RSD	
Radon Determination of characteristic exposure conditions for radon at indoor workplaces on behalf of IAF-Radioökologie GmbH, Radeberg TROPOS: AMP	
RWB Leipzig Residential Wood Burning in Leipzig during the 2022 Energy Crisis TROPOS: AMP, Modeling**, ACD	
S2VSR Investigation of the small-scale spatial and temporal variability of solar radiation TROPOS: RSD	University of Oklahoma, Atmospheric Research Measurement Programm, USA
SOPORTE Source apportionment of size-resolved atmospheric particulate matter and their oxidative potential in Córdoba (Argentina) and Leipzig (Germany) TROPOS: ACD	National University of Cordoba, Multidisciplinary Institute of Plant Biology IMBIV-CONICET, Argentina
ULTRAFLEB Stationary and mobile field measurements of ultrafine particles (UFP) and other quantities in the vicinity of Berlin Brandenburg Airport BER TROPOS: AMP	Brandenburg State Office for the Environment, Technische Universität Braunschweig, Technische Universität Berlin, Airport Berlin Brandenburg GmbH, Ingenieurbüro Janicke GbR, Society for Environmental Physics, IVU Umwelt GmbH
TINIA Investigations on ice crystal growth under turbulent temperature and humidity conditions TROPOS: AMP	Michigan Tech, USA; University of Hamburg
VACCINE Variation of Antarctic Cloud Condensation (CCN) and ice nucleating particle concentrations (INP) at Neumayer Station TROPOS: AMP	Alfred Wegener Institute, Helmholtz Center for Polar and Marine Research, Germany
EDIAQI Evidence driven indoor air quality improvement TROPOS: AMP	IMROH, KNOW, TALTEC, Wings, LAS Analytica, ...
Continuous ammonia immission measurements TROPOS: ACD	
ATMO ACCESS rehearsal campaign in preparation for EarthCARE Cal/Val TROPOS: RSD	ACTRIS remote sensing consortium, ATMO ACCESS partners

Appendices: International and national field campaigns / Cooperations

Campaign	Project partner
SOURCE FFR measurements, modelling: 1. emission measurement campaign at Frankfurt airport TROPOS: RSD	DLR Institute of Combustion Technology, Institute for Atmosphere and Environment at Goethe University Frankfurt am Main, Dresden University of Technology
BASS Mesocosmen TROPOS: ACD	University Oldenburg, GEOMAR - Helmholtz Center for Ocean Research Kiel, Alfred Wegener Institute, Helmholtz Center for Polar and Marine Research, Germany

* Atmospheric Chemistry Department

** Department Modeling of Atmospheric Processes

*** Department Atmospheric Microphysics

**** Department Remote Sensing of Atmospheric Processes

***** Experimental Aerosol and Cloud Microphysics Department

Cooperations

International cooperations

Research project	Cooperation partners
ACD-C Atmospheric Chemistry Chamber	University of British Columbia, Dept. of Chemistry, Vancouver, Canada; University College Cork, Ireland; Institute of Chemistry, Slovenia
ACLOUD Arctic Cloud Observations Using airborne measurements during polar Day	Max Planck Institute for Chemistry, Mainz; Alfred Wegener Institute, Helmholtz Center for Polar and Marine Research; Karlsruhe Institute for Technology; University of Mainz, Germany; University of Clermont-Ferrand, France
ACORES Project about clouds, aerosols, and radiation at the Azores	Michigan Technological University, Houghton; ARM Facilities of DOE, USA; Storm Peak Laboratory, DRI, USA; Max Planck Institute for Chemistry, Mainz; TU-Berlin, Germany; University Warsaw, Poland; Universitat Politècnica de Catalunya, Barcelona, Spain
ACROSS Atmospheric ChemistRy Of the Suburban foreSt	> 10 partners from France and USA
ACTRIS Aerosol, Clouds and Trace Gases Research Infrastructure	more than 100 partners from 21 European countries
ACTRIS-CAMS Aerosol, Clouds and Trace Gases Research Infrastructure - Copernicus Atmosphere Monitoring Service	Norwegian Institute for Air Research, Kjeller, Norway; Centre National de la Recherche Scientifique, Paris, Verneuil-en-Halatte, France
ACTRIS measurement station Melpitz Cooperation partners involved in research projects at the TROPOS Research Station Melpitz	Norway, UK, Italy, Switzerland, Czech Republic, Hungary, Ireland, Finland, Austria, Sweden, Bulgaria, Belgium, France, Greece, The Netherlands, Spain, Denmark, Latvia, Poland, Portugal

Appendices: Cooperations

Research project	Cooperation partners
Aeolus DISC (Data, Innovation, and Science Cluster) - ESA's data quality framework to support the Aeolus mission	German Aerospace Center, DoRIT, Germany; Centre National de la Recherche Scientifique, France; European Centre for Medium-Range Weather Forecasts, Royal Netherlands Meteorological Institute, The Netherlands; ASEA Brown Boveri, Zürich, Switzerland
AQMEII Air Quality Model Evaluation International Initiative	Austria, Australia, Belgium, Canada, Switzerland, Cyprus, Germany, Denmark, Finland, France, Greece, Italy, Luxembourg, Malta, The Netherlands, Norway, Poland, Portugal, Sweden, UK, USA
ATMO-ACCESS Sustainable Access to Atmospheric Research Facilities	Cooperation of the European Research Infrastructures ACTRIS, ICOS and IAGOS
ATTO Amazon Tall Tower Observatory	18 partners from Brazil and Germany
BBComp Biomass burning organic aerosol in Europe and Asia: Molecular composition and impact on air quality	Chubu University, Japan
BRACE MY Boosting ReseArch CapabilitiEs of Romanian Cloud MicrophYsics Centre	National Institute for Aerospace Research "Elie Carafoli", Bucharest, Rumania; University Oslo; Andøya Space Center, Andenes, Norwegen
CAFE-Brazil aircraft measurement campaign of HALO in combination with measurements at the ATTO tower to study the new particle formation in the upper troposphere of the amazonian rainforest	Max Planck Institute for Chemistry, Goethe University Frankfurt, Germany
CARDINAL Clouds, Aerosol, Radiation – Development of INtegrated ALgorithms	9 partners from The Netherlands, Germany, Belgium, Canada, Spain, UK, France
CEOS protocol: Best practices for the validation of Aerosol, Cloud, and Precipitation Profiles	Multiple international partners, mainly from the US, Europe and Japan
CLOUD – DOC Cosmics Leaving OUtdoor Droplets	Germany, Switzerland, Finland, Austria, UK
CLOUD Cosmics Leaving OUtdoor Droplets	16 partners from Germany, Switzerland, Finland, Austria, Portugal, Russia, UK, USA
CLIMB How do aerosol-cloud interactions influence the surface mass balance in East Antarctica?	Royal Meteorological Institute of Belgium, Uccle; Catholic University of Leuven; Royal Belgian Institute for Space Aeronomy, Uccle; Ghent University, Belgium
COST Chemistry transport model intercomparison	Germany, Denmark, Finland, France, Bulgaria, Estonia, Italy, Malta, Spain, The Netherlands, Norway, Poland, Switzerland, UK, Greece, Israel
DACAPO-PESO Dynamics, Aerosol, Cloud and Precipitation Observations in the Pristine Environment of the Southern Ocean	University de Magallanes, Punta Arenas, Chile; Leipzig Institute for Meteorology, Germany

Appendices: Cooperations

Research project	Cooperation partners
DUSTRISK A risk index for health effects of mineral dust and associated microbes	The University of Cape Verde, The National Institute of Meteorology of Cape Verde, The National Directorate of Environment, The Instituto Nacional de Saúde Pública, Dr. Baptist de Sousa Hospital, and Dr. Agostinho Neto Hospital Praia, Cabo Verde
EARLINET European Aerosol Research Network	Germany, Italy, Spain, Greece, Switzerland, Sweden, Portugal, Poland, Belarus, France, Bulgaria, Romania, Norway, The Netherlands, Finland, Ireland, Cyprus
ESA-Aeolus European Space Agency, Atmospheric Dynamics Mission	European Space Research and Technology Center, Noordwijk, The Netherlands, ESA Centre for Earth Observation, Frascati, Italy
ESA-EarthCARE European Space Agency, Earth Clouds, Aerosol and Radiation Explorer	European Space Research and Technology Center, Noordwijk, The Netherlands; Japan Aerospace Exploration Agency, Chofu
EXCELSIOR ERATOSTHENES: EXcellence Research Centre for Earth SurveyLlance and Space-Based Monitoring Of the EnviRonment	Cyprus, Germany, Greece
GoSouth Measurements to better understand the aerosole population in the southern hemisphere.	National Institute of Water and Atmospheric Research, Auckland; University of Canterbury, Christchurch; University Auckland, New Zealand; University Hannover, Germany
GreenFjord Greenlandic Fjord ecosystems in a changing climate: Socio-cultural and environmental interactions	Extreme Environments Research Laboratory; École Polytechnique Fédérale de Lausanne, Switzerland
HAMMOZ hosting	ETH Zurich; C2SM Zurich, Switzerland; University Oxford, UK; Finish Meteorological Institute; GEOMAR - Helmholtz Center for Ocean Research Kiel, Max Planck Institute Hamburg, Leipzig Institute for Meteorology, Leipzig University, Germany
H-AMS/ACROSS Developing an on-line parameterization approach for predicting the ambient organic aerosol hygroscopicity based on High- Resolution AMS measurements	Laboratoire des Sciences du Climat et de l'Environnement, Université Paris-Saclay, Gif-sur-Yvette, France; Institut National de l'Environnement Industriel et des Risques, Verneuil-en-Halatte, France
HALO-AC3 Characterisation of Arctic aerosol particles, cloud particle residues, cloud condensation nuclei and ice nucleating particles	Max Planck Institute for Chemistry; Alfred Wegener Institute, Helmholtz Center for Polar and Marine Research; German Aerospace Center; University of Mainz, Germany; University of Clermont-Ferrand, France
IAPOS-CARIBIC In-service Aircraft for a Global Observing System - Civil Aircraft for Remote Sensing and In situ measurement in Tropospheric and Lower Stratosphere based on the Instrumentation Container Concept	Germany, UK, France

Appendices: Cooperations

Research project	Cooperation partners
ICON Cloud Issues Assessment of cloud forecast with the ICON model	Israel Meteorological Service, Beit Dagan; German Weather Service; Karlsruhe Institute of Technology, Germany
ICON-HAMMOZ Development Model development	Max Planck Institute for Meteorology, Germany, ETH Zurich, Institute for Atmospheric and Climate Science, Switzerland, Oxford University, UK; University of Leipzig, Germany
Impact of the COVID-19 lockdown on the Asian summer monsoon	Indian Institute of Tropical Meteorology
LACIS-T Turbulent Leipzig Aerosol Cloud Interaction Simulator	Leibniz Institute for Solid State and Materials Research Dresden; University of Ilmenau, Germany, Michigan Technological University, Houghton; University of Utah, Salt Lake City, USA; University of Warsaw, Poland; University of Hamburg, Germany
OSCM Ocean Science Center Mindelo	Instituto Nacional de Desenvolvimento das Pescas, Mindelo, S. Vicente, Republic of Cape Verde; GEOMAR Helmholtz Centre for Ocean Research Kiel, Germany
OzonEval Development and application of an approach to assess the uncertainty of model computations of air pollution dispersion with a focus on ozone	FU Berlin, Research Institute for Sustainability – Helmholtz Centre Potsdam; TNO, Utrecht; IVU Umwelt GmbH, Freiburg, Germany
PARAMOUNT Production of Aerosol paRticle orgAnic Matter in CLOUDs: chamber and laboratory studies, mechanisms, modelling and iNTegration	University Paris-Est Créteil Val de Marne; Institut Pierre Simon Laplace; Laboratoire Inter-universitaire des Systèmes Atmosphériques, Paris; Aix-Marseille Université; Laboratoire de Chimie de l'Environnement, Oleans, France
PHOSDMAP Phosphorus speciation in dust and marine aerosol particles	GOBABEL, Namibia; Institute for Meteorology and Geophysics, Mindelo, S. Vicente, Cabo Verde
PM03 ozone and PM air pollution in China	Fudan University, China
PolarCAP Polarimetric Radar Signatures of Ice Formation Pathways from Controlled Aerosol Perturbations	ETH Zurich, Switzerland
PollyNet Development and application of Polly systems	11 partners from Finland, Poland, Portugal, Korea, Greece, Israel, Tajikistan, Cyprus, Cabo Verde, Germany
RI-URBANS Research Infrastructures Services Reinforcing Air Quality Monitoring Capacities in European Urban & Industrial Areas	Spain, Finland, France, Germany, Italy, Netherlands, United Kingdom, Greece, Switzerland, Belgium, Norway, Romania, Poland
SOPORTE Source apportionment of size-resolved atmospheric particulate matter and their oxidative potential in Córdoba (Argentina) and Leipzig (Germany)	National University of Cordoba, Multidisciplinary Institute of Plant Biology IMBIV-CONICET, Argentina

Appendices: Cooperations

Research project	Cooperation partners
SOURCE FFR measurements • modelling Ultrafine particles in the Frankfurt airport region	TU Darmstadt, TU Braunschweig; DLR Institute of Combustion Technology, Stuttgart; Institute for Atmosphere and Environment Frankfurt; DLR Institute of Atmospheric Physics Oberpfaffenhofen; IVU Umwelt GmbH, Freiburg; Institute for Environment & Energy, Technology & Analytics Duisburg, TNO Utrecht, ACH Gladbach, HEREON Geestacht, The Netherlands, ETH Zurich, Switzerland
Tobac Development of an Open-Source-Python Software for Tracking and Object-based Analysis of Clouds in Observations and Simulations	University of Oxford, UK; Colorado State University; Texas Tech University; Argonne National Laboratory, USA
TRACE Transport and transformation of atmospheric aerosol across Central Europe with emphasis on anthropogenic sources	Institute of Chemical Process Fundamentals of the CAS (ICPF-CAS)
TINIA Investigations on ice crystal formation and growth under turbulent temperature and humidity conditions	Michigan Technological University, Houghton, USA; University of Hamburg, Germany

National cooperations

Research project	cooperation partners
(AC)³ projekt A-01 DFG-SFB/Transregio 172 Radiative closure studies and cloud radiative effects	Leipzig Institute for Meteorology, University Leipzig; University of Cologne
(AC)³ project D-02 DFG-SFB/Transregio 172 Modelling marine organic aerosol and its impact on clouds in the Arctic	Leipzig Institute for Meteorology, University Leipzig; University Bremen; Alfred Wegener Institute, Helmholtz Center for Polar and Marine Research, Bremerhaven and Potsdam
(AC)³ project A-02 DFG-SFB/Transregio 172 Tethered balloon-borne energy budget measurements in the cloudy central Arctic	Leipzig Institute for Meteorology, University Leipzig; Alfred Wegener Institute, Helmholtz Center for Polar and Marine Research, Bremerhaven and Potsdam
(AC)³ project B-03 DFG-CRC/Transregio 172 Characterization of Arctic mixed-phase clouds by airborne in-situ measurements and remote sensing	Leipzig Institute for Meteorology, University Leipzig; University of Cologne
(AC)³ project B-04 DFG-SFB/Transregio 172 Properties and sources of Arctic ice nucleating particles and cloud condensation nuclei by ship-based in-situ measurements	Leipzig Institute for Meteorology, University Leipzig; Alfred Wegener Institute, Helmholtz Center for Polar and Marine Research, Bremerhaven and Potsdam

Appendices: Cooperations

Research project	cooperation partners
ACTRIS-D Aerosol, Clouds and Trace Gases Research Infrastructure - Deutschland	10 project partners
AEROVIR Aerosol chamber studies to characterize the SARS-CoV-2 transmission through aerosol	Helmholtz Centre for Environmental Research, Leipzig; Institute for Virology, Leipzig University Hospital
BASS Mesocosmen Biogeochemical processes and ocean-atmosphere exchange processes in marine surface films	University Oldenburg, GEOMAR - Helmholtz Center for Ocean Research Kiel, Alfred Wegener Institute, Helmholtz Center for Polar and Marine Research, Germany
ALADINA Investigating the Small-Scale Vertical and Horizontal Variability of the Atmospheric Boundary Layer Aerosol using Unmanned Aerial Vehicles	Technical University Braunschweig; University Tübingen
APAICA (within ATWAICE) measurements on Polarstern (aerosol / turbulenz) in the Arctic	Technical University Berlin, Alfred Wegener Institute, Helmholtz Center for Polar and Marine Research, Bremerhaven
AVANTI Aerosol variability across the North Polar Ocean and sea ice	Technical University Braunschweig
AirPlast Abundance and Fate of Synthetic Materials in Atmospheric sub-10 µm Particles	Leibniz Institute of Polymer Research, Dresden; Helmholtz Centre for Environmental Research, Leipzig; Institute for Chemistry and Biology of the Marine Environment, University of Oldenburg, Technical University Berlin
BeCoLe UVC air disinfection indoors	8 project partners
CARIBIC-AMS An Automated Aerosol Mass Spectrometer for the Regular Chemical Characterization of Aerosol Particles in the Upper Troposphere and Lowermost Stratosphere	Max Planck Institute for Chemistry, Mainz
ChemTAL Chemical transformations in the plant-related dispersion calculation according to TA Luft	Federal Environmental Agency, Dessau-Roßlau; Janicke Consulting, Überlingen; Lohmeyer Consulting, Dresden
CIRRUS-HL The HALO mission on cirrus in high latitudes	7 partners
Colrawi Combined Observations with Lidar RAdar and WInd profiler	German Weather Service, Lindenberg
DUSTRISK A risk index for health effects of mineral dust and associated microbes	Leibniz Institute DSMZ (German Collection of Microorganisms and Cell Cultures), Braunschweig; Leibniz Research Institute for Environmental Medicine, Düsseldorf; Leibniz Lung Center, Borstel
Influence of the use of energy-efficient wood stoves on lung health	atmosfair gGmbH, Berlin

Appendices: Cooperations

Research project	cooperation partners
EVAA Experimental Validation and Assimilation of Aeolus observations: Validation of aerosol and wind products with ground-based instruments of TROPOS	German Weather Service, Ludwig-Maximilians-Universität Munich
GoSouth measurements to better understand the aerosole population in the southern hemisphere.	University Hannover, Germany
GUAN German Ultrafine Aerosol Network	Federal Environmental Agency, Dessau-Roßlau, Langen, Garmisch-Partenkirchen, Hofsgrund; German Weather Service, Hohenpeißenberg; IUTA Duisburg e. V.; Helmholtz Zentrum München - German Research Center for Environmental Health, University Augsburg
IFCES2 SCALEXA With Intra-model Functional Concurrency towards Efficient Exascale Earth System Predictions	TU Dresden - Center for Information Services and High Performance Computing, Max Planck Institute for Meteorology Hamburg, German Climate Computing Center Hamburg, Jülich Supercomputing Centre , ParTec, Munich
Leibniz Research Alliance “Crisis in a Globalized World”	22 partners
LoCo-PM Use of miniaturized low-cost PM2.5 and PM10 measurement devices in order to increase the spatial density in air quality networks, Application in Leipzig-Lindenau	Dr. Födisch Environmental Measurement Technique AG, Makranstädt, Germany
Machine learning algorithm to predict black carbon (BC) optical properties at various stages of aging	Technical University Kaiserslautern
MMS Leibniz Network “Mathematical Modeling and Simulation (MMS)”	24 partners
MesSBAR Automated airborne measurement of pollutant levels in the near-earth atmosphere in urban areas.	Technical University Braunschweig; Leichtwerk Reserch GmbH, Braunschweig; Research Center Jülich; Federal Environment Agency, Dessau; German Federal Office for Roads and Traffic, Bergisch-Gladbach; Physikalisch-technische Bundesanstalt, Braunschweig
Measurements of ammonia in Saxony	Saxon State Agency for Environment, Agriculture and Geology, Dresden
MODEX Modellers Exchange	Leipzig Institute for Meteorology, Leipzig University
PICNICC Polarimetry Influenced by CCN aNd INP in Cyprus and Chile	Leipzig Institute for Meteorology, Leipzig University
PolarCAP Polarimetric Radar Signatures of Ice Formation Pathways from Controlled Aerosol Perturbations	PROM Initiative

Appendices: Cooperations / Boards

Research project	cooperation partners
Prototype Doppler Lidar (design phase)	ABACUS-Laser Göttingen; Licel Berlin
Trends, causative factors and effects of ozone pollution in Saxony	Saxon State Agency for Environment, Agriculture and Geology, Dresden
UFP exposure study Frankfurt airport and region	University Frankfurt; Helmholtz Centre HEREON, Geesthacht; Leibniz Research Institute for Environmental Medicine, Düsseldorf
UV Monitoring Network Deutschlandweites Netzwerk zur Beobachtung der UV-Strahlung und Vorhersage des UV-Index	Federal Office for Radiation Protection, Salzgitter; German Weather Service, Federal Environmental Agency
VACCINE Variation of Antarctic Cloud Condensation (CCN) and ice nucleating particle concentrations (INP) at Neumayer Station	Alfred Wegener Institute, Helmholtz Centre for Polar and Marine Research, Bremerhaven

Boards

Boards of trustees

Name	Institution
Dr. K. Hess	Federal Ministry of Education and Research
RORin C. Liebner	Saxon State Ministry for Science, Culture and Tourism
Prof. Dr. F.-J. Lübken	Leibniz Institute of Atmospheric Physics at the University of Rostock (IAP)

Scientific advisory board

Name	Institution
Dr. F. Beyrich	Meteorological Observatory Lindenberg
Prof. Dr. A. Engel	GEOMAR Helmholtz Centre for Ocean Research Kiel
Dr. C. Fittschen	University of Lille, PhysicoChemistry of Combustion Processes and Atmosphere
Prof. Dr. C. Hoose	Karlsruhe Institute of Technology (KIT), Institute of Meteorology and Climate Research

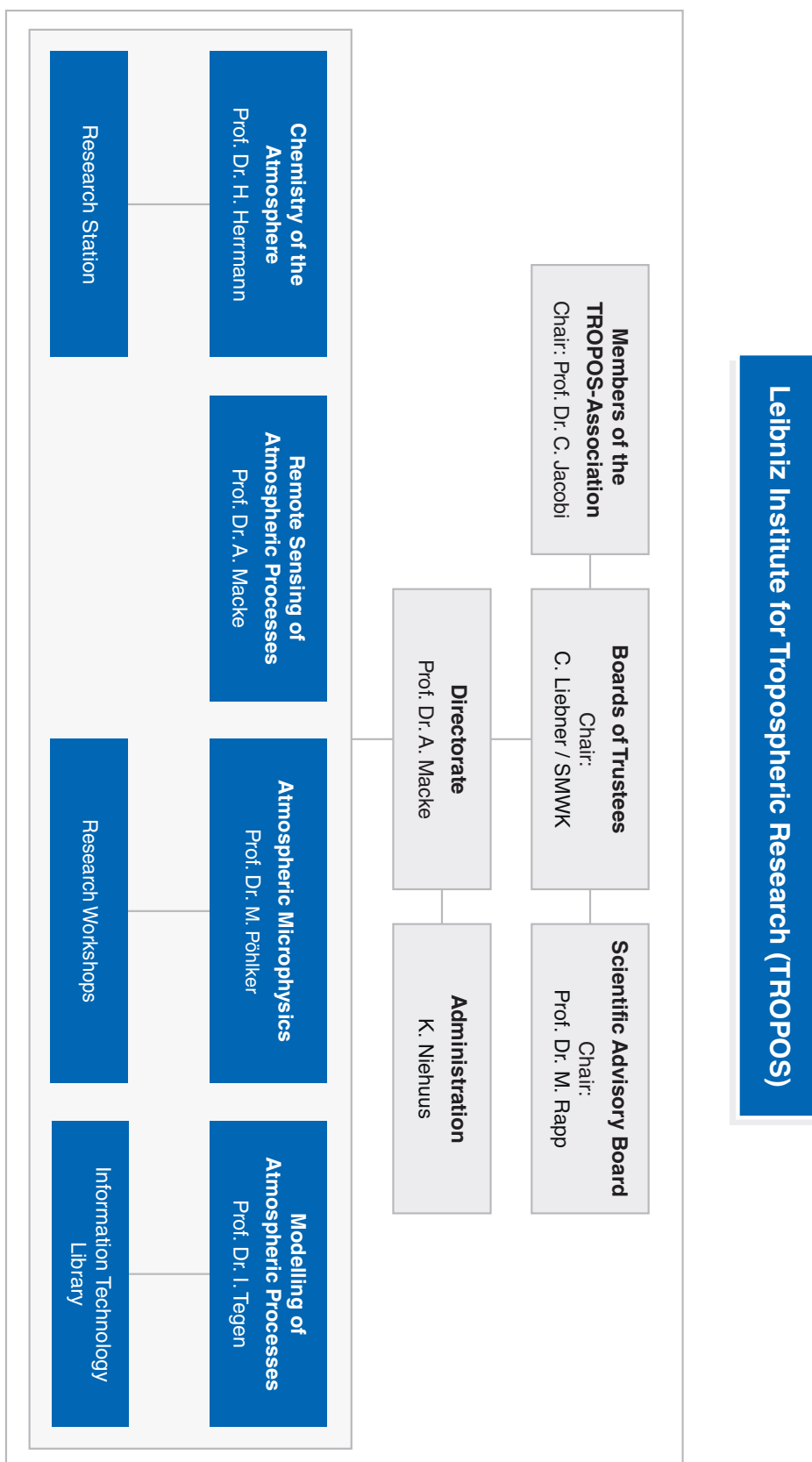
Appendices: Boards

Name	Institution
Prof. Dr. T. Koop	Bielefeld University, Faculty of Chemistry
Prof. Dr. M. Lawrence	RIFS Potsdam, Research Institute for Sustainability
Prof. Dr. H. Pawlowska	University of Warsaw, Faculty of Physics / Institute of Geophysics
Prof. Dr. J. Quaas	University Leipzig, Leipzig Institute for Meteorology (LIM)
Prof. Dr. M. Rapp (Chairman)	German Aerospace Center, Director of the Institute of Atmospheric Physics
Prof. Dr. Bernadett Weinzierl	University Vienna, Faculty of Physics

Members of the TROPOS association

Name	Institution
Prof. Dr. C. Jacobi (Chairman)	Leipzig University, Leipzig Institute for Meteorology (LIM)
RORin C. Liebner	Saxon State Ministry for Science, Culture and Tourism
Dr. Karsten Hess	Federal Ministry of Education and Research
Prof. Dr. B. Abel	University of Leipzig, Institute of Technical Chemistry
Prof. Dr. B. Brümmer	University of Hamburg, Meteorological Institute
Prof. Dr. W. Engewald	Leipzig University, Faculty for Chemistry and Mineralogy
Prof. Dr. J. Quaas	Leipzig University, Leipzig Institute for Meteorology (LIM)
Dr. H.-H. Richnow	Helmholtz Centre for Environmental Research (UFZ)
Prof. Dr. C. Simmer	Rhineland Friedrich Wilhelm University Bonn, Institute for Meteorology
Prof. Dr. E. Renner, honorary member	Professor emeritus
Prof. Dr. J. Heintzenberg, honorary member	Professor emeritus

Appendices: Organigram



TROPOS

Leibniz Institute for Tropospheric Research
Leibniz-Institut für Troposphärenforschung e.V. Leipzig
Member of the Leibniz Association

Permoserstraße 15
04318 Leipzig
Germany

Phone: ++49 (341) 2717-7060
Fax: ++49 (341) 2717-99-7060
Email: info@tropos.de
Internet: www.tropos.de